A LIGHT AND ELECTRON MICROSCOPIC STUDY OF CLARKE'S COLUMN IN THE CAT.

by

MADELEINE JANE NICOL BSc. (Hons.).

Experimental Neurology Unit,
John Curtin School
of Medical Research
Australian National University.

A thesis submited for the degree of
Doctor of Philosophy
of the Australian National University.
November, 1988

PREFACE

This thesis reports findings from several series of experiments investigating the morphology of DSCT neurones in Clarke's column, and the ultrastructural details of primary afferent terminations within Clarke's column. This work was commenced in January, 1984 in the John Curtin School of Medical Research.

A series of experiments on physiologically identified afferent inputs to Clarke's column was carried out in collaboration with Dr. R.E.W. Fyffe. The preparation of the initial experiments was shared equally between Dr. Fyffe and myself. Following each experiment, the histology and subsequent analysis of the tissue was all my own work. The results of this series of experiments are presented in Chapter 3, Sections II and III.

All other series of experiments described in this thesis were carried out in collaboration with Dr. B. Walmsley. These consisted of a series of experiments on the morphology of DSCT neurones which receive identified ankle extensor muscle input, and a series of experiments in which muscle afferents were physiologically identified and labelled, and their terminations in Clarke's column examined under the electron microscope. Again, responsibility for the preparation of the initial experiments was shared equally. The subsequent light and electron microscopic results were my own work, and are presented in Chapter 3, section I, Chapter 4 and Chapter 5.

A series of experiments was also carried out in collaboration with Dr. B. Walmsley and Dr. E. Wieniawa-Narkiewicz. The initial experiments and histology were performed by myself and Dr. Walmsley. In the first study, presented as Appendix I, the subsequent electron microscopy was performed by Dr. Wieniawa-Narkiewicz. The electron microscopy was shared by myself and Dr. Wieniawa-Narkiewicz in the second study, presented in Appendix II.

The following abstracts and papers have been published during the course of the present work:

Walmsley, B., Wieniawa-Narkiewicz, E. and Nicol, M.J. (1985) The ultrastructural basis for synaptic transmission between primary muscle

afferents and neurones in Clarke's column of the cat. The Journal of Neuroscience 5(8):2095-2106

Walmsley, B., Wieniawa-Narkiewicz, E. and Nicol, M.J. (1987) Ultrastructural evidence related to presynaptic inhibition of primary muscle afferents in Clarke's column of the cat. The Journal of Neuroscience 7(1):236-243

Wieniawa-Narkiewicz, E., Walmsley, B. and Nicol, M.J. Electron microscopy of the synaptic connection between primary afferents and DSCT neurones. Neurosci. Lett. (Suppl.) 15:S63

Walmsley, B. , Wieniawa-Narkiewicz, E., Nicol, M.J. and Tracey, D.J. (1984) Synaptic connections between primary muscle afferents and dorsal spinocerebellar tract neurones of the cat spinal cord. Neuroscience Abstracts, Vol X(1), No. 142.8

Walmsley, B., Wieniawa-Narkiewicz, E. and Nicol, M.J. (1985) The ultrastructure of identifed primary afferent terminals in Clarke's column of the cat spinal cord. Proc. Aust. Physiol. Pharmacol. Soc. 16(2):237P

Apart from the collaborations outlined above, the results contained in this thesis are my own original work, and I certify that none of the work contained in this thesis has previously been submitted for a degree or other examination.

ACKNOWLEDGEMENTS

The work contained in this thesis has been carried out in the Experimental Neurology Unit, J.C.S.M.R., and in the School of Anatomy, University of New South Wales. Financial support was provided by an Australian National University Graduate Scholarship, for which I am most grateful.

Firstly, I wish to thank my supervisor, Dr. R.E.W. Fyffe, currently at the University of North Carolina, for his support, encouragement and advice over the past 4 years. I value not only his teaching, but also his friendship very highly.

Thanks are due to Dr. S.J. Redman, Experimental Neurology Unit, J.C.S.M.R for providing continued financial support for these studies, and to Professor. M. Rowe for taking on the role of "local supervisor" over the last year. I also wish to thank the School of Anatomy, U.N.S.W for allowing me to continue my studies in Sydney.

At the John Curtin School, I would like to thank Mr. Ken Collins, especially in his role of liason between me and the two departments, Garry Rodda and Terrina Thompson for assistance in setting up the experiments in the Experimental Neurology Unit, and especially Lesley Maxwell and Elzbieta Wieniawa-Narkiewicz for teaching me serial section electron microscopy. Also, I am grateful to Mr. Stuart Butterworth and his staff for their careful reproduction of the final figures.

At the University of New South Wales, I am deeply indebted to Mr. Collin Yeo, for his ready advice, and for his heroic achievement in managing to keep all the machines running smoothly during the course of my studies.

For critical reading and advice of this thesis I am grateful to Drs. B. Walmsley, R.E.W. Fyffe, and D.J. Tracey.

I would like to thank my family, the Nicols and the Walmsleys, for all their involvement. Thanks are also due to the Fyffes, the Robertsons and the Gardiners for their continued support .

My greatest debt of thanks is due to my husband, Bruce, for his support, advice and encouragement throughout, and for his unfailing sense of humour during the final frantic days. He has helped enormously in the production of the final figures, especially of the schematic drawings depicted in Chapter 4.

I would like to dedicate the work in this thesis to my parents, Val and David Nicol, and to my husband Bruce.

ABSTRACT

A number of morphological studies have been carried out on Clarke's column in the cat spinal cord.

In one series of experiments, the location and morphology of physiologically identified dorsal spinocerebellar tract (DSCT) neurones in Clarke's column was investigated. DSCT neurones were intracellularly identified, labelled by injection of horseradish peroxidase, and reconstructed under the light microscope. The results of these experiments do not support previous proposals concerning a strict somatotopic location, nor a distinct morphology of DSCT neurones according to their location, or receptor type of their afferent input from the hindlimb.

A major ultrastructural study was subsequently undertaken. This study examined the ultrastructural features of an entire Ia afferent collateral branch within Clarke's column. The results of this study reveal a wide diversity in the structural features of the collateral branches and myelination, and of the synaptic boutons and the synaptic specializations contained within these boutons. The collateral exhibited nodes synaptically specialized with a single *en passant* bouton, nodes specialized to include a series of *en passant* boutons, and terminal heminodes, without myelination. The synaptic specializations contained within the boutons were found to exhibit a range of sizes and morphologies, including the presence of perforated contacts. These ultrastuctural features were interpreted as playing an important role in the shaping and generation of a presynaptic action potential, and subsequently to synaptic transmission at afferent connections in Clarke's column.

An Ultrastructural Sonnet

In sombre beauty in her room she broods.
'Tis night - and all her pumps are deathly still
And thus she slumbers peacefully until
The morn, when unkind amperes end this interlude.

With steady beat, her motors wheeze and keen,
Industrious vapours drain the inner core
That Bohr's electrons shortly will explore
In headlong torrent downwards to her screen.

What truths does she uncover with her beam?
How much is artefact produced by man,
And how much really fits into the plan
Of nature? That believed is easily seen!

But even as she may promote confusion,
It is at least an elegant illusion.

N.D. Yeomans

TABLE OF CONTENTS

CHAPTER ONE

BACKGROUND AND LITERATURE REVIEW

CHAPTER ONE: BACKGROUND AND LITERATURE REVIEW

1.1 Clarke's Column.

In 1851, Clarke first described a major nucleus which he called the posterior vesicular columns, lying dorsolateral to the central canal and extending the full length of the spinal cord in dogs, pigs, calves, sheep, rabbits, cats, guinea pigs, frogs and man (Clarke, 1851). He later modified his earlier finding to note that this nucleus dorsalis, or Clarke's column, extends only from lower thoracic to mid-lumbar segments of the spinal cord (Clarke, 1859).

Figure 1.1 shows a cross section of the spinal cord prepared by Ramon y Cajal (1909), which clearly shows Clarke's column lying dorsolateral to the central canal.

In his cytoarchitectonic atlas of the cat spinal cord, Rexed (1954) suggested that Clarke's column arises at level Th2 in the newborn, and Th3 in the adult. At the upper thoracic levels, the column consists of individual cells or small cell groups. It expands to its fullest by segments Th11-L3, and then diminishes caudally to end abruptly, always terminating rostral to L5 (Rexed, 1954; Matsushita, et al., 1979). Clarke's column extends from Th1-L4 in the dog (Petras and Cummings, 1977), and rhesus monkey (Petras, 1977), from Th1-L5 in the rat (Matsushita and Hosoya, 1979) and from C8-L3 in the primate *Galago senegalesis* (lesser bushbaby, Allbright and Haines, 1973). Clarke's column maintains a similar position in the cord throughout its extent, dorsolateral to the central canal, in a medial part of the grey matter corresponding to Rexed's lamina VII (Mann, 1973), although in thoracic segments it is more lateral, shifting dorsal and then dorsomedial as it extends caudally, and lying

FIGURE 1.1

Transverse section of the spinal cord prepared by Cajal (1909), in which Clarke's column (Colonne de Clarke) is seen lying dorsolateral to the central canal.

The neurones labelled "A" to the right of the figure are the large, complex focal cells which comprise Clarke's column.

Afferent collaterals (labelled "B") from the dorsal columns are shown terminating throughout the same region occupied by the focal cells.

(Reprinted from Cajal, 1909).

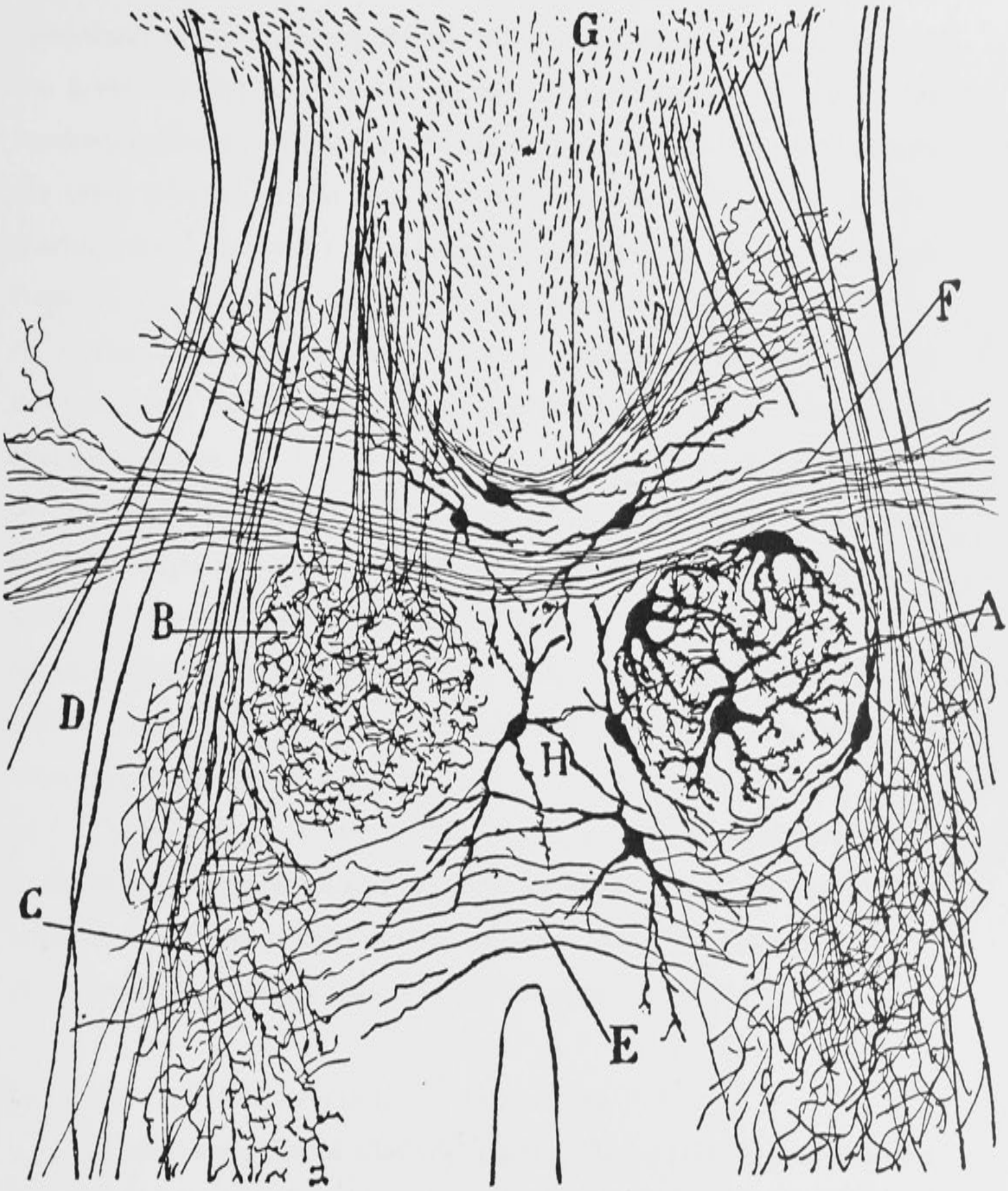
G
F
A
B
D
H
C
E

quite dorsal to the central canal in the lower thoracic/upper lumbar segments (Rexed, 1954).

In cross section, the nucleus cervicalis centralis of the cervical cord (demonstrated in the cat by Rexed, 1954) and Stilling's sacral nucleus of the lower lumbar and sacral segments (demonstrated in the spider monkey by Chang, 1951; and in the rhesus monkey by Petras, 1977) occupy the same position in the cord as Clarke's column. Both have cellular morphologies similar to that observed in Clarke's column, although these are distinct nuclei, and are not continuous with Clarke's column.

The structure of Clarke's column has traditionally been described by the following four distinctive characteristics: 1) a "close" nature, with sharp restriction of the cells to the nuclear confines, 2) longitudinal orientation of the cells and dendrites within the column, 3) a dorsal funicular origin of collaterals to the column, 4) the axons of the main cells travel to the dorsolateral fascisulus (DLF), giving rise to the dorsal spinocerebellar tract (DSCT) (Rethelyi, 1968). Each of these characteristics will be examined in greater detail, as each has bearing on the aims and objectives of the present study.

The material presented in this chapter includes that published prior to the onset of the present study, that is, up to and including 1984. Studies which have been published during the execution of the present study are discussed in the relevant experimental chapters.

1.2 Morphological Cell types in Clarke's column.

In his description of Clarke's column, Clarke (1859) noted that the constituent cells were characteristically large, of oval, pyriform, stellate or fusiform shape, with longitudinal dendritic processes extending quite some distance, intermingling with the processes of other large cells and of small cells within the column, and occasionally leaving the boundaries of

the column. Lenhossek (1895, in Loewy, 1970) described two cell types within the column, the focal and marginal cells, whose existence was confirmed by Cajal (1909; see Figure 1.1).

Using Golgi techniques in the kitten, Rethelyi (1968) re-examined the cytoarchitecture of Clarke's column, recognizing both the main (or focal) cells, and the marginal cells, which he described as local interneurones. The main cells clearly corresponded to the focal cells described by Lenhossek (1895, in Loewy, 1970) and Cajal (1909), with large spherical or elliptical cell bodies. Their dendrites extended 400-500 μm in the rostrocaudal direction, but only 70-80 μm in the transverse plane, and were never seen to leave the column.

Boehme (1968) described the architecture of the column in 1-10 day old kittens using Golgi and Nissl staining techniques, basing the categories on cell shape and size. Three cell types were described; 1) Large bodied cells, rostrocaudally oriented, with long dendrites (500-1000 μm) confined entirely to the column, 2) smaller bodied rostrocaudally oriented cells with fewer trunk dendrites, and 3) large bodied cells whose dendrites extended up to 1500 μm in length, primarily rostrocaudally, but also extended ventrally into the intermediate nucleus. Boehme (1968) did not describe the previously reported marginal cells as a separate category.

In 1970, Loewy proposed a classification scheme for the cell types in Clarke's column of the adult cat. The classes were based on soma shape and size, and number and orientation of the dendrites observed in Golgi and Nissl stained tissue. The three cell types observed in the Golgi study were 1) Type A cells, soma diameter 10-25 μm, with 2-5 main or trunk dendrites which take a curvilinear course and have no preferred orientation, 2) Type B cells, 25-50 μm in diameter, multipolar or fusiform in shape, with 5-7 primary dendrites, and 3) Type C cells, oval to lenticular cell bodies up to 135 x 60 μm, primarily rostrocaudally oriented, with 5-13

main or trunk dendrites extending from the rostral and caudal poles. These dendrites could extend up to 1000 μm, and were seen to leave the column ventrally, laterally and dorsally. Three dendritic specializations were described for Type C cells, a) dendritic spines, (although quite rare, seen on less than 25% of the cells and restricted to the soma and proximal dendrites), b) varicosities or beading along the dendrites, and c) small branchlets, 3-90 μm in length. The axons of Type C cells take a lateral course to the DLF, where they give rise to the dorsal spinocerebellar tract (DSCT), and ascend ipsilaterally to terminate as mossy fibres in the anterior lobe of the cerebellum (Grant, 1962). The axons of type A and Type B cells could not be followed. The Type C, or DSCT, neurones have been studied extensively because of their large size and distinctive character. However, in the cat they are not the most numerous of the cell types within Clarke's column, being outnumbered 3:1 by the smallest type A cells (Loewy, 1970). In the lesser bushbaby, type B and C cells predominate in Clarke's column (Allbright and Haines, 1973).

The classification scheme proposed by Loewy (1970) appears to adequately describe the cytoarchitecture of Clarke's column, and has since been used almost exclusively to describe the column. Loewy (1970), in accordance with Boehme (1968) did not include the marginal or border cell group as Clarke's column cells, noting that most of the cells fitting this description have their cell bodies and the majority of their dendrites outside the column, and simply send a few of their dendrites into the column, as do other cells situated in the dorsal horn and intermediate nucleus.

In summary, the cell types described in Clarke's column in the cat and kitten are as folows: Type A cells are the smallest and most numerous cell type. Type B cells correspond to the smaller bodied cells described by Boehme (1968) and may account for some of the marginal cells described

by Lenhossek (1895, in Loewy, 1970), Cajal (1909) and Rethelyi (1968). Type C cells (Loewy, 1970), the DSCT cells, are the largest cell type in the column, and correspond to the two large cell types described by Boehme (1968), and the main or focal cell types decribed by Lenhossek (1895, in Loewy, 1970), Cajal (1909) and Rethelyi (1968). It has since been confirmed that the same three cellular types are found in Clarke's column of the dog (Petras and Cummings, 1977), rhesus monkey (Petras, 1977), lesser bushbaby (Allbright and Haines, 1973) and rat (Matsushita and Hosoya, 1979).

Although Golgi studies have provided much information on the cytoarchitectonic structure of Clarke's column, they are, as emphasized by Boehme (1968), at best random, providing no conclusive evidence on total numbers or types of cells in the column. Nor do they offer any information regarding the functional nature of the cells visualized. The advent of micropipettes for intracellular recording, and relatively recent advances in techniques for intracellular application of dyes and tracers such as horseradish peroxidase (HRP) have greatly increased our ability to correlate neuroanatomical and neurophysiological information (Snow et al., 1976; Jankowska et al., 1976). It is now possible for individual cells to be functionally characterized and subsequently identified histologically, thus providing a direct correlation between physiological data and morphological detail.

In 1981, Randic, Miletic and Loewy labelled DSCT neurones in Clarke's column of adult cats using intracellular injection of HRP. Cells at the L2 and L3 segments were identified as DSCT neurones by antidromic activation of the DLF at the C2 level, and classified as receiving muscle, cutaneous or convergent (cutaneous + muscle) afferent input. Randic et al. (1981) recovered 19 intracellularly labelled DSCT neurones in Clarke's column. These neurones were grouped on the basis of size, shape and

dendritic complexity, and an attempt was made to correlate these morphological groups with the three functionally based categories: muscle, cutaneous or convergent input. On this basis, Randic et al. (1981) determined that their largest cells, all of which received muscle input, were consistent with Loewy's Type C cells (Loewy, 1970), with cell bodies up to 40 x 140 μm, and 5-7 trunk dendrites extending up to 1250 μm rostrocaudally (see Figure 1.2B). They noted that the dendrites were smooth, with relatively few branch points. In the cases where the axon was stained, no collaterals were observed. Thirteen of the nineteen neurones recovered histologically received muscle input. However, this, was regarded as sampling bias due to the larger size of the cell bodies of these neurones. Randic et al. (1981) suggested that the DSCT neurones which received convergent input had smaller cell bodies (up to 50 x 75 μm, see Fig. 1.2C), although their orientation, dendritic branching patterns and axonal trajectory were very similar to that seen for cells receiving muscle input. They showed that most of the cells receiving purely cutaneous input at L3 were located outside Clarke's column, although they recorded two cells which received purely cutaneous input within Clarke's column. These two cells were not morphologically similar, and one was believed to be a type B cell.

Houchin et al. (1983) subsequently labelled cells in Clarke's column of the adult cat, identified as DSCT neurones through antidromic activation of the DLF at C2, which received input from the sciatic nerve. Subsequent histological recovery of the cells showed them to be extremely morphologically complex, and very similar in their appearance. Cell bodies were 70-100 x 30-70 μm, with long dendritic trees extending up to 3200 μm in the rostrocaudal plane (see Figure 1.2A). In the transverse plane, the dendritic spread was much more closely restricted, with most branches confined to the column, and only a few extending beyond. These

FIGURE 1.2

A. Reconstructions in the sagittal plane of HRP labelled DSCT neurones which received group I afferent input following stimulation of the sciatic nerve, showing large cell bodies, and complex, profusely branched dendritic trees.
(Reprinted from Houchin et al., 1983).

B. Reconstructions in the sagittal plane of HRP labelled DSCT neurones which received identified group I muscle afferent input.
(Reprinted from Randic et al., 1981).

C. Reconstructions in the sagittal plane of HRP labelled DSCT neurones which received convergent (muscle + cutaneous) input.
(Reprinted from Randic et al., 1981).

The reconstructions in A, B and C have all been printed to exactly the same magnification.

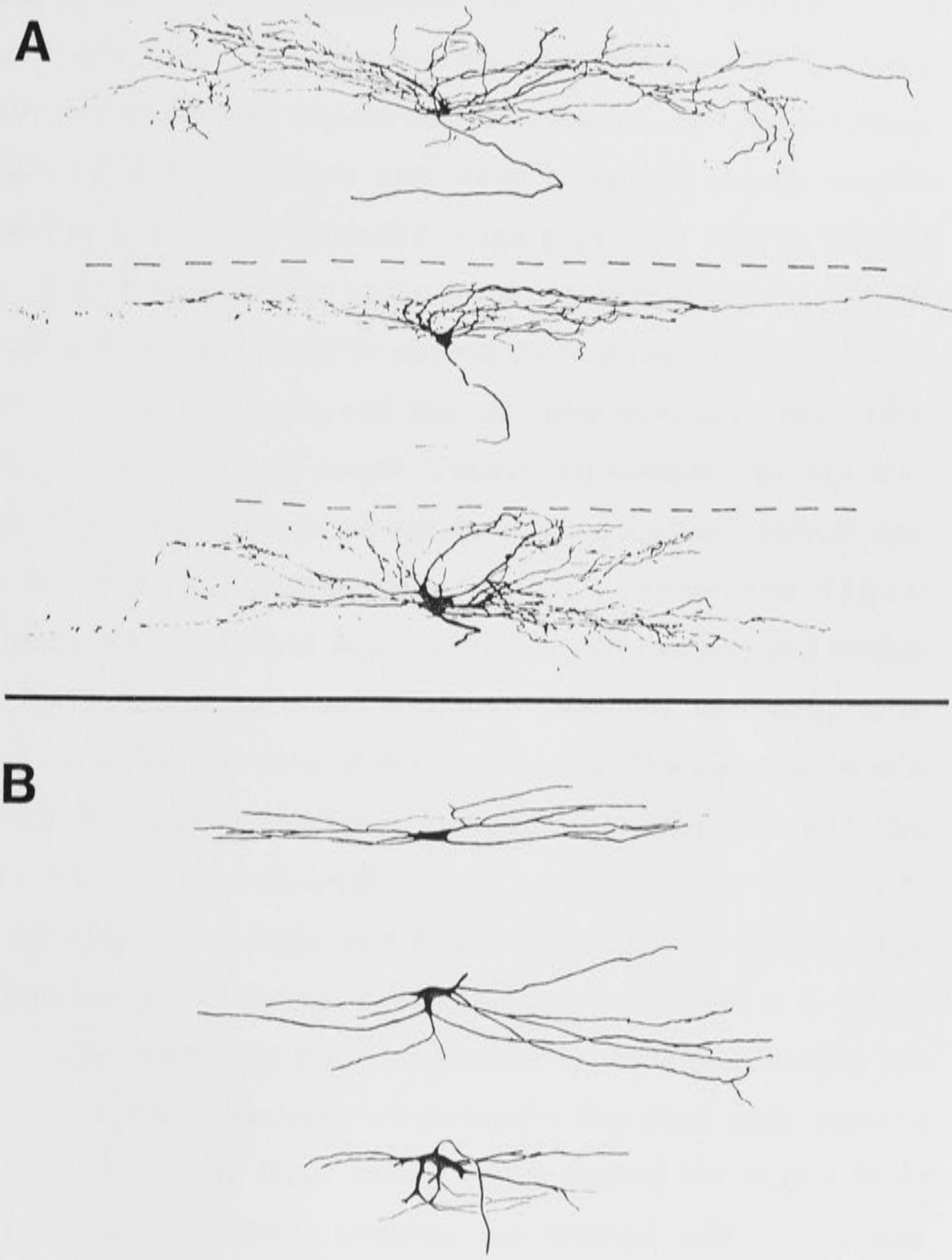
A
B
C
100 μm

cells exhibited 5-9 primary dendrites, all of which branched profusely and were of extremely complex appearance. Houchin et al., (1983) also noted the same three dendritic specializations described by Loewy (1970); spines, branchlets and varicosites. The varicosities were subsequently examined under the electron microscope, and found to contain grossly swollen mitochondria, and signs of internal damage, suggesting that the beading may be in part artefact. The computer aided reconstruction methods employed by Houchin et al. (1983) allowed the HRP labelled DSCT cells to be observed from any angle, and also provided statistical information about the dendrites such as length, volume and surface area. The total length of dendrites of any one cell was found to be approximately 35 mm, slightly shorter than the total dendritic length of a motoneurone (Ulfhake and Kellerth, 1981; Egger and Egger, 1982). The total volume and surface area of DSCT neurone dendrites were also measured, and found to be large, but not as large as those of the motoneurone. The axons of the cells were well stained and were followed to the DLF (Houchin et al., 1983). No recurrent collaterals were observed.

Figure 1.2 shows large type C cells from Clarke's column taken from the studies of A) Houchin et al. (1983), B and C) Randic et al. (1981). In view of the conflicting results presented in these two studies, the morphology of DSCT neurones which receive identified input remains inconclusive. In light of Golgi studies which showed the large cells of Clarke's column to exhibit complex morphology with extensively branched dendritic trees, the anatomical simplicity of the neurones presented by Randic et al. (1981) (see Figure 1.2B and C) seemed quite surprising. Their reconstructions illustrated far less morphological complexity than those observed by (for instance) Boehme (1968) and Loewy (1970). The subsequent finding by Houchin et al. (1983) that the DSCT neurones in Clarke's column were in fact extremely

morphologically complex with profusely branched dendritic trees (Figure 1.2A), led them to suggest that the HRP labelling achieved by Randic et al. (1981) had not been entirely succesful, and that the cells were not completely filled.

In summary, the morphology of functionally identified DSCT cells in Clarke's column has not been properly resolved. Golgi studies provide a limited picture of morphological detail, and provide no functional information. Randic et al. (1981) intracellularly labelled DSCT neurones which received identified input, but more recent evidence suggests that the morphological details presented by them were not complete. This means, therefore, that their proposal that the morphological characteristics of DSCT neurones might indicate their function, and vice versa, is not conclusive. Houchin et al. (1983) have presented convincing evidence for the morphological complexity of DSCT neurones in Clarke's column, but their functional identification of the cells was limited. Clearly, more evidence is required on these issues concerning the morphology and location of DSCT neurones which receive identified muscle, cutaneous and convergent inputs from the hindlimb of the cat.

The following section explores the origin, pathway and termination of the DSCT, and examines the relationship between the tract and the cells of Clarke's column.

1.3 The Dorsal Spinocerebellar Tract

i) Cells of Origin of the DSCT

In 1876, Flechsig first described the connection between the nucleus dorsalis (Clarke's column) and a myelinated fibre tract running in the dorsolateral column which terminated in the cerebellum, the dorsal spinocerebellar tract (DSCT; in Petras and Cummings, 1977). Van Gehuchten found after lesion of the DSCT that only the largest Clarke's

column cells showed signs of degeneration (in Petras and Cummings, 1977). Subsequent studies in which the DSCT was transected confirmed this finding (see e.g. Sherrington and Laslett, 1903; Liu, 1956). Grant (1962) showed that lesion of the spinal cord caudal to Clarke's column produced no degeneration in the cerebellum, thus concluding that Clarke's column was the site of origin of the tract. Until quite recently, there was general agreement that the largest Clarke's column neurones were the sole cells of origin of the DSCT (see Oscarsson, 1965,1973; Mann, 1973; Burke and Rudomin, 1977 for reviews). This presumption has been challenged in two different ways:

1) Petras and Cummings (1977) studying cerebellar projections from the spinal cord in the dog, used retrograde HRP labelling and degeneration techniques to show that in fact both the large and the medium sized Clarke's column neurones (Types B and C of Loewy, 1970) projected to the cerebellum. The axons of both types were shown to take a similar or identical course, and almost all their projections were ipsilateral. Snyder et al. (1978) in a retrograde labelling study of spinocerebellar neurones in cat, rat and squirrel monkey found labelled small, medium and large cells which projected ipsilaterally to the cerebellum, and suggested that the size of the cell bodies in Clarke's column is not sufficient to indicate whether or not they project to the cerebellum. Matsushita, Hosoya and Ikeda (1979) conducted a similar experiment, injecting HRP into the cerebellum of the cat and following its retrograde transport to the cells of the spinal cord. They concurred with Petras and Cummings (1977) that both large and medium sized Clarke's column neurones were cerebellar projecting. Matsushita et al. (1979) also observed some labelling of oval cells on the circumference of Clarke's column which they considered to be the marginal or border cells described by Rethelyi (1968). (As noted previously, Loewy (1970) suggested that the majority of marginal cells are

in fact located outside the boundary of Clarke's column, and that oval cells within the boundary of Clarke's column may be medium sized (type B) neurones. This suggestion received support from an observation by Saito (1979), that within Clarke's column, the large and medium neurones which label retrogradely on cerebellar injection of HRP are located both centrally and marginally). In accordance with Snyder et al. (1978), Matsushita et al. (1979) observed occasional labelling of small (type A) cells. Thus it appears that cells other than the largest cells may contribute to the DSCT.

2) In a study of supraspinal control of the DSCT, Hongo, Okada and Sato (1967) recorded from DSCT units which received cutaneous and high threshhold muscle afferent input. These cells were situated at spinal segments L4-L6. Although this spinal level was considered caudal to the extent of Clarke's column, these cells were identified as DSCT neurones on the basis of antidromic activation from the ipsilateral anterior lobe of the cerebellum. This suggests that cells of origin of the DSCT which receive cutaneous and high threshold muscle input may lie outside Clarke's column.

Prior to this study, suggestions that the cells of origin of the cutaneous component of the DSCT lay caudal or lateral to Clarke's column had been explained by assigning extra-Clarke's column cell types to ascending tracts other than the DSCT, such as the spino-olivary or spinocervical tracts (Grundfest and Carter, 1954). In 1959, Lundberg and Oscarsson, recording DSCT axons at cervical levels, suggested that all units which received muscle inputs were located in Clarke's column, but that some units receiving group II and group III muscle input or cutaneous input from receptors with large receptive fields could be located caudal to Clarke's column. Units receiving input from cutaneous receptors with restricted fields (such as hair follicle afferents) had their cell bodies caudal to

Clarke's column, and were not included as DSCT units due to lack of activation on cerebellar stimulation. Oscarsson (1965) concluded that the DSCT units receiving cutaneous input were not necessarily located caudal to Clarke's column, but that there was no proof of their location within the column, although the course and termination of their axons appeared to be as for proprioceptive units.

Mann (1971) subsequently sampled a small group of neurones in laminae III-VI in segments L6-S1, and was unable to record any units driven by cerebellar stimulation. Kuno, Munoz-Martinez and Randic (1973a,b) were able to record from cells in Clarke's column at L2 and L3 which received input from cutaneous receptors. However, they also recorded from units which they classified as DSCT, receiving joint or cutaneous input, whose cell bodies lay lateral to the boundary of Clarke's column. Aoyama, Hongo and Kudo (1973) physiologically demonstrated a group of cells whose properties resembled DSCT units situated in segments L5 and L6 in a location resembling, but caudal to, Clarke's column. These cells were monosynaptically activated by both group Ia and Ib muscle input, and their axons ascended ipsilaterally in the DLF. The primary differences between these units and DSCT neurones in Clarke's column included the predominance of extensor muscle input and extensive convergence. Identification of cells recorded at segments L5 and L6 was based on antidromic activation of the DLF at C1, thus projection to the cerebellum was not unequivocally established (Aoyama et al., 1973). Activation of the DLF at C1 is an adequate means of identification for DSCT axons whose somata are subsequently determined to be located in Clarke's column. However, as Oscarsson (1965) pointed out, three other ascending tracts occupy regions of the DLF (Lundberg and Oscarsson, 1961), and therefore rigorous identification is required if a unit is to be included as DSCT without subsequent histological localization to Clarke's

column. Nevertheless, Aoyama et al. (1973) believed that their data represented evidence of an uncrossed spinocerebellar tract with cells of origin caudal to Clarke's column. It was not determined whether the cells in L5 and L6 represented a new subgroup of the DSCT or an alternative spinocerebellar pathway.

Tapper, Mann, Brown and Cogdell (1975) recorded the response of cells in spinal segments L4-L6, (caudal to Clarke's column) in laminae IV and V in response to stimulation of cutaneous nerves of the hindlimb of the cat. All units were tested for cerebellar projection. The location of the neurones, and the extent of convergent input which they received, suggested that they were the same cell group recorded previously by Aoyama et al. (1973), who had tested their projection only as far as the C1 level. Tapper et al. (1975) found no difference in axonal trajectory or receptive field characteristics between the cells they recorded within, or caudal to Clarke's column, suggesting that the only reason these cells had not previously been identified was the prior assumption that all cells of origin of the DSCT were located within Clarke's column. Tapper et al. (1975) concluded that the definition of the dorsal spinocerebellar tract should be based on axonal pathway and site of termination, and thus expanded to include these cells situated caudal to Clarke's column.

Randic, Myslinski and Gordon (1976) examined mid-lumbar segments for evidence of DSCT cell bodies outside Clarke's column. They recorded from neurones in the dorsal horn at L3 and L4, which responded to hair movement. These neurones had ipsilaterally ascending axons, and some were identified as DSCT after activation from the cerebellum, while some were assigned to the spinocervical tract. They concluded that all DSCT neurones receiving muscle inputs, or cutaneous input from the foot, were located in Clarke's column, but that those with receptive fields on the proximal leg could be located outside Clarke's column in laminae

IV-VI, and that some of the cells included in this group were not DSCT, but spinocervical tract cells.

The proposal by Tapper et al. (1975) that the definition of the DSCT should be expanded to include the cells outside Clarke's column which appeared to contribute to the tract, was subsequently contradicted by the suggestions of Matsushita et al. (1979). From a study of cerebellar projecting spinal cord neurones in the cat, Matsushita et al. (1979) concluded that the term dorsal spinocerebellar tract was no longer appropriate, and proposed its replacement with three alternate terms, each of which represented an individual fibre tract. These were: 1) the Clarke's column-Spinocerebellar tract, comprising large and medium sized neurones in Clarke's column from upper thoracic to mid-lumbar segments, 2) the lamina V-Spinocerebellar tract from lower cervical to lumbar segments, and 3) the medial lamina VI-Spinocerebellar tract in the lumbar cord. A study by Matsushita and Hosoya (1979) suggested that the ascending spinocerebellar neurones in the rat were similarly organized, with cell bodies traced to Clarke's column, lamina V of segments L1-L3 and a group in the L6-caudal segments which appeared to lie within Stilling's sacral nucleus. This same sacral nucleus had been described in the spider monkey by Chang (1951) and more recently in the rhesus monkey by Petras (1977), who concluded that the neurones of this sacral nucleus were cytologically and topographically similar to those of Clarke's column, and therefore consistent with Stilling's proposed continuation of Clarke's column. In contrast, Snyder, Faull and Mehler (1978) comparing spinocerebellar projecting neurones of the cat, rat and squirrel monkey, found large multipolar neurones in the caudal and sacral segments in the rat and monkey, which they concluded were similar in position and orientation to Clarke's column, but not in projection or cytoarchitecture. Despite this, they considered these cells to

be those described as Stilling's sacral nucleus and concluded that the posterior vesicular columns described by Clarke (1851) constituted the central cervical nucleus, Clarke's column and Stilling's sacral nucleus described in continuity. Apart from heavy labelling of Clarke's column neurones in all three animals, Snyder et al. (1978) also observed labelling in cells immediately caudal, rostral and lateral to Clarke's column, which had similar cytology and axonal projection to DSCT neurones, but could not determine whether these were displaced Clarke's column neurones or a distinct cell group.

Randic et al. (1981) recorded from DSCT units in L3 and L4 which received input from hairy skin mechanoreceptors. Some of these units were located outside the boundary of Clarke's column. A similar location for such neurones was determined by Grant et al. (1982) in the kitten, who also observed ipsilaterally projecting spinocerebellar cells caudal to Clarke's column.

The location of functionally identified DSCT neurones remains unclear. As a general guide, the DSCT is probably best described as originating from the large and medium cells of Clarke's column, with possible contributions from lamina V neurones in the cervical to lumbar cord, and medial laminae V-VII neurones in segments L5 and L6. Even so, reports regarding the location of DSCT cells receiving cutaneous and convergent inputs are largely conflicting (Mann, 1971; Kuno et al., 1973a,b; Aoyama et al. 1973; Tapper et al., 1975).

ii) Pathway of the DSCT.

The axons of Clarke's column neurones, which constitute the main body of the dorsal spinocerebellar tract, leave the column and travel laterally to the DLF, in which they ascend as an uncrossed tract, terminating in the ipsilateral anterior lobe of the cerebellum. Rethelyi

(1968) suggested that the axons of the DSCT cells may have recurrent collaterals which contacted other cells within Clarke's column. However, in more recent intracellular labelling studies no such collaterals have been observed (Randic et al., 1981; Houchin et al., 1983).

Yoss (1952) determined that in macaque monkeys, the DSCT axons are located deep in the DLF at their most caudal extent, and shift dorsally and peripherally as they ascend. This represents a simple stratification pattern, with the longest fibres found at the periphery and the shortest more medial. This same stratification has been described for the cat (Pass, 1933; Grant, 1962), with the longest fibres most dorsal at cervical levels. This shift indicates that at more rostral segments, fibres are recruited to the ventromedial aspect of the tract, which suggests that the DLF may be topographically (or perhaps segmentotopically) organised. Yamomoto and Miyajima (1959) proposed a medial to lateral arrangement of fibres from cranial to caudal. Yamomoto and Miyajima (1959) may, however, have been recording in a separate tract from the DSCT, as this finding is inconsistent with earlier findings of dorsal and peripheral shift at rostral segments (Yoss, 1952; Grant, 1962). Kitai and Morin (1962) saw no evidence of somatotopic organization of the DSCT fibres at C2 based on sensory modality, although Lundberg and Oscarsson had demonstrated a somatotopic arrangement of the DLF fibres at upper lumbar and lower thoracic levels (Lundberg and Oscarsson, 1961). Oscarsson (1965) noted that neither Yamomoto and Miyajima (1959) nor Kitai and Morin (1962) identified the fibres from which they recorded as belonging to the DSCT, and that since three other ascending tracts occupy this region (Lundberg and Oscarsson, 1961), they may well have been recording responses from other pathways.

Mann (1971) found that the DLF was quite inhomogeneous, with DSCT axons found throughout, except in the most dorsomedial region,

which is occupied by the spinocervical tract. Mann (1971) showed a tendency for the fibres mediating cutaneous information to be located more lateral and those mediating muscle information to be more medial, but that there was considerable overlap. Within sensory modalities, DSCT units receiving muscle, or muscle + cutaneous input were not shown to be somatotopically organized. Units receiving cutaneous input from receptive fields on the foot were recorded throughout the DLF, those with input from receptors on the lateral or medial leg were found in the lateral DLF and those with input from receptive fields on the trunk were found more medial.

Hongo, Okada and Sato (1967) suggested that since somata of DSCT cells receiving muscle input from foot and calf were located more caudally, their axons should be found more dorsolateral than those of cells receiving input from thigh muscles. This, however, was not found (Mann, 1971). Since the cell bodies of the cutaneous component of the DSCT were suggested to be located more caudal than those which received muscle input, it was also suggested that muscle input cells would join the tract at more rostral (and thus more ventromedial) aspects of the tract, resulting in a more peripheral location of the axons mediating cutaneous information. This, again, was not found to be the case (Mann, 1971).

Thus, although there is a tendency for DSCT fibres to shift dorsal and lateral as they ascend, strict somatotopic arrangement of the fibres based on sensory modality, or on receptor type, is not found, with considerable intermingling of the DSCT and non-DSCT fibres within the DLF.

Grant (1962) found the majority of the DSCT fibres to be quite large, a finding expected due to the size of the contributing cell bodies. Van Beusekom (1955) concluded that 7,000-10,000 fibres constitute the DSCT, with 2% > 15 μm in diameter, 56% > 3um, and 17% < 1.5 μm, but Mann

(1973) pointed out that van Beusekom sampled a region of the DLF, which is inhomogenous, with DSCT and non-DSCT axons intermingled. Mann (1973) suggested that the DSCT fibres were all > 3 μm in diameter.

iii) Termination of the DSCT.

DSCT fibres reach the cerebellum directly, without synaptic interruption, but have been suggested to send collaterals to three other sites. Cajal (1909) suggested that the lateral cervical nucleus might receive input from DSCT collaterals. This was re-examined by Morin (1955) who implicated the DSCT as a mediator of cutaneous information in a spinothalamic pathway via collaterals to the lateral cervical nucleus. However, this connection was denied by Brodal and Rexed (1953), and it is now known that input to the lateral cervical nucleus comes largely from the spinocervical tract. A possible cutaneous pathway via DSCT collaterals to the inferior olivary nucleus was ruled out by Grundfest and Carter (1954). Low et al. (1986) concluded that 92% of the afferent input to nucleus Z is via DSCT collaterals, as a medullary relay for proprioceptive information from the hindlimb to the sensory cortex. It thus appears that nucleus Z is the only non-cerebellar recipient of DSCT input.

It is generally well agreed that on entering the cerebellum, DSCT axons course through the white matter, sending collaterals to the folia and becoming narrower before terminating as mossy fibres on the granule cells (Brodal and Grant, 1962). Grundfest and Campbell (1942) recorded responses to stimulation of the DSCT in the rostral vermis in the cat, with some response in the declive and pyramids, but none in the cerebellar hemispheres. Occasionally, inputs to the contralateral lobulis centralis and folia of the culmen were recorded.

Yoss (1952) used degeneration techniques to determine a similar result in the monkey, with most fibres terminating in the anterior lobe of

the ipsilateral vermis, with some termination in the pyramids, declive and uvula. He found no somatotopy to these terminations.

Morin, Lindner and Catalano (1957) found a direct connection to the paramedian lobule of the posterior lobe for DSCT fibres mediating tactile input.

Grant (1962) studied degenerating terminals of DSCT fibres in cerebellar cortex after lesion of the tract in the cat. Lesion of the cord caudal to Clarke's column caused no degeneration in the cerebellum, leading to the conclusion that the cells of origin of the DSCT were situated only in Clarke's column. Grant (1962) found that section of the DSCT rostral to L3 always produced the same result, degeneration in the anterior lobe (lobules I-V of Larsell , 1953), in lobule VI, VIIB, VIII, and IX, the paramedian lobule and parafloccus, with almost the entire projection confined to the ipsilateral side. Since these areas are representative of the trunk and hindlimb, it was expected that some degree of somatotopic organization of the terminations would eventually be found.

Grant (1962) reported that lesion of the DSCT did not result in any degeneration in the cerebellar nuclei. However, Matsushita and Ikeda (1970) using the same technique as Grant (1962) concurred with Szentagothai (in Matsushita and Ikeda, 1970) that there is some nuclear termination, concluding that DSCT fibres may terminate in nucleus medialis, and nucleus interpositus, primarily ipsilaterally. Matsushita and Ikeda (1970) suggested that these nuclear terminations are of collaterals whose parent DSCT axons terminate in the cerebellar cortex.

Allbright and Haines (1973) found that the majority of DSCT fibres terminate in the cortex of the vermal and paravermal functional zones of the anterior lobe of the cerebellum in the lesser bushbaby, especially in the central and culminate lobes, with some fibres terminating in the uvular and pyramidal lobules of the posterior lobe.

The termination of DSCT fibres in the cerebellar areas which are involved in control of movement in the trunk and hindlimb thus lends support to the proposed role of the DSCT in mediating information relating to posture, stance, balance and movement.

1.4 Afferent Input to the cells of Clarke's column.

The principal source of afferent input to the cells of Clarke's column is from fibres ascending in the dorsal columns (Pass, 1933; Liu, 1956; Mann, 1973), although other inputs have been described from the lateral columns (Boehme, 1968), descending fibres in the dorsal columns (Liu, 1956) and from the cortex (Hongo et al., 1967). The DSCT receives input from the hindlimb and trunk, almost exclusively from the ipsilateral side of the body (Petras and Cummings, 1977). Afferent input to the cells of Clarke's column has been investigated in great detail using physiological, and to a lesser extent anatomical methods.

i) Physiological Studies of Afferent Inputs to Clarke's column.

Prior to 1958, when the first intracellular recordings from cell bodies in Clarke's column were made (Curtis et al., 1958), the input to Clarke's column neurones had been studied almost exclusively through examining mass discharge or single unit responses in the tract axons running in the DLF at the cervical and upper thoracic levels.

Grundfest and Campbell (1942) recorded responses from the DSCT axons in the DLF on stimulation of tibial, peroneal and saphenous nerves, concluding that the tract received input from the muscles of the hindlimb, but that the response was mediated by a chain of interneurones.

Lloyd and McIntyre (1950) reinvestigated the latency of the responses. They found that the DSCT responded only to group I muscle

input, and that since the conduction velocity through the pathway averaged 109 m/sec, saw no reason to assume interneurones in the connection, claiming instead that DSCT neurones received monosynaptic excitatory input from the hindlimb muscles, and conveyed stretch evoked activity to the cerebellum. They also observed that while motoneurones required considerable summation of afferent input to fire, DSCT units could respond to a single input with transmission approaching 1-1, and that the DSCT therefore acted solely as a relay pathway, with no integrative function.

Lundberg's group carried out an extensive series of experiments to determine the nature of information relayed in the tract. Laporte et al. (1956a) recorded the mass discharge response in the DSCT on stimulation of both skin and muscle nerves of the hindlimb of the cat, and found the conduction velocity of each fibre type to average 100-110 m/sec. Grundfest and Carter (1954) had previously dismissed the DSCT as a mediator of cutaneous information, with the assertion that units relaying the cutaneous impulses had their cell bodies caudal to Clarke's column. Using single unit recording techniques, Laporte et al. (1956b) again demonstrated DSCT units in the DLF which received cutaneous or muscle inputs. They also demonstrated convergent excitation from more than one muscle onto one DSCT cell, excitation and inhibition from more than one muscle, and, occasionally, convergent excitation from the skin and muscle nerves onto one cell.

On the basis of their own, and earlier studies, Laporte et al., (1956b) divided the recorded units into two subgroups. They defined the classic Flechsig's tract as the true DSCT, receiving group I muscle inputs and making direct connection with the anterior vermis of the cerebellum. The second subgroup received input from group II and III muscle afferents and skin afferents, and represented an entirely different pathway, with

cells of origin outside Clarke's column, and a high probability of receiving input from more than one receptor type. Thus the DSCT was considered to be a purely proprioceptive pathway. Laporte et al. (1956b) found, in accordance with Lloyd and McIntyre (1950) that DSCT cells did not require the extent of summation required by the motoneurones to cause them to fire. Laporte and Lundberg (1956) studied the response of DSCT neurones to stimulation of stretch receptors in hindlimb muscles, demonstrating the excitatory action of muscle spindle afferents (group Ia) to these neurones. They concurrently tested discharges in other units of Flechsig's fasciculus, recording units responsive to light touch, pressure or bending of joints, or pressure on foot pads, which they attributed to an alternate spinocerebellar pathway. Lloyd and McIntyre (1950) reported volleys from both Ia and Ib muscle afferents in Clarke's column. Laporte and Lundberg (1956) clearly demonstrated the existence of the group Ia responses in DSCT units, but noted that the group I response in the DLF consisted of two components. Subsequently, Lundberg and Oscarsson (1956) studied the involvement of group Ib inputs to the DSCT. After determination that Ib fibres arrived at the correct spinal levels to contact Clarke's column DSCT neurones, and that the mass discharge recorded in the DLF increased on recruitment of the Ib fibre input, Lundberg and Oscarsson (1956) proposed that the DSCT consisted of two functional subgroups, the first receiving group Ia (muscle spindle primary afferent) and the second Ib (Golgi tendon organ) input. However, they then made the seemingly contradictory observation that both Ia and Ib afferents most probably converge on the same cell, in which case such a division would seem unwarranted.

Oscarsson (1957) determined that the course taken by Ia and Ib afferents to contact DSCT neurones was not identical. He found that as Ia and Ib afferents ascend in the dorsal columns, the Ib afferents drop

collaterals to the grey matter at a more caudal level than the Ia afferents from the same dorsal root. These Ib collaterals then ascend in Clarke's column for some distance before contacting DSCT neurones at the same spinal level as the Ia collaterals, which drop to the grey matter in a perpendicular manner at more rostral levels, contacting DSCT neurones almost immediately. Oscarsson (1957) also determined that despite earlier suggestions of Ia and Ib convergence onto the same DSCT neurone (Lundberg and Oscarsson, 1956), most units received either group Ia or Ib inputs. Oscarsson (1957) made the concurrent finding that group Ia and group II muscle spindle afferents took a similar topographic course to contact DSCT cells. This was of interest, as Laporte et al., (1956b) had determined that the group II muscle responses recorded in the DLF were attributable to pathways other than the DSCT.

In 1959, Lundberg and Oscarsson recorded from DSCT axons in the DLF identified by antidromic activation from the cerebellum and a lack of direct stimulation from the spinal cord caudal to L5. They defined three groups of DSCT axons: 1) units monosynaptically activated by impulses in muscle spindle afferents (group Ia and group II), 2) units activated monosynaptically by group Ib muscle inputs, and 3) a group activated by inputs from group II and group III muscle receptors and skin or joint receptors. All three types were regarded as DSCT axons, although not all the axons responding to the third group of afferent inputs were included as DSCT, as some had their cell bodies caudal to Clarke's column and were considered to constitute another pathway. A group of units activated caudal to L5 which received low threshhold cutaneous inputs from receptors with restricted receptive fields, were also regarded as non-DSCT.

Yamomoto and Miyajima (1959) studied responses of the spinocerebellar (including DSCT) axons at C2, recording units responsive to touch, pressure or deep receptors. They found that the number of units

responsive to exteroceptive impulses approximately equalled the number of proprioceptive units, and that hindlimb responses were twice as frequently observed as forelimb. This suggested to Yamomoto and Miyajima (1959) that the DSCT, classically considered a proprioceptive pathway, was in fact functionally non-specific, with the implication that the cerebellum was more complex than previously thought. However, as noted above, many of the units probably belong to the SCT rather than the DSCT.

Of the DSCT units recorded by Kitai and Morin (1962), 53% responded to touch, 31% to pressure, 2% to touch and pressure, and 14% to joint input. They found tactile responses more numerous for the forelimb, and pressure from the hindlimb. Joint units responded to one joint only, and adjusted their firing frequency to the rate and degree of displacement. Fields of touch and pressure receptors varied from very small to quite large, with large fields suggesting a high degree of convergence. Unfortunately, Kitai and Morin did not identify the fibres from which they recorded as belonging to the DSCT, therefore these results cannot be considered conclusive.

Jansen and Rudjord (1965) concluded from the response pattern of DSCT fibres to muscle stretch that the cerebellum receives information about the mechanical situation in the muscle from three receptor types. Group Ia receptors provide a mixed signal about the muscle length and speed of stretch, group II receptors provide information about muscle length, and group Ib on the degree of muscle contraction.

Cutaneous inputs to the cerebellum were reinvestigated by Mann and Tapper (1970) who recorded from axons in the DLF identified as DSCT by antidromic activation from the cerebellum. Four classes of neurones with cutaneous input were identified: 1) those activated by rapidly adapting receptor (such as hair) and slowly adapting Type I (SAI)

receptors, 2) those activated only by SA receptors, 3) those activated only by rapidly adapting receptors, and 4) those activated by both cutaneous and muscle receptors. They showed that DSCT neurones receive extensive convergent input, but that a single presynaptic impulse could trigger a post synaptic response. Mann (1971) subsequently found that, of units recorded in the DLF (identified as DSCT by activation from the cerebellum), 53% responded to deep or muscle input (of which many responded to more than one, and up to four muscle groups), 19% to cutaneous inputs, and 8% to convergent cutaneous + deep inputs. Both Yamomoto and Miyajima (1959) and Kitai and Morin (1962) had shown that more than half the recorded DSCT units responded to cutaneous impulses. However, the fibres were not conclusively identified as DSCT tract axons in either of the latter studies. Of the cutaneous units recorded by Mann (1971), 30% responded to hair follicle afferent inputs, and were rapidly adapting, 15% responded to slowly adapting units with large receptive fields, and 54% responded to both slowly adapting and hair afferent input. From these findings, Mann proposed that up to 37 afferents might converge on one DSCT neurone. Thus both 'unimodal' and 'multimodal' units comprise the cutaneous as well as the muscle components of the DSCT.

Although cutaneous units of the DSCT had been confirmed, Kuno et al. (1973a,b) reexamined sensory inputs to the DSCT neurones on the basis that the role of the DSCT as a relay for cutaneous information was tenuous. Cutaneous volleys from the hind limb of the cat were found to activate cerebellar mossy fibres and the DSCT was proposed as the pathway for transmission of this information. However, limited numbers of DSCT neurones in Clarke's column had been found to be activated in response to cutaneous volleys. It was proposed that either 1) the number of DSCT neurones in Clarke's column relaying cutaneous information

may be much smaller than the numbers relaying muscle impulses, or that 2) cells of origin of the cutaneous component of the DSCT may reside outside Clarke's column. Kuno et al., (1973a,b) recorded intra and extracellularly from cells in the region of Clarke's column which responded to antidromic activation from the cerebellum, and demonstrated transmission of four separate types of input through the DSCT; those responding to muscle input, cutaneous input, joint input, or receiving convergent input from more than one receptor type, with no difference in conduction velocity recorded between axons of different unit types. (This suggests that axonal size, and therefore soma size, are similar between unit types, and that sampling bias will not have been introduced by ease of microelectrode penetration of one or other type of unit). Kuno et al. (1973a) found that most units (up to 65% of the total population studied) received muscle input. Cells receiving cutaneous input represented up to 25%, with the joint and convergent cell types up to 15 % and 20% respectively. All neurones receiving muscle and cutaneous inputs were found to be located within Clarke's column, although some convergent and one joint input cell were located lateral to Clarke's column, and it was not clear whether these cells were of the DSCT or an alternate pathway.

Petras and Cummings (1977) concluded that the DSCT receives group Ia, Ib and cutaneous inputs, with the proprioceptive information arising from single muscles or synergistic muscles at a common joint, and that therefore the DSCT mediates information that is modality and space specific.

It is therefore well established that the DSCT neurones in Clarke's column receive monosynaptic excitatory input from group I, II and III muscle receptors, joint receptors and a variety of cutaneous receptors in the hindlimb. However, questions regarding the proportion of DSCT

units receiving information from various sensory receptors, and the degree to which afferents converge on DSCT cells remains uncertain.

ii) Presynaptic Modulation of afferent input.

In a study of the synaptic action of muscle afferent input to DSCT cells, Eccles, Schmidt and Willis (1963) noted inhibition of the discharge, which could last 100 msec or more, and which they believed to be presynaptic in origin. Jankowska, Jukes and Lund (1964) subsequently showed pharmacologically that this inhibition was similar to the presynaptic inhibition demonstrated at the monosynaptic connection between primary muscle afferents and motoneurones. That is, the duration of the inhibition was prolonged by pentobarbitone and further prolonged by strychnine nitrate. They suggested two possible mechanisms for this pharmacological increase in presynaptic inhibition on DSCT cells: 1) that after application of strychnine the interneurones may be more effectively activated and 2) pentobarbitone application may impede removal of the transmitter responsible for depolarization of the primary afferent.

Jankowska, Jukes and Lund (1965) examined the pattern of this proposed presynaptic inhibition, and showed that mediation of presynaptic inhibition of the DSCT neurones was equally effective from flexor or extensor muscle nerves, and also from skin afferents. Separation of the Ia and Ib volleys clearly showed a powerful inhibitory effect from Ib, skin and joint afferents, and no effect from Ia afferents of either flexor or extensor muscles. Tests of Ia terminal excitability on DSCT neurones confirmed an increase on stimulation of Ib, skin and joint afferents, and no change on stimulation of Ia afferents. However, excitability was increased in both Ia and Ib terminals by conditioning volleys in skin and high threshold muscle afferents. Thus, the terminals of Ia and Ib

collaterals contacting DSCT cells were found to be subject to presynaptic inhibition from conditioning volleys in Ib, skin, joint and high threshold (Group II and III) muscle afferents, but not Ia afferents.

In an ultrastructural study, Gray (1962) observed an axo-axonic arrangement which he proposed as the morphological basis of presynaptic inhibition in the central nervous system Subsequently, terminals have been observed in Clarke's column presynaptic to the giant boutons which contact DSCT neurones (Rethelyi, 1970; Saito, 1974,1979; Houchin et al., 1983). It therefore seems likely that this arrangement also represents the morphological correlate of presynaptic inhibition of afferent input to neurones in Clarke's column. A more detailed discussion of this issue is presented in Appendix II: "Ultrastructural Evidence Related to Presynaptic Inhibition of Primary Muscle Afferents in Clarke's Column of the Cat".

iii) Anatomical Studies of Afferent Inputs to the Cells of Clarke's column.

Clarke (1859) first indicated that the column was "traversed and surrounded" by fibres from the dorsal spinal roots, and this has since been confirmed (e.g. Pass, 1933; Liu, 1956; Szentagothai and Albert, 1955; Rethelyi, 1968). Most studies have suggested that the principal inputs to Clarke's column are from the lower extremities and the trunk. Prior to the use of micropipette electrodes for intracellular staining and recording, anatomical studies of the afferent input to Clarke's column relied heavily on the use of degeneration techniques subsequent to experimentally placed lesion of the dorsal roots.

Pass (1933) showed that section of dorsal roots could cause degeneration in Clarke's column in up to 6 segments rostral to the

interruption, a finding confirmed electrophysiologically by Lloyd and McIntyre (1950).

Liu (1956) determined that Clarke's column showed extensive signs of ipsilateral degeneration in up to 8 spinal segments after section of any of the spinal roots except C1-4. Section of the coccygeal, sacral and lower lumbar roots was believed to interrupt fibres ascending in the dorsal columns, while section of roots C5-8 was believed to cause degeneration through damage to descending fibres. On section of roots T1 to L4, collaterals of both ascending and descending fibres apparently degenerated in Clarke's column. Liu (1956) found that the degeneration was greatest at the level of entry of the severed dorsal root, and diminished both rostral and caudal to that segment. Liu (1956) therefore concluded that Clarke's column received input from the tail, the hindlimbs, trunk and forelimbs, but not the head and neck, with the principal input from the trunk and hindlimbs, and a considerable degree of overlap in the terminal distributions of each dorsal root in Clarke's column.

Szentagothai and Albert (1955) utilized Nauta techniques to visualize degenerating collaterals in Clarke's column of the dog after lesion of dorsal roots. They demonstrated that collaterals enter Clarke's column, and ascend for some distance before making synaptic contact with DSCT neurones.

Grant and Rexed (1958) found that cutting of any dorsal root caudal to Th2 could lead to ipsilateral degeneration in Clarke's column of up to 7 spinal segments (i.e. less extensive degeneration than that observed by Liu, 1956, but greater than that demonstrated by Pass, 1933), and also that Clarke's column in any one spinal segment could receive input from more than one dorsal root, suggesting, in accordance with Liu (1956), that there was an extensive overlap of terminations within Clarke's column. In direct contradiction to Liu (1956), Grant and Rexed (1958) found no

degeneration in Clarke's column on section of cervical or Th1 roots, finding instead that the fibres degenerating on section of those roots passed around Clarke's column and not into it. They therefore concluded that Clarke's column receives information from the trunk and hindlimb, and not the forelimb as proposed by Liu (1956). In accordance with earlier studies (Laruelle and Reumont, 1938, in Grant and Rexed, 1958; Szentagothai and Albert, 1955), Grant and Rexed (1958) showed that the most caudal extent of the degeneration observed on severance of any one dorsal root was situated laterally in Clarke's column, that on moving rostral through the terminal field, the degeneration was found throughout the cross section of Clarke's column, and finally that the rostral degeneration was found in the most dorsomedial part of Clarke's column.

Szentagothai (1961) re-examined both the course of afferent input to Clarke's column, and the extent of somatotopic organization of the afferents. He determined that the primary afferents enter the cord through the spinal dorsal roots, and initially ascend in the dorsal columns for at least two spinal segments before dropping collaterals into the grey matter. Thus transection of dorsal root L4 led to degeneration in segments L2-Th10, section of L3 led to degeneration rostral to L1 and so on. This finding was in accordance with Szentagothai and Albert (1955) but not with the findings of Liu (1956) and Grant and Rexed (1958). With regard to the somatotopic arrangement of afferent inputs to Clarke's column, Szentagothai (1961) noted, in accordance with Szentagothai and Albert (1955) and Grant and Rexed (1958), that the collaterals are found in the lateral part of the column at their caudal extent, and shift medially as they ascend in the column. This mirrors the somatotopy of the afferent fibres, which shift medially as they ascend in the dorsal columns. He suggested that the full termination pattern for any one dorsal root could be

represented as parallel oblique slice running rostromedially through the column (see Figure 1.3), but again concurred with Liu (1956) and Grant and Rexed (1958) that much overlap was evident between collateral terminations of neighbouring and more distant segments.

Both Boehme (1968) and Rethelyi (1968) examined the origin and distribution of collaterals to Clarke's column in newborn kittens. Boehme (1968) reported that the fibre groups which terminated in Clarke's column included: 1) collaterals from the dorsal columns which enter Clarke's column and divide into fibrils which run longitudinally in the column, 2) fibres from other tracts which were of fine caliber and entered Clarke's column from the lateral columns, and 3) fibres which arose from cells of the dorsal horn. Rethelyi (1968) described only the afferent inputs to Clarke's column which arose from the dorsal columns. He subdivided them on the basis of their position in the dorsal columns, and collateralization, into three groups. These were: 1) collaterals terminating exclusively in Clarke's column, which branched to take a longitudinal course within the column (most branches ascending, but some branches descending), and which gave off many side branches. These collaterals demonstrated a particular topography, with those arising from fibres running in the lateral region of the dorsal columns terminating in the lateral part of Clarke's column, and those arising from fibres in the medial region of the dorsal columns terminating medially in Clarke's column. All these collaterals, however, terminated in the dorsomedial 2/3 to 3/4 of Clarke's column, sparing the ventrolateral region. 2) a group of fibres situated in the lateral dorsal columns sent collaterals which curved around the lateral boundary of Clarke's column to terminate primarily in the intermediate region and ventral horn, but which branched at the base of the dorsal horn, sending lateral or ventrolateral side branches to terminate in the ventrolateral sector of Clarke's column.

3) The third group were collaterals arising from afferents in the medial part of the dosal columns which travel to their termination in the dorsal horn, but could send collaterals branches to run longitudinally and terminate in the dorsolateral region of Clarke's column. Rethelyi (1968) concurred with Szentagothai (1961) that the terminal fields of fibres entering Clarke's column encompassed a rostromedially directed slice of the column.

Rethelyi (1968) speculated on the nature of each of the three fibre groups, suggesting that the first group, with exclusive termination in Clarke's column, were group Ia muscle afferent collaterals; the second, collaterals from group Ib muscle afferents; and that the third group may be the cutaneous collaterals.

Tracey and Walmsley (1984) labelled DSCT cells in Clarke's column by retrograde transport of HRP injected into the cerebellum, and subsequently identified and intraaxonally labelled Ia and Ib muscle afferents ascending in the dorsal columns at L3 and L4 levels. They showed that collaterals of both afferent types descend ventrally to Clarke's column, then divide into secondary collaterals which terminate in a zone of Clarke's column restricted to <1 mm rostrocaudally. The study of Tracey and Walmsley (1984) wasthe first to examine the morphology of functionally identified afferent terminations within Clarke's column.

Although the trajectory of degenerating and identified primary afferents to Clarke's column have been examined, few studies have extended to an examination of bouton types, or morphology of the synaptic connection made between these afferents and Clarke's column cells. The following section outlines the ultrastructural morphology of synaptic boutons located within Clarke's column.

1.5 Synaptology of Clarke's column

Knowledge of the nature of synaptic connections within Clarke's column was limited prior to 1955, when Szentagothai and Albert used Nauta techniques to observe the degeneration of three bouton types within the column on section of dorsal roots in the dog. These were: 1) the "giant synapse" - large boutons believed to arise from muscle afferents, which run parallel to the dendrites and are characterized by large, elongated contact zones, 2) small, terminal boutons, 1-3 μm in diameter, thought to arise from local intraspinal neurones, and 3) a meshwork of fine fibres, also from spinal interneurones, and believed to be inhibitory.

Sedar and Moskowitz (1967) examined the utlrastructure of normal Clarke's column tissue from the cat, and noted the appearance of S and F type boutons. S type boutons, also called Gray type 1 (Gray, 1959), or E (excitatory) type (Uchizono, 1965) contained spherical vesicles, 400-600 angstroms in diameter, while F type boutons (Gray type 2, Gray 1959), or I (inhibitory) type (Uchizono, 1965), contained elliptical or flattened vesicles, 200-300 x 400-600 angstroms. S type boutons accounted for 50% of the axodendritic, and 56% of the axosomatic boutons (Sedar and Moskowitz, 1967).

In a Golgi study of Clarke's column in the kitten, Boehme (1968) showed collaterals from fibres in the dorsal columns to enter the grey matter and divide into fibrils, which run longitudinally in the column. These fibrils were characterized by numerous, knoblike expansions up to 5 x 10 μm, which, although irregularly spaced, appeared to be more concentrated towards the end of the fibril, which terminated in a larger knob. Boehme (1968) concurred with Szentagothai and Albert (1955) that the giant contacts appeared to be made only with dendrites of the DSCT neurones, and that axosomatic contacts were of smaller types.

Rethelyi (1970), using degeneration techniques, determined the existence of three synaptic types in Clarke's column (see Figure 1.3). The first group were the giant terminals observed previously by Szentagothai and Albert (1955), recognized at the ultrastructural level as being 8-10 x 4-5 μm, containing large, spherical vesicles of irregular size, and contacting the dendrites or cell bodies of the largest Clarke's column or DSCT cells. The giant boutons made asymmetric synaptic contacts, with clustering of vesicles presynaptically, thickening of the postsynaptic membrane, and were generally not terminal, instead making *en passant* connection and continuing on to contact the same or other dendrites. The contact surfaces of these giant boutons were often invaginated by small, spinelike processes from the dendrites or somata of the cells, which were apparently non-synaptic. Rethelyi (1970) suggested that each of the giant boutons may contain multiple sites for transmitter release, perhaps as many as six (see Figure 1.4). These boutons were presumed to arise from primary muscle afferents, and were often accompanied by small, presynaptic boutons. The second group were small boutons with spherical vesicles, which contacted the somata of small cells, or small dendrites which may have been distal dendrites of the DSCT cells. A third group was divided into type 3a and type 3b boutons. Type 3a) were delicate axons containing flattened vesicles which were occasionally dense cored, surrounding the cell bodies and dendrites of the large Clarke's column cells, with which they made symmetric synaptic connections. Type 3b) were small boutons containing flattened vesicles, observed in close apposition to the giant terminals. These small boutons could show full synaptic specialization, or simply appear in close proximity to the giant terminals, but generally appeared to be presynaptic axo-axonic contacts. Rethelyi (1970) compared the Type 3b boutons with small boutons discovered to contact primary afferent terminations on motoneurones (Conradi, 1969). These axo-axonic contacts

FIGURE 1.3

Schematic representation of the ultrastructural synaptology of Clarke's column, prepared by Rethelyi (1970).

The bouton labelled "EIT" represents an excitatory terminal, presumed to arise from an interneurone.

The boutons labelled "IIT" are *en passant* terminals, presumed to be inhibitory, and also of interneuronal origin.

A giant axon terminal (GAT) is shown making multiple synaptic connections with a dendrite. In turn, the GAT is shown to be contacted by a small, presynaptic terminal, which is presumed to be inhibitory.

(Reprinted from Rethelyi, 1970).

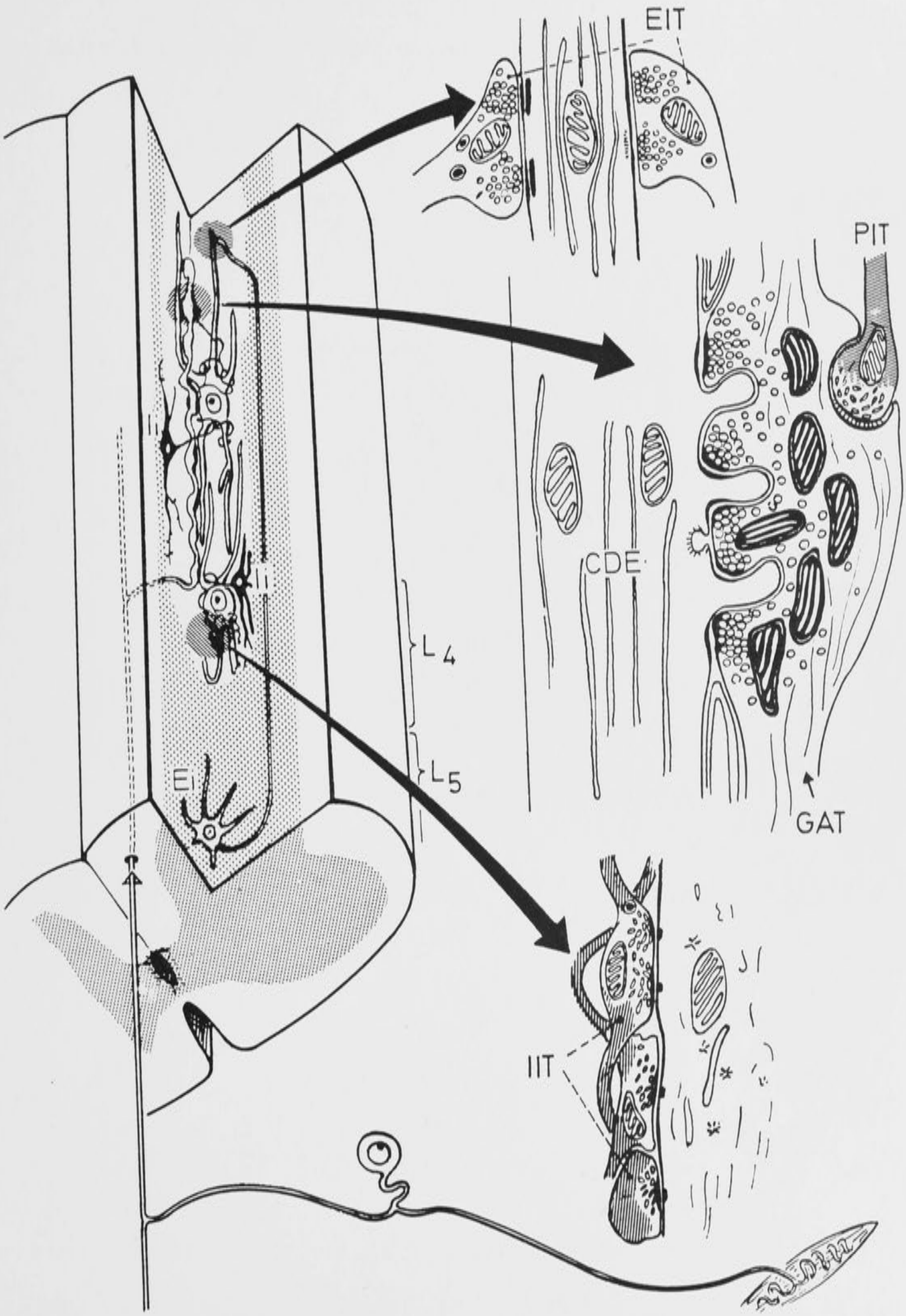
EIT
PIT
CDE
L4
L5
GAT
EI
IIT

FIGURE 1.4

Electron micrograph of a "GAT", giant axon terminal, or giant bouton, found contacting a dendrite of a Clarke's column neurone, prepared by Rethelyi (1970). This bouton is shown to make multiple synaptic connections with the same post synaptic dendrite.

(Reprinted from Rethelyi, 1970).

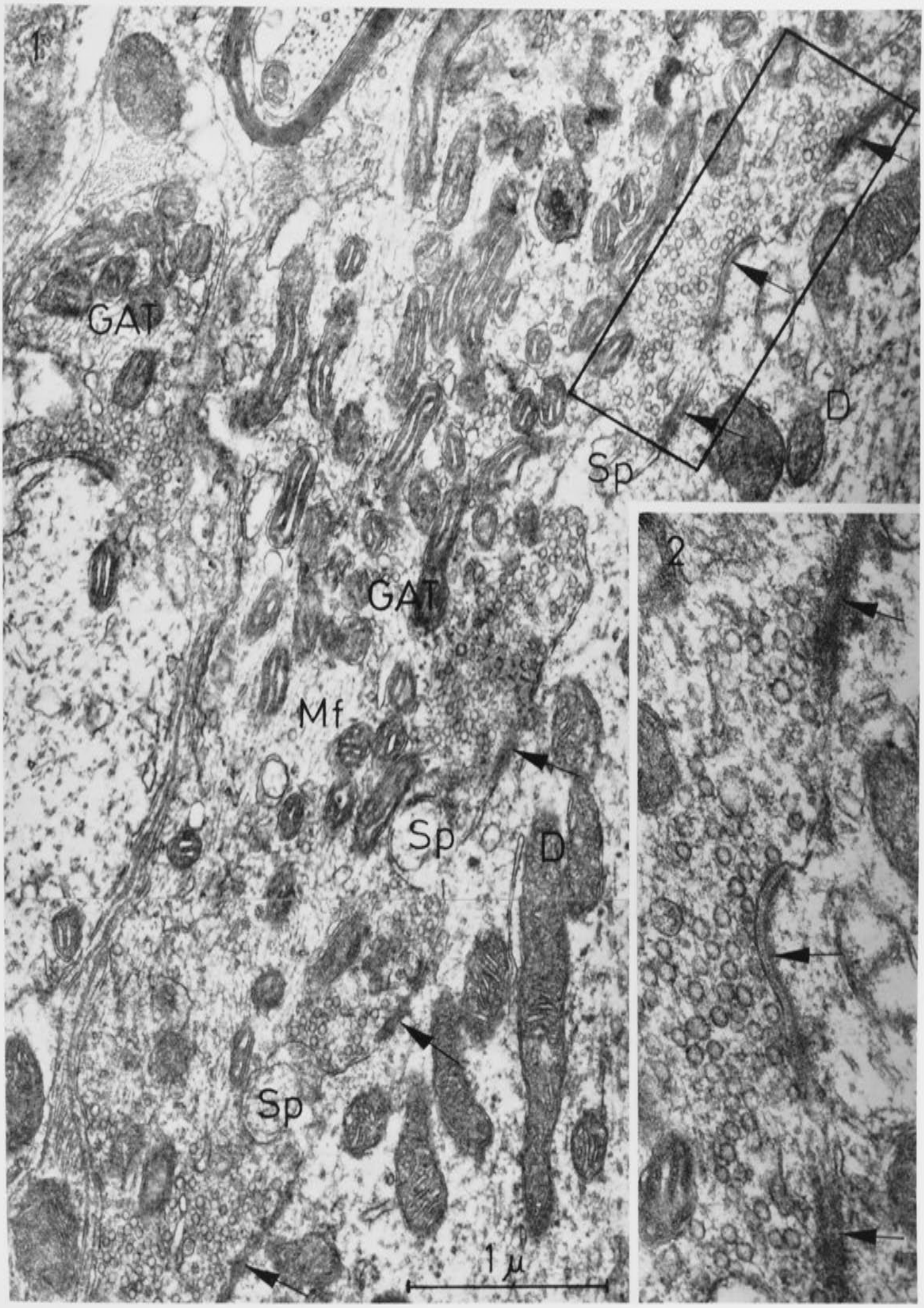
1
GAT
Sp
D
GAT
Mf
Sp
D
Sp
1 μ
2

were suggested to represent the morphological correlate of presynaptic inhibition.

In a further study, Kuno et al., (1973b) observed giant boutons on or close to the soma of DSCT neurones in Clarke's column. Kuno et al., (1973b) concluded that some of the giant boutons arise from primary afferents, and suggested that the size of a bouton may correlate directly with the receptor type. They compared the size and position of terminals on DSCT neurones and motoneurones, and found that while no difference was obvious between dendritic contacts on the two cell types, DSCT neurones were contacted by giant boutons on or close to the soma. Thus, while both dendritic and somatic terminals on motoneurones ranged from 1-4 μm, somatic terminals on DSCT neurones ranged from 1-14 μm. The large number of *en passant* connections seen by Rethelyi (1970) was also reported by Kuno et al. (1973b) who agreed that the strong synaptic actions seen on DSCT neurones might result from a large number of *en passant* synaptic contacts, or the large size of the somatic terminals.

An extensive ultrastructural study by Saito (1974) on normal tissue from Clarke's column at the L3 segment of the adult cat revealed 6 bouton types, differentiated on the basis of size, vesicle shape, and nature of synaptic complex: Type 1) Elongated boutons, 5-25 x 1-2.5 μm, characterized by short active zones, a dense accumulation of clear circular vesicles at the presynaptic site and asymmetric synapses with a wide synaptic cleft. These boutons could be *en passant* in nature, making multiple synaptic connections along the cell soma and proximal dendrites. Type 2) differed from type 1) primarily in having flattened vesicles, only moderately clustered at the presynaptic site, and symmetric synaptic complexes, with long active zones and a narrow synaptic cleft. 3) Type 3 boutons were small, contact lengths 1-3.5 μm, containing 1-2 short

active zones with a dense accumulation of vesicles at the presynaptic site, asymmetric density and a wide synaptic cleft. 4) Type 4 boutons differed from type 3) by having 1 long active zone which resembled that described for type 2) boutons. Both type 3 and type 4 boutons were seen densely packed over the soma, main dendrites and axon hillock, but not the initial segment of DSCT neurones in Clarke's column (Saito, 1972). 5) Type 5, the "club giant" bouton, named on the basis of size and shape, was thought to correspond to the giant axon terminal described previously by Rethelyi (1970) and Szentagothai and Albert (1955). These boutons had contact lengths of 4.0-7.5 μm and diameters of 2.5-6.0 μm, with large synaptic complexes of the types described for bouton types 1) and 3). The boutons were often invaginated by small spinous processes of the DSCT neurone soma or proximal dendrites. These type 5) boutons were characteristically contacted by small type 6) boutons, containing pleomorphic vesicles. These boutons were apparently presynaptic to type 5) boutons, although the symmetric nature of the synapse made determination of the postsynaptic profile difficult (Saito, 1974; Rethelyi, 1970). Bouton types 1-5 were distributed randomly over the soma and proximal dendrites of the large cells. Saito (1974) considered that the three bouton types described by Rethelyi (1970) corresponded to those listed as 4), 5) and 6), such that type 4) correspond to small inhibitory boutons, type 5) to the giant synapses, and type 6) to small boutons presynaptic to giant boutons. Due to similarities with boutons found to contact motoneurones (Conradi, 1969), Saito (1974) proposed that bouton types 1) and 5) may arise from muscle spindle afferents.

In 1977, Chen, Chambers and Liu examined synaptic connections on Clarke's column neurones after lesion of the DSCT and subsequent cellular degeneration. They observed the six bouton types described by Saito (1974) but added that although the giant boutons were found

degenerating on DSCT neurones, they were rarely observed contacting the soma of the DSCT neurones, instead most often found contacting the proximal dendrites. The DSCT neurone soma was contacted primarily by small bouton types. Also, they found the density of boutons contacting the primary dendrites to be 3 times higher than that contacting the soma.

In 1979, Saito studied the synaptic connections of DSCT neurones in Clarke's column at the L3 level after retrogradely labelling the cells by injection of HRP into the anterior lobe of the cerebellum. Having thus identified the postsynaptic profile, Saito (1979) examined the number of small vs large, and S vs F type (after Sedar and Moskowitz, 1967) boutons found contacting the cell body, proximal and distal dendrites. Giant boutons were most frequently observed contacting the proximal dendrites of labelled cells, where they accounted for 27.6% of the total boutons, as compared to 18.1% on the soma and 10.1% on distal dendrites. F type boutons were most frequent on the soma (55%) and primary dendrites (59%) while S type boutons accounted for 62.6% of those observed on distal dendrites. Saito (1979) concurred with Boehme (1968) that the majority of boutons found contacting retrogradely labelled DSCT neurones in Clarke's column were of the small S type, and that the distribution density of giant boutons is quite low. It was again suggested (Saito, 1979) that the giant boutons which receive small, presynaptic contacts, might correspond to the M-type (muscle spindle afferents) terminations described on motoneurones by Conradi (1969).

These studies left a number of questions unanswered. Saito equated all boutons in close apposition to presumed (Saito, 1974) or identified (Saito, 1979) DSCT neurones as contacts, whether or not synaptic specializations were observed, and measured the contact lengths of all boutons as the length of membrane apposition, rather than length of specializations. Also, identification of the afferent had not been made, so

although speculation was drawn as to the nature of the bouton types, the studies were functionally non-specific. Saito (1979) emphasized that the only true classification of the function of DSCT neurones would come with electron microscopic observations of identified afferent connections with the DSCT neurones, and analysis of the contacts such as had been performed with the motoneurones.

Houchin et al. (1983) examined the ultrastructural morphology of boutons found contacting DSCT neurones labelled intracellularly by injection of HRP. The proximal dendrites received synaptic connections from three terminal types: 1) large or giant synaptic boutons (> 5 μm) containing small, agranular vesicles and making asymmetric synaptic contact on the main dendritic shaft or on small spinous processes, 2) small boutons, also making asymmetric contact, containing circular, agranular vesicles, and some larger, dense cored vesicles, and 3) small boutons, 1-3 μm in diameter, containing flattened vesicles. These boutons could contact DSCT neurones or giant boutons, and could, in fact, contact both a DSCT neurone and a giant bouton simultaneously. As noted previously, Houchin et al. (1983) determined that the observed beading or varicosity of the DSCT neurone dendrites contained swollen mitochondria and signs of internal disruption. However, these swellings could give rise to fine projections, which often received synaptic contact. Two terminal types were found contacting distal dendrites of identified DSCT neurones, 1) terminals containing flattened vesicles, and 2) terminals containing both clear and dense cored vesicles.

Tracey and Walmsley (1984) demonstrated the termination pattern of identified, intra-axonally labelled group Ia and Ib muscle afferents on DSCT neurones in Clarke's column which had been labelled retrogradely after injection of HRP into the cerebellum. Both Ia and Ib boutons contacted the neurones in an *en passant* or a terminal manner, with

boutons of small or giant types, ranging from 5-20 x 2-5 μm (the largest corresponding to the giant synapse described by Szentagothai and Albert, 1955; and Rethelyi, 1970). Tracey and Walmsley (1984) concurred with Kuno et al. (1973b) that the large EPSPs recorded in DSCT neurones may be explained to some extent by the unusual synaptology of these cells.

In summary, 6 distinct bouton types have ben observed contacting cells in Clarke's column. To date, no ultrastructural investigation has examined identified afferent terminations in Clarke's column. Thus, although various authors have speculated on the physiological nature of the bouton types, strict functional characterisation of each type has not been achieved. Questions therefore remain as to the nature of the excitatory and inhibitory connections on DSCT neurones in Clarke's column, and the origins of synaptic boutons.

1.6 Aims and Objectives.

This chapter has provided a review of the organization and synaptology of Clarke's column and the dorsal spinocerebellar tract prior to 1985. Much conflicting evidence has emerged from these studies.

The morphology of DSCT neurones in Clarke's column which receive identified afferent input has not been completely determined. Golgi studies suggested that the cells were large, with extremely complex dendritic trees. Such studies provide no information about the functional nature of the cells. Two studies have utilized intracellular labelling techniques to visualize DSCT cells. The results of these two studies were largely conflicting. Randic et al. (1981) labelled cells with identified afferent inputs but the reconstructions presented by them showed the cells to exhibit a simpler morphology than suggested by earlier Golgi studies. In contrast, Houchin et al. (1983) showed intracellularly labelled DSCT neurones to be large and extremely complex, with long, extensively

branched dendritic trees. The cells reconstructed by Houchin et al. (1983) were, however, identified only on the basis of sciatic nerve stimulation. It was therefore considered important to examine the detailed morphology of DSCT neurones in Clarke's column which receive specific, identified afferent inputs. Two series of experiments on the morphology and location of these cells were therefore carried out, and the results are presented in Chapter Three.

The DSCT neurones in Clarke's column represent a major pathway for the processing and transfer of sensory information from receptors in the hindlimb to the cerebellum. To date, no study has examined the ultrastructural synaptology of contacts between identified primary afferents and DSCT neurones. Such a study is extremely important in describing the morphological basis for synaptic transmission at this connection. The only study to examine terminations of functionally identified primary afferents within the column prior to 1985 was that of Tracey and Walmsley (1984) who did not examine the ultrastructure of these terminations. Several investigations to examine the ultrastructure of identified contacts between sensory afferents and DSCT neurones in Clarke's column were therefore carried out. The results of two of these studies have already been published in the Journal of Neuroscience and are presented in Appendices I and II. The results of a further study, which represents a major part of this thesis, is presented in Chapter 4. Further results on the ultrastructural morphology of identified afferent inputs to Clarke's column are included in Chapter 5, which presents a General Discussion of all of the studies contained in this thesis.

CHAPTER TWO

METHODS

CHAPTER TWO: METHODS

Many of the procedures used are common to all the studies presented in the following chapters. This chapter describes these techniques, including surgical procedures, recording, intracellular labelling, histology and analysis. Where necessary, the different experimental procedures are separated under appropriate headings.

2.1 Preparation and Surgical Procedures

Young adult cats 1.5-3.5 kg were used in these experiments. The cats were anaesthetised with an initial dose of sodium pentobarbitone (Nembutal, Abbot Laboratories) 35 mg/kg i.p. and maintained with supplementary doses of 5 mg/kg i.v. as required. Anaesthetic level was monitored by constant observation of blood pressure, reflex response and pupil size. The animals were shaved around the throat, back and left hindlimb to facilitate surgical procedures. The right carotid artery was exposed and cannulated to allow constant monitoring of blood pressure, and the right jugular vein, or the left cephalic vein was cannulated to allow intravenous anaesthetic administration. A tracheal cannula was inserted to provide the animal with a free passage of air, and also to allow easy connection to a respiration pump should a pneumothorax be required to stabilize the preparation. End tidal CO_2 was monitored continuously throughout the experiment, as was body temperature, which was maintained at 37^{o}C by the use of heating blankets and infra-red lamps.

The animal was clamped into a rigid animal frame, and fixed at the head, shoulders and hips. The spinal cord was exposed by conventional laminectomy from L2 to L7 segments, and at C2 or C3 for antidromic

stimulation. The sciatic nerve was exposed and cleared in the left hindlimb. In some experiments nerves from lateral gastrocnemius (LG), medial gastrocnemius (MG), soleus (Sol) and plantaris (Pl) muscles were exposed and cleared for part of their length. These muscle nerves were left in continuity with their respective muscles. The tendon from each of the four muscles was separated and cut at its insertion. This allowed individual stretch responses of each muscle to be determined.

The skin was drawn up to form pools around the exposed nerves and spinal cord. The pools were filled with mineral oil which was maintained at 37^{o}C throughout the experiment by infrared heat lamps. Bipolar stimulating electrodes were placed on the exposed sciatic and/or muscle nerves. A stimulating electrode was situated over the DLF at the C2 level to allow antidromic identification of DSCT neurones (Houchin et al., 1983; Tracey and Walmsley, 1984). Another bipolar electrode was situated at L7 such that the cord dorsum potential could be monitored. This assisted with determining presence and strength of signals travelling to the cord from the periphery, and with assessment of any possible damage to the exposed hind limb nerves and receptors. The dura mater was slit longitudinally under an operating microscope, along the entire length of the exposed spinal cord. The dura was then carefully drawn up and secured at the L3 and L4 segments, effectively creating a sling in which to support the cord, particularly at the recording site. This procedure was considered necessary for stabilization of the preparation, as it effectively isolated the spinal cord recording site from the normal movement caused by breathing or changes in the animals' blood pressure.

Recording electrodes were pulled on a Kopf vertical puller using thin walled glass capillary tubing (Clark electromedical). Electrodes were filled with 8-10% HRP dissolved in either 1M KCl/tris buffer, or 2M K-Methyl-SO_4. Immediately prior to use, the electrodes were subjected to a

vaccuum in order to eliminate air bubbles from the tip. Electrodes had a tip diameter of 0.5-1.5 μm, and an impedence of 4-20 M ohms.

2.2. *Recording and Identification*

Recording electrodes were advanced into the spinal cord at L3-L4 spinal segments, at an angle of approximately 45°. This angle was used to achieve more stable intracellular penetrations (Tracey and Walmsley, 1984). The electrodes were advanced into the cord at a variable rate in steps of 1 μm. Electrical potentials recorded through the electrode were monitored both by loudspeaker, and visually on an oscilloscope screen.

I. Cells

An antidromic field potential was generally recorded from a depth of approximately 1800 μm, and most cells were penetrated at approximately 2100-2600 μm depth. Penetration of a cell was indicated by a recorded membrane potential of -40mV or greater. Cells were further identified as DSCT neurones by their response to antidromic activation of the DLF at cervical levels.

i). Cells which received muscle input: Cells identified in experiments in which the ankle extensor muscles were the sole source of synaptic input were tested for response to stretch of each of the four muscles (MG, LG, Sol or Pl), or to stimulation of each of the muscle nerves. Once a cell was shown to receive input from one or more of the ankle extensor muscles, the input was identified as group I or group II on the basis of conduction velocity and threshhold. Only those cells receiving group I input were stained in these experiments. An attempt was then made to further divide the input into group Ia (muscle spindle afferent) or group Ib (Golgi tendon organ). Ia inputs were characterized by a high dynamic sensitivity to passive muscle stretch, and were silent during the active muscle

contraction. Ib afferent inputs were characterized by a higher threshhold, a lower dynamic sensitivity to passive muscle stretch and were activated during the muscle contraction or twitch. (These same criteria were used to divide group Ia and Ib afferents during studies of the muscle afferents themselves).

ii). Cells which received cutaneous and convergent inputs: For these experiments, all hindlimb nerves were left intact. Penetration and identification of the cells as belonging to the DSCT were as described above for cells with muscle input. Sensory input to the cells was subsequently identified as follows. The hair of the hindlimb was first brushed and stroked using a fine paintbrush in an attempt to identify possible inputs from hair follicle receptors. If this was successful in identifying afferent input to the penetrated cell, the type of hair follicle afferent (HFA) was further categorized as Down, Guard, or Tylotrich (after Brown and Iggo, 1967). Next, the skin itself was stroked and pinched, with particular attention to the base of the claw and foot pads in a search for Slowly Adapting Type I (SATypeI, Merkel), Slowly Adapting Type II (SAType II, Ruffini), or Rapidly Adapting Pad (RAPAD, Krause) input to the penetrated cell. Input from Paccinian corpusles was determined on the basis of extremely high sensitivity both to manipulation of the hindlimb, and to bumping or knocking of any object in the vicinity of the receptor. Paccinian corpuscles are also capable of firing very rapidly, and could follow extremely high frequency (512 Hz) stimulation in a 1-1 manner. High frequency stimuli were applied using a tuning fork. Receptive fields for the cutaneous receptors ranged from extremely small, (1 hair or touch receptor), to many cm^2. Cells identified as receiving input from cutaneous receptors were subseqently tested for deep (muscle or joint) inputs. This was achieved by flexion and extension of the toe, ankle and knee joints, and squeezing or manipulation of the bellies of the intact

hindlimb muscles. Cells were categorized as convergent if they received input from a deep receptor in addition to an identified cutaneous receptor.

II. Afferents

Both muscle and cutaneous afferents were usually encountered in the dorsal columns at a depth of 400-1400 μm. Penetration was generally established by the recording of an afferent action potential driven by the search stimulus applied to the sciatic nerve. The afferents had resting membrane potentials of approximately -40 mV or greater and exhibited action potentials of 30-90 mV.

i). Muscle afferents: The muscle of origin was determined either by stimulation of mounted muscle nerves, or by stretching of individually separated ankle extensor muscles. Muscle afferents were first divided into group I or group II on the basis of their threshold and conduction velocity. Group II afferents were not stained in this series of experiments. Group I afferents were next further divided as described previously, Ia muscle afferents had a high dynamic sensitivity to passive stretch and were silent during the active muscle twitch, whereas Ib afferents were higher threshhold, had lower dynamic sensitivity to stretch and were activated during the muscle contraction.

ii). Cutaneous afferents: Cutaneous afferents of five sensory modalities were sought. Their identification was as follows:

1) Hair follicle afferents responded to movement of hairs after light brushing or blowing; little mechanical movement of the hairs was required to elicit a rapidly adapting response. 3 categories were identified, down, guard and tylotrich (after Brown and Iggo, 1967).

2) SATypeI (Merkel cells, touch domes): respond to stroking of the skin, slowly adapting in response to stimulation, response to displacement irregular.

3) SATypeII (Ruffini endings): also slowly adapting, respond to movement of the claw or manipulation of skin at the claw base with regular discharge.

4) RAPad (Krause corpuscles): rapidly adapting receptors found in the foot and toe pads.

5) Paccinian corpuscles: highly sensitive to any movement or vibration of the surrounding area, and able to follow high frequency (> 500 Hz) stimulation 1-1.

2.3. *Staining*

Once identification was satisfactorily completed, ionophoretic current or pressure injection was used to fill the cell or afferent with HRP (Jankowska et al, 1976; Snow et al., 1976). Ionophoresis was achieved by passing depolarizing current pulses of 4-40 nA through the electrode for up to 1 hour. Good staining was generally achieved if the charge transfer was approximately 400 nA mins. A simple tool for pressure injection was developed utilizing a 10 ml disposable syringe and a spring. These were arranged such that the syringe was used to compress the solution in the electrode, forcing minute amounts of HRP from the tip. On release of the plunger, the spring ensured the return of the system to atmospheric pressure. Pressure was administered in pulses, with return to atmospheric pressure between each pulse. Sufficient staining could be achieved using pressure injection in a very short period, usually 1-5 minutes.

i) Cells: HRP was delivered to the cells via ionophoretic current/and or pressure injection, only while the cell was exhibiting a visible action potential. Usually, two to four cells were stained in each experiment.

Separation of approximately 0.5-1.0 mm was maintained between cells, which generally ensured easy identification and reconstruction at completion of histological procedures.

ii) Afferents: Ionophoresis was usually employed to label afferents with HRP (Snow et al., 1976). HRP was delivered to the afferents only while an action potential of 10 mV or greater could be observed. In experiments in which muscle afferents were stained, only group Ia or Ib afferents were stained in each experiment. This, in addition to a maintained separation between injection sites of 0.5-1.0 mm ensured lack of confusion during reconstruction and during electron microscopic viewing. Greater separation was maintained between injection sites when cutaneous afferent were stained, and 4-5 afferents from various receptor types were usually stained in each experiment.

2.4. *Perfusion*

After 2-5 hours post-injection survival time, the animal was given an anaesthetic overdose immediately prior to perfusion. The perfusion involved first passing two litres of cold saline via the left ventricle through the aorta to wash out the blood, before perfusing with two litres of fixative, also at 4^{o}C. The fixative generally consisted of 2.5% EM grade glutaraldehyde in phosphate buffer (0.1 M, pH 7.2-7.4). In some cases 2% glutaraldehyde + 2% paraformaldehyde was used. The perfusion took approximately 1 hour to complete. The L3 and L4 segments of the spinal cord were removed, the pia and dura peeled away, and the segments left to post fix overnight at 4^{o}C in the same fixative.

2.5. *Histology*

After approximately 10 hours post-fixation, the tissue was washed in phosphate buffer and cut at 70 - 100 μm on a Vibratome tissue slicer

(Camden Instruments). This was necessary for tissue prepared for electron microscopy, as cutting the tissue on a freezing microtome causes ultrastructural damage. Sections were collected serially in phosphate buffer, then stained using either di-amino benzedine (DAB), or cobalt enhanced DAB (Adams, 1977, 1981), or the method described by Hanker, Yates, Metz and Rustioni (1977).

2.6. Light Microscopy

After washing, tissue for light microscopic analysis was mounted on gelatine coated microscope slides and allowed to air dry overnight. The sections were dehydrated through a graded series of alcohols (50, 70, 90, 95, 100, 100%) then passed through two changes of xylene before being coverslipped. DPX was used as the mounting medium.

Photographs were taken of the sections using either a Zeiss or an Olympus microscope with camera attachment. Stained profiles were also traced and subsequently reconstructed manually using one of the same two microscopes fitted with a drawing tube attachment.* Landmarks such as large blood vessels, and the boundaries of Clarke's column and the dorsal columns were mapped onto each tracing. This made the drawings from each of the 70-100 µm thick sections easier to overlay, and gave a more positive location of the profile within the cord or column. The tracings were combined to produce composite reconstructions of the stained cells or afferents. These reconstructed profiles were then measured and/or photographed.

* Camera Lucida drawings were made at a magnification of 250x using a Leitz x25 FLUOTAR water immersion objective.

2.7. Electron Microscopy

I. Fixation and Embedding

Tissue to undergo electron microscope analysis was fixed, sliced and chromogen reacted in an identical manner to that described above. The primary consideration for all tissue to undergo electron microscopy is preservation of ultrastructure, thus extreme care is required in the handling of the sections.

The sections were thoroughly washed in phosphate buffer, and then examined using glyerol as a clearing agent under the light microscope. Sections containing stained profiles were identified and selected under the light microscope. The selected sections then underwent one of two embedding procedures as follows:

i). Flat or Sandwich embedding.

The section containing the stained profiles was rinsed with phosphate buffer. The section remained intact while the embedding procedures were carried out. The section first underwent secondary fixation for 1 hour in 1% OsO_4. (Provided the OsO_4 is aqueous, the tissue may then be stained en bloc with uranyl acetate. However, if the OsO_4 had been made up in PO_4 buffer, uranium salts cannot be used, as uranyl phosphate formation may contaminate the material for electron microscopy). After fixation (and *en bloc* staining where possible), the sections were rinsed in 2 changes of distilled water, then dehydrated through a graded series of alcohols (50,70,90,95,100,100%EtOH), with 10 mins in each change. They were then impregnated with a mixture of EtOH/Spurr's resin (Spurr, 1969), 50%:50%, for 1-8 hours. This was then replaced with 100 % Spurr's resin for 2-10 hours. Impregnation took place

under constant agitation provided by a rotating table. This ensured even infiltration of resin into the tissue.

The sections were subsequently "sandwiched" flat between two sheets of Melinex, and allowed to cure in a 70^{o}C oven overnight.

This procedure was particularly useful in that light microscope reconstruction of the stained profiles could then carried out without fear of damage to the tissue, or loss of stain. When the tissue was to undergo analysis, the Melinex sheets were peeled away. This left a thin wafer of embedded tissue, from which small blocks 1 x 1 mm were excised for electron microscopy. These blocks were cured or glued to blank blocks of resin. One disadvantage of this technique was that the background tissue, which normally appears pale under the light microscope, was rendered quite dark by the osmium fixation.* This occasionally resulted in difficulty in locating small stained profiles such as boutons. When boutons were of major interest, the following procedure was more successful:

ii) Section Embedding

The chromogen reaction was carried out, and tissue was chosen for EM after scanning at the light microscope level under glycerol. Under glycerol, the HRP stained profiles were readily identified, photographed and traced using a drawing tube attachment on the light microscope. This meant that all photographs and tracings required had to be finished prior to secondary fixation. The length of time before commencement of secondary fixation naturally increased the possibility of tissue contamination or damage. However, even tissue left under glycerol for some weeks before being drawn, photographed and taken for EM procedures gave acceptable results. It was, however, preferable to conclude all tracings and photographs such that EM procedures commenced within 10-12 hours of sectioning.

* This problem may be alleviated using the method of Cullheim, S. and Kellerth, J-O. (1976) Neuroscience Letters 2:307-313

Small pieces of tissue (approximately 0.3-0.5 x 1 mm) were excised from the tissue using a scalpel blade, and taken through secondary fixation, staining, dehydrating and infiltration procedures as described previously. Once resin infiltration was completed, the pieces of tissue were embedded in small plastic beem capsules. Such pieces sink to the bottom of the capsule, and their size ensures that they remain almost entirely flat throughout the embedding procedure. They were then allowed to cure in a 70^{o}C oven overnight.

II. Ultramicrotomy

Pieces of tissue excised from sandwich embedded sections were either cured, or glued to blank blocks of cured resin. Section embedded tissues were generally flat in the bottom of a cylindrical block of resin whose circumference was much greater than that of the section. In both cases, the block to be cut for EM had to be trimmed substantially to provide a block face of reasonable size for ultramicrotomy. This was achieved using a binocular microscope and a single edged razor blade. The section is very dark against the clear holding resin. Precise trimming is necessary to ensure that the block assumes the correct shape and size. The block was trimmed to present as a pyramid, with the block face trapezoidal. The trapezoidal block face served two purposes. 1) The irregular shape could be recognised under the electron microscope, and allowed determination of position within the block, 2) the parallel edges top and bottom ensured that the sections cut properly, and came away from the knife face as a neat ribbon. Once the block face was small enough to be manageable at the ultramicrotome, and the correct shape, sectioning began.

Serial thin sections 70-100nm (silver/gold) were cut using a Diatome diamond knife. The sections were collected on single slot (2 x 1

mm) copper grids coated with a nitrocellulose support film (collodion). The sections were dried overnight, then drop stained using lead citrate (Reynolds, 1963) and 1% aqueous uranyl acetate. The grids were floated, sections down, over a drop of the stain, then washed by dipping in distilled water a number of times. They were then allowed to dry, and were ready for examination under the electon microscope.

For much of the current work, serial electron microscopy was required. This technique is particularly difficult as it requires perfect cutting and collection of many sections. These must then be kept in perfect order and condition throughout the collection, staining and examination procedures.

III. Examination and Photography

Two electron microscopes were used. 1) a Philips 301, (J.C.S.M.R.) and a Jeol 100C (U.N.S.W.). The tissue was first scanned at low power (2,600x or 3,300x). At this magnification, HRP stained profiles were recognised as darker areas against the lighter background. Maps drawn previously under the light microscope were extremely useful at this point for determining the location of stained profiles. This was especialy useful in the cases where large blocks (1 x 2 mm) were viewed under the electron microscope.

At higher powers, (5,000x or greater) HRP stained profiles were unmistakeable. The HRP itself accumulates in and on membranous structures and remains within the intracellularly labelled profile. Thus the HRP filled structures have very dark, well defined membranes, vesicles, and mitochondria. In some cases the reaction product was so dark that it obscured the ultrastructural details of interest. This problem was somewhat alleviated by discontinuation of the cobalt enhancement step during the chromogen reaction, but even then the stain intensity was

variable. Profiles were generally photographed at a low and medium magnification (2,000 and 5,000x), and profiles of particular interest (e.g. boutons, synapses) were photographed again at a higher power (10,000 or 20,000x). The Philips microscope used a 35 mm camera, and the Jeol used cut plate 70 mm film. Due to the nitrocellulose coating, some tissue to be examined in the Philips microscope required carbon coating for strength prior to examination. Carbon coating prior to examination generally proved unnecessary under the Jeol microscope.

IV. Reconstruction and Analysis

Reconstruction and measurement of the analysed tissue was carried out from the series of collected electron micrographs. For reconstruction, photos taken at 5,000x were traced directly, and the tracings combined to reconstruct the stained profile.

All measurements of length, diameter and width were taken directly from the EM micrographs.

CHAPTER THREE

MORPHOLOGY, LOCATION AND SOMATOTOPY OF DORSAL SPINOCEREBELLAR TRACT NEURONES IN CLARKE'S COLUMN

CHAPTER THREE: MORPHOLOGY, LOCATION AND SOMATOTOPY OF DSCT NEURONES IN CLARKE'S COLUMN.

3.1 Introduction

Three major types of cells have been found to exist within Clarke's column, the largest of which (the Type C cells) are the primary cells of origin of the dorsal spinocerebellar tract (Loewy, 1970). Golgi and Nissl staining have shown the Type C cells to be large bodied, with many primary dendrites oriented primarily in a rostrocaudal direction, and which exhibit complex branching patterns (Boehme, 1968; Loewy, 1970). The dendrites of these cells have variously been described as totally confined to the column, or to have a few branches which extend beyond the boundary (Clarke, 1851; Rethelyi, 1968; Boehme, 1968). However, there is presently very little information available on the morphology of DSCT neurones in Clarke's column which have been positively identified physiologically.

Randic et al. (1981) labelled physiologically identified DSCT neurones in Clarke's column with intracellular injections of HRP. They recovered stained cells histologically, showing them to have large cell bodies and smooth dendrites, with few branch points (see Fig. 1.2 B and C). Randic et al. (1981) proposed that DSCT neurones fell into morphological categories which correlated well with their function. Cells receiving muscle input were morphologically similar, and larger than cells which received convergent (deep + cutaneous) input. A small number of cells which received purely cutaneous inputs were stained, but were morphologically dissimilar to each other, and to the cells which received muscle or convergent inputs. The cells presented in the study by Randic et al. (1981) were surprising in their lack of morphological

complexity, especially in light of the detail provided by earlier studies using Golgi techniques.

Houchin et al. (1983) subsequently labelled DSCT neurones in Clarke's column which received afferent input on stimulation of the sciatic nerve, and found that these DSCT neurones have an extremely complex morphology, with large cell bodies and multiple primary dendrites which branch profusely, but are mostly confined to the boundaries of the column (see Fig. 1.2A). The discrepancies between the cells labelled by Houchin et al. (1983) and those presented by Randic et al. (1981), led Houchin et al. (1983) to the conclusion that the cells presented in the earlier study "were less well filled with HRP reaction product".

Golgi studies have limited usefulness, due to the lack of identification of the cells. The likelihood that the cells presented by Randic et al. (1981) were not completely filled, and the limited identification of the cells reconstructed by Houchin et al. (1983) (i.e. receiving group I input from the sciatic nerve), means that the morphology of DSCT neurones in Clarke's column which receive identified afferent inputs has not yet been properly determined.

Hongo and co-workers (Hongo et al., 1967; Hongo, 1985) have proposed that DSCT cells within Clarke's column are somatotopically organized with respect to the muscle providing their primary input. Hongo (1985) has suggested that, in cross section, DSCT neurones receiving input from toe muscles are located in the dorsomedial region of Clarke's column, those with input from thigh muscles are located ventrolaterally, and those with input from shank muscles are found in the intermediate region of the column. Hongo (1985) stated that not only the cell body, but the entire dendritic tree of these cells is confined to the "appropriate" somatotopic location. This finding has recently been correlated with the observation that group I muscle afferents terminate in

Clarke's column in a strictly musculotopic arrangement (Hongo et al., 1987). Kuno et al. (1973b) had previously observed such a "musculotopic" arrangement of the DSCT cells, with those cells receiving inputs from biceps femoris muscle located more laterally in the column than those receiving input from gastrocnemius/soleus muscles. This observation is consistent with the finding of Hongo (1985) that somatotopic division in the column is based on the proximity of the muscle providing primary input.

It has been suggested that DSCT neurones receiving input from other than group I muscle afferents might be located outside Clarke's column. Hongo et al. (1967), Kuno et al. (1973a,b) and Randic et al. (1981) have recorded from identified DSCT neurones lateral to Clarke's column (at levels L3 and L4) which receive afferent input from a variety of cutaneous receptors. Aoyama et al. (1973) and Tapper et al. (1975) have suggested that the cells of origin of the cutaneous component of the DSCT might be located caudal to Clarke's column in segments L4 to L6. These particular cells were characterised as receiving a high proportion of convergent inputs.

The evidence available on the location and morphology of DSCT neurones in Clarke's column which receive identified inputs is both limited and conflicting. It was therefore proposed, in the present study, to intracellularly record, identify and label DSCT neurones in Clarke's column which received muscle, cutaneous or convergent inputs. These cells were to be recovered histologically and reconstructed, thus providing a detailed picture of the morphology and location of functionally identified DSCT neurones in Clarke's column.

3.2 Methods

Intracellular recordings were obtained from DSCT neurones located in Clarke's column at the L3-L4 spinal level. The identification and HRP labelling of these cells has been described in detail in Chapter 2: Methods, as have the subsequent histological procedures.

3.3 Results

The Results are presented in two sections. The first section deals with the location and morphology, in the transverse plane, of DSCT neurones in Clarke's column which receive identified input from a specific muscle group, the ankle extensor muscles. The second section describes the comparative morphology of DSCT neurones in Clarke's column whose input has been physiologically identified as deep (muscle or joint), cutaneous, or convergent (muscle + cutaneous). Both series of experiments involved intracellular penetration, identification and labelling of DSCT neurones in Clarke's column.

Previous reports have suggested that, despite their size, DSCT cells are extremely difficult cells to record from intracellularly (e.g. Curtis et al, 1958; Tracey and Walmsley, 1984). In accordance with these reports, it was found to be extremely difficult to obtain stable intracellular recordings from these neurones, due in part to movement caused by respiration and blood pressure pulsations. A number of measures were employed to improve the stability of the preparation to ensure better recordings. These measures included performing a pneumothorax (used only in some experiments), securing the dura in the form of a sling around the recording site, and using an acute angle of approach with the electrode (Tracey and Walmsley, 1984, and see Chapter 2). Even so, stable recordings were extremely difficult to obtain in comparison with, for example, the motoneurones of the lumbar spinal cord.

I. Location and Morphology of DSCT neurones which receive group I afferent input from ankle extensor muscles.

In this study, DSCT neurones were identified as receiving group I input from one or more of the ankle extensor muscles, medial gastrocnemius (MG), lateral gastrocnemius (LG), soleus (Sol) or plantaris (Pl), and were labelled intracellularly with HRP. Experiments were performed on 23 cats weighing 1.5-2.5 kg. Intracellular recordings were obtained from 40 DSCT neurones positively identified as receiving group I afferent input from one or more of the ankle extensor muscles.

Figure 3.1 shows a DSCT neurone which received group I input from plantaris muscle. Figure 3.1A shows a photomicrograph of the cell as it appeared in a single, transverse section of the spinal cord, in the ventromedial region of Clarke's column, close to the central canal. The cell is shown at higher magnification in Figure 3.1B. Other large cell bodies in Clarke's column can be seen in this counterstained section.

The degree of staining of the axon has previously been used as an indication that a DSCT neurone is well filled (Randic et al., 1981; Houchin et al., 1983). The fully reconstructed cell is shown in Fig. 3.1C. The soma and dendrites of this DSCT neurone were extremely well stained, as was the axon, which could be followed over 1.5 mm as it travelled ventrally and then laterally to ascend in the dorsolateral fasciculus (DLF). No axon collaterals were observed. This cell has a soma size of 48 x 43 μm in this plane, and its dendrites are confined almost entirely to the column. The dendrites appear as a complex tangled web, which spread laterally and dorsally, extending over half the column in cross section. A few of the dendrites are shown to extend dorsally from the column, one reaching almost 200 μm into the white matter.

FIGURE 3.1

A. An HRP labelled DSCT neurone which received input from plantaris muscle, shown in transverse section.

B. Higher magnification photomicrograph of the neurone shown in A. This counterstained section shows the HRP labelled cell in Clarke's column. Other large Clarke's column neurones can also be seen.

C. Full reconstruction in the transverse plane of the HRP labelled DSCT neurone in Clarke's column shown in A and B.

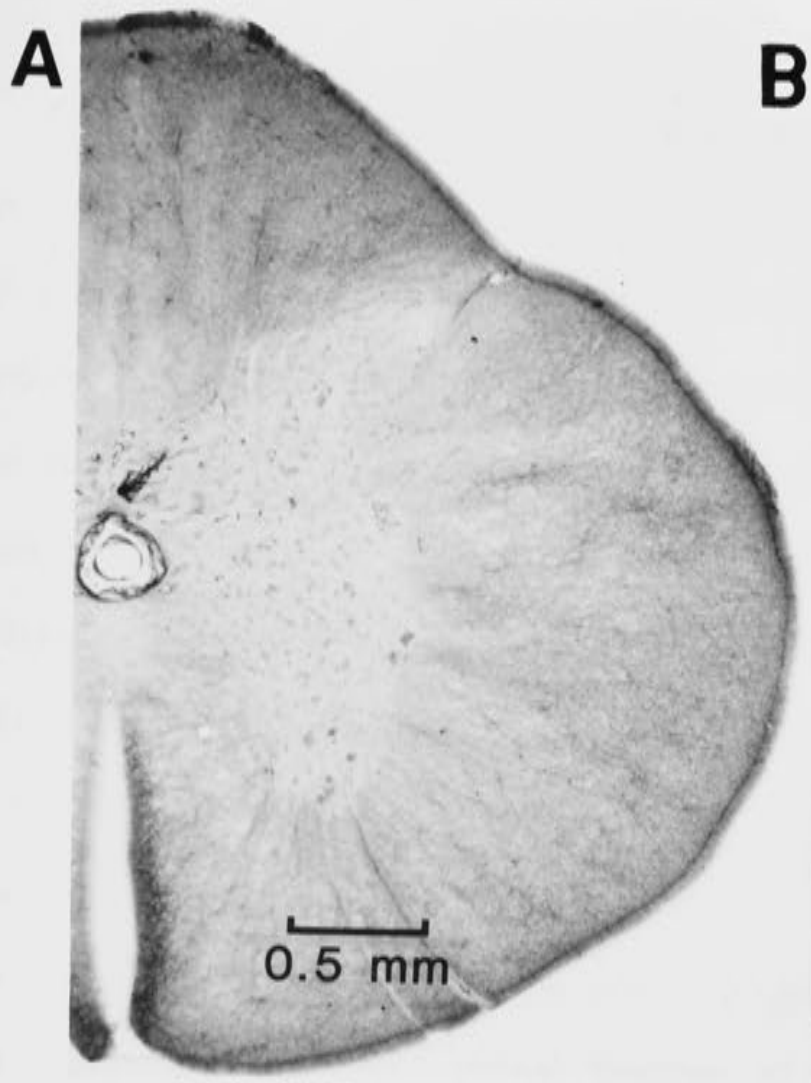
A
0.5 mm

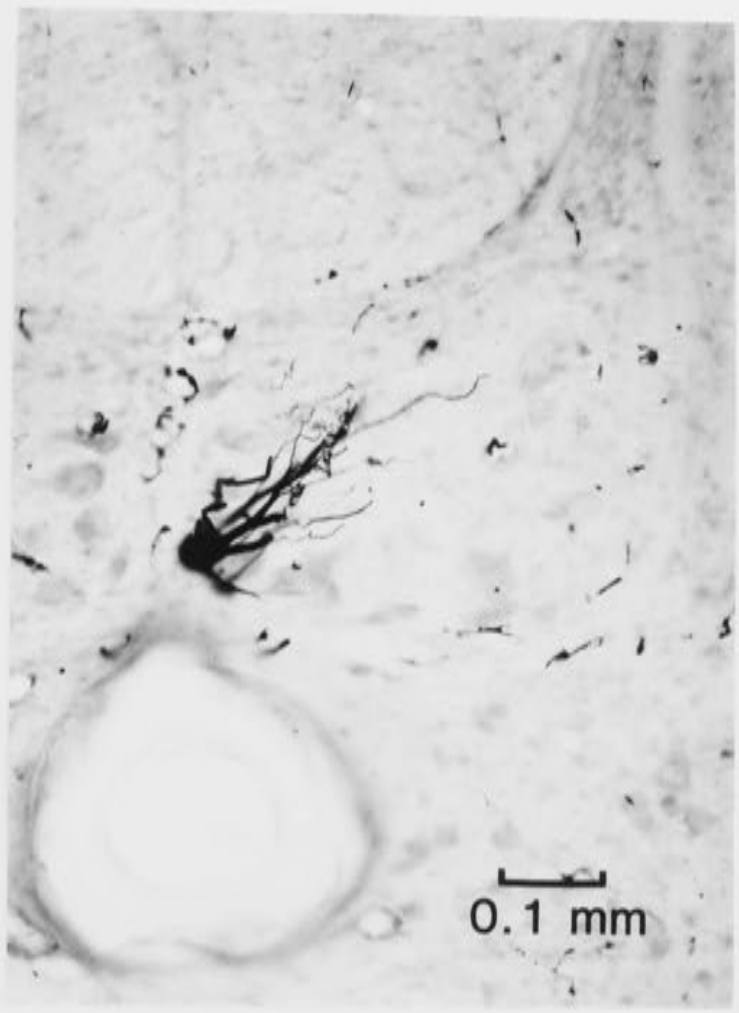
B
0.1 mm

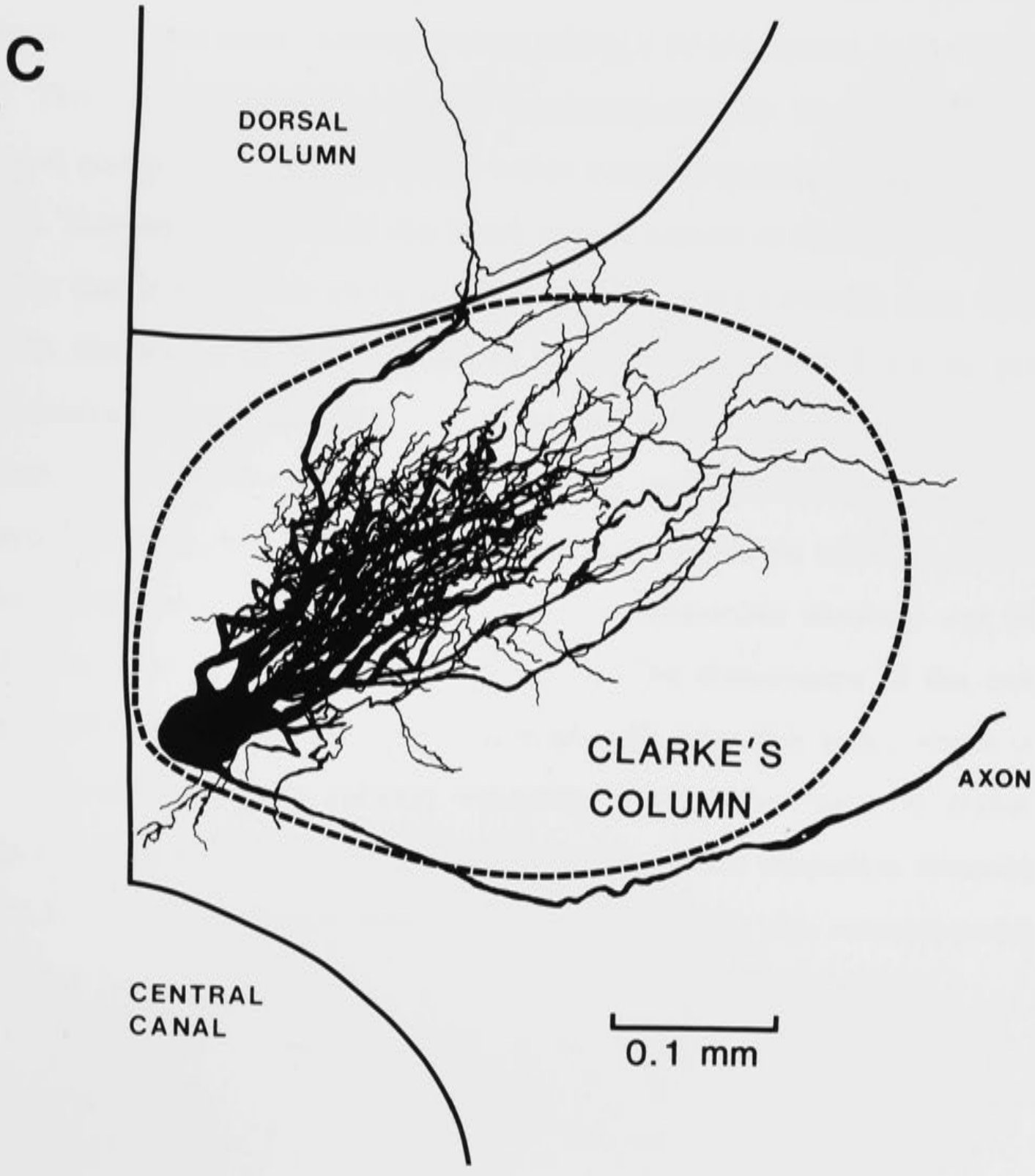
C
DORSAL
COLUMN
CLARKE'S
COLUMN
AXON
CENTRAL
CANAL
0.1 mm

Figure 3.2 shows a cell which received synaptic input from all of the ankle extensor muscles; MG, LG, Sol and Pl. The soma was measured to be 27 x 65 µm. The dendrites of this cell extend 500 µm in the mediolateral direction. The total extent of the dendritic spread in the dorsoventral plane is 670 µm, although the majority obviously occupy a much tighter region. The cell soma is located in the dorsomedial region of Clarke's column, and most of its dendrites also occupy the dorsal zone. A few dendrites are seen to extend ventrally into the column, and a few are shown leaving the column in the dorsal direction, reaching well beyond it into the white matter, in one case for over 430 µm. The axon of this cell is also well stained, and can be seen to leave the ventral surface of the soma, travelling to the ventral border of the column and continuing ventrolaterally for some distance before taking a lateral course to the DLF.

The DSCT neurones shown reconstructed in Figure 3.3 also received group I input from all four ankle extensor muscles, MG, LG, Sol and Pl. This cell is located in the ventrolateral region of Clarke's column, and has dendrites which cover a much greater cross sectional area than the cell illustrated in Fig. 3.2. These dendrites extend 770 µm in the mediolateral plane, and 490 µm dorsoventrally. The majority of the dendritic branches are directed back into the intermediate region of the column, covering over 60% of the area of the column. In addition, some of the dendrites are seen to extend for a considerable distance out of Clarke's column in a ventrolateral direction. The dimensions of the cell body in this plane were measured to be 48 x 43 µm. The axon, which is well stained, leaves the column ventrally, and is then seen to travel medially before doubling back on itself to take a lateral projection towards the DLF. Axon collaterals were not observed along the reconstructed length.

FIGURE 3.2

Reconstruction in the transverse plane of an HRP labelled DSCT neurone in Clarke's column. This neurone received group I afferent input from all 4 ankle extensor muscles; LG, MG, Sol and Pl.

The axon is shown leaving the cell and the column ventrally.

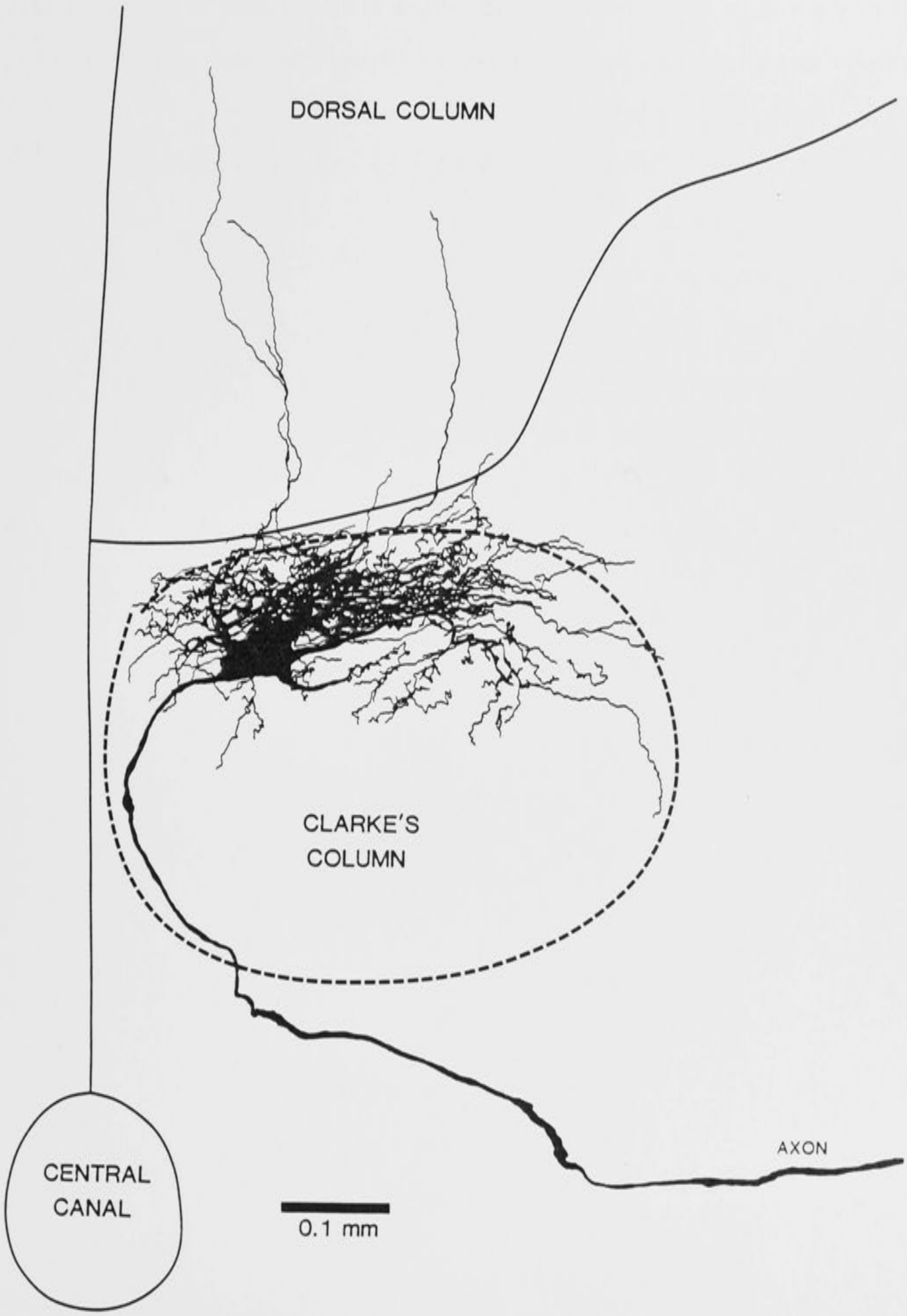
DORSAL COLUMN
CLARKE'S
COLUMN
CENTRAL
CANAL
AXON
0.1 mm

FIGURE 3.3

Reconstruction in the transverse plane of an HRP labelled DSCT neurone in Clarke's column. This neurone received group I afferent input from all 4 ankle extensor muscles; LG, MG, Sol and Pl.

The axon is seen leaving the cell ventrally, then travels medially before taking a lateral projection towards the DLF.

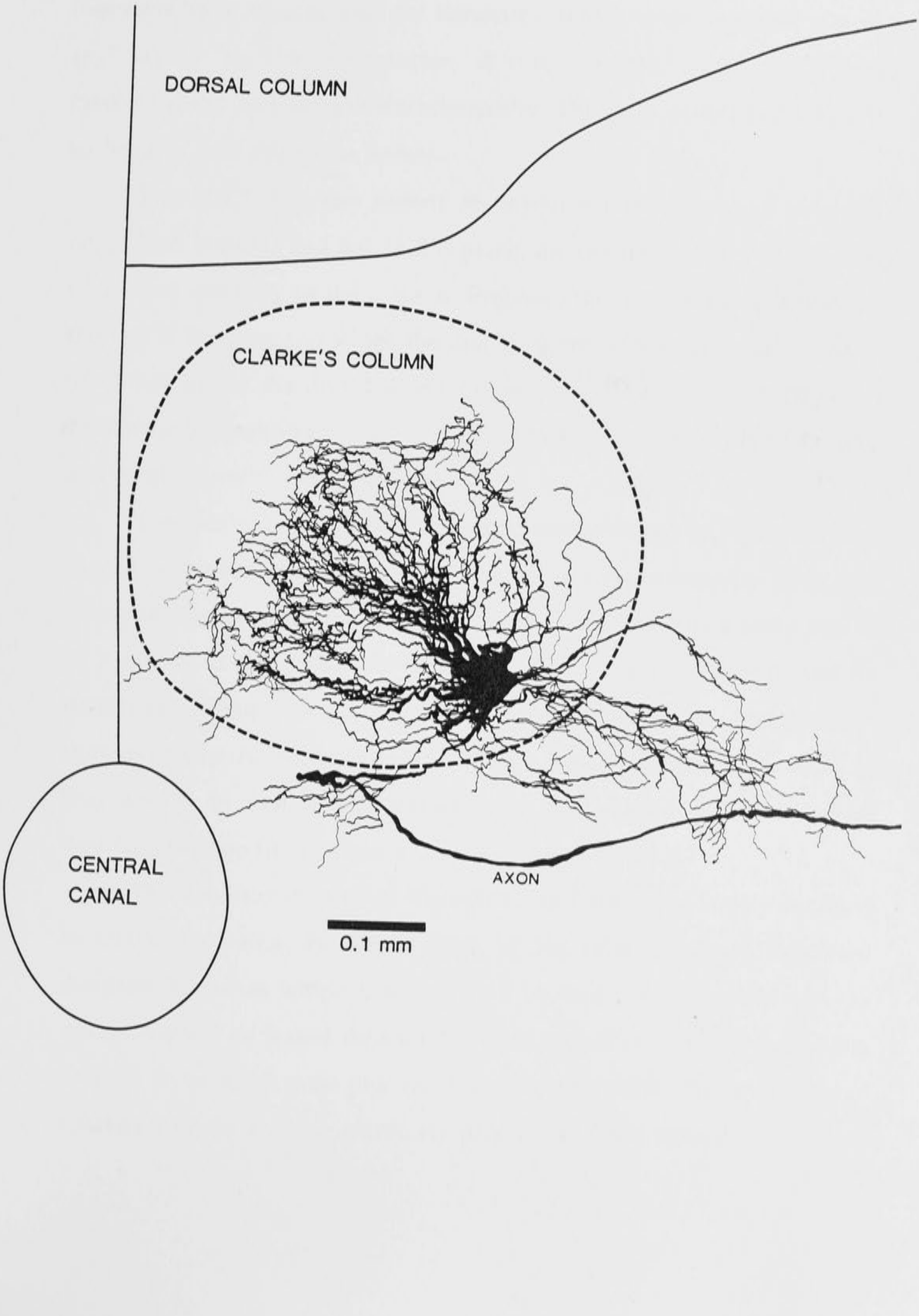
DORSAL COLUMN
CLARKE'S COLUMN
CENTRAL
CANAL
AXON
0.1 mm

Figure 3.4 shows a reconstructed DSCT neurone in Clarke's column which received input from plantaris muscle. This cell was relatively compact, and one of the smallest examined. In this plane, the cell body measures 35 x 45 µm, and the dendrites, which were confined almost exclusively to the boundaries of the column, extend 390 µm mediolaterally and 460 µm dorsoventrally. The axon of this cell was not sufficiently well stained to follow.

The DSCT neurone shown reconstructed in Figure 3.5 received input from both LG and Sol. In this plane, the cell body is 65 x 53 µm, and is situated centrally in the column. Probably the most striking feature of this cell is the extent to which the dendrites are seen to leave the column, up to 620 µm in the dorsal direction, and up to 450 µm ventrolaterally. The entire dorsoventral extent of the dendrites is approximately 1350 µm, and mediolaterally they extend for 770 µm.

The dendrites of the DSCT neurone reconstructed in Figure 3.6 also extend well beyond the column, up to 340 µm ventrolaterally. This cell, which received input from plantaris muscle only, exhibits a soma size of 55 x 50 µm in this plane. Its situation in the column is lateral, and its dendrites extend 700 µm in the mediolateral direction and 500 µm dorsoventrally. After leaving the soma, the axon takes a similar course to that shown in Figure 3.3, travelling in the medial direction before doubling back on itself to take a lateral course to the DLF.

The dendritic trees of all the cells reconstructed are largely confined to Clarke's column. However, most of the cells examined exhibited dendritic branches which extended well beyond Clarke's column in the dorsal, ventral or lateral directions. These projections can be quite long, and are on occasion quite profuse. The dendrites within the boundaries of Clarke's column are also extremely profuse, and can spread to occupy a

FIGURE 3.4

Reconstruction in the transverse plane of an HRP labelled DSCT neurone in Clarke's column. This neurone received group I afferent input from Pl.

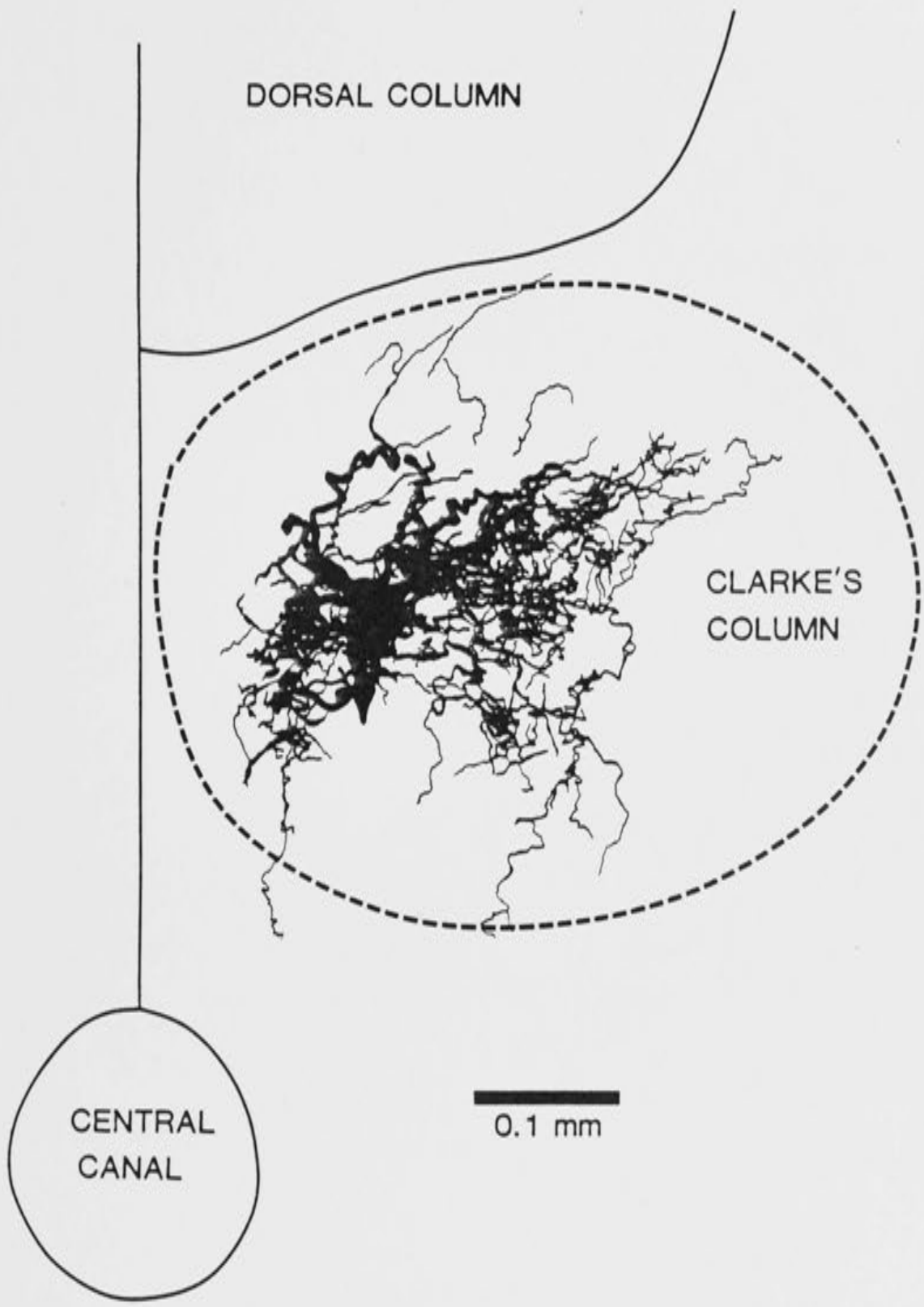
DORSAL COLUMN
CLARKE'S
COLUMN
CENTRAL
CANAL
0.1 mm

FIGURE 3.5

Reconstruction in the transverse plane of an HRP labelled DSCT neurone in Clarke's column. This neurone received group I afferent input from LG and Sol.

Note the dosoventral spread of dendrites, which extend beyond the Clarke's column boundary.

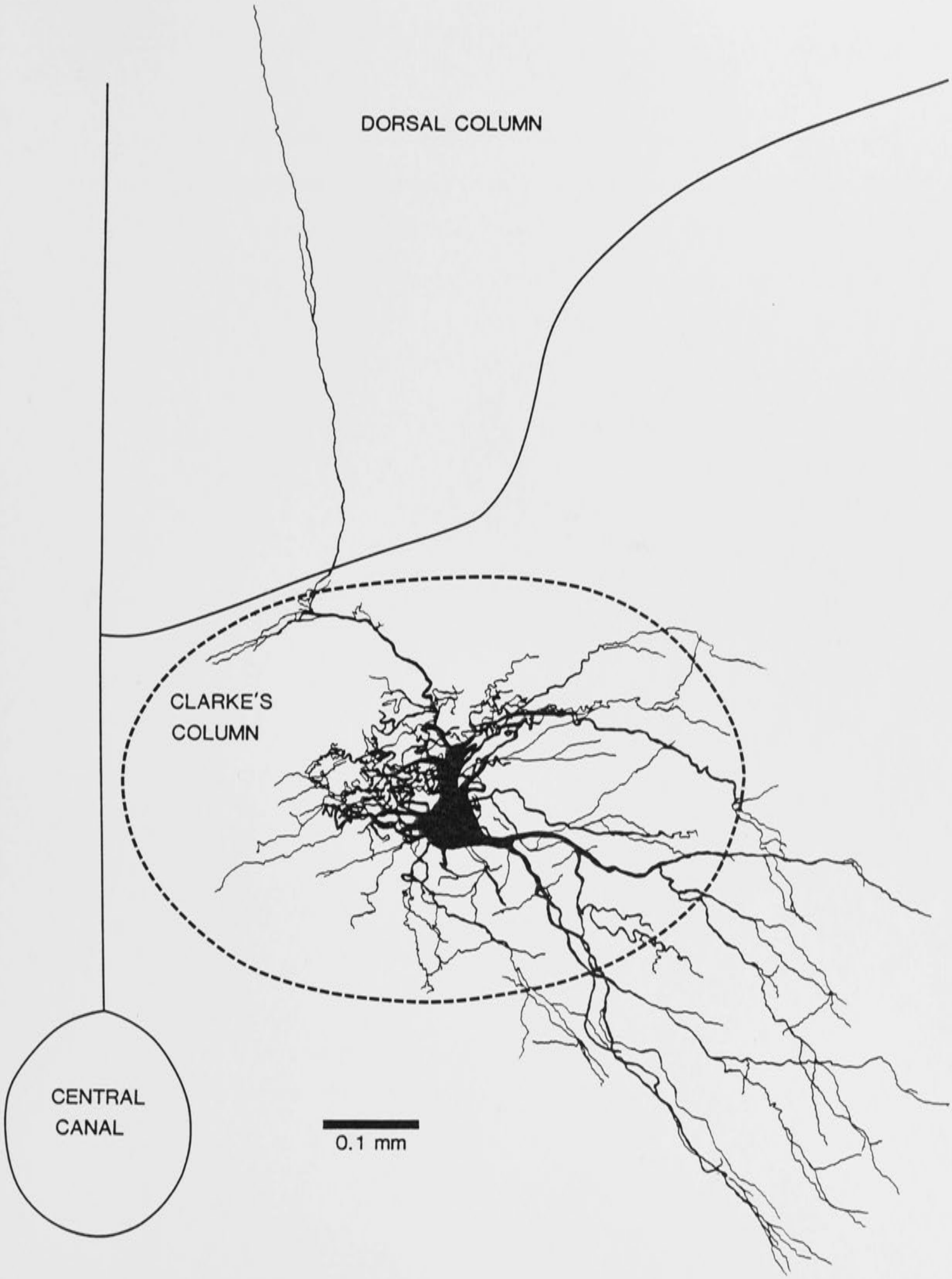
DORSAL COLUMN
CLARKE'S
COLUMN
CENTRAL
CANAL
0.1 mm

FIGURE 3.6

Reconstruction in the transverse plane of an HRP labelled DSCT neurone in Clarke's column. This neurone received group I afferent input from Pl. Note the lateral location of this cell within Clarke's column.

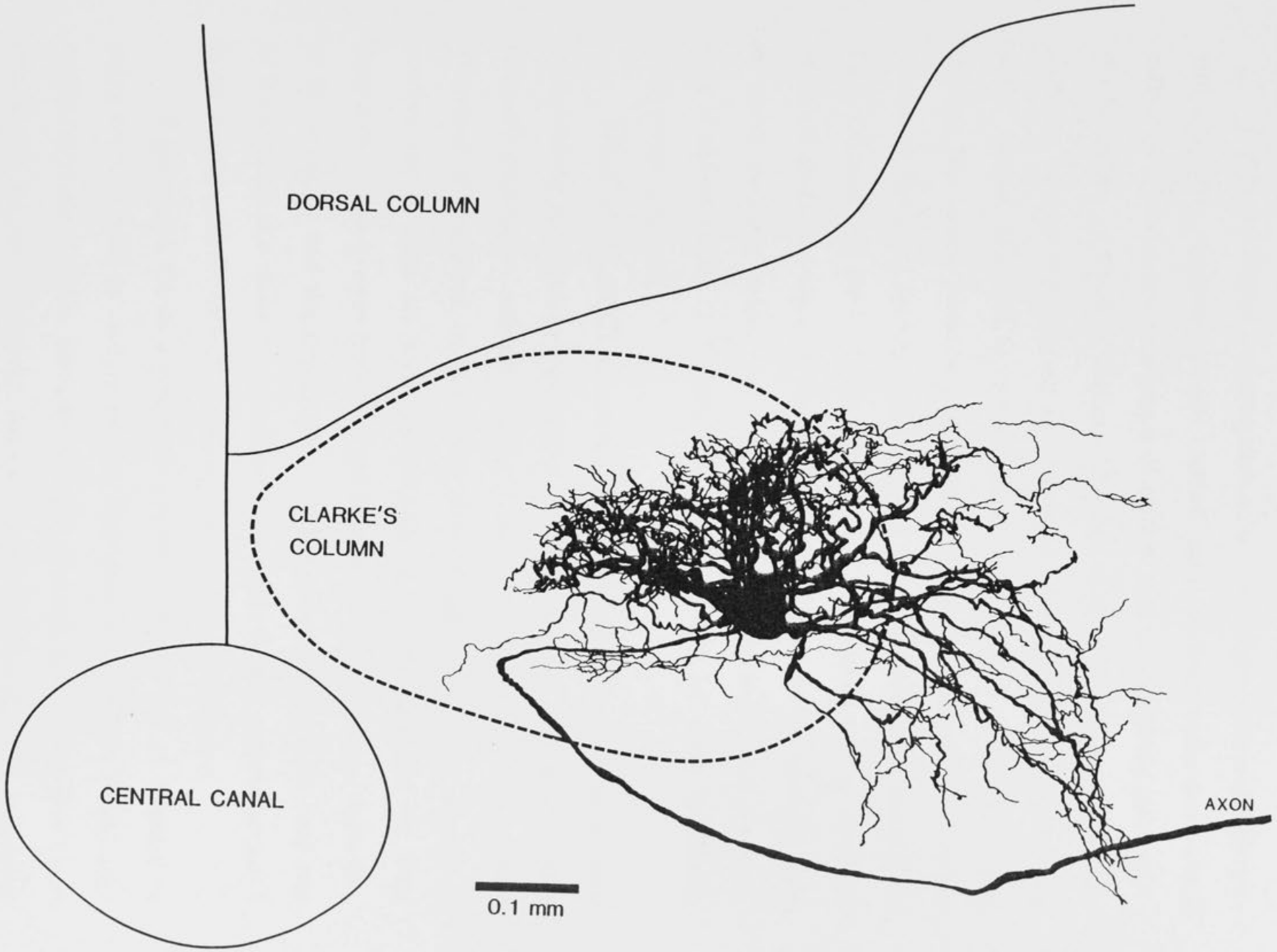
DORSAL COLUMN
CLARKE'S
COLUMN
CENTRAL CANAL
AXON
0.1 mm

region representing over 60% of the area of Clarke's column in cross section.

Figure 3.7 shows a reconstruction of the complete axonal trajectory and dendritic envelope (black shaded area) of four individual DSCT neurones. The dendritic envelope of cells A and C is confined entirely to the boundary of Clarke's column. The dendrites of cell B extend a short distance beyond the column in the dorsal direction, reaching into the white matter, and cell D exhibits more than half its dendritic spread beyond the lateral boundary of Clarke's column. Figure 3.7 shows the course of the axon leaving each cell and travelling laterally toward the DLF. On reaching the DLF, the axons of DSCT neurones change direction abruptly to ascend towards the cerebellum. Axons were occasionally seen to travel medially before changing direction and taking a lateral course. This is shown in Fig. 3.7D, and also in Fig. 3.3 and 3.6. Axon collaterals were never observed.

Many of the DSCT neurones recorded during the course of these experiments received group I input from more than one of the ankle extensor muscles. A summary of the muscle inputs received by 40 DSCT neurones is presented in Table 3.1. Five of these cells were shown to receive input from all 4 of the muscles, LG, MG, Sol and Pl. Two neurones received input from 3 of the muscles, 8 received input from two of the muscles, and the remaining 25 cells received input from only one of the muscles. Of these, two received input from lateral gastrocnemius, 8 from medial gastrocnemius, 7 from soleus and 8 from plantaris.

Figure 3.8A shows a schematic reconstruction of the L3 dorsal root entry zone, viewed in sagittal section. The location of 28 DSCT neurones receiving group I ankle extensor input is plotted, and shows that these cells could be recorded from rostral L3 past caudal L3. The apparent grouping or clustering of the cells towards the caudal end of L3 is not

TABLE 3.1

Summary of group I monosynaptic afferent input from ankle extensor muscles to 40 DSCT neurones recorded intracellularly in Clarke's column. Each cell received input from one or more of the ankle extensor muscles (LG, MG, Sol or Pl) as indicated by a dot.

CELL#	PL	SOL	MG	LG
1	•	•	•	•
2	•	•	•	•
3	•	•	•	•
4	•	•	•	•
5	•	•	•	•
6	•	•		•
7		•	•	•
8	•	•		
9	•	•		
10	•			•
11	•			•
12		•		•
13			•	•
14			•	•
15			•	•
16	•			
17	•			
18	•			
19	•			
20	•			
21	•			
22	•			
23	•			
24		•		
25		•		
26		•		
27		•		
28		•		
29		•		
30		•		
31			•	
32			•	
33			•	
34			•	
35			•	
36			•	
37			•	
38			•	
39				•
40				•

FIGURE 3.7

Reconstruction in the transverse plane of the axonal trajectory and dendritic envelope (black shaded area), of 4 DSCT neurones in Clarke's column. These neurones all received group I afferent input from ankle extensor muscles.

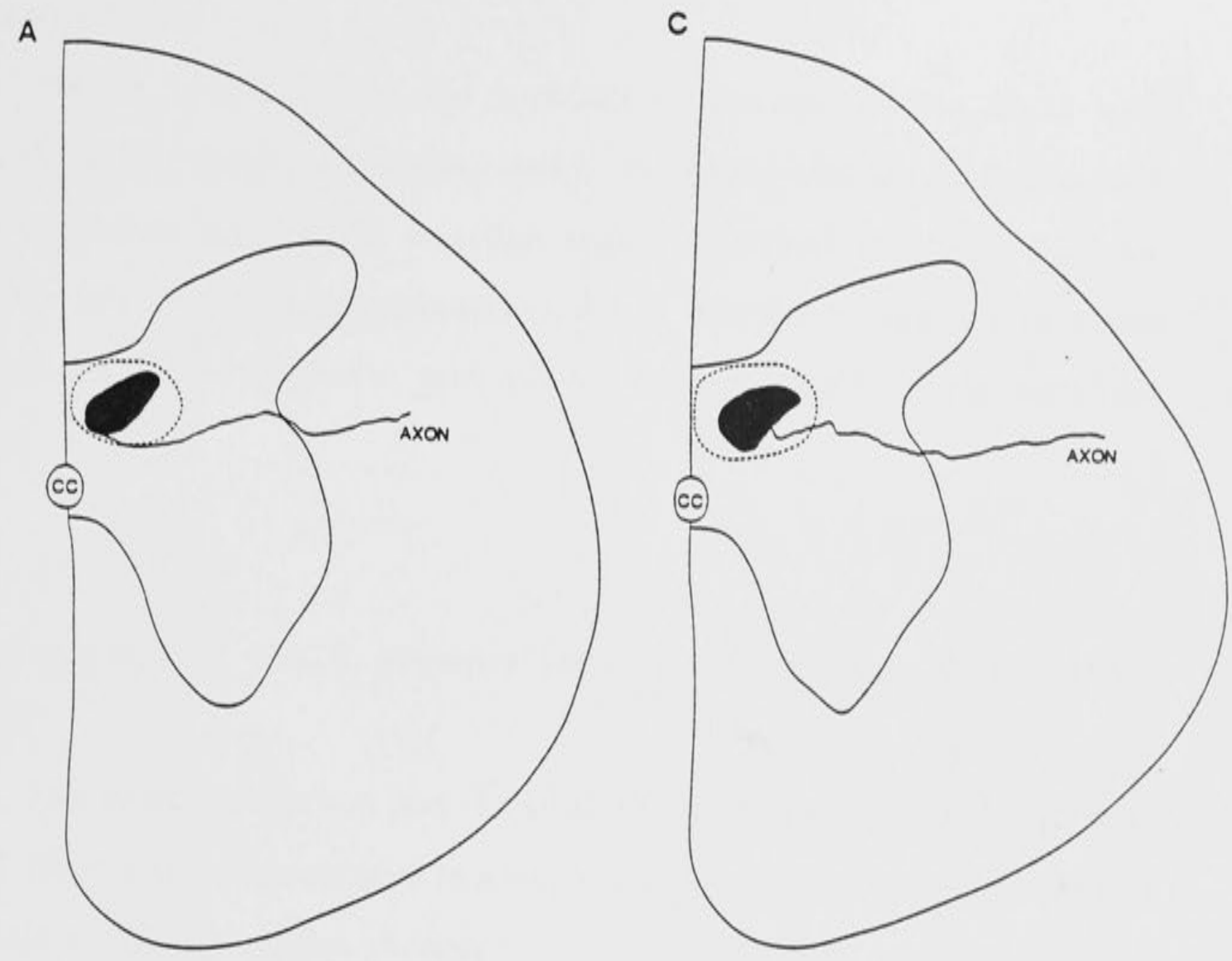
A
AXON
CC
C
AXON
CC
B
AXON
CC
D
CLARKE'S
COLUMN
CC
AXON
0.5 mm

thought to be significant, since this was the region in which most tracking was carried out.

Figure 3.8B indicates the location of the cell bodies of 12 well stained DSCT neurones, reconstructed in the transverse plane. Again each dot represents one DSCT neurone which received input from ankle extensor muscles. This reconstruction shows that these cells can be found throughout Clarke's column, and are not strictly confined to a particular region.

II. Morphology of DSCT neurones which receive functionally identified input.

The previous section has detailed the morphology and location of DSCT neurones which receive monosynaptic input from group I afferents of ankle extensor muscles. Access to these muscles was achieved through an extensive surgical procedure which required separation of the muscles, and dissection of their nerves and tendons.

This section describes results from a different series of experiments, in which the hindlimb was left intact, apart from placing a stimulating electrode on a small length of the sciatic nerve. Occasionally, short lengths of sural nerve, and/or triceps surae nerves, were also cleared and mounted on stimulating electrodes. Each DSCT neurone impaled was subsequently characterised as receiving input from deep (muscle and/or joint), cutaneous or convergent (deep + cutaneous) receptors (see Chapter 2: Methods), and the results for each of these groups, obtained from 36 experiments on adult cats, are now presented.

i) DSCT neurones which receive deep input.

Deep input to the DSCT neurones, which included input from both muscle and/or joint receptors, was established on the basis of their response to squeezing or manipulation of various joints and muscles in the intact hindlimb. Figure 3.9 shows a DSCT neurone which received input from muscles in the region of the thigh, reconstructed in the sagittal plane. The soma of this neurone measures 47 x 119 μm, and 10 primary dendrites are exhibited. The dendritic tree of this neurone is oriented primarily along a rostrocaudal axis, extending over 2760 μm in this direction. Several dendritic branches can also be seen to leave the soma in a ventral direction, and the total dorsoventral extent of the dendritic tree is 570 μm. The dendritic tree of this cell shows a profuse, extremely complex branching pattern, with many small branchlets and extrusions from the dendrites.

Figure 3.10 shows a DSCT neurone reconstructed in the sagittal plane, which received group I input from triceps surae muscles only, (identified by electrical stimulation of the muscle nerves). The soma of this cell measures 58 x 100 μm, and its 8 primary dendrites give rise to a more closely confined dendritic tree than that of the cell shown in Fig. 3.9, reaching 2570 μm in the rostrocaudal direction, and only 276 μm in the dorsoventral direction. However, the dendrites are shown to branch and exhibit many fine branchlets and extrusions along their length. The axon (marked with an arrow) of this cell is clearly shown leaving the ventral surface of the cell body, before taking a lateral course to the DLF.

The cell shown reconstructed in Fig. 3.11 received group I muscle input from the toe extensor muscles. This cell was situated almost exactly in the centre of Clarke's column, as can be seen from the reconstruction. The soma of this cell is 56 x 135 μm, and again the well filled axon (arrow) can be seen leaving the ventral surface of the soma. The 13 primary

FIGURE 3.8

A. Schematic reconstruction in the sagittal plane of the L3 dorsal root entry zone, with the recorded position of 28 DSCT neurones receiving ankle extensor input marked as individual dots.

B. Schematic reconstruction in the transverse plane showing the position of 12 DSCT neurones in Clarke's column. These neurones all received group I afferent input from ankle extensor muscles.

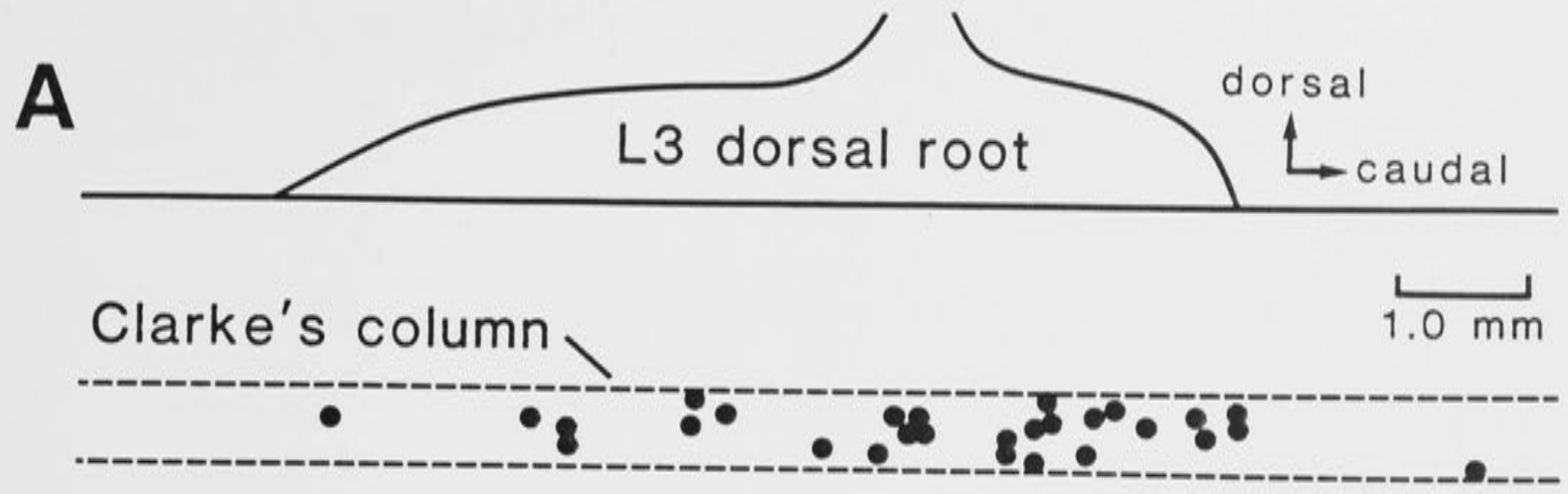
A
L3 dorsal root
dorsal
caudal
Clarke's column
1.0 mm

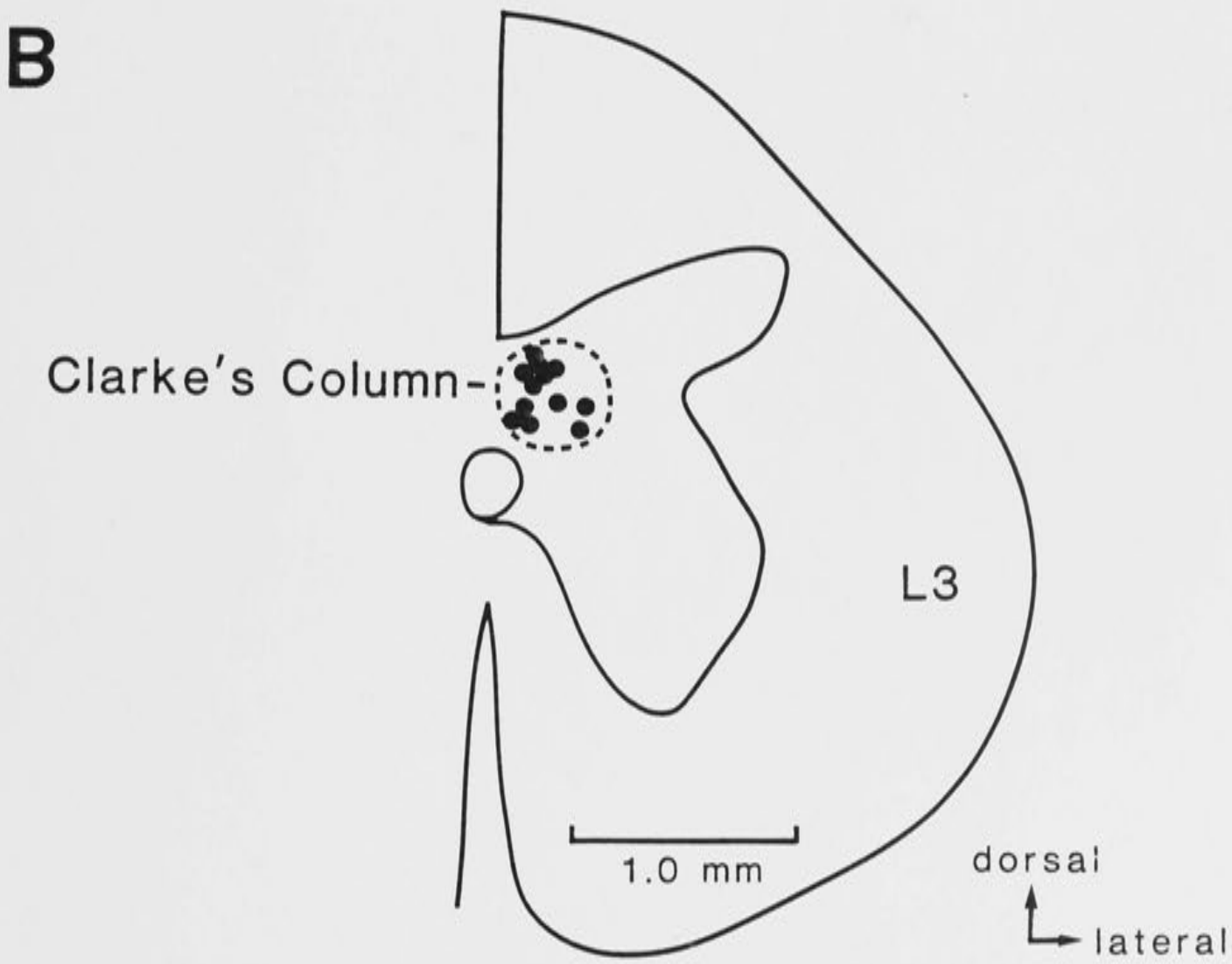
B
Clarke's Column
L3
1.0 mm
dorsal
lateral

FIGURE 3.9

Reconstruction in the sagittal plane of an HRP labelled DSCT neurone in Clarke's column. This neurone received muscle input from the thigh. The dorsal boundary of Clarke's column is indicated by an unbroken line. The axon is indicated with an arrow.


100 um

FIGURE 3.10

Reconstruction in the sagittal plane of an HRP labelled DSCT neurone in Clarke's column. This neurone received group I afferent input from triceps surae muscles.

The dorsal boundary of Clarke's column is indicated by an unbroken line.

The axon is indicated with an arrow.

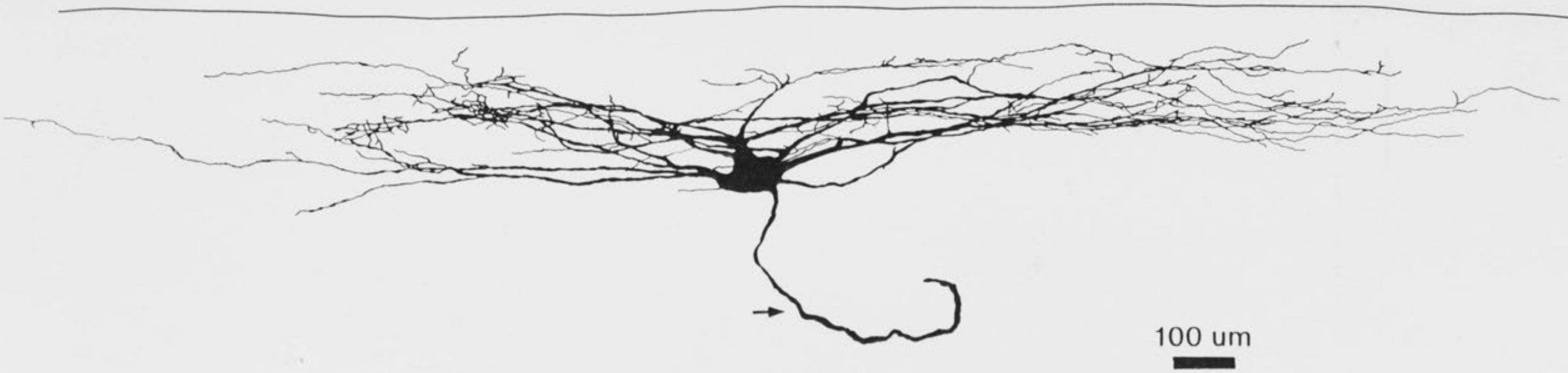
100 um

FIGURE 3.11

Reconstruction in the sagittal plane of an HRP labelled DSCT neurone in Clarke's column. This neurone received group I afferent input from toe extensor muscles.

The boundary of Clarke's column is indicated by unbroken lines.

The axon is indicated with an arrow.

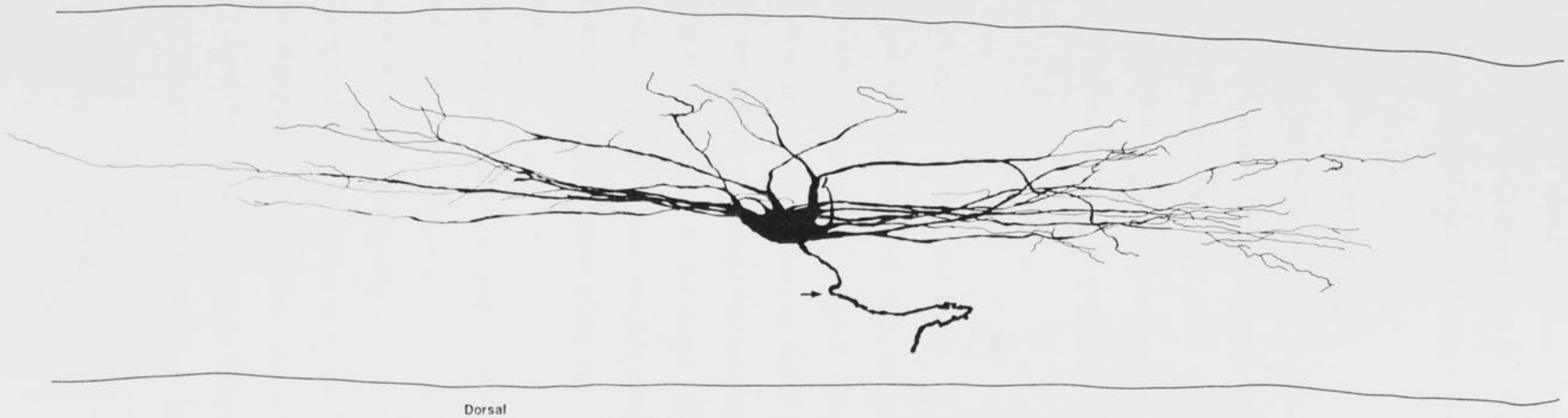
Dorsal
Rostral
100 um

dendrites of this cell branch and reach 2470 μm rostrocaudally, and although they are not as profuse and complex as those shown in previous reconstructions, are shown to exhibit many fine branchlets.

ii) DSCT neurones which receive cutaneous input.

In the present series of experiments, only 6 DSCT neurones were found to receive purely cutaneous input. Although attempts were made to inject HRP into these cells, unfortunately none were sufficiently well stained to attempt reconstruction. However, these observations verify the existence of such cells in Clarke's column, in accordance with Randic et al. (1981).

iii) DSCT neurones which receive convergent input.

Cells were classified as convergent if they were demonstrated to receive both cutaneous and deep input. In each case, the cutaneous receptor type and field was identified, and deep input was examined as described previously, by squeezing of muscle bellies and manipulation of joints. These cells were generally found at the same spinal level as those which receive muscle afferent input from the hindlimb, at the caudal region of the L3 dorsal root entry zone through to the rostral root of the L4 dorsal root entry zone.

Figure 3.12 shows a reconstruction in the sagittal plane of a DSCT neurone which received input from group I muscle afferents of triceps surae muscles, in addition to Slowly Adapting Type I and Hair Follicle afferent input from the foot, and was thus classified convergent. The cell body of this neurone was elongated and flattened, measuring 103 x 33 μm, and exhibiting 9 primary dendrites. These dendrites branch profusely, and extend 2470 μm in the rostrocaudal direction. In the dorsoventral

FIGURE 3.12

Reconstruction in the sagittal plane of an HRP labelled DSCT neurone in Clarke's column. This neurone received convergent input from triceps surae muscles, in addition to Slowly Adapting Type I and Hair Follicle afferent input from the foot, and was thus classified convergent.
The dorsal boundary of Clarke's column is indicated by an unbroken line.
The axon is indicated with an arrow.


100 um

direction, the dendrites extend 577 µm, and some are shown to leave the column in the dorsal direction.

Dendrites are also shown to leave the column in the reconstruction in Fig. 3.13, again in the dorsal direction. This DSCT neurone received input from the hair receptors on the toes, and also received deep input from the foot region, and is thus classified as convergent. This cell had a soma size of 105 x 38 µm, and 12 primary dendrites extending 2790 µm rostrocaudally, and 602 µm dorsoventrally.

III. Cutaneous afferent input to Clarke's column.

During the course of the 36 experiments in which attempts were made to label DSCT neurones receiving cutaneous or convergent input, attempts were also made to label cutaneous afferents in the dorsal columns, and to examine the termination patterns of their collaterals in Clarke's column.

Figure 3.14 shows a reconstruction, in sagittal section, of a hair follicle afferent, which was located in the dorsal columns at the boundary of L3 /L4, and whose receptive field was located on the lateral surface of the foot. This afferent was intensely labelled with HRP reaction product, and could be followed over 7.7 mm rostrocaudally in the dorsal columns. A single collateral left the afferent in the ventral direction and could be followed 460 µm towards the grey matter. This collateral could not, however, be followed to termination in Clarke's column, despite the extremely intense labelling of the parent axon.

A similar situation is shown in Fig. 3.15. This is a further example of a hair follicle afferent, labelled at the L3/L4 boundary in the dorsal columns. This afferent was intensely stained, and could be followed for over 6 mm in the dorsal columns (total extent not shown in the reconstruction). Over this lengh the afferent branched twice, sending two

FIGURE 3.13

Reconstruction in the sagittal plane of an HRP labelled DSCT neurone in Clarke's column. This neurone received convergent input from muscle and hair afferents from the foot region.

The dorsal boundary of Clarke's column is indicated by an unbroken line.

The axon is indicated with an arrow.

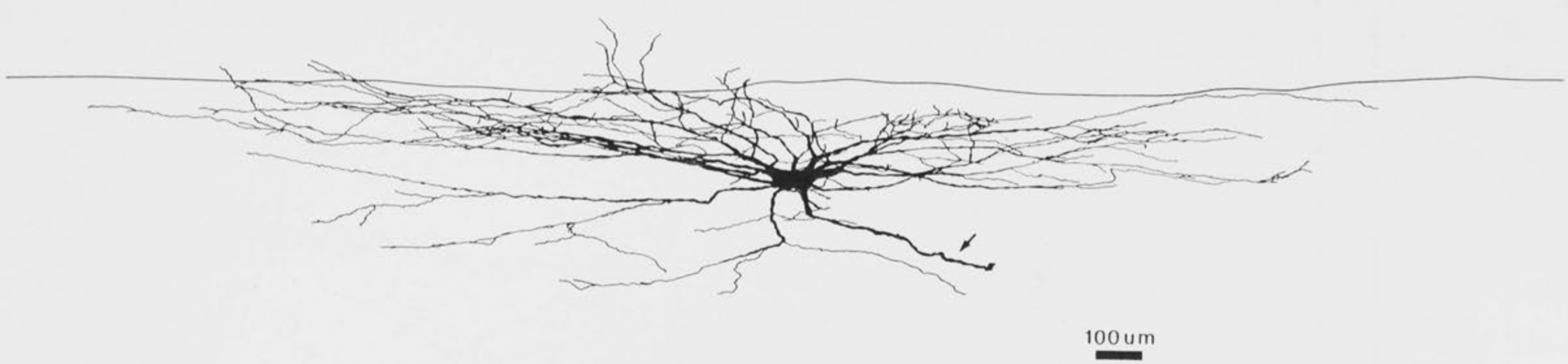
100 um

FIGURE 3.14

Reconstruction in the sagittal plane of a hair follicle afferent in the dorsal column at the L3/L4 spinal level.

One collateral leaves the afferent ventrally, but could not be followed into the grey matter.

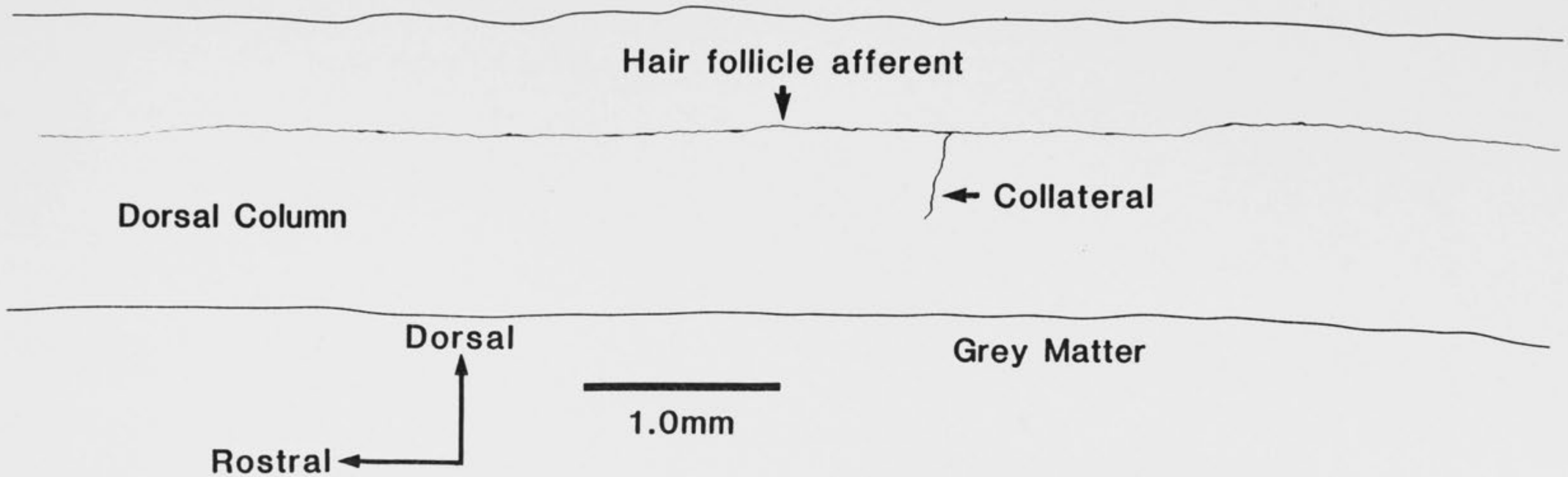
Hair follicle afferent
Collateral
Dorsal Column
Grey Matter
Dorsal
Rostral
1.0mm

FIGURE 3.15

Reconstruction in the sagittal plane of a hair follicle afferent in the dorsal column at the L3/L4 spinal level.

Arrows at both ends of the main fibre indicates that the reconstruction does not show the full recovered length of that fibre, which extended over 6 mm.

Two collaterals leave the afferent ventrally, but could not be followed to termination in the spinal grey.

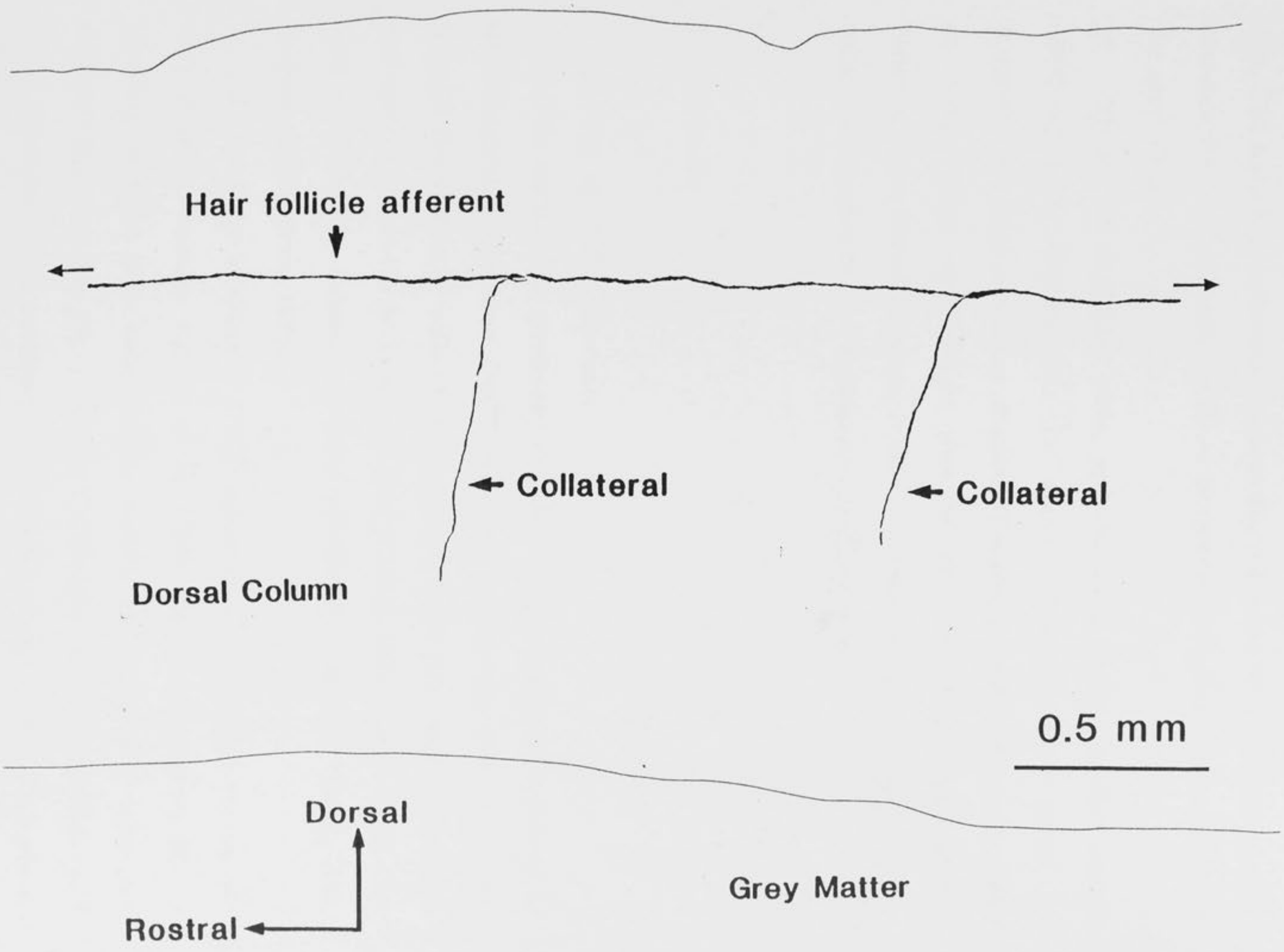
Hair follicle afferent
Collateral
Collateral
Dorsal Column
0.5 mm
Dorsal
Rostral
Grey Matter

collaterals ventrally towards the grey matter in the same manner described in Fig. 3.14. The distance between these two collaterals was 1.15 mm. The collaterals were followed for 850 μm and 670 μm. However, this distance was not sufficient to allow observation of their terminations in the grey matter.

These two examples were, unfortunately, typical of the results obtained from experiments in which attempts were made to intracellularly label cutaneous afferents. Despite intense labelling of many cutaneous fibres, which could often be followed over a considerable distance in the dorsal columns, it was not possible to follow any of their collateral branches to their destination in the grey matter.

3.4 Discussion

Morphology of DSCT Neurones

This chapter has presented results on the detailed morphology of physiologically identified DSCT neurones in Clarke's column. In his original description of cells in the column, Clarke proposed an intricate and complex dendritic branching pattern (Clarke, 1851,1859), and this has been supported by subsequent Golgi studies of these cells (Cajal, 1909; Boehme, 1968; Loewy, 1970).

Intracellular labelling of DSCT neurones with HRP has shown two very different results. Randic et al. (1981), in the first intracellular labelling study on these cells, showed them to be simple, with truncated dendritic branches (see Fig. 1.2 B and C). Houchin et al. (1983) examined DSCT neurones which receive group I afferent input from the hindlimb, and showed these cells to be large, with extremely complex, profusely branched dendrites which exhibited many fine branchlets and extrusions.

The results of the present study are in direct accordance with the findings of Houchin et al. (1983). DSCT neurones which receive muscle or convergent (deep + cutaneous) input from the hindlimb were shown to be large bodied cells, whose dendrites can extend approximately 3 mm in the rostrocaudal direction, and up to 800 μm dorsoventrally (see 3.3 Results). In the transverse plane, the dendritic spread is much more restricted (see 3.3 Results, section I.) Both Szentagothai (1961) and Rethelyi (1968) suggested that if the cells were to occupy neatly defined geometric spaces, then in an idealized situation, 6 such cells could fit across the column with little intermingling. However, the present results show that the dendritic branches of any one cell can cover an extensive area of Clarke's column, spreading throughout 50% or more in cross section, and often extending well beyond the column in the dorsal, lateral or ventral directions. An interesting observation was that individual dendrites were occasionally seen to reach some distance into the white matter of the dorsal columns.

White matter dendrites have been observed arising from cervical motoneurones by Rose and Richmond (1981). Electron microscopy further showed these dendrites to receive synaptic contacts within the white matter (Rose and Richmond, 1981). Hongo (1985) noted, in accordance with Houchin et al. (1983), that very few of the dendrites of DSCT neurones are seen to extend beyond the boundaries of Clarke's column. In contrast, the findings of the present study show that the dendrites of DSCT neurones commonly extend well beyond the column boundary, and one example was illustrated in which over half the dendritic spread was outside Clarke's column.

The axons of DSCT cells which receive group I muscle input from the ankle extensor muscles were all seen to take a similar path, leaving the column in a ventral direction before travelling laterally to the DLF (in

which they ascend to the cerebellum as the DSCT). Axon collaterals were never observed in the cells labelled in this study, in accordance with Houchin et al. (1983).

Both the study of Houchin et al. (1983) and the present study show DSCT neurones to be more highly complex than suggested by the reconstructed cells presented in the study by Randic et al. (1981). Houchin et al. (1983) suggested that the cells presented in that earlier study were not completely HRP filled, and subsequent observations, made during the course of this study, of cells which did not receive sufficient HRP, also suggest this possibility. Randic et al. (1981) attempted to categorize DSCT cells into morphological groupings, which they proposed might correlate with the function of the neurone. Thus they suggested that DSCT neurones with muscle input had larger cell bodies and longer, more complex primary dendrites than those which receive convergent input. DSCT neurones which receive convergent input were suggested to have smaller cell bodies, with fewer primary dendrites, exhibiting simple branching patterns. In contrast, the present study has shown that DSCT neurones which receive convergent input can be large, with profusely branched dendritic trees, and of a similar morphology to DSCT neurones receiving purely muscle afferent input.

It should be noted that, because of the considerable difficulties in obtaining stable intracellular recordings of DSCT neurones, both the present observations and those of Randic et al. (1981), are based on a restricted sample size. However, the present observations clearly indicate that subclasses of DSCT neurones cannot be immediately identified on the basis of their size or dendritic morphology.

Location and Somatotopy of DSCT cells in Clarke's column.

Kuno et al. (1973a,b) proposed that the somata of the DSCT neurones in Clarke's column were somatotopically organized, showing that cells which receive input from gastrocnemius/soleus muscles were more medially located than cells which receive triceps femoris input.

Hongo and coworkers (Hongo et al., 1982; Hongo, 1985) have returned to the question of somatotopic location of the cell bodies of DSCT neurones, concluding that, in the transverse plane, the cells are arranged with respect to the proximity of the muscle supplying their major synaptic input. In this scheme, DSCT neurones which receive toe muscle input are located dosomedially in the column, those with shank input in the intermediate region, and those receiving input from thigh muscles in the ventrolateral zone. Hongo (1985) has proposed that these regions are quite definite (although they exhibit some overlap), with both the cell body and the dendrites confined to their respective functional regions.

In the present study, cells which receive input from ankle extensor muscles were physiologically identified and labelled intracellularly before reconstruction in the transverse plane. These cells correspond with those receiving shank muscle input under the classification of Hongo (1985). Examples presented in 3.3 Results, of DSCT neurones which receive group I input from ankle extensor muscles show that these cells can be located throughout Clarke's column in the transverse plane. This does not mean, of course, that there may not be a general trend for these cells to be located in a particular region of Clarke's column. In fact, a plot of the location of DSCT neurones presented in Figure 3.8 indicates a possible clustering of these cells towards the medial region, which would concur with Kuno et al. (1973a,b) and Hongo (1985) that DSCT neurones receiving input from ankle extensor muscles are medially located in the column.

Nevertheless, DSCT neurones receiving ankle extensor input were located in other regions of the column, including the dorsomedial and the ventrolateral regions. Furthermore, the cell bodies of these neurones are extremely large, and the dendritic trees, rather than being confined to functional zones, were found to branch and occupy up to 60 % or more of the transverse area of Clarke's column, and often to extend well beyond the column.

The results presented in this chapter do not, therefore, provide convincing support for a strict musculotopic arrangement of the cell bodies in Clarke's column. The wide spread of the dendrites both within and outside Clarke's column raises interesting questions regarding the nature and origin of synaptic input to these cells, and this issue is discussed further in Chapter 5.

CHAPTER FOUR

A SERIAL SECTION ELECTRON MICROSCOPE STUDY OF AN IDENTIFIED, HRP-LABELLED Ia COLLATERAL IN CLARKE'S COLUMN.

CHAPTER FOUR: A SERIAL SECTION ELECTRON MICROSCOPE STUDY OF AN IDENTIFIED, HRP LABELLED Ia COLLATERAL IN CLARKE'S COLUMN.

4.1 Introduction

The anatomy of afferent input to Clarke's column has been studied using degeneration techniques after lesion of dorsal roots in the cat (eg. Pass, 1933; Liu, 1956; and Grant and Rexed, 1958) and in the dog (Szentagothai and Albert, 1955). Golgi techniques have also been employed to determine the trajectory of afferent collaterals to the column (Boehme, 1968; Rethelyi, 1968). Such studies have provided much useful information on the pattern of afferent terminations within the column, although the source of the afferent input was unknown.

More recently, Tracey and Walmsley (1984) examined intracellularly labelled group Ia and Ib muscle afferent collateral terminations in Clarke's column, after first retrogradely labelling DSCT neurones by injection of HRP into the anterior lobe of the cerebellum. They showed the rostrocaudal extent of the terminations of any one collateral to be restricted to < 1mm in the column. Both Ia and Ib afferents were shown to make *en passant* and terminal connections with the soma and proximal dendrites of labelled neurones, and both Ia and Ib afferents were shown to exhibit a range of bouton sizes from small (1 x 1 μm) to giant boutons (up to 18 x 3 μm). Prior to the study of Tracey and Walmsley (1984) giant boutons in Clarke's column were believed to be terminations of group Ia muscle afferents. This was due to their degeneration after lesion of the dorsal roots (Szentagothai and Albert, 1955; Rethelyi, 1970) and their similarity to the Ia afferent terminations observed by Conradi (1969) on motoneurones (Saito, 1974, 1979).

During the course of the present study, Hongo et al. (1987) have carried out an examination of the trajectory of identified HRP labelled collaterals of Ia and Ib afferents into Clarke's column. They found that the ascending hindlimb muscle afferent fibres were segregated in the dorsal funiculus according to the proximity of the muscle of origin, and that this topographic organization was carried over to collateral ramification within the column. The afferent termination patterns described by Hongo et al. (1987) were similar to those recognized in an earlier Golgi study by Rethelyi (1968). Fibres from toe muscles were found to enter the column dorsomedially, terminating in the dorsal third of the column. Fibres from shank muscles entered Clarke's column from the dorsal direction, and terminated both in the intermediate region of the column, and also in laminae V-VII. Collaterals from thigh muscles passed through the lateral portion of Clarke's column, or passed laterally to it, and terminated in the ventrolateral part of the column or in laminae V-VIII. Afferents of hip muscle origin generally passed lateral to Clarke's column, terminating in laminae VII-IX (Hongo et al., 1987). This indicated that both the afferents in the dorsal columns, and the collateral ramifications in Clarke's column obeyed somatotopic patterns of organization. This organization appeared to depend on the proximity of the muscle of origin, rather than to the fibre type, or site of entry to the cord. Hongo et al. (1987) subsequently attempted to correlate this finding of topographic organization of the afferent terminations in Clarke's column with a previous finding of somatotopic organization of the cell bodies within Clarke's column (Hongo, 1985: see Chapter 3). This study (Hongo et al., 1987) was also the first study to decribe giant boutons situated outside the boundary of Clarke's column.

Neither the study of Tracey and Walmsley, (1984) nor that of Hongo et al. (1987), examined the ultrastructure of identified terminations in

Clarke's column. Sedar and Moskowitz (1967) determined that both E and I type boutons (Uchizono, 1965) or Gray type 1 and Gray Type 2 boutons (Gray, 1959) existed within Clarke's column. Rethelyi (1970) examined bouton types within Clarke's column, and confirmed ultrastructurally the presence of the giant boutons first described in a degeneration study by Szentagothai and Albert, (1955). Rethelyi (1970) observed 3 other bouton types within Clarke's column, including small boutons presynaptic to the giant boutons, which, in accordance with Gray (1959) were presumed to represent the morphological correlate of presynaptic inhibition within the column. Rethelyi (1970) also showed that the giant boutons could exhibit more than one synaptic specialization, or release site (see Chapter 1, Figs. 1.3 and 1.4).

Saito (1974) subsequently carried out an ultrastructural study of Clarke's column, and reported 6 distinct bouton types. Ultrastructural observations of DSCT cells in Clarke's column labelled retrogradely by injection of HRP into the anterior lobe of the cerebellum, have confirmed that each of the 6 bouton types in Clarke's column are associated with these cells (Saito, 1979; Houchin et al., 1983).

Despite these ultrastructural findings, no previous study has attempted an ultrastructural examination of identified afferent terminations in Clarke's column. Such a study was regarded as being extremely important to our understanding of synaptic transmission between primary afferent fibres and neurones in Clarke's column, and more generally to an understanding of synaptic transmission in the central nervous system.

Electrophysiological experiments on synaptic input to DSCT neurones in Clarke's column have attempted to relate properties of the synaptic potentials to morphological specializations at the synaptic connection. Kuno et al. (1973a,b) proposed that the different size of the

EPSP evoked in DSCT neurones on stimulation of muscle, or cutaneous afferents, might be related to different types of synaptic boutons contacting these cells. Thus ultrastructural observation of the bouton was proposed as a method for identifying the afferent type from which it arose. Tracey and Walmsley (1984) based their hypothesis regarding fluctuations in the amplitude of single fibre EPSPs evoked in DSCT neurones on the existence of multiple synaptic transmitter release sites in the giant boutons at this connection, as demonstrated by Rethelyi (1970). In fact, many of the current theories concerning synaptic transmission rely on ultrastructural observation of boutons and release sites.

In view of a need for ultrastructural evidence, several series of experiments were initially carried out with the aim of determining the ultrastructural morphology of identified afferent terminations in Clarke's column. The results of two of these studies have already been published in the Journal of Neuroscience, and they are presented as Appendices I and II. Further results from these studies are also included in Chapter 5.

Following these studies, it was proposed that a project be attempted in which full ultrastructural details of identified afferent collateral terminations in Clarke's column would be examined. All previous electron microscope studies of identified afferent terminations in the spinal cord, including those presented in Appendices I and II and Chapter 5, have examined selected boutons arising from a particular afferent collateral. Most concentrate directly on the synaptic surface and specializations, and present little other morphological detail on the bouton or collateral. Although these observations are extremely useful, they do not present a full picture of the branching and termination pattern of the afferent collateral at an ultrastructural level. Such features as the myelination pattern of the collateral, and its relationship to the synaptic boutons arising from the collateral, could provide information

important to the understanding of the nature of propagation of the presynaptic action potential, and subsequently to the nature of transmitter release.

The present study provides these results in an ultrastructural examination of an entire afferent collateral, including its branches and terminations, within Clarke's column. Although this study was extremely time consuming, taking over two years to complete, the results provide a unique and valuable picture not obtained by previous ultrastructual studies of identified afferent terminations in the spinal cord. The implications of these results are discussed at the end of this chapter, and in conjunction with other results in the General Discussion of Chapter 5.

4.2 Methods

The experimental method is described in full in Chapter 2. An electrophysiological experiment was performed in which horseradish peroxidase was ionophoresed into a plantaris Ia muscle afferent at the L3/L4 boundary of the dorsal columns. Five such experiments were conducted before a satisfactory staining result was achieved. Perfusion and fixation were carried out as described in Chapter 2, and spinal segments L3 and L4 removed. 100 μm thick sagittal sections were subsequently cut on a Vibratome vibrating tissue slicer, and reacted using DAB as the chromogen (Adams, 1977, 1981). After rinsing, the sections were immersed in glycerol and carefully scanned under the light microscope. Sections containing the collateral were easily identified. The collateral was observed in two consecutive 100 μm thick sections. The collateral was photographed and carefully traced out using a drawing tube attachment. Other landmarks such as blood vessels were also traced in order to

facilitate later orientation of the sections under the electron microscope. Small sections of tissue including and surrounding the stained collateral were then excised. Those blocks underwent secondary fixation in $Os0_4$ and were dehydrated, impregnated and embedded in Spurr's resin as described in Chapter 2: Methods. After curing, each block was trimmed to present as a pyramid, with a trapezoidal block face, largest dimensions 1 x 1 mm. The large size of the block face was necessary to ensure inclusion of all the HRP stained collateral. This large size was somewhat unfortunate as it made handling of the tissue more difficult, and meant that a maximum of two sections could be retrieved on any one slot grid. This naturally meant a huge increase in the time taken coating slot grids and post staining sections. Serial sections were cut using a Diatome diamond knife on a Reichert Ultracut E ultramicrotome. In order to include the entire collateral, a large number of sections were required. 1275 sections were taken from the first block, and 764 from the second. The sections were collected on copper slot grids, and drop stained with lead citrate and uranyl acetate as described in Chapter 2. Great care was taken to ensure that the grids (and thus sections) were kept in order, and the inevitable loss or damage kept to a minimum.

Each section was subsequently examined and photographed using a JEOL 100C electron microscope operating at 80 kV. Some initial technical service problems with this microscope are, unfortunately, reflected in the quality of some of the sections presented. For serial section electron microscopy, stability of the machine and reliability of performance are of utmost importance throughout the duration of the project. Unfortunately, for the first 6 months of this study these were less than optimal. This particular study involved use of the microscope over a 2 year period, with approximately 15,000 micrographs taken, using 70 mm cut plate film. Every photograph was developed and contact printed.

From these contact prints, a sequence of sections through each bouton was chosen for presentation. These sections were chosen for clarity and inclusion of morphological detail, and are presented in the following section, 4.3 Results.

4.3 Results

Initial observation of the HRP stained plantaris Ia collateral was carried out using an Olympus microscope while the sections were immersed under glycerol. The complete collateral appeared in two 100 µm thick sagittal sections of the lumbar spinal cord. The collateral was traced out at 400x using a drawing tube attachment, and photographed. Figure 4.1 shows one of the sagittal sections in which the HRP labelled Ia afferent appeared. Although the afferent is not in the plane of focus throughout this micrograph, 3 regions of the collateral are clearly indicated as A,B and C. This micrograph shows the contrast which existed between the HRP labelled profile and the background tissue. Figure 4.1 also shows 3 examples at higher magnification of HRP labelled boutons photographed while the sections were immersed in glycerol.

Figure 4.2 shows a reconstruction of the entire collateral from its entry to the spinal grey matter to its termination in Clarke's column. The collateral entered the spinal grey at the mid L3 level amongst a thick bundle of fibres. Approximately 120 µm into the grey matter the collateral abruptly changed direction to orient in a ventrocaudal direction for most of its length. A number of branch points were identified under the light microscope, and these were carefully traced. Boutons were recognized as dark, dense areas, often wider than the diameter of the collateral itself. At a number of points the true nature of the collateral morphology was difficult to determine. However, extreme care was taken to reproduce the

FIGURE 4.1

The upper photomicrograph shows a single 100 μm thick sagittal section of lumbar spinal cord in which the HRP labelled plantaris Ia afferent collateral can be seen. The collateral is not in the plane of focus throughout the micrograph, but is clearly indicated in three distinct places (A, B and C).

A, B and C. Examples of HRP labelled boutons along the length of the plantaris Ia afferent collateral.

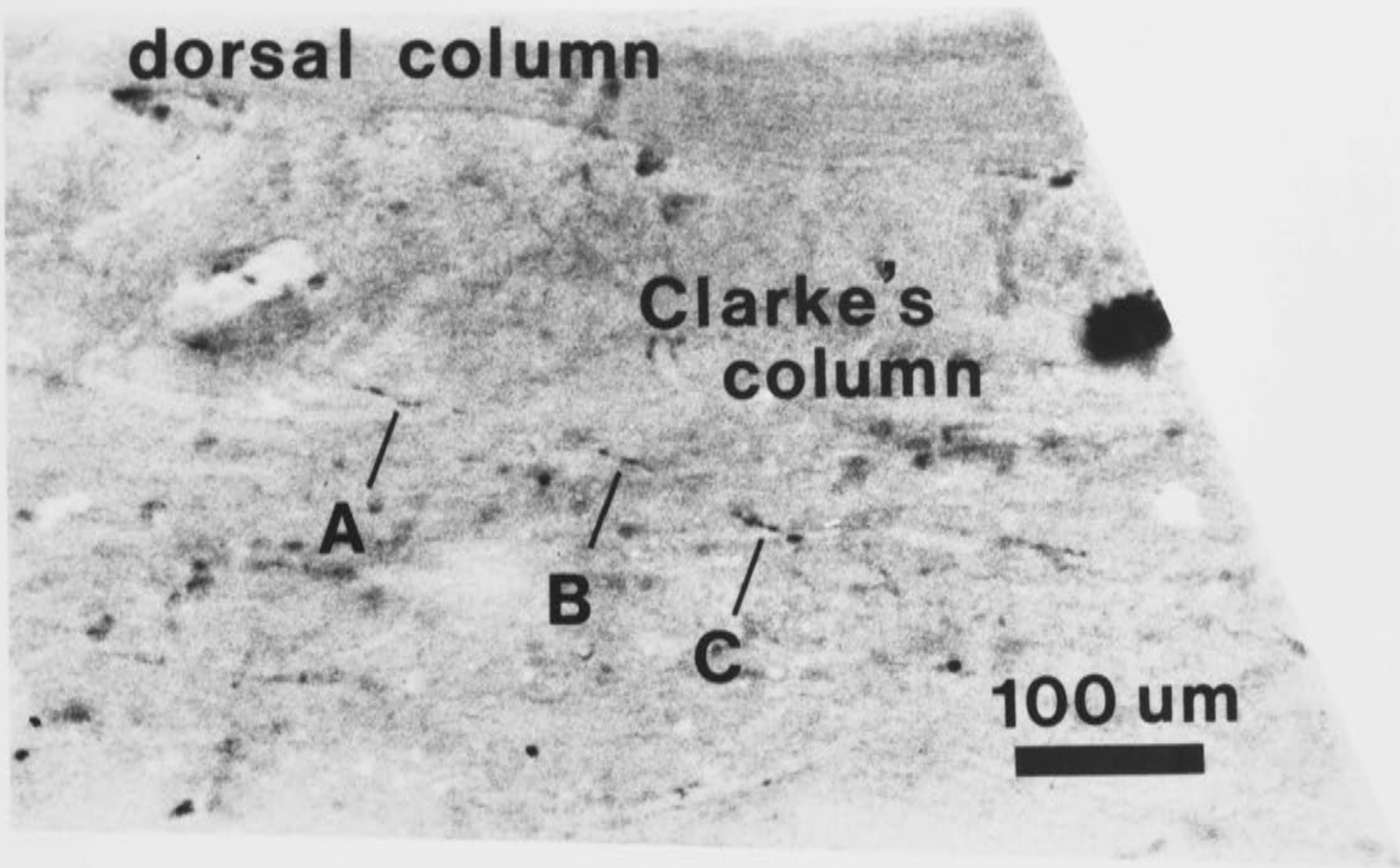
dorsal column
Clarke's column
A
B
C
100 um


A


B


C
10 um

FIGURE 4.2

Full reconstruction of the HRP labelled plantaris Ia afferent collateral presented in this chapter. Tracings were made of the collateral in each of two 100 μm thick sagittal sections. Resolution of the light microscope occasionally made it difficult to determine whether or not a bouton was present. The 37 arrows shown on the tracing indicate the position of boutons regarded as probable. Four further possible boutons are indicated with an arrow head marked with a p, making a total of 41 possible and probable boutons along the length of the collateral.

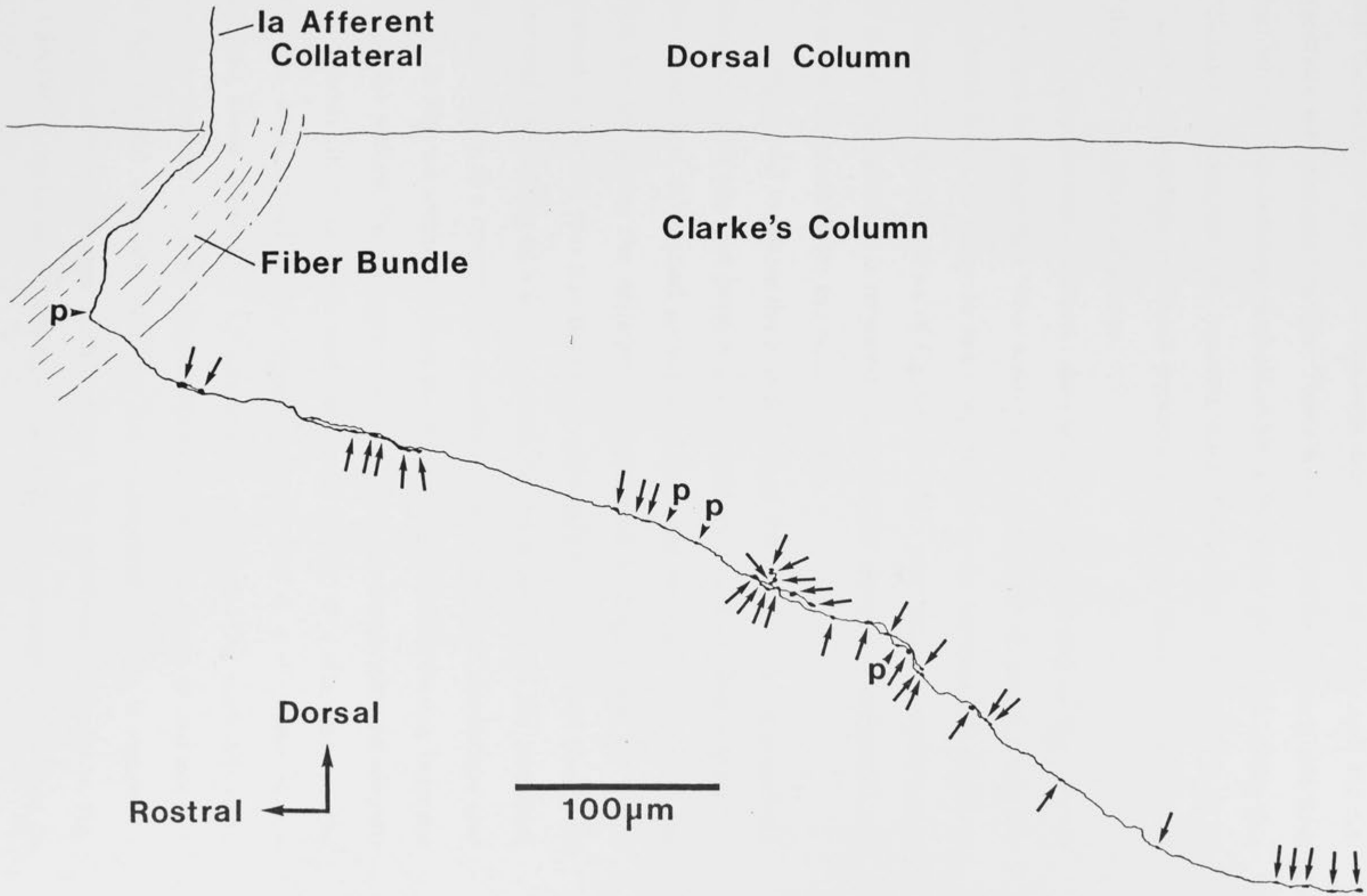
Ia Afferent
Collateral
Dorsal Column
Clarke's Column
Fiber Bundle
p
p
p
p
Dorsal
Rostral
100µm

collateral faithfully. On the basis of this reconstruction it was determined that the collateral extended approximately 600 µm caudally and 400 µm ventrally into the grey matter. Thirty seven probable (arrow), and four further possible boutons (indicated by a 'p') were predicted along this collateral. Under the EM, boutons were dealt with individually, or in clusters, depending on their proximity, and on their orientation in relation to the plane of section.

Complete ultrastructural details of each bouton and of the afferent will now be described. The boutons are presented in order along the collateral from its entry to the grey matter to its termination. Prior to presentation of each series of figures, the light microscope reconstruction of the entire collateral is repeated, such that the electron micrographs can be easily correlated with the reconstruction.

Figure 4.3 indicates the first section of the collateral to be presented. The location of the first bouton is indicated by an arrow, and enclosed in the dotted box. A selected sequence of the serial sections cut through the first bouton along the collateral is presented in Figure 4.4. Of initial interest is the fact that this bouton is extremely small, and that due to its size and its position at a turning point on the trajectory of the collateral, its appearance as a bouton was questioned under the light microscope (see Fig. 4.2). Fig. 4.4 section 1 shows the myelinated afferent entering from the top of the section. Two diameters will be given for the myelinated afferent throughout (in accordance with Berthold, 1978). D = diameter of the afferent fibre including the myelin sheath, and d = diameter of the afferent alone. Here D = 1.5 µm and d = 1.0 µm. The dark structure towards the bottom of the section indicates the first traces of this bouton. In Fig. 4.4 and wherever possible, the sequence of sections is numbered from the first appearance of the bouton. The myelinated afferent in Fig. 4.4 section 1 can be see to lose its myelin sheathing through the sections to

FIGURE 4.3

Reconstruction of the HRP labelled plantaris Ia afferent collateral terminating in Clarke's column.

The following figures (Fig. 4.4 and Fig. 4.5) are of the first bouton on the collateral, indicated on the reconstruction by an arrow and enclosed by a dotted box. This first bouton was one of the "possible" rather than probable boutons (see Fig. 4.2).

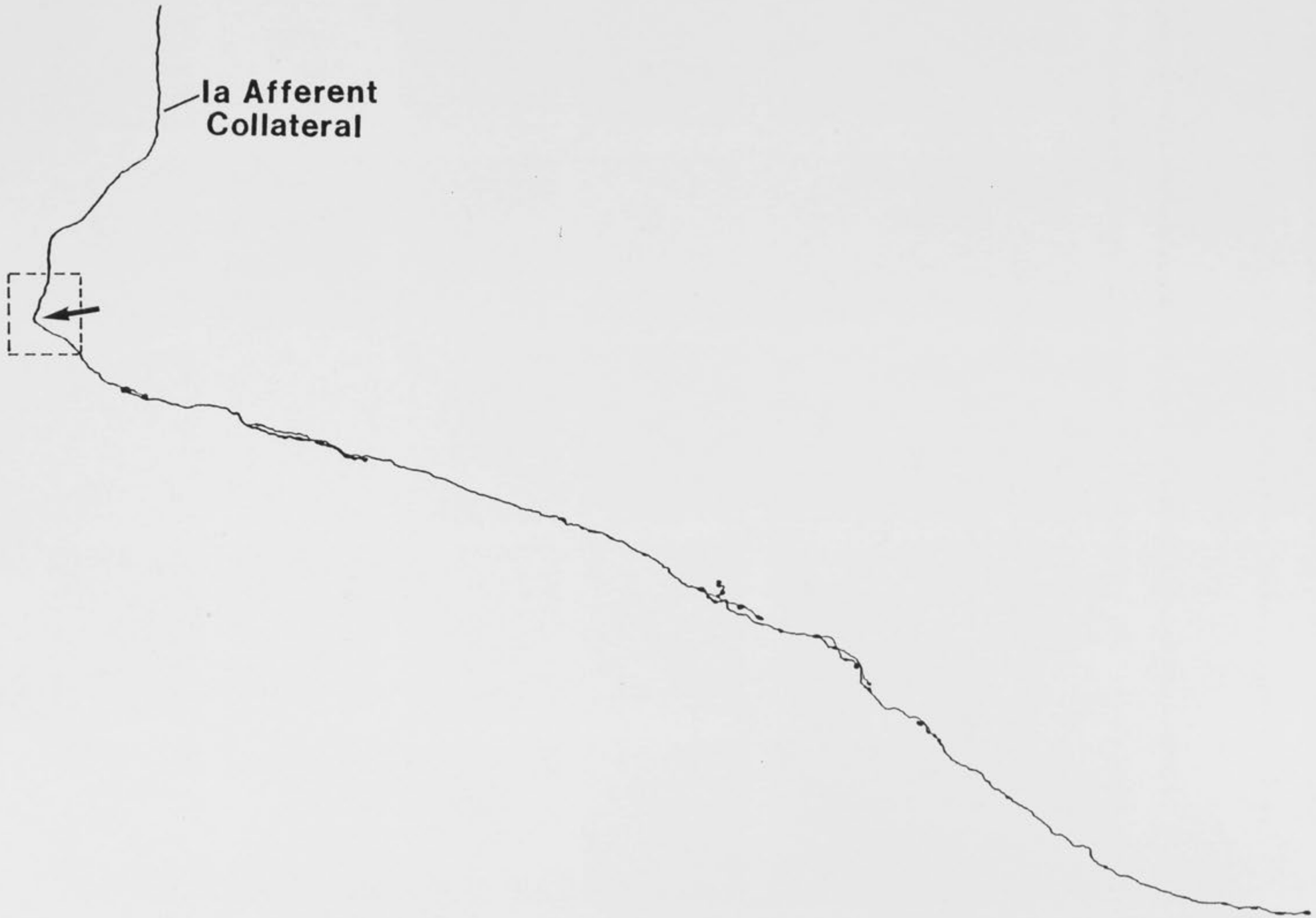
Ia Afferent
Collateral

FIGURE 4.4

This sequence of photomicrographs was selected from the serial sections taken through the first bouton on the labelled plantaris Ia collateral. The position of this bouton is indicated on the previous figure (Fig. 4.3).

Wherever possible throughout the chapter, sections are numbered relative to the first appearance of the bouton. Section 1 shows the very first traces of this bouton.

This bouton exhibits two synaptic specializations, indicated by double arrows (A and B) in sections 15 and 16.

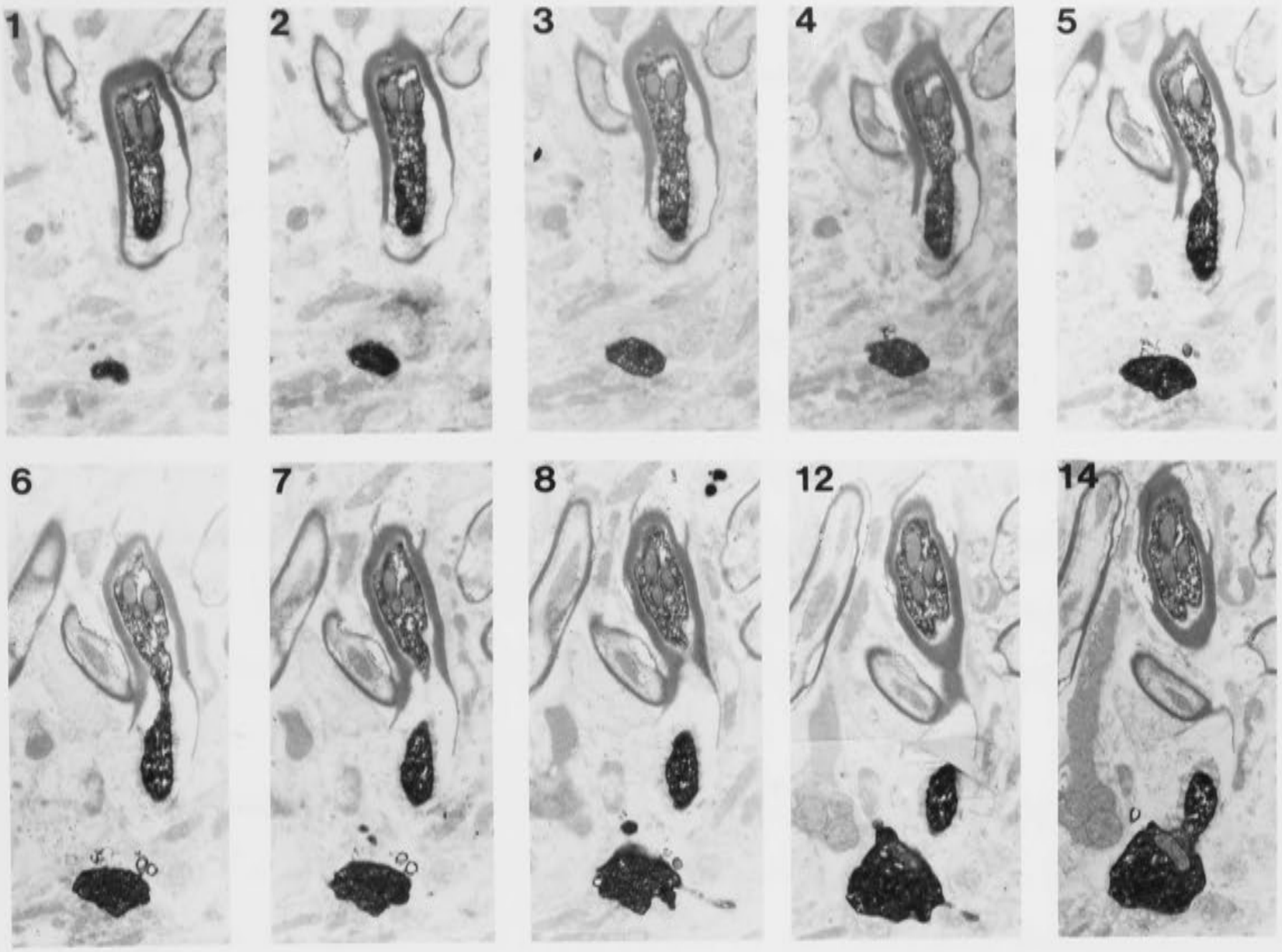
1
2
3
4
5
6
7
8
12
14
15
A
16
B
17
18
19
22
23
24
25
26
27
28
29
30
31
32
33
35
39
41
1 μm

14. Due to the characteristic helical unwinding of the myelin layers, dense strands can be seen close to the neck of the bouton. These are not artefact, but remaining myelin shreds, and this area of unwinding constitutes the paranodal zone. This bouton is of an *en passant* nature, and the bouton itself consitutes a synaptically specialised CNS node of Ranvier. Wisps of myelin are seen again in Fig. 4.4 sections 39 and 41. These indicate the rewinding of the myelin sheath and thus the remyelination of the afferent distal to the bouton. The paranodal region on the distal side of the bouton is 1.2 μm in length. The unwinding and rewinding of the myelin sheathing is characteristic of the nodal region of myelinated fibres in the CNS (see review by Waxman, 1972).

Two synaptic specializations are apparent in this bouton, defined by double sets of arrows as A and B in Fig. 4.4 sections 15 and 16. Synaptic specializations were identified on the basis of the following criteria: 1) postsynaptic thickening, 2) presence of synaptic cleft, and 3) clusters of vesicles at the presynaptic site, although these were often difficult to identify due to the intensity of the HRP staining (see review by Szentagothai, 1970). The two synaptic specializations are shown at higher power in Figure 4.5B. A post synaptic dense band and an increased density in the synaptic cleft are clearly visible in both cases. Vesicles can be seen clustered close to the presynaptic membrane at both specializations, particularly at the specialization on the left. The position of these proposed release sites and the orientation of the dendrite which they presumably contact are shown clearly in the drawing, Fig. 4.5A. This drawing was reconstructed from tracings of the series of photomicrographs. For purposes of orientation, the arrow at the top indicates the direction of travel of an incoming action potential. The montage presented in Fig. 4.5A shows clearly the complete configuration of this bouton. As with the series in Fig. 4.4, the myelinated afferent is

FIGURE 4.5

A. This montage was reconstructed from the same serial sections presented in the previous figure (Fig. 4.4). The line drawing to the right of the montage was reconstructed from tracings of the same serial sections. The drawing shows the position of the two synaptic specializations exhibited by this bouton, and also indicates the orientation of the postsynaptic dendrite. The arrow at the top of the line drawing indicates the direction of travel of an incoming action potential.
The calibration bar on the line drawing also refers to the montage.

B. This high power inset photomicrograph shows more clearly the nature of the proposed synaptic specializations (indicated by arrows) exhibited by this bouton.
Calibration bar = 1 μm.


A
D

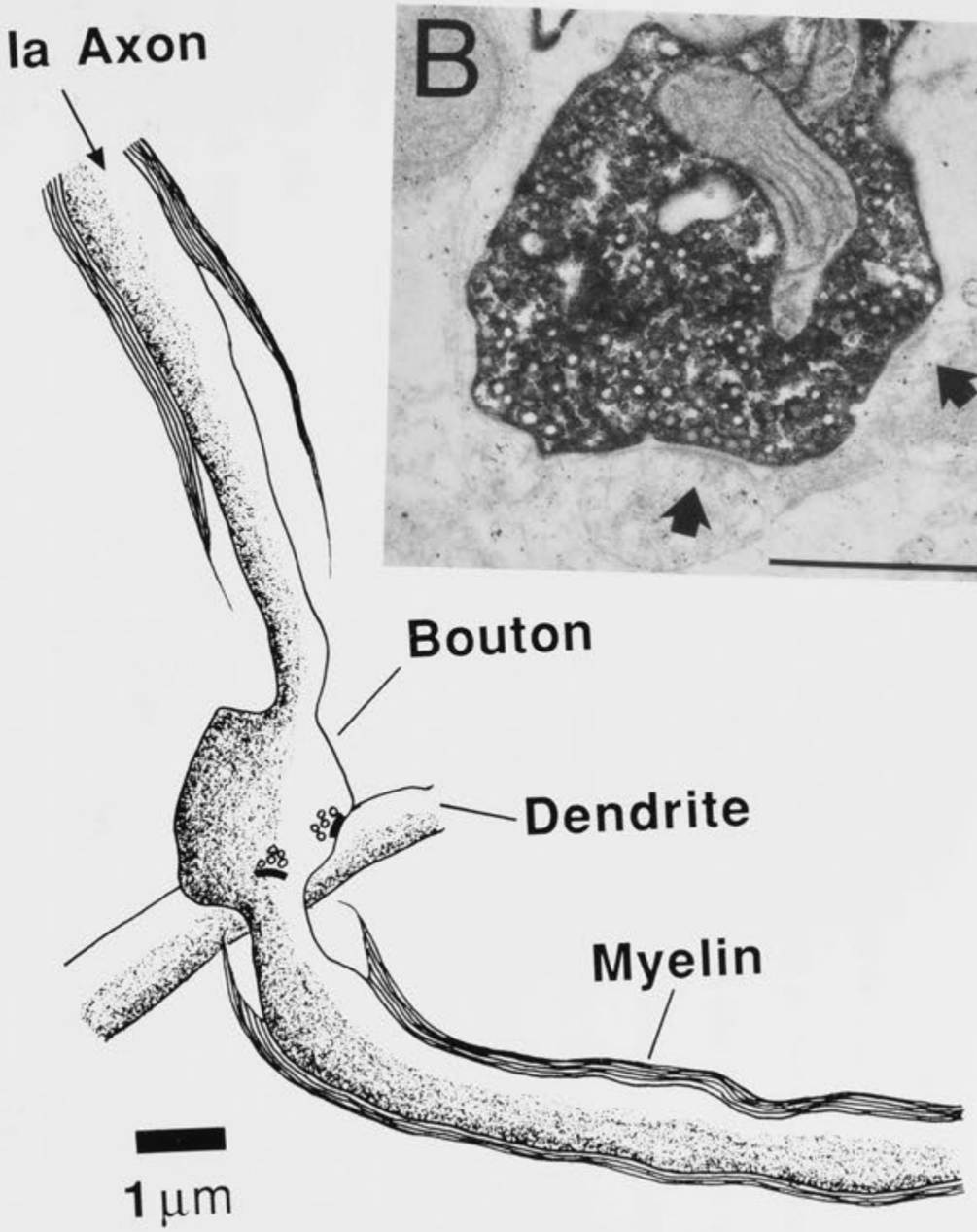
Ia Axon
Bouton
Dendrite
Myelin
1 μm

B

shown descending, and the myelin unwinding at the paranodal region. In this region the diameter of the afferent without sheathing is reduced from d = 1.0 μm to d = 0.5 μm. It is clear from the montage that the diameter of the bouton, 1.8 μm, is only marginally greater than that of the myelinated fibre either side of the bouton, and this probably explains the difficulty encountered identifying this bouton under the light microscope.

The wide separation of the myelin sheathing from the afferent in the paranodal region may be partly artefact caused by less than optimal fixation. However, the unwinding of the myelin sheathing in the paranodal region, and the resulting appearance of banding across this region, accompanied by scalloping of the axolemma where the myelin layers contact it, have been described previously for myelinated fibres in the central nervous system (Peters, 1966). The paranodal region prior to this bouton is longer than that following the bouton, but the last vestiges of the myelin contact the bouton itself on both sides. After remyelination, the afferent resumed its former diameter of (on average) D = 1.5 μm, and continued for approximately 55 μm before giving rise to a second group of boutons.

The reconstruction of the collateral is repeated in Figure 4.6, and illustrates the next region of the collateral to be presented. Two boutons, A and B, are indicated by arrows, and enclosed within the dotted box. Fig. 4.6 indicates that under the light microscope, the afferent was seen to give rise to a large bouton, A, which constituted a branch point. One branch continued in a caudal direction, while the second appeared to give rise to a smaller, terminal bouton, B.

Figure 4.7 shows a selected sequence of serial sections through the first, or larger, of the two boutons, bouton A, again with the sections numbered relative to the first appearance of the bouton. The myelinated fibre, shown on the left in Fig. 4.7 sections 3-16, has an average diameter

FIGURE 4.6

Reconstruction of the HRP labelled plantaris Ia afferent collateral terminating in Clarke's column.

The following figures (Figs. 4.7-4.9) describe the next two boutons on the plantaris Ia collateral. The two boutons are indicated on this reconstruction by arrows, as bouton A and bouton B within the dotted box.


Ia Afferent
Collateral
A
B

FIGURE 4.7

This sequence of photomicrographs was selected from the serial sections taken through bouton A (indicated on the previous reconstruction, Fig. 4.6). This bouton is an example of an *en passant* giant bouton, which exhibits 7 individual synaptic specializations. Each specialization is indicated by double arrows, and labelled A-F.

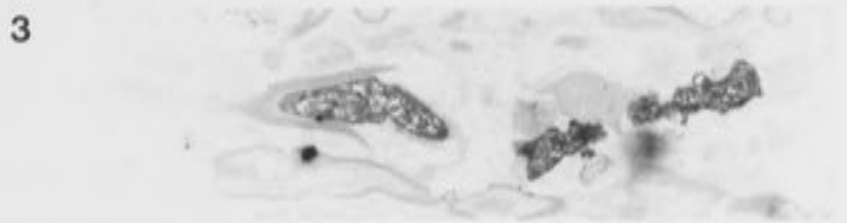
3

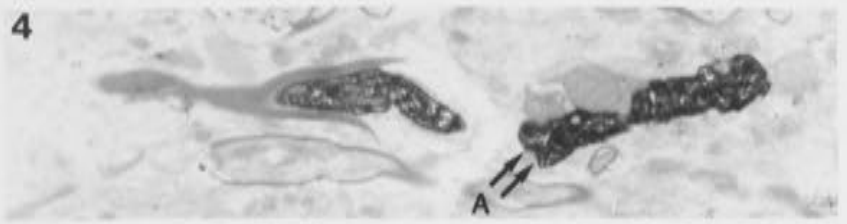
4
A


6


8


12
B


13
C


14


15


16


18

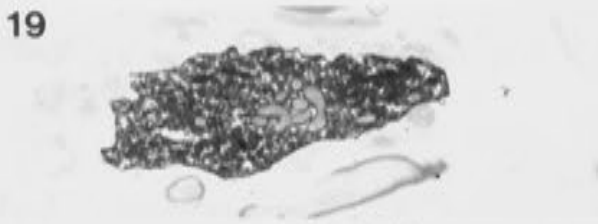
19


20


22
D


23


24
E


26
F

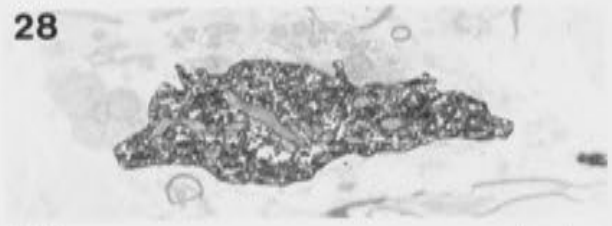
28


36
1.0 µm

of D = 1.6 μm (d = 0.9 μm). The helical unwinding of the myelin sheath is shown taking place in the same way described previously. The afferent itself narrows quite substantially to approximately d = 0.6 μm in the paranodal region. Again the final layers of the myelin can be seen to contact the very edge of the bouton itself. The banding pattern in the paranodal zone is very clear in Fig. 4.7 section 12. This bouton was very large and irregularly shaped, with a length of approximately 9.2 μm, and a diameter of 3.1 μm at its widest point. A length of over 9 μm indicates that this is a giant bouton. Six clear synaptic specializations were identified in this bouton. These all appeared to be contacting the same postsynaptic structure, possibly a dendrite of a DSCT neurone in Clarke's column. Each of these synaptic specializations is seen at higher power in Figure 4.8. In each case, the postsynaptic density and cleft are quite clear. However presynaptic clusters of vesicles were not always observed as distict entities, due partly to the intensity of the HRP staining, but largely to the dense overall packaging of the vesicles within the bouton. This dense packaging of vesicles was quite characteristic of many of the boutons examined. Mitochondria also seemed to be densely packed within these HRP labelled boutons, generally close together and located away from the proposed synaptic contact region. Figure 4.8D shows an example of a specialization contacting a small, spinelike protrusion of the postsynaptic profile.

In Figure 4.9, the last two sections of Fig. 4.7 (sections 28 and 36) are repeated to include the afferent approaching and emerging from the bouton. An interesting observation, shown in Fig. 4.9 sections 28, 36 and 47, and clearly illustrated in the reconstruction, is that the large bouton gave rise to two axonal branches. The first, represented as Axon Branch 1, emerged from the upper right corner of the bouton. Remyelination occurred on this branch approximately 2.0 μm distant from the bouton, at

FIGURE 4.8

The photomicrographs show the synaptic specializations (double arrows, A-F) exhibited by bouton A, at higher magnification.

The line drawing indicates schematically the position of each of the specializations on the bouton.

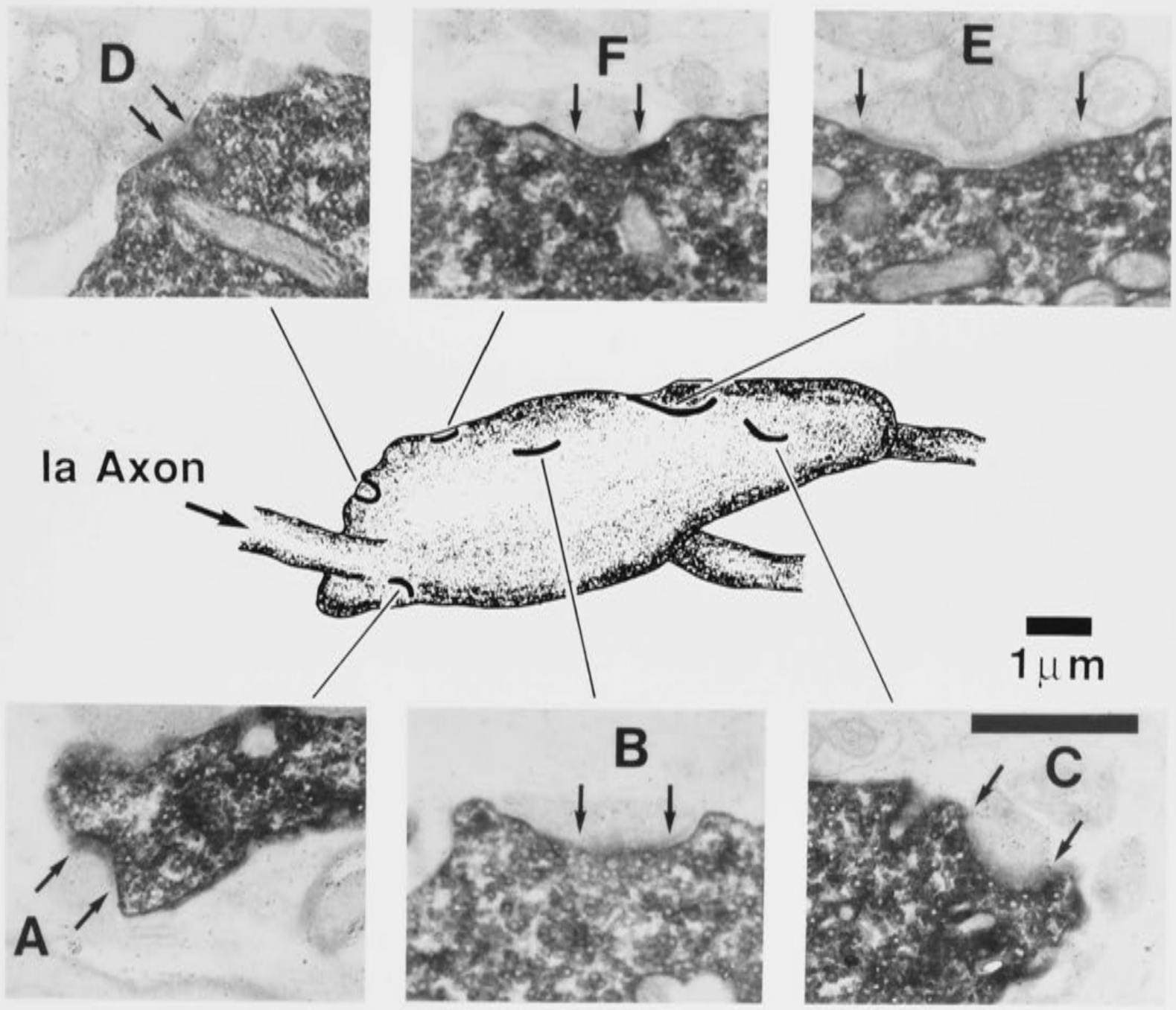
D
F
E
la Axon
1 µm
A
B
C

FIGURE 4.9

Sections 28, 36 and 47 show the configuration of the afferent approaching and emerging from the giant bouton, bouton A. Bouton A proved to constitute a complicated branch point, giving rise to axon branch 1 and axon branch 2. This is shown schematically in the line diagram. Axon branch 1 subsequently gives rise to a small, terminal bouton, Bouton B. The lower series of photomicrographs, sections 48-62, were selected from the serial sections through Bouton B, which shows no clear synaptic specializations.

The arrow in Section 47 indicates the characteristic banding pattern exhibited by the paranodal region.

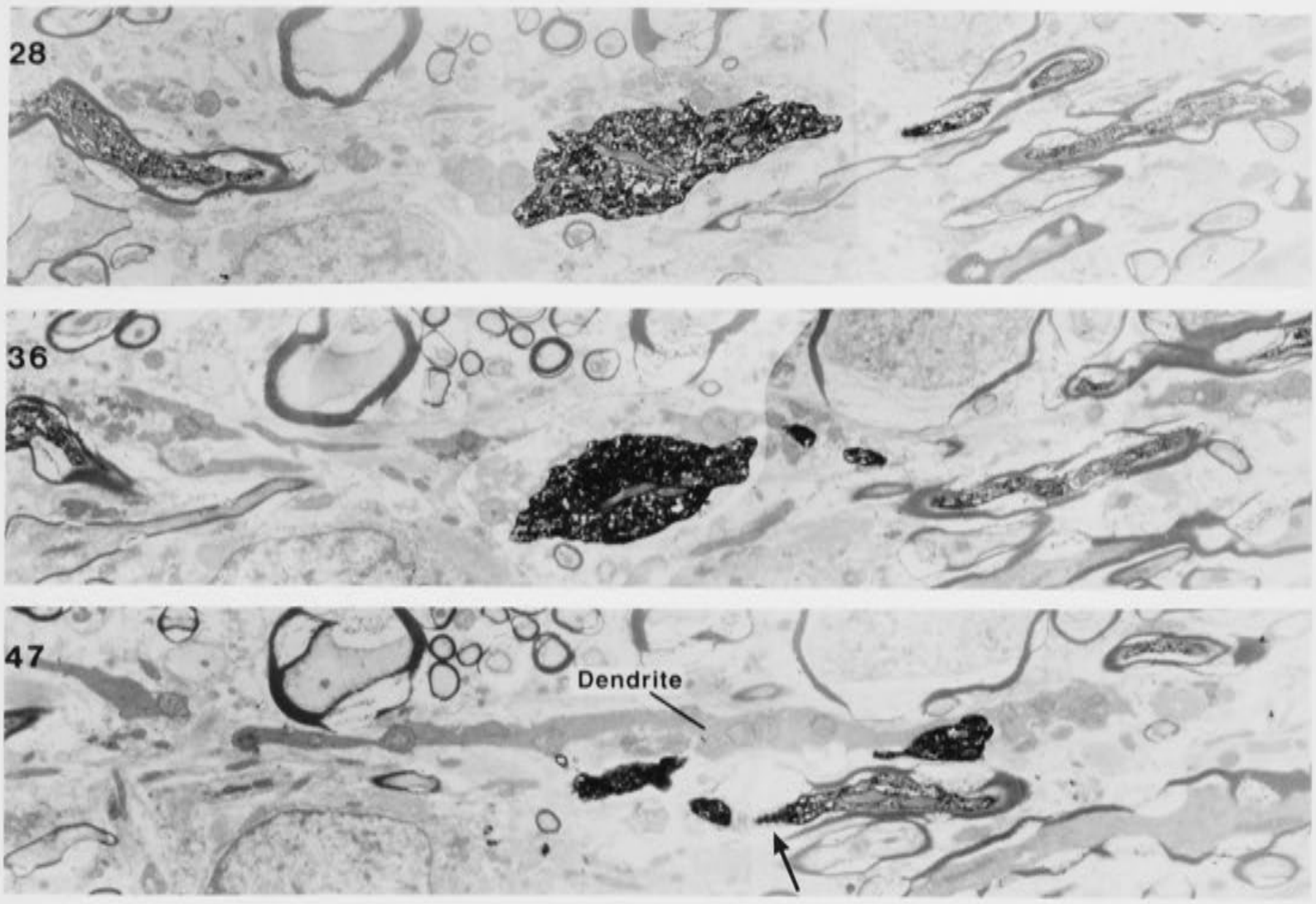
28
36
47
Dendrite

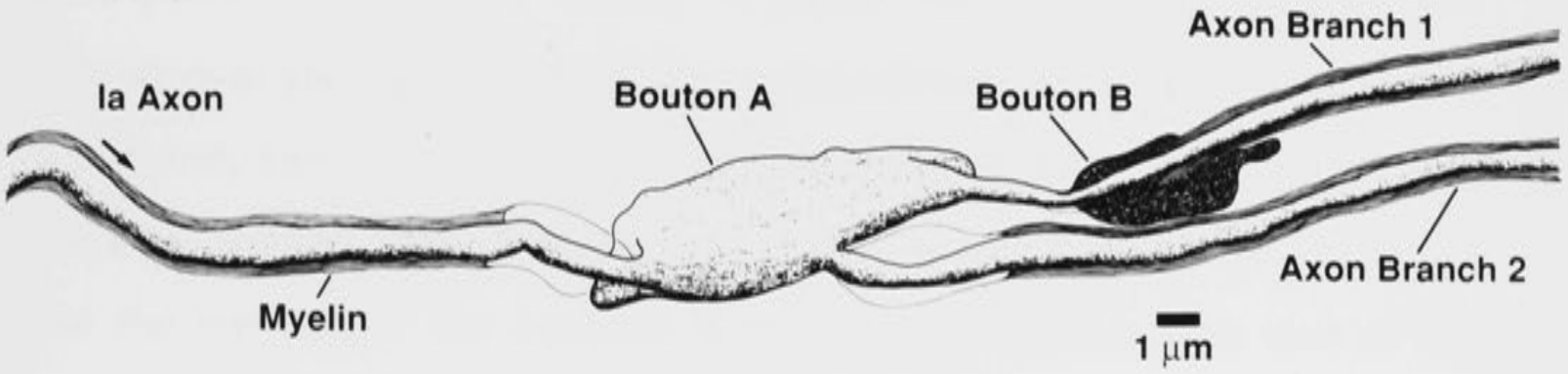
Ia Axon
Bouton A
Bouton B
Axon Branch 1
Axon Branch 2
Myelin
1 μm

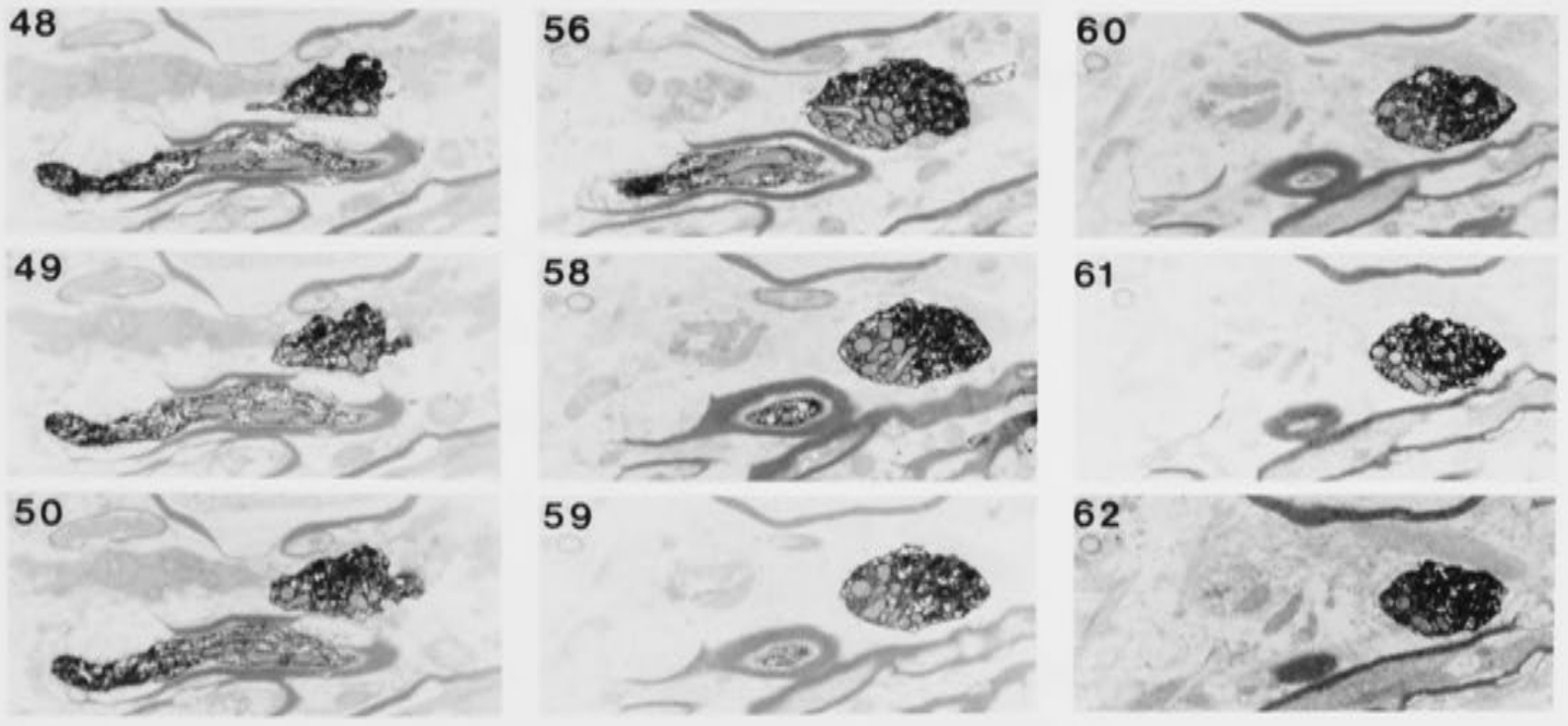
48
49
50
56
58
59
60
61
62

which point this axon branch exhibited a further branch point. This subsequent small, very narrow unmyelinated branch gave rise to the second bouton of this series, (bouton B), recognised initially under the light microscope. A sequence of photomicrographs taken through this second bouton is presented in Fig. 4.9 sections 48-62. This bouton was 3.8 μm in length, and its maximum width was approximately 1.9 μm. This small bouton was terminal, and exhibited no obvious synaptic specializations. After this second branch point, Axon Branch 1 continued on in parallel with Axon Branch 2, which emerged from the lower right corner of the bouton. After remyelination, over 3.7 μm in both cases, both axon branches resumed at a similar diameter, D = 1.0 μm, and d = 0.6 μm. The characteristic bars of the paranodal region were clearly observed, especially in Fig. 4.9 section 47 (Axon Branch 2). The two axon branches subsequently continued closely together for the next 80 μm. The resolution of the light microscope was insufficient to allow determination of this fact, and thus the reconstruction indicated only one axon, not two (see Figs. 4.2 and 4.6). Of possible relevance to this observation is the fact that the staining of the boutons is much more intense than that of the myelinated portions of the axon collateral branches.

The reconstruction of the collateral is repeated in Fig. 4.10. No bouton is marked in the indicated region on the tracing, as it was not recognized under the light microscope. However, the S-shaped dip in the axon correlates well with the configuration shown in Fig. 4.11. At this point, a distance of 40 μm from the branch point, the two parallel axon branches (which emerged from the large bouton in the previous series) separated sufficiently to be resolved individually under the light microscope (see reconstruction, Fig. 4.10). This had the effect of suggesting a branch point at this site, although serial section electron microscopy has now shown that this is definitely not the case. On the branch giving rise

FIGURE 4.10

Reconstruction of the HRP labelled plantaris Ia afferent collateral terminating in Clarke's column.

The following figure, Figure 4.11 shows a bouton which was overlooked during the initial light microscopic tracing of this collateral (see Fig. 4.2). The position at which this bouton appears is indicated on this reconstruction by an arrow, and surrounded by a dotted box.


Ia Afferent
Collateral

FIGURE 4.11

This small bouton was not included in the reconstruction under the light microscope (see Fig. 4.2). Its position is marked by the arrow and dotted box on the previous reconstruction (Fig. 4.10).

Sections 1 through 51 were selected from the serial sections taken through this bouton and the collateral.

The line drawing shows the configuration of the collateral as it approaches the bouton, and subsequently emerges from it.

Individual layers of the rewinding myelin sheath were identified close to the neck of this bouton in the paranodal zone. They are shown schematically on the line drawing, and are indicated by the star in the higher power inset micrograph. Calibration bar for the higher magnification photomicrograph = 1 μm.


1


2


3


4

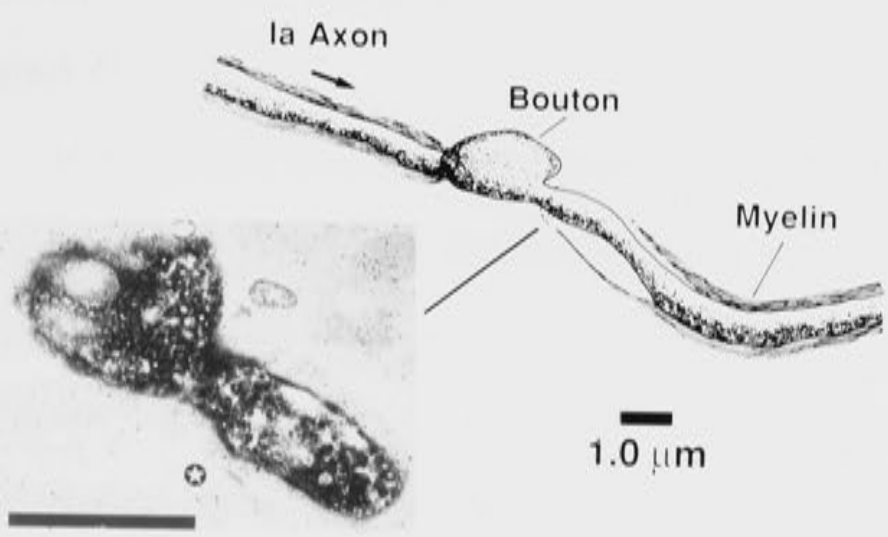
Ia Axon
Bouton
Myelin
1.0 µm

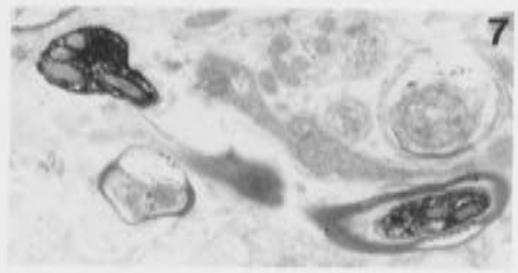
7


8


11


12


14

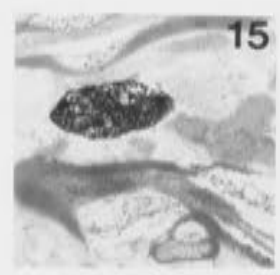
15


17


19


20


21


22


23


24


36


38


51

to the bouton, the incoming myelinated fibre is situated directly behind the bouton, and was masked by it, as is indicated in the line drawing in Fig. 4.11. The myelinated fibre shown has a total diamter D of 1.0 μm (d = 0.6 μm) as it approaches the bouton (seen in cross-section in Fig. 4.11 section 51) and a similar diameter as it emerges from the bouton (Fig. 4.11 sections 1-12). Although this bouton has a length of 2.4 μm, its width is only 1.0 μm, and the resulting small difference between bouton diameter and diameter of the myelinated fibre probably explains the oversight of this bouton under the light microscope. As the fibre approaches the bouton, it is seen to lose its myelin sheath in Fig. 4.11 sections 36 and 38. Due to the orientation of this bouton in relation to the cutting plane, the fibre leaving the bouton is seen in the first sections cut, shown in Fig. 4.13 sections 1-4. As the afferent becomes remyelinated, individual myelin layers can be identified close to the neck of the bouton. These are shown in Fig. 4.11 on the drawing, and are indicated by the star on the higher magnification inset micrograph. On remyelination, the afferent resumes approximately the same dimensions exhibited prior to the bouton, d = 0.6 μm and D = 1.0 μm.

Figure 4.12 shows the reconstructed collateral, indicating by arrows, (unlabelled, A, B and C), the next four boutons to be presented. Although it appears from the reconstruction that each of the four boutons is situated along the same branch of the collateral, serial section electron microscopy showed that this was not the case. A sequence of the sections cut through this first bouton is presented in Fig. 4.13. This bouton is a very small, *en passant* bouton, and represents an example of a synaptically specialised CNS node. The paranodal region is approximately 3.2 μm in length and the final myelin layers finish close to the bouton itself. The characteristic banding of the paranodal region, and scalloped effect along the axolemma, are in evidence on both sides of this bouton. As the myelinated fibre (D =

FIGURE 4.12

Reconstruction of the HRP labelled plantaris Ia afferent collateral terminating in Clarke's column.

The four boutons indicated on this reconstruction by arrows, surrounded by the dotted box, appear to lie on the same branch of the collateral, but this is not the case. The first bouton is situated on one of the branches, and the other three arrows (A, B and C) indicate a series of three boutons on the other branch.

The first bouton is presented individually in Figs. 4.13 and 4.14, and the following three (A, B and C) are presented as a series in Figs. 4.15 - 4.19.

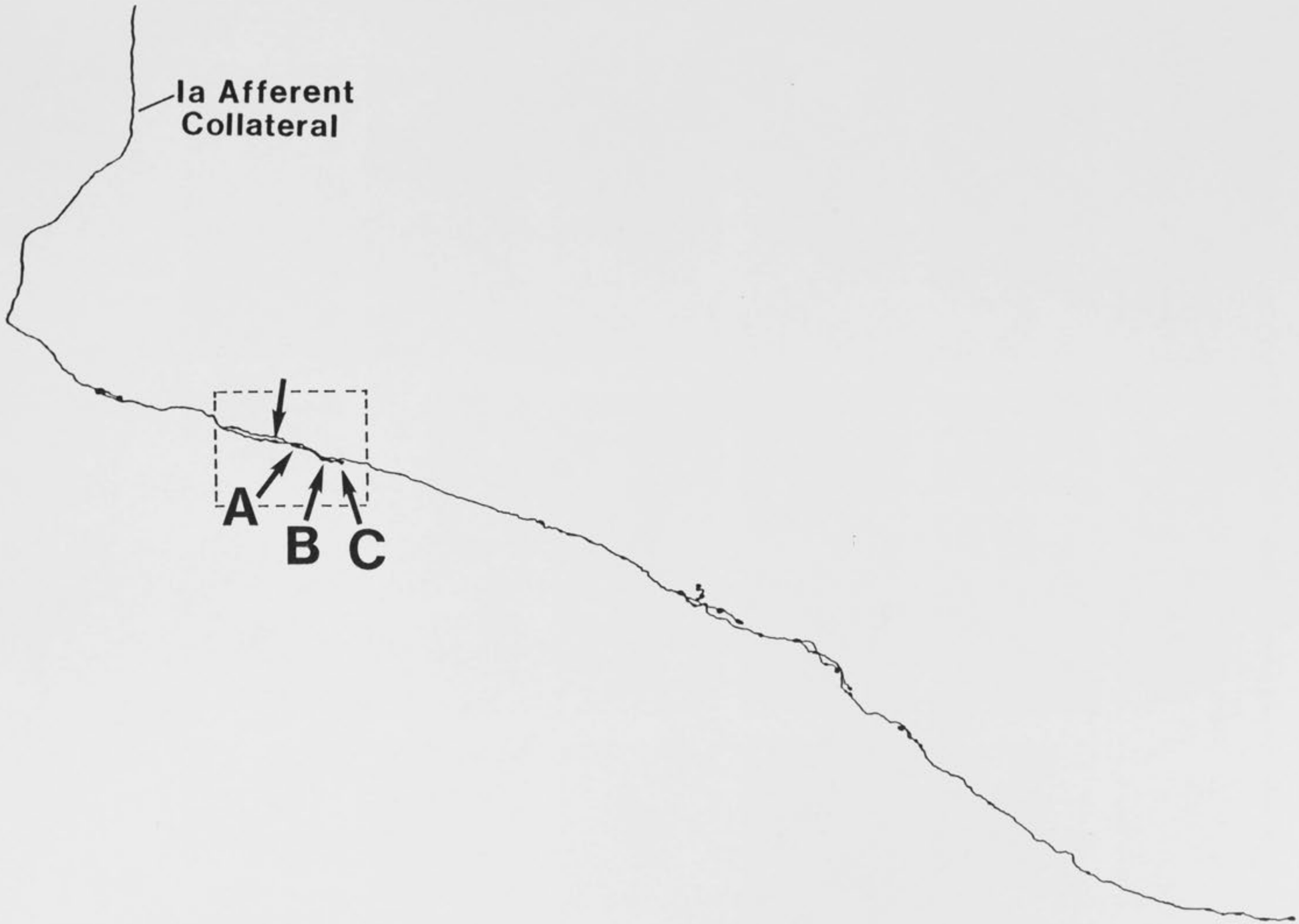
Ia Afferent
Collateral
A
B
C

FIGURE 4.13

This small *en passant* bouton is an example of a synaptically specialized node in the central nervous system. A single synaptic specialization is indicated by double arrows in section 16.

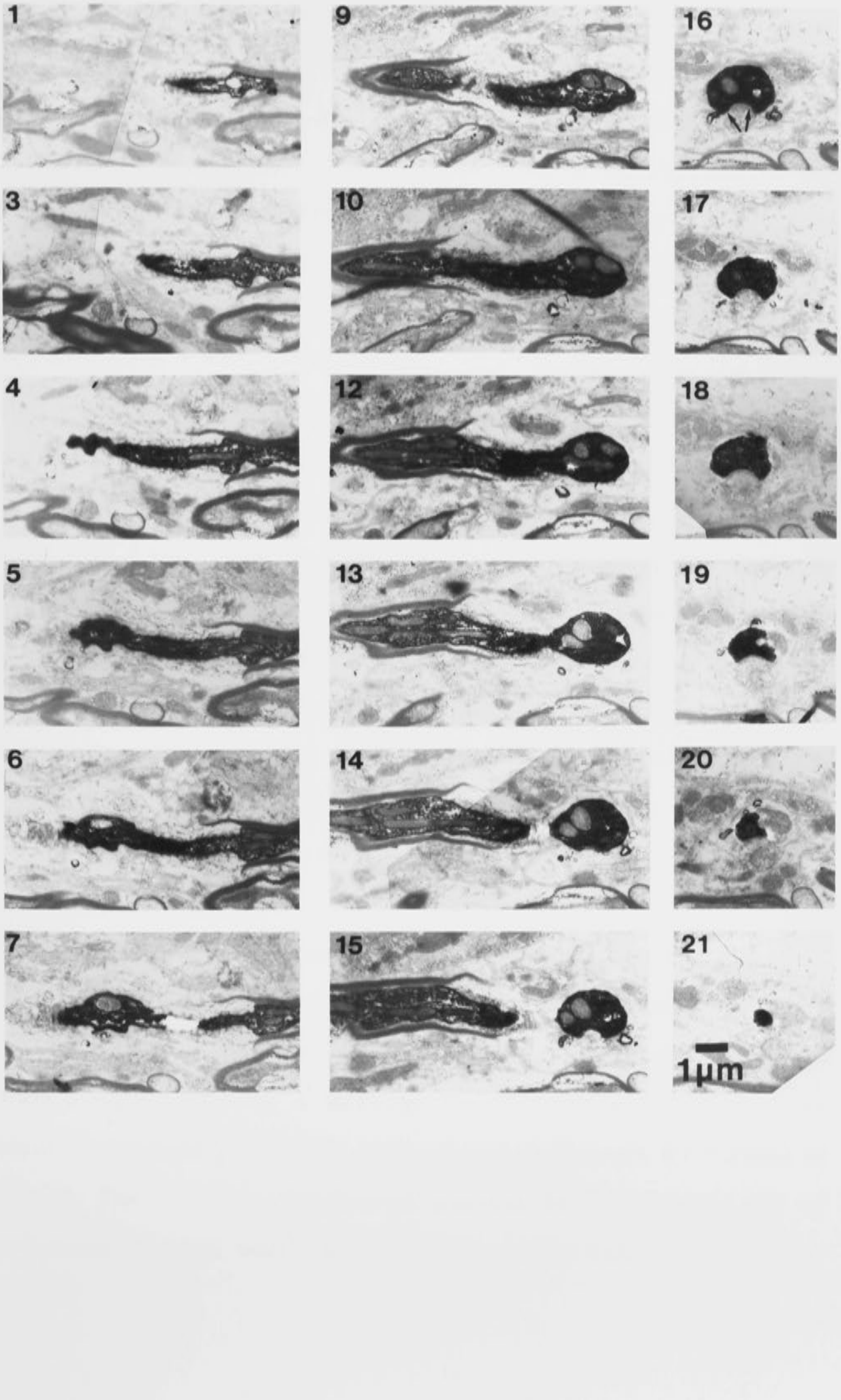
1
9
16
3
10
17
4
12
18
5
13
19
6
14
20
7
15
21
1µm

1.7 µm) approaches the bouton, d is reduced from 1.1 µm to approximately 0.7 µm. The bouton itself is approximately 2.4 µm long, but only 1.6 µm wide. The diameter of this bouton is therefore less than that of the myelinated fibre on either side of it. The fact that this bouton was recognized as such while other larger boutons were missed is probably due to the intensity of the HRP staining within this bouton, and the necking down of the fibre on either side. This is seen clearly in the montage in Figure 4.14A, where the afferent on either side of the bouton is less intensively HRP labelled than the bouton itself. The proximity of the myelin layers to the edge of the bouton, and the scalloped appearance of the axolemma are shown in the reconstruction, Fig. 4.14B. The helical unwinding of the myelin layers are presumably responsible for the effect of scalloping along the axolemma, and the banding across the afferent in the paranodal region, seen both before the bouton in Figure 4.14C, and after in Fig. 4.14E. Each band is highlighted by a small dot. A single synaptic specialisation was identified in this bouton, shown in Fig. 4.13 section 16, but seen more clearly at higher magnification in Fig. 4.14D. The post synaptic membrane thickening and dense cleft are clear in this figure, although the close packaging of the vesicles within the bouton, and the intensity of the HRP label makes it difficult to define a separate and distinct cluster of presynaptic vesicles. However, it apears that the vesicles are lined up in parallel rows at the presynaptic site.

The three boutons indicated on the reconstruction in Fig. 4.12 as A, B and C are in fact situated on the other axon branch, and constitute a terminal series of boutons. In order to describe the series more easily, a summary figure showing a montage and line drawing of the three boutons is presented prior to the series of sections through the boutons as Fig. 4.15. The incoming myelinated afferent has a diameter (D) of approximately 1.4 µm, which does not differ greatly from the diameter D

FIGURE 4.14

A. This montage was constructed using the same series of sections presented in the previous figure (Fig. 4.13).

B. The nodal and paranodal regions are shown clearly in the line drawing, which was reconstructed from tracings of the serial sections presented in the previous figure (Fig. 4.13). The scalloped appearance of the axolemma is a characteristic feature of the paranodal region. The arrow to the left of the drawing indicates the direction of travel of an incoming action potential.

C and E. Banding across the paranodal region. A small dot indicates the peak of each band in the paranodal region before (C) and after (E) the bouton.

D. The single synaptic specialization exhibited by this bouton is shown between the set of arrows. The dense post-synaptic band and cleft underlie a region where the vesicles appear to have lined up in neat rows, rather than "clustered", at the presynaptic membrane.

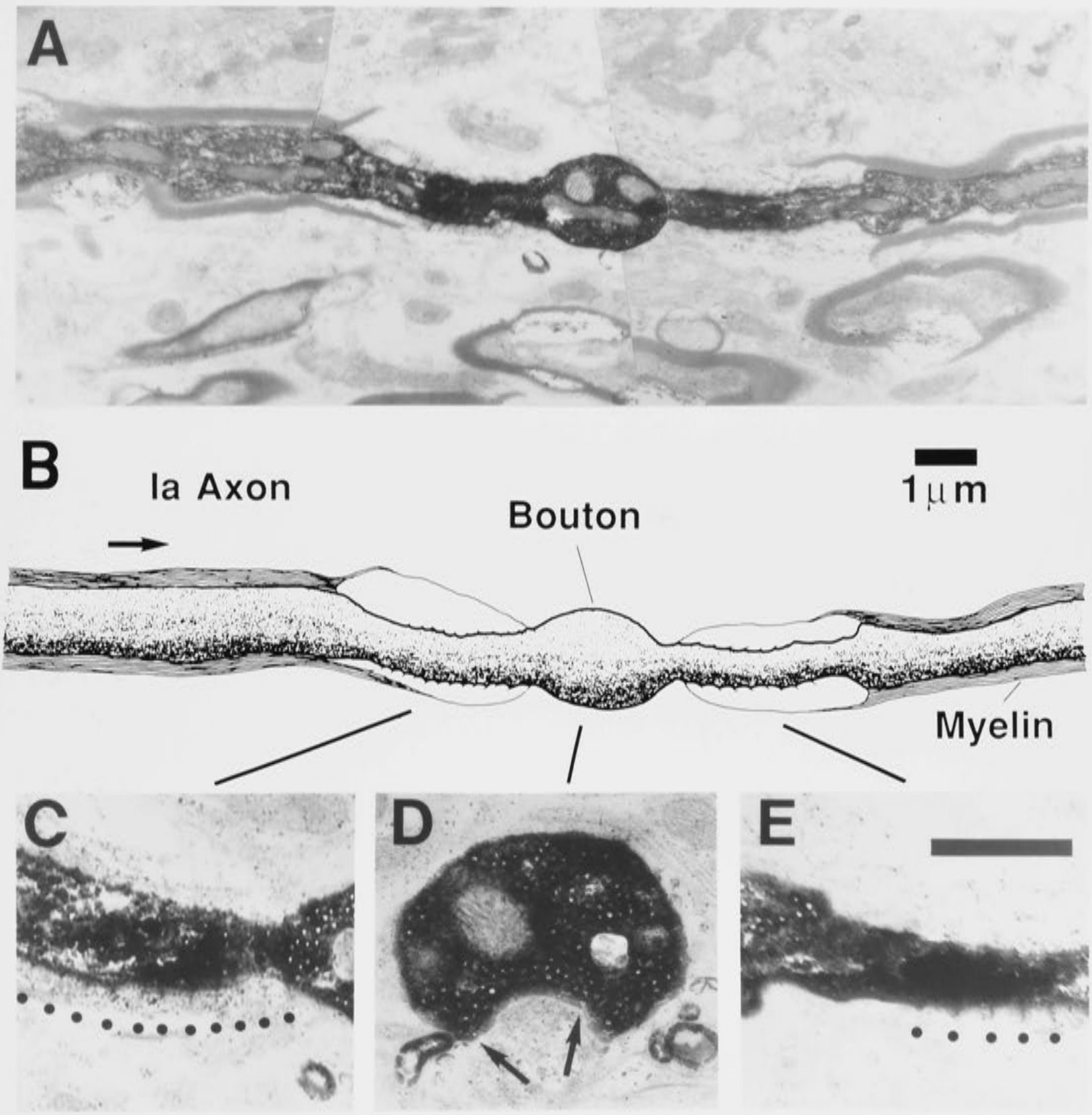
A
B
Ia Axon
1 μm
Bouton
Myelin
C
D
E

FIGURE 4.15

Summary figure illustrating the configuration of the series of three boutons, A, B and C, presented in serial sections in the following four figures (Fig. 4.16-4.19).

A. Montage, reconstructed from the same photomicrograph series presented in Figs. 4.16-4.19 shows that this particular collateral branch loses its myelin prior to bouton A and does not remyelinate prior to termination with bouton C.

B. Reconstruction of the three boutons, A, B and C.

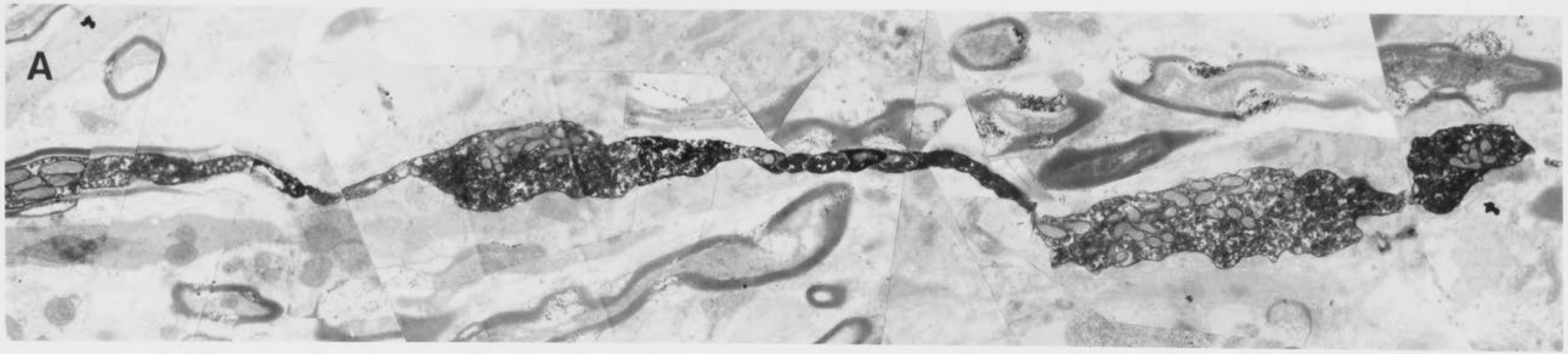
A
B
Ia Axon
Myelin
Bouton A
Bouton B
Bouton C
Dendrite
1 μm

of 1.5 μm at the entry of the collateral to the spinal grey matter. The myelin layers unwind in the same helical fashion described previously over a distance of 3.4 μm. In contrast to previous descriptions however, the myelin sheathing does not butt against the bouton itself. Instead, the afferent diameter (d) necks down from 1.0 μm to approximately 0.4 μm, and continues bare of myelin sheathing for 2.8 μm before the initial swelling of the first bouton in this series. Bouton A is 9.0 μm long, and 2.2 μm in diameter at its widest point. Due to its unusual configuration, the light reconstruction shows bouton A as two individual boutons (see Fig. 4.2). The true configuration of bouton A can be seen in Fig. 4.16 sections 20-25. Complete separation of the bouton into two sections is then seen in Fig. 4.16 section 26, and in Fig. 4.17. Again, serial section electron microscopy was used to show that in fact only one bouton existed at this point on the collateral. As the afferent emerged from bouton A, no remyelination occured. Instead, a fine unmyelinated bridge 0.5 μm in diameter, and 7.0 μm in length is present between bouton A and bouton B (see Fig. 4.15A and B). The second bouton, bouton B is also very large, with a length of 8.3 μm and a width of 2.1 μm at its widest point. After leaving bouton B, the collateral is again very narrow, approximately 0.5 μm in diameter, and remains unmyelinated. This bridge, 2.3 μm long, then gives rise to bouton C. Bouton C is the smallest bouton of this series of three, 2.1 x 3.8 μm, and is terminal as suggested by the original reconstruction. The montage and line drawing presented in Fig. 4.15A and B clearly indicate the nature of the boutons and of the afferent bridges which join them. A further interesting point illustrated in the line drawing Fig. 4.15B is that all three boutons in this series lie along the same dendrite, which, due to its large size, is possibly that of a DSCT neurone.

FIGURES 4.16 - 4.19

The following four figures show a selection of the serial sections cut through boutons A, B and C, shown in the previous figure (Fig. 4.15).
The orientation of these sections was such that the sections are numbered relative to the first appearance of bouton C.
Seven individual synaptic specializations were recognized in bouton A, and these are labelled with double sets of arrows as A1-A7. One specialization was seen in bouton C, labelled with a double set of arrows as C1 in Fig. 4.16 section 14.

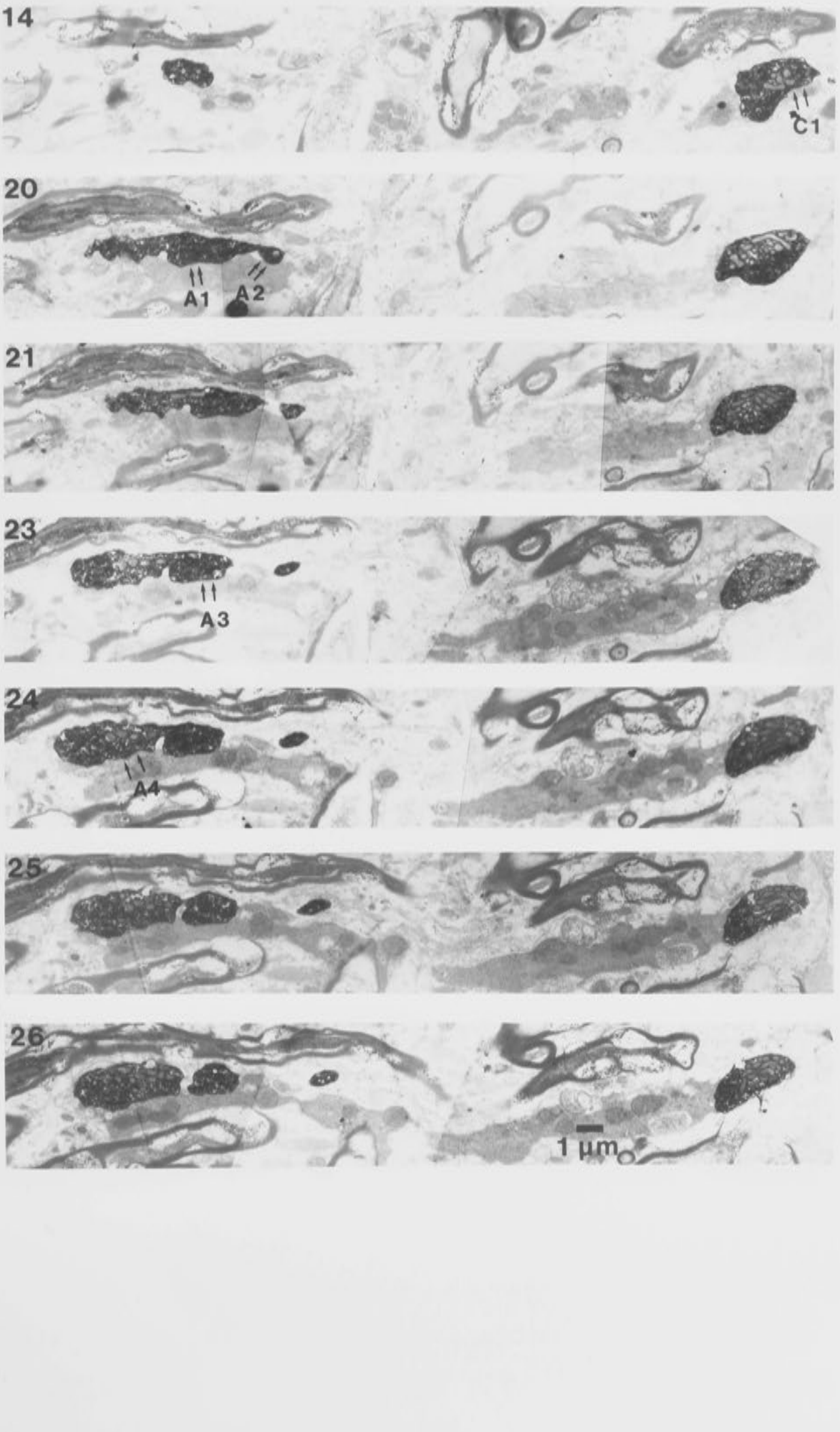
14
C1
20
A1
A2
21
23
A3
24
A4
25
26
1 µm

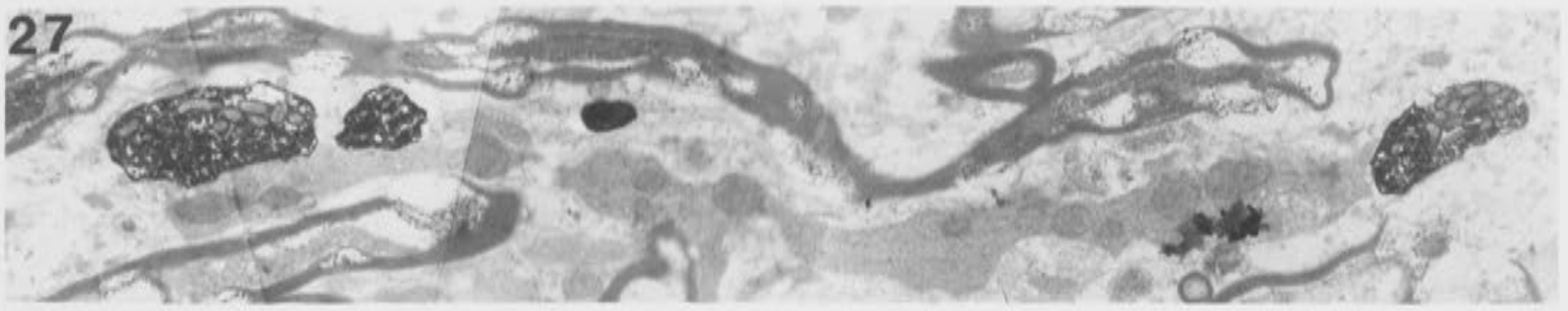
27

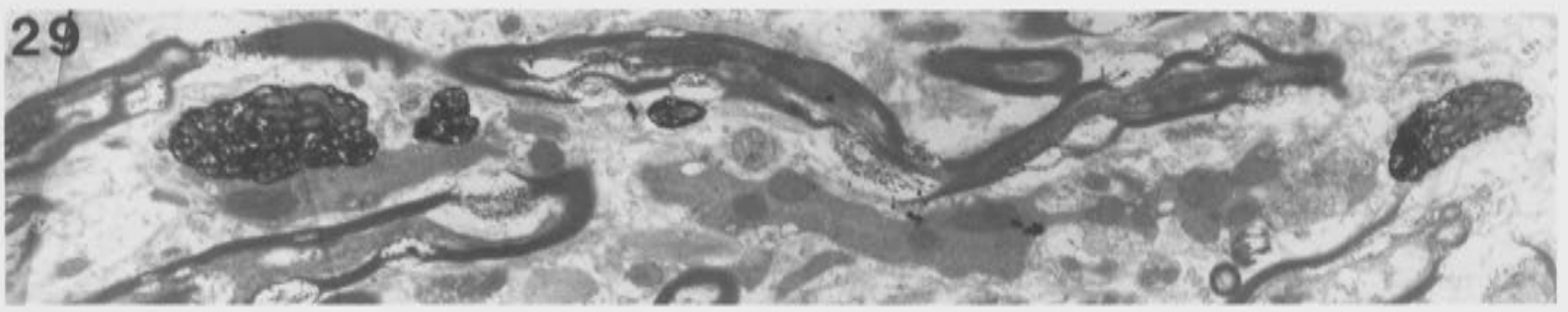
29

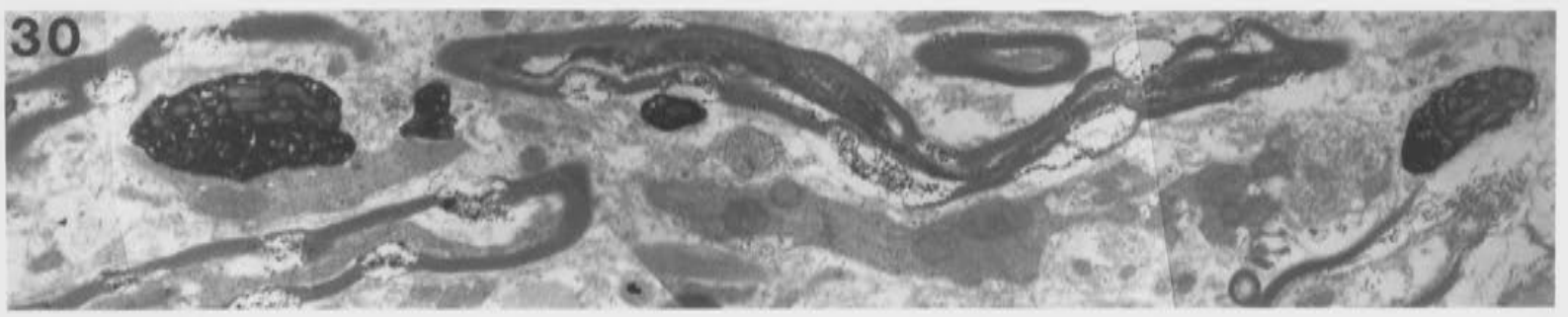
30


31

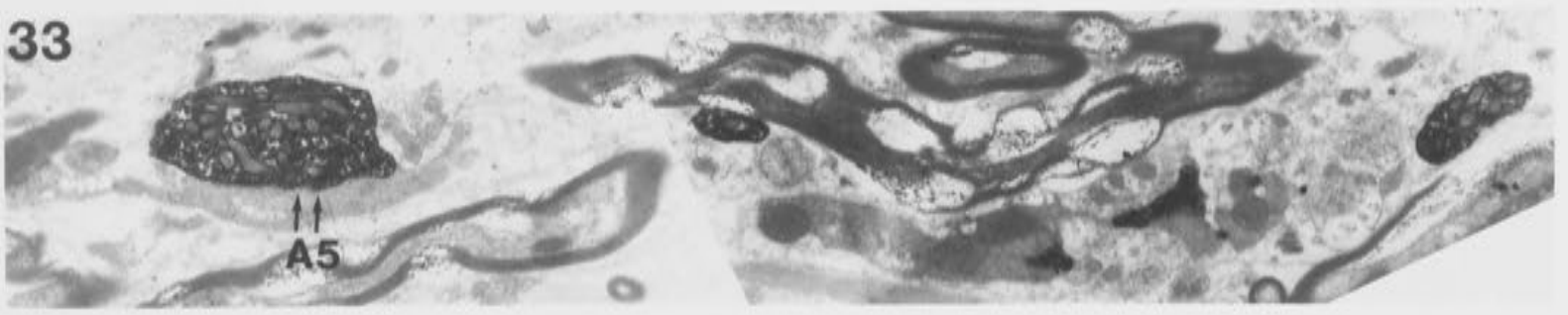
33
A5


34
A6
1 µm

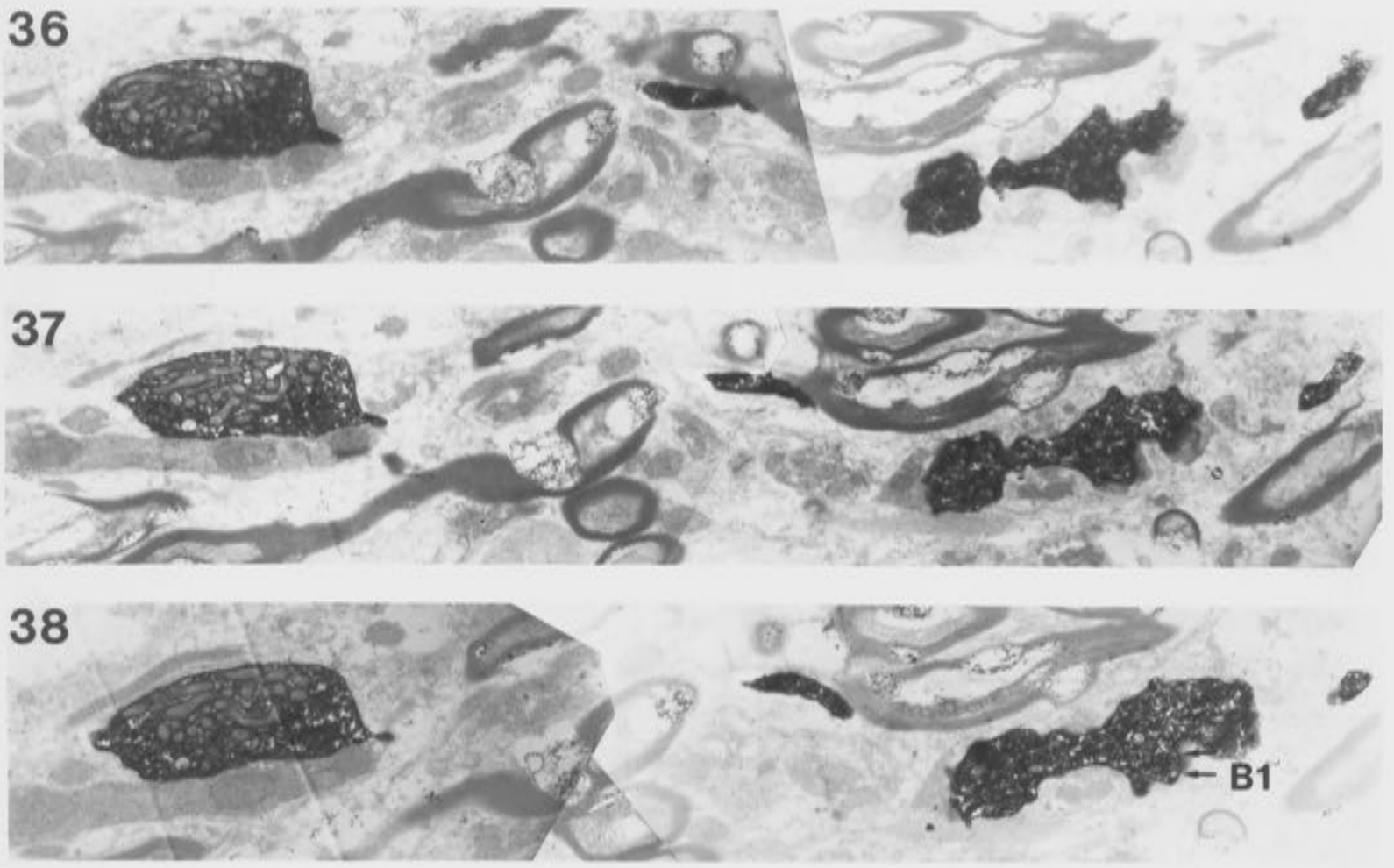
36
37
38
B1

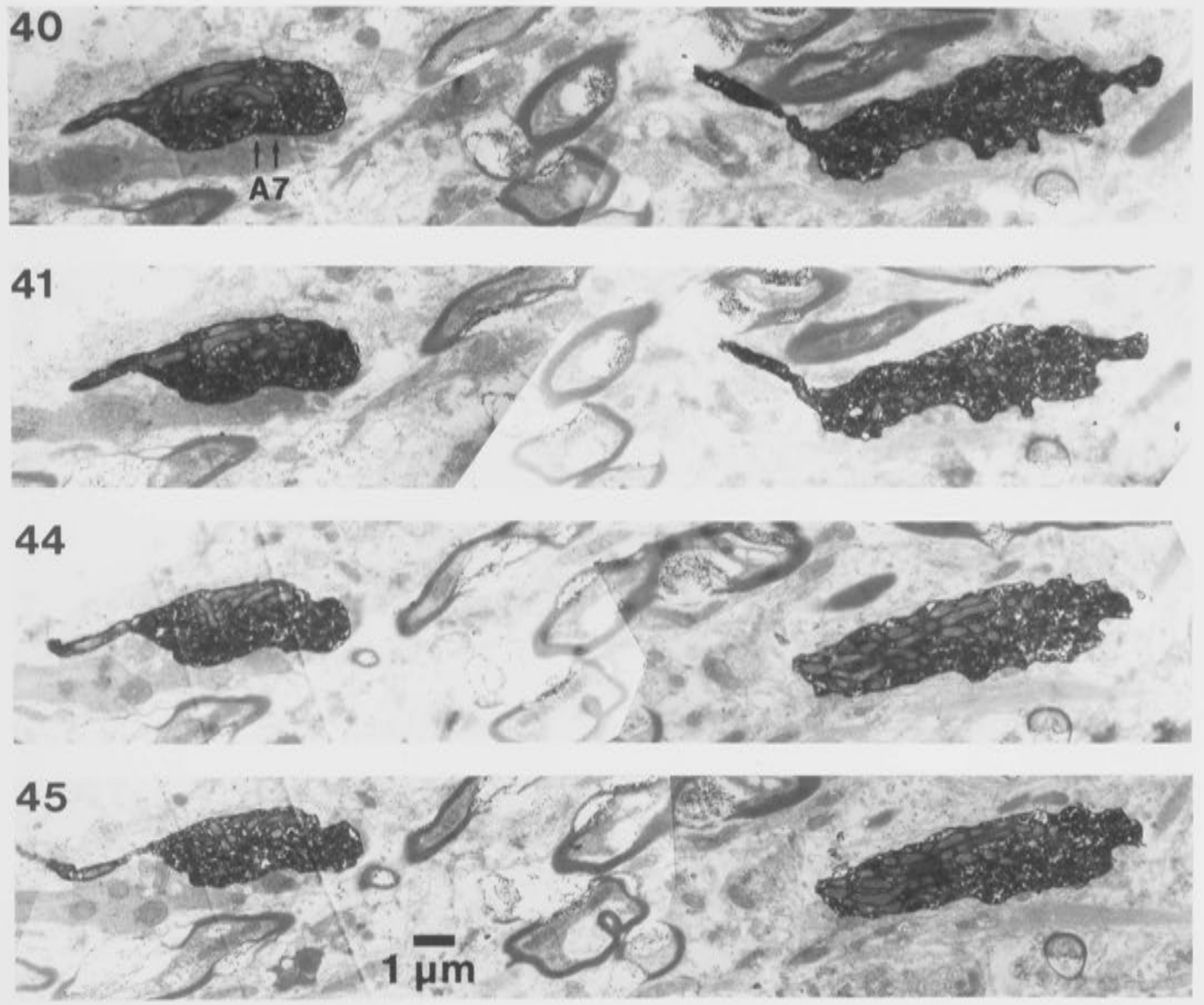
40
A7
41
44
45
1 µm

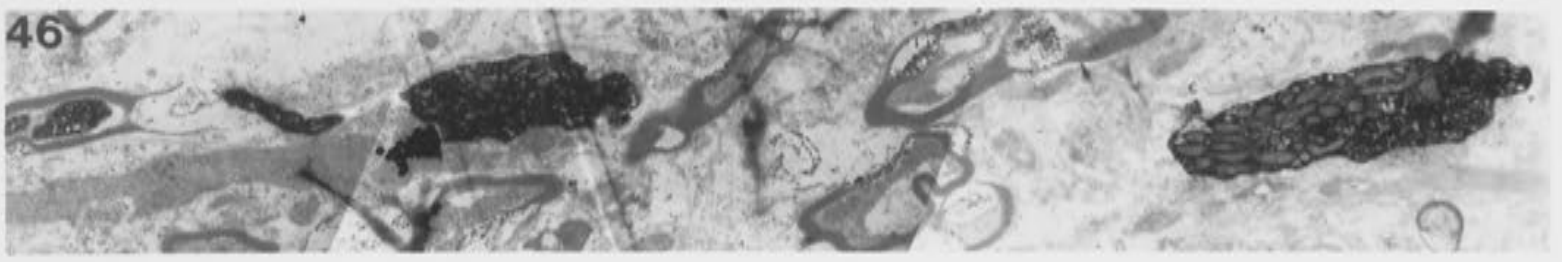
46

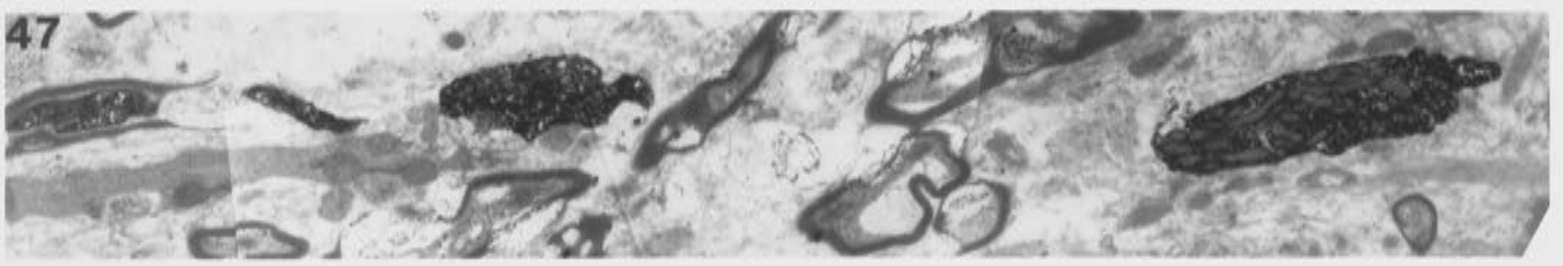
47

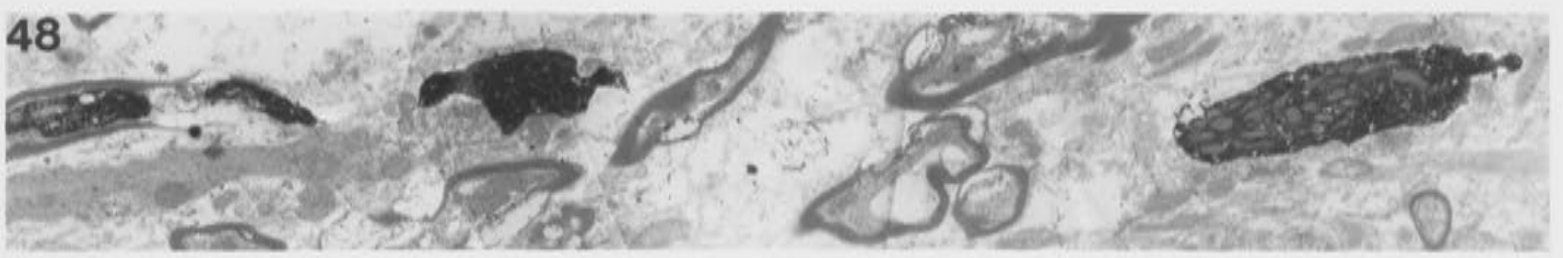
48


49

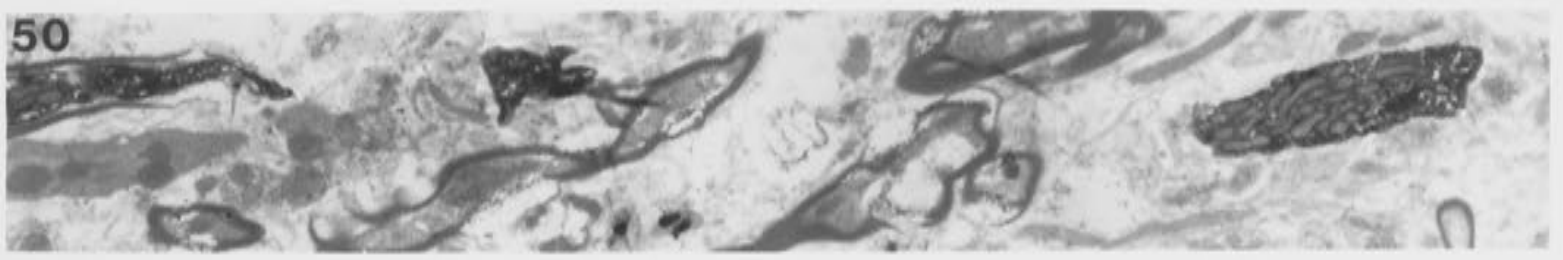
50


53


54
1 µm

FIGURE 4.20

The photomicrographs, 1-7, show examples at higher magnification of the specializations labelled A1-A7 in Figs. 4.16-4.19.

A. Contour map showing the shape and size of each of the synaptic specializations on the surface of the bouton. The separation between the contours is not to scale.

B. The synaptic surface of the bouton which overlies the dendrite is shown, drawn exactly to scale, with the synaptic specializations marked. The labels 1-7 correspond directly to the numbered photomicrographs.

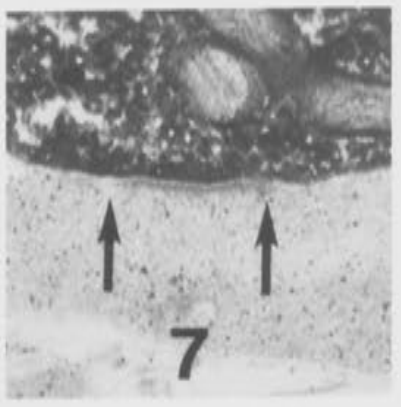

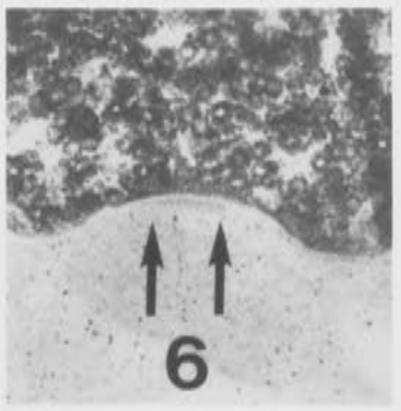

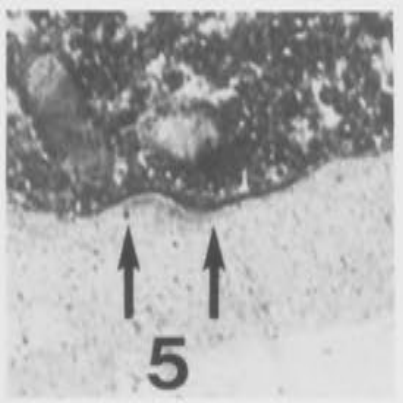

A

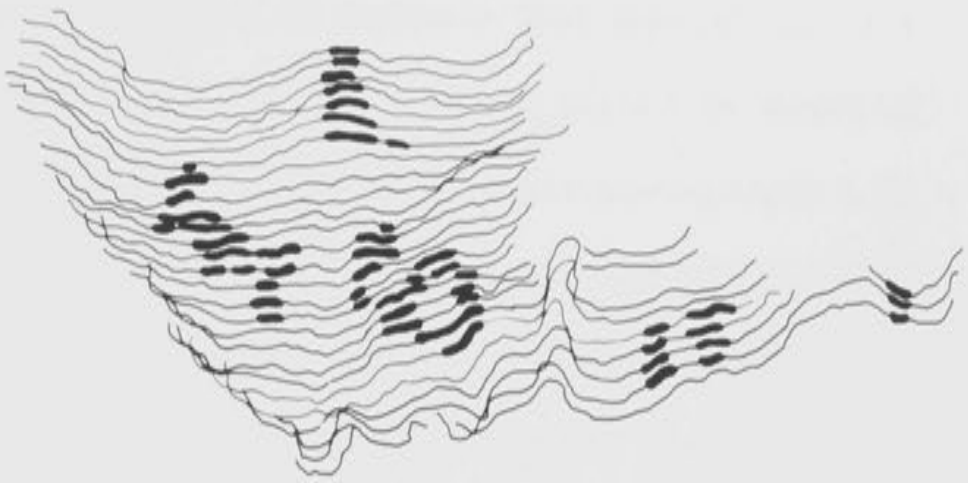

1 μm

B

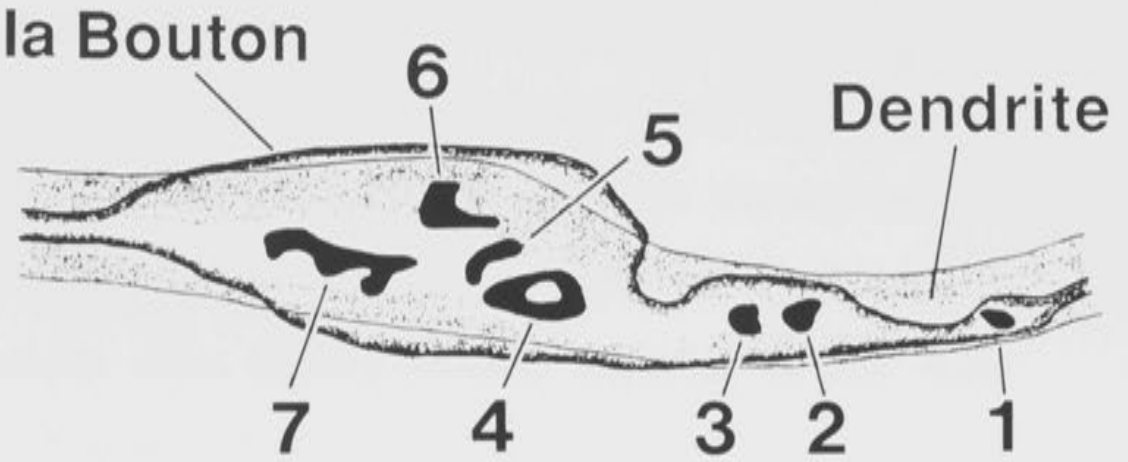

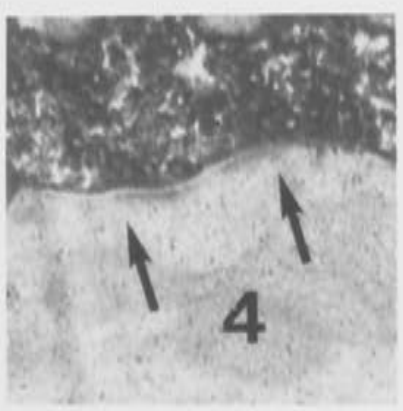

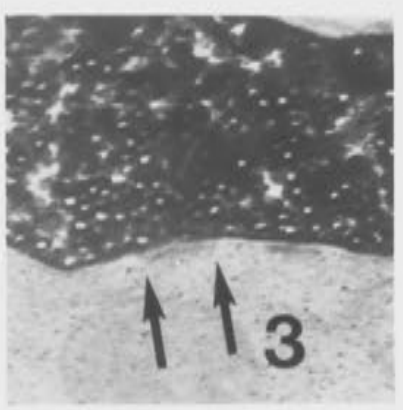

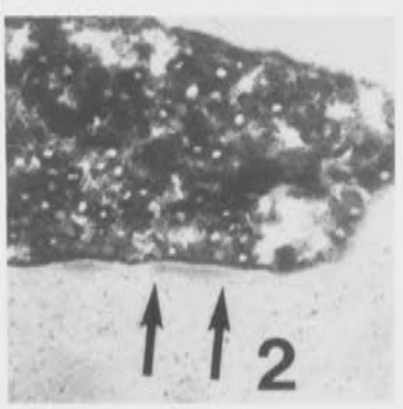

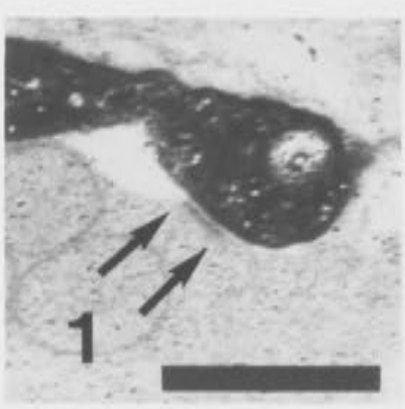

numbering of the photomicrographs in Fig. 4.20, and to the specializations A1 to A7 in Figs. 4.16 to 4.19. Fig. 4.20B indicates the unusual shapes of the synaptic specializations exhibited by this bouton. Serial section electron microscopy was required to determine the irregular shape of the largest specialization (7) and to indicate that specialization 4 was continuous, rather than two individual sites as suggested by some of the individual sections. For instance, in the inset photomicrograph 4 in Fig. 21, the specialization appears to be discontinuous. Serial EM showed that this was an example of a perforated synapse. Specializations 2 and 3 were discontinuous, although they were in close proximity to each other. The same was true of specializations 4 and 5. It is interesting to speculate that these may be examples of synaptic specializations which were previously perforated, and then became discontinuous (see 4.4 Discussion). These maps (Fig. 4.20A and B) indicate that the synaptic specializations may demonstrate a wide variety of sizes and shapes. Obviously, as in this case, serial EM is necessary to determine the continuous or discontinuous nature of the postsynaptic thickening. Mitochondria in this bouton were tightly packed together as has been described previously, and were situated well away from the synaptic surface of the bouton.

Figure 4.21 again shows the reconstructed collateral and indicates the boutons (A, B and C) presented in the next series of figures. The reconstruction shown in Fig. 4.22 summarizes the configuration of the three boutons. The incoming afferent (D = 1.1 μm), begins to lose its myelin sheath 5.4 μm from the edge of the bouton. In this paranodal zone, the scalloped appearance of the axolemma is exhibited, and the axon diameter d begins to narrow, (from d = 0.7 μm to d = 0.5 μm). The myelin layers do not come into direct contact with the bouton itself, instead leaving bare a narrow afferent bridge, 0.7 μm in length and only 0.2 μm in

FIGURE 4.21

Reconstruction of the HRP labelled plantaris Ia afferent collateral terminating in Clarke's column.

The following series of figures (Figs. 4.21, 4.22 and 4.23) represent the three boutons indicated by arrows (A, B and C) and enclosed by the dotted box in this reconstruction.

Two other swellings on the collateral, (contained within the dotted box), were shown on the original reconstruction as possible boutons (see Fig. 4.2). Serial electron microscopy demonstrated that these were not boutons, but probably darker or more densely labelled regions of the collateral itself.

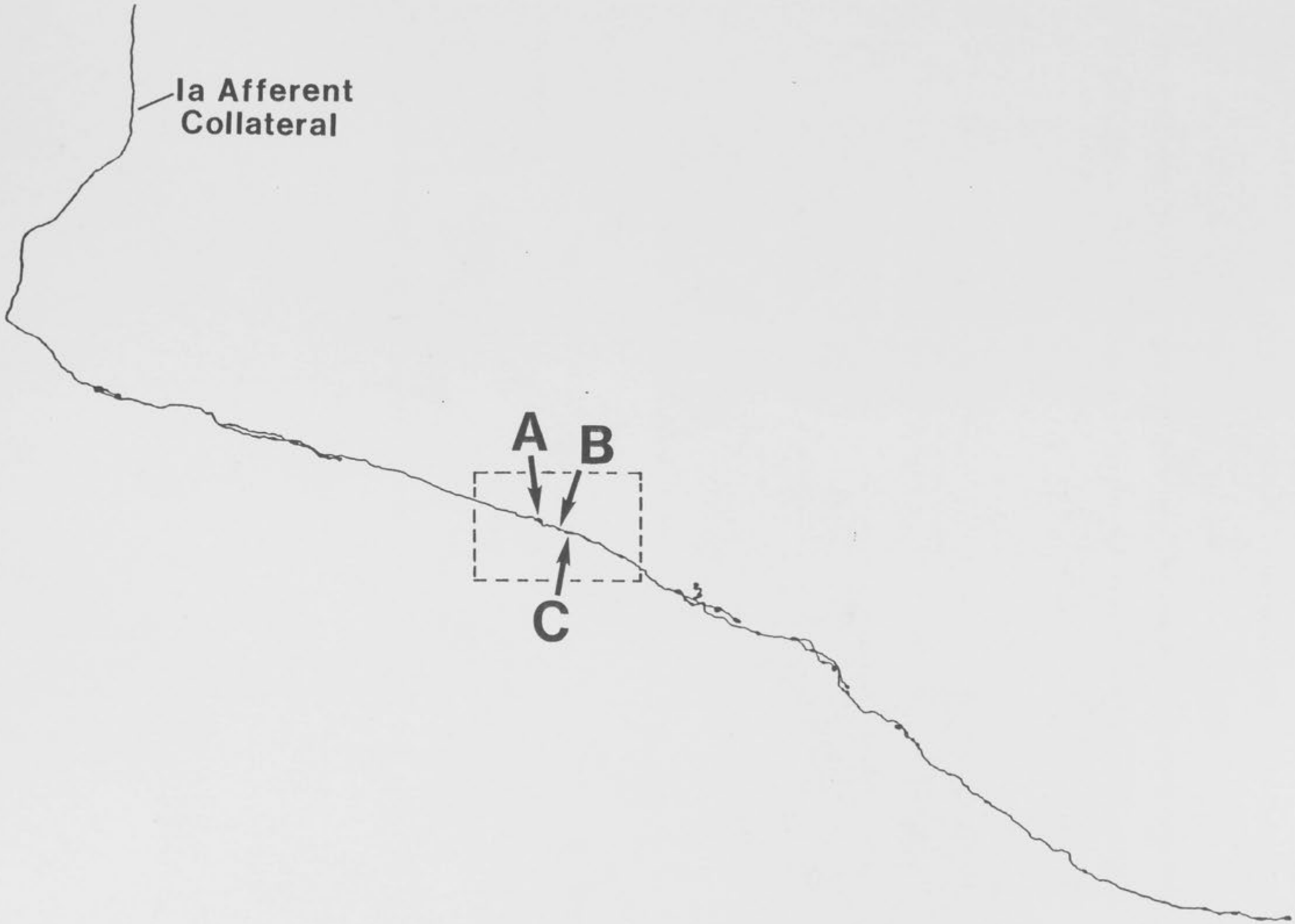
Ia Afferent
Collateral
A
B
C

FIGURES 4.22 - 4.24

The following three figures show a series through the three boutons indicated on the previous reconstruction (Fig. 4.21).

The line diagram at the bottom of figure 4.22 summarizes the configuration of this series of three boutons. Synaptic specializations are indicated with double sets of arrows as C1 and C2 in Fig. 4.22; B1, B2 and B3 in Fig. 4.23; and A1 and A2 in Fig. 4.24.

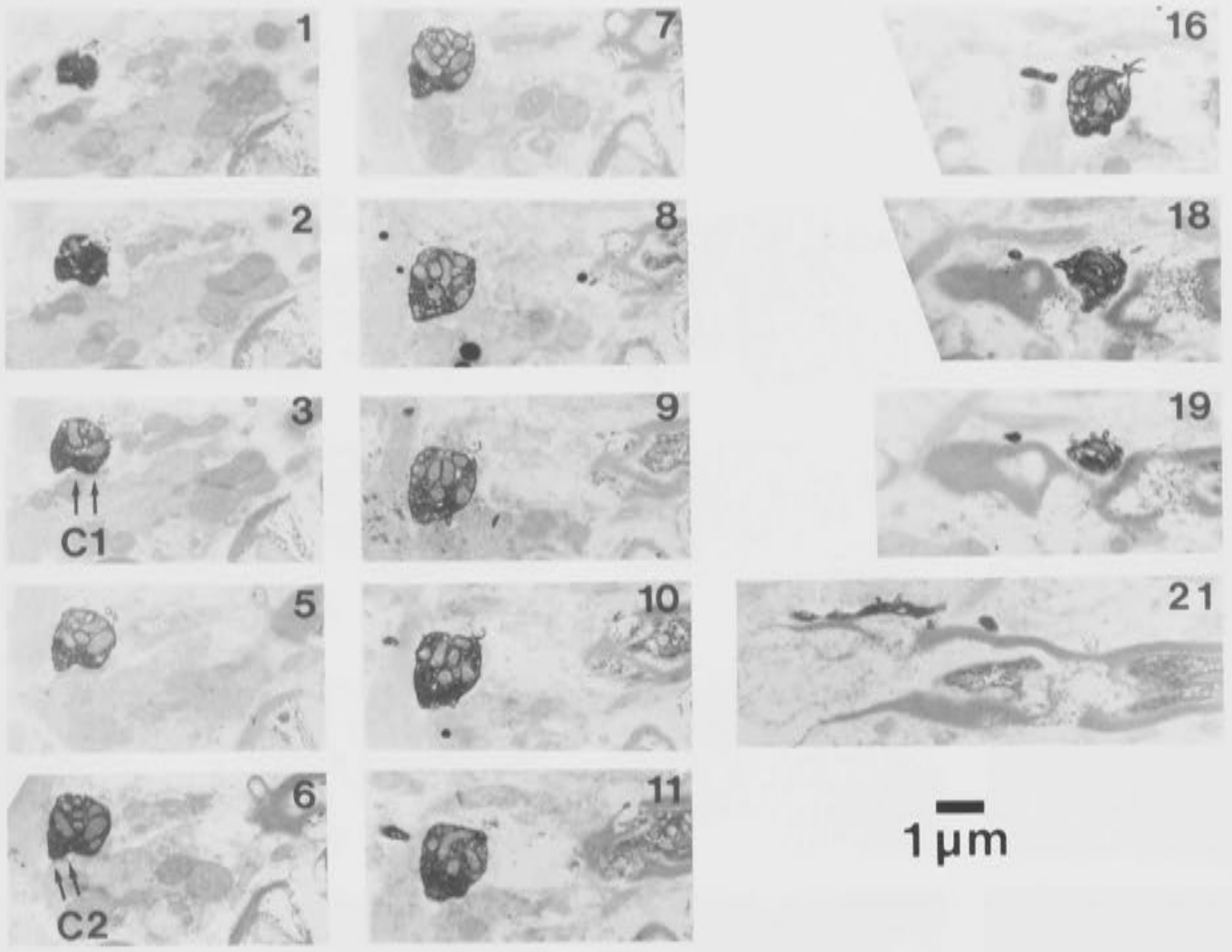
1
7
16
2
8
18
3
9
19
C1
5
10
21
6
11
C2
1 µm

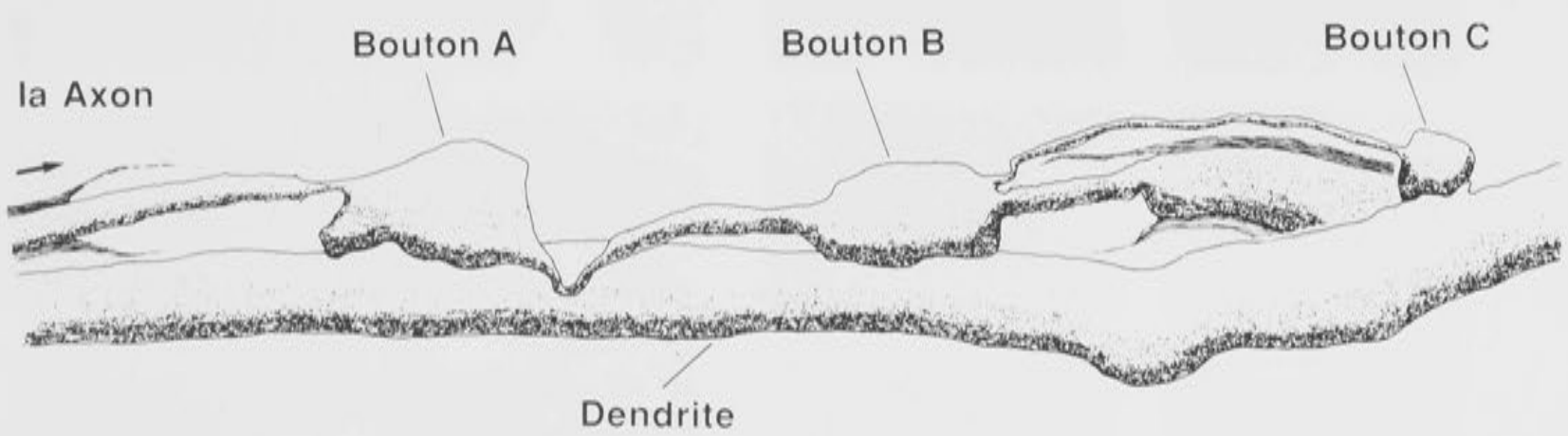
Ia Axon
Bouton A
Bouton B
Bouton C
Dendrite

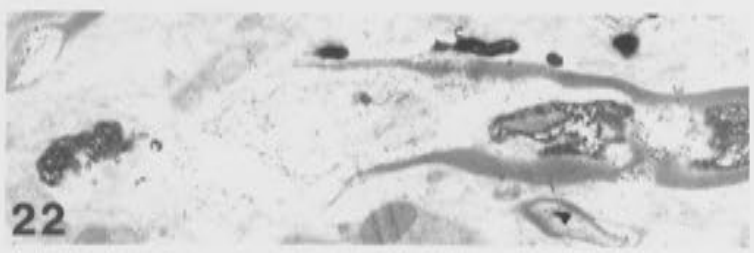
22


24


25


26


27


28
B1

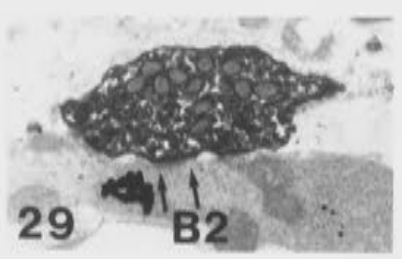
29
B2


30


31
B3


32

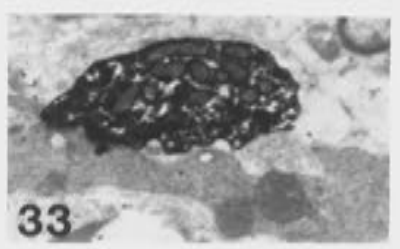
33


35


36


48


52

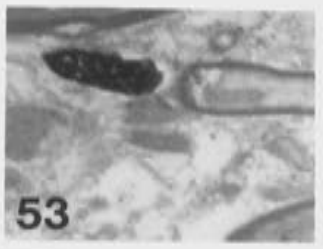
53


54

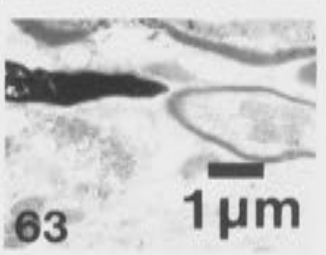
63
1µm

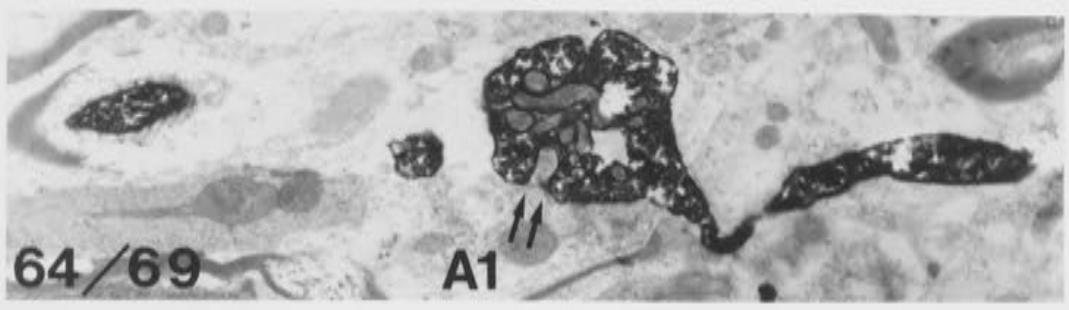
64/69
A1


79


73


85


74
A2

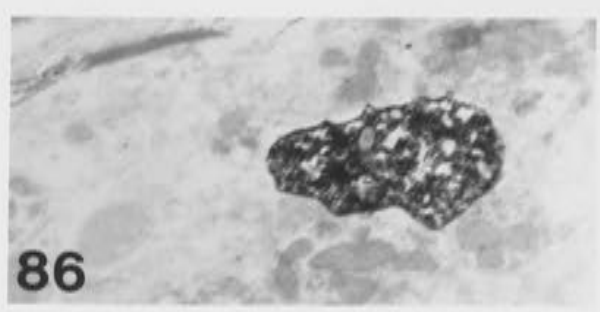
86

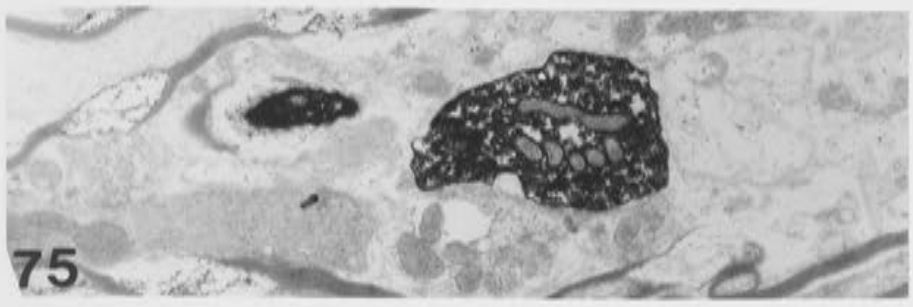
75


88


76


89

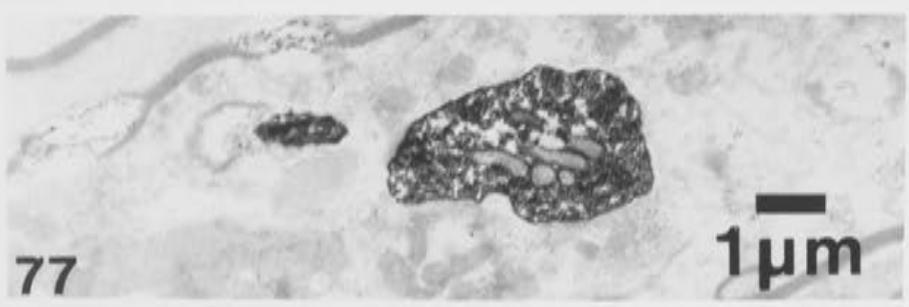
77
1µm

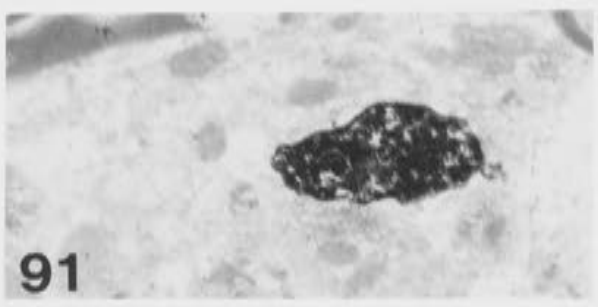
91

diameter, leading to the first bouton, labelled bouton A in the drawing of Fig. 4.22. Bouton A is approximately 4.1 x 2.4 µm. After emerging from bouton A, the fibre does not remyelinate, instead exhibiting a now familiar unmyelinated narrow bridge or neck, 0.5 µm in diameter and 5.5 µm in length, giving rise to bouton B. Bouton B of this series is approximately 3.8 x 2.0 µm, and constitutes a further branch point on the collateral. The major branch is the continuation of the afferent itself. A paranodal zone is exhibited on this major branch, prior to remyelination of the fibre. On remyelination, the fibre diameter d increases abruptly from 0.5 µm to 1.5 µm, and the caudal continuation of the myelinated fibre has a total diameter D of 1.9 µm. The second branch is an extremely narrow neck or bridge of unmyelinated afferent fibre, which averages 0.17 µm in diameter, and reaches 8.3 µm in length. This branch gives rise to a tiny spherical terminal bouton, approximately 1.4 µm in diameter.

As with the previous series, each of these three boutons lies along the same postsynaptic dendrite. The orientation of the boutons in relation to this dendrite is clearly shown in the line drawing of Fig. 4.22. The photomicrographs of Fig. 4.22 are a selected sequence of the serial sections taken through the terminal bouton, bouton C. Two probable synaptic specializations are indicated in Fig. 4.22 sections 3 and 6 with double arrows as C1 and C2. The unusual configuration of this small bouton meant that, under the light microscope, the very narrow branch was not resolved (see Fig. 4.2). Instead, it was believed that boutons B and C of this series existed in a peanut or dumbell shaped arrangement, as observed under the light microscope. Serial section electron microscopy was used to show the true nature of the configuration, with the terminal bouton overlying the continuation of the myelinated afferent. Bouton B established three probable synaptic specializations, illustrated in Fig. 4.23 sections 28 and 29 with double arrows as B1, B2 and B3. Bouton B can be

seen to be packed with vesicles, and the tightly clustered mitochondria are situated well away from sites of possible transmitter release. Two synaptic specializations observed in bouton A of this series are illustrated in Fig. 4.24 sections 64/69 and 74. Section 64/69 is a montage of the two sections (64 and 69). The specialization labelled A1 in Fig. 4.24 section 64/69 is a further example of a synaptic specialization on a spine-like protrusion, where the bouton appears to wrap around the postsynaptic process. The vesicles are very clearly lined up around the spine at the presynaptic site. The second synaptic specialization on this bouton, marked A2 in Figure 4.24 section 74 was of a more conventional configuration. Again the bouton is packed full of vesicles, and the mitochondria are clumped together in the center of the bouton.

Two further possible boutons were indicated on the original light microscopic reconstruction and are shown marked as 'p' in the reconstruction of Fig. 4.2. Neither proved to be synaptically specialized, and each was simply a darker, denser area of the HRP stained myelinated collateral.

The afferent continuation of this series travelled in parallel with a second branch of the collateral which had not been resolved under the light microscope (and is therefore not indicated in the tracing of Fig. 4.2) for 55 μm before any further specializations were seen. The fact that the second branch had not been identified under the light microscope meant that the traced configuration actually appeared more complex than the true morphology, which has now been determined using serial section EM techniques. Figure 4.25 again shows the reconstructed collateral. The four arrows indicate the next series of boutons to be presented. This series, enclosed by the dotted box, and indicated with arrows as A, B, C and D, was in fact a straight forward *en passant* series of boutons with no branch points involved. This did not appear to be the case from the original

FIGURE 4.25

Reconstruction of the HRP labelled plantaris Ia afferent collateral terminating in Clarke's column.

The configuration of the series of four boutons indicated by arrows as A, B, C and D on this reconstruction was in fact simpler than appears from this reconstruction. These four boutons are presented in the following series of figures, Figs. 4.26 - 4.28.

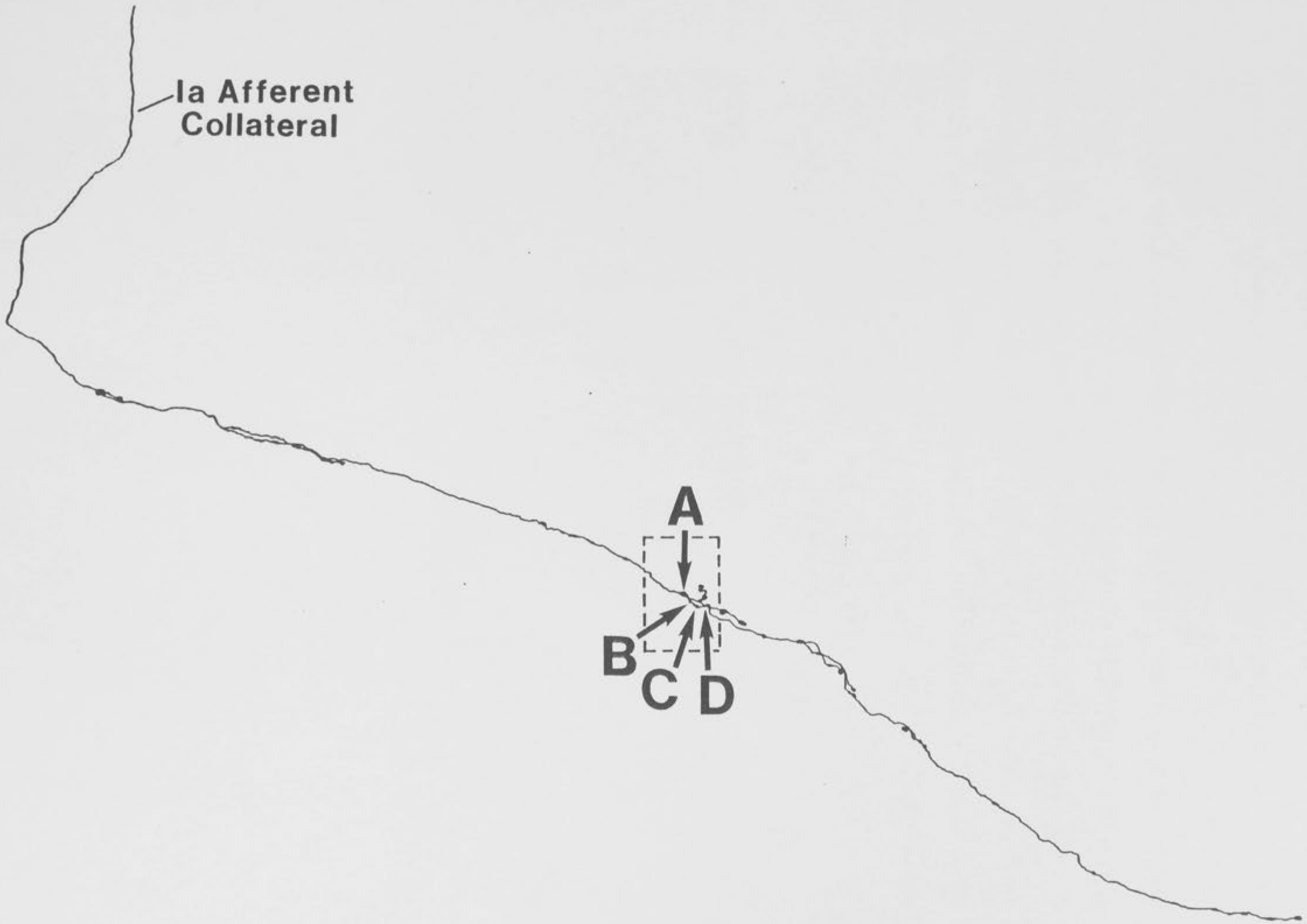
Ia Afferent
Collateral
A
B
C
D

FIGURES 4.26-4.28

These three figures show a series of photomicrographs taken through the four boutons indicated by arrows as A, B, C and D on the reconstruction of Fig. 4.25.

The line drawing at the bottom of Fig. 4.28 summarizes the configuration of the four boutons, which were an *en passant* series.

A single synaptic specialization was recognized in Bouton A, marked with a double set of arrows as A1 in Fig. 4.27. Boutons C and D also exhibited single synaptic specializations, indicated with double sets of arrows as C1 and D1 in Fig. 4.26.

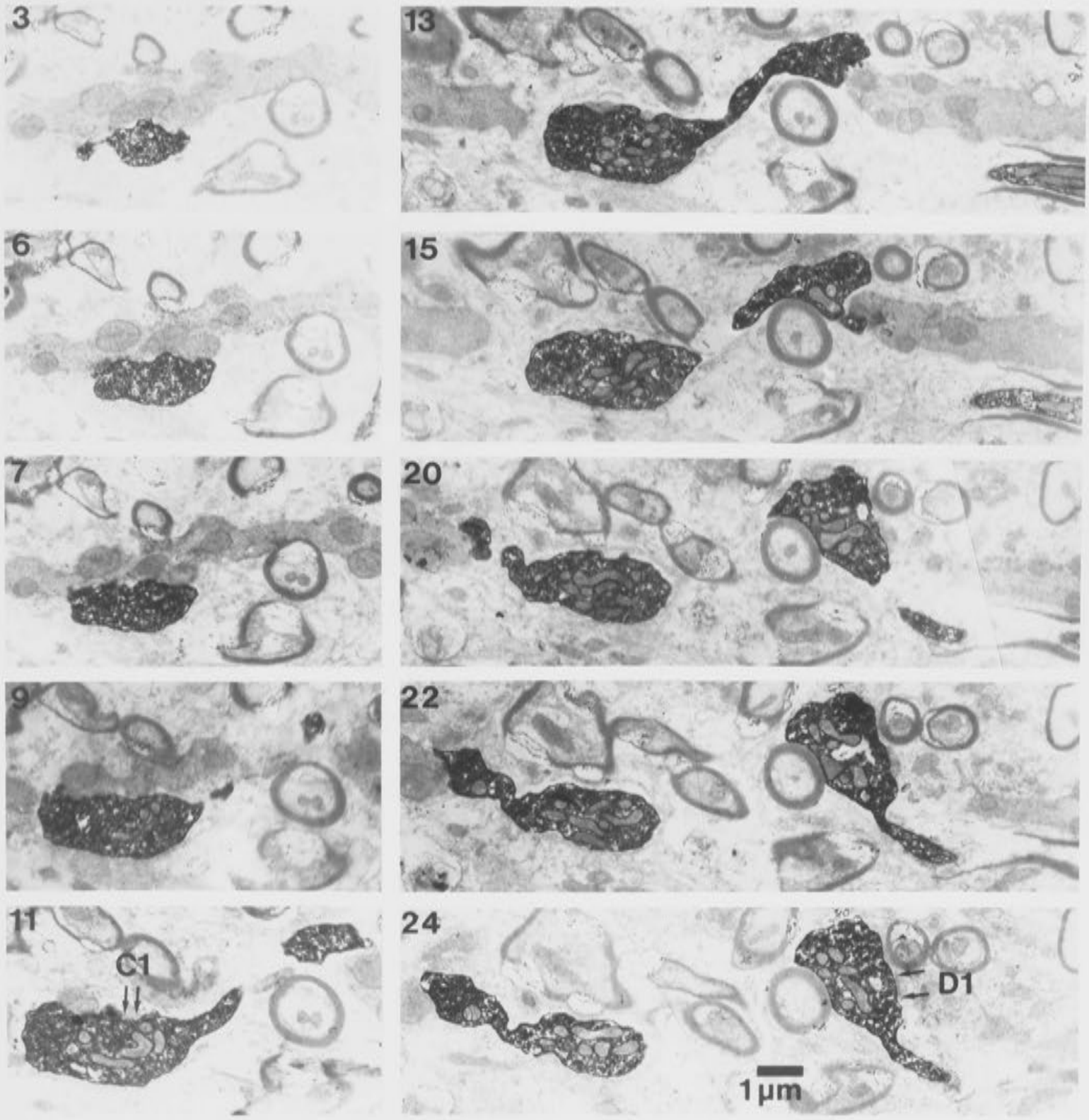
3
13
6
15
7
20
9
22
11
C1
24
D1
1 µm

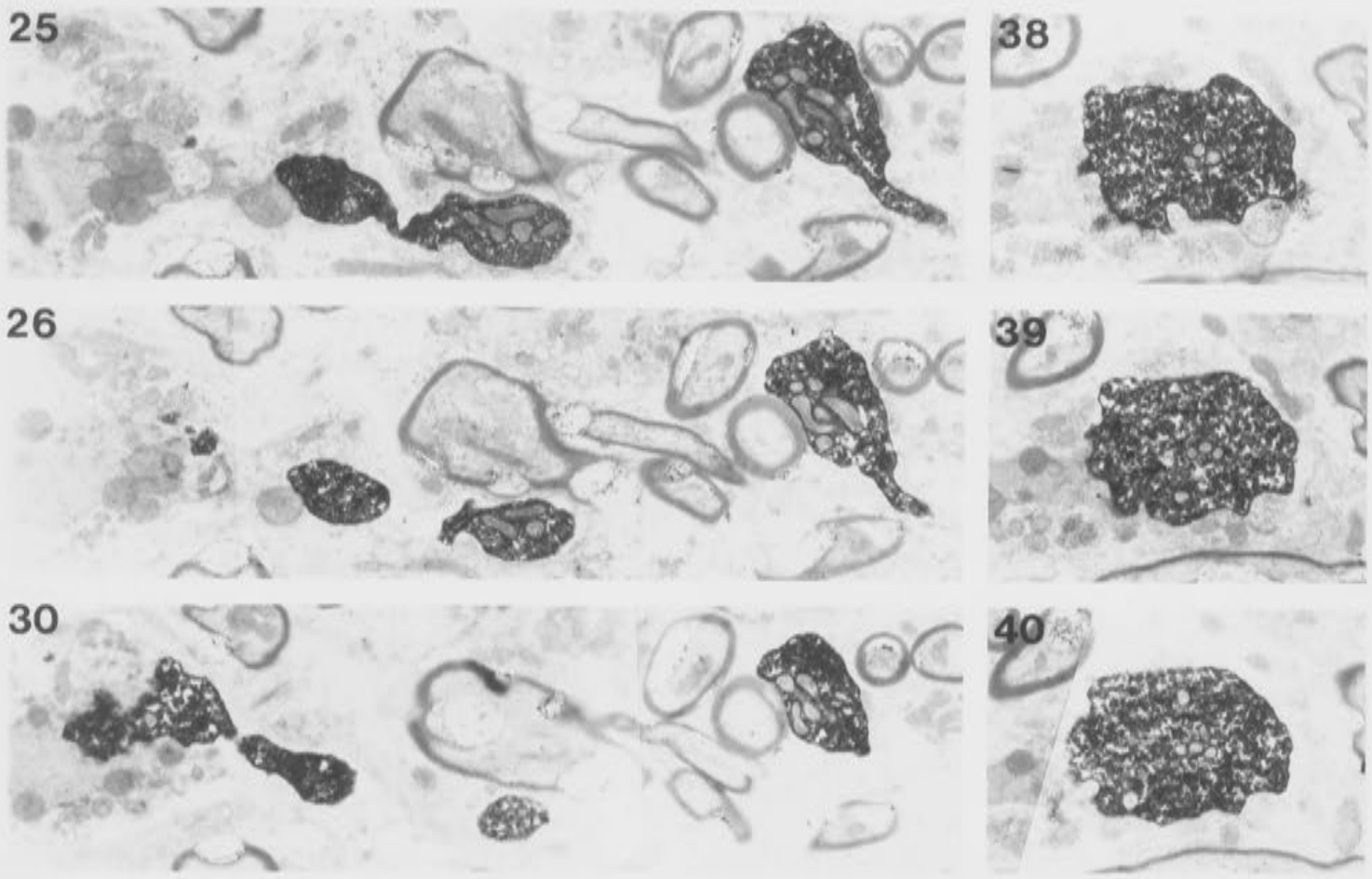
25
38
26
39
30
40
31
41
A1
37
42
1µm

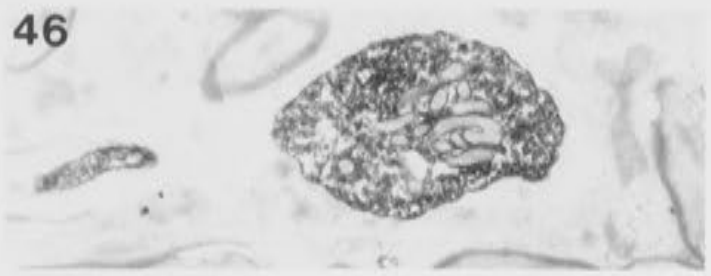
46


47


48

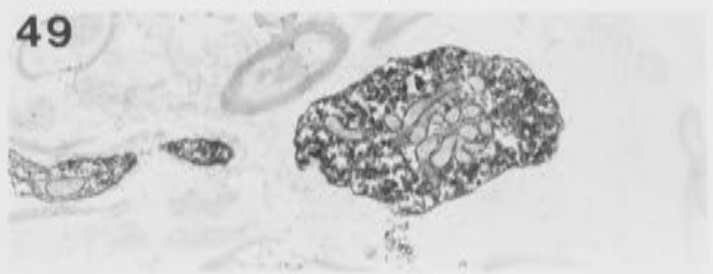
49


52


54


55

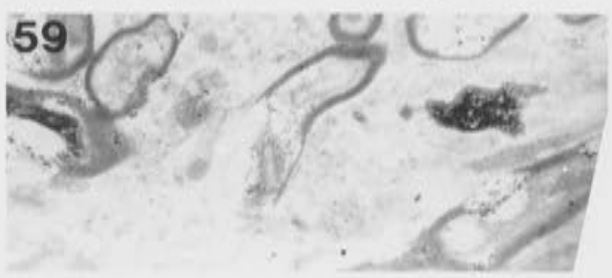
59

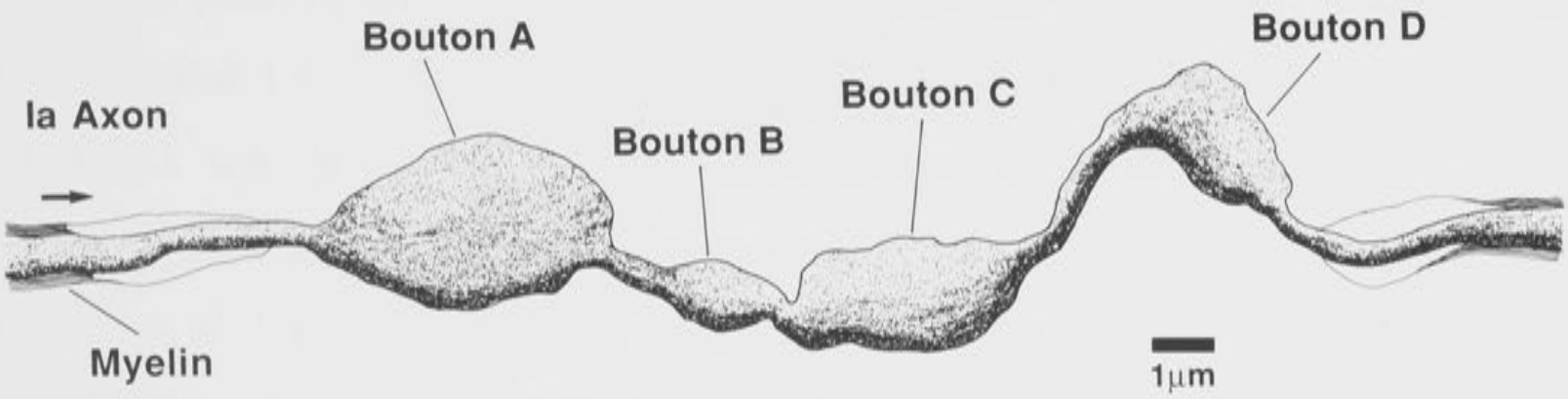
Bouton A
Bouton D
Ia Axon
Bouton C
Bouton B
Myelin
1μm

tracing (Fig. 4.2) but is clearly illustrated in the summary line drawing of Figure 4.28. The confusion arose for two reasons. Firstly, the second, parallel collateral branch had not been resolved by the initial light microscopic observation of the collateral, and secondly, bouton D appeared to overlay the parallel collateral branch, thus appearing to belong to both branches. Serial electron microscopy established that this was not the case, and the configuration of this next branch was quite simple.

Figure 4.28 shows the myelinated branch of the collateral D = 1.0 μm and d = 0.7 μm, on the left. As previously, the arrow on the line drawing indicates the direction of travel of an incoming action potential. A paranodal region 3.0 μm in length is exhibited, over which the afferent loses its myelin sheath, and the diameter of the fibre is reduced from d = 0.7 to d = 0.4 μm. The myelin sheathing does not reach the first bouton, instead leaving an 0.7 μm length of the collateral bare. Bouton A is approximately 4.6 x 2.7 μm. After emerging from bouton A, the collateral does not remyelinate. A small unmyelinated fibre neck 0.4 μm in diameter and 1.0 μm in length connected boutons A and B. Bouton B was 1.4 x 1.1 μm, and the bridge which joined it to bouton C was unmyelinated, 0.4 μm in diameter and less than 0.3 μm in length. The small size of this bridge made it difficult to determine whether boutons B and C were separate, or in fact parts of the same bouton. They were reconstructed as individual boutons on the tracing (see Figs. 4.2 and 4.25), in view of the narrow bridge separating them. Bouton C is 3.6 x 1.9 μm, and is connected to bouton D by a further unmyelinated afferent branch, 0.4 μm in diameter and 2.7 μm in length. Bouton D, (2.7 x 1.6 μm) is the final bouton in this *en passant* series. The configuration of bouton D was quite unusual, as recognised under the light microscope (see Figs. 4.2 and 4.25), and easily correlated with the accompanying series of

photomicrographs presented in Figures 4.26-4.28. After emerging from bouton D, the afferent did not remyelinate immediately, leaving a short neck 0.7 μm long and 0.3 μm wide bare of sheathing. Remyelination occurred over a region 3.0 μm in length, and the fully myelinated continuation of the afferent had a diameter D of 1.0 μm (d = 0.7 μm). A selected sequence of the photomicrographs taken through this series of 4 boutons is presented in Figs. 4.26 - 4.28. Due to the order of appearance of this series of boutons, the sections are numbered relative to the first appearance of bouton C. A single synaptic specialization was recognized in bouton C, and this is shown marked by double arrows as C1 in Figure 4.26 section 12. Bouton C is seen giving rise to the final bouton of the series, bouton D, in Fig. 4.26 sections 12-15. As already noted, bouton D had an unusual configuration, appearing as a hump on the tracing under the light microscope (Figs. 4.2 and 4.25). In Fig. 4.26 sections 15 to 24, the reason for this configuration is obvious, as bouton D appears to fold around a myelinated axon which runs perpendicular to it, viewed in cross section. Bouton D also exhibited a single synaptic specialization, seen marked by double sets of arrows as D1 in Figure 4.26 section 24. Bouton B was very small, and situated very close to bouton C, but the narrow neck which established them as individual boutons is shown in Fig. 4.27 section 25. Bouton A was the largest of this series. Only one clear synaptic specialization was visible in bouton A, marked with double arrows as A1 in Fig. 4.27 section 41.

Running parallel to, and behind the series of boutons presented in Figs 4.25-4.28, was a second collateral branch. This branch was somewhat more complex, exhibiting a number of further branch points, each giving rise to synaptic boutons. Figure 4.29 again shows the reconstructed collateral. Enclosed in the dotted box, and indicated by the arrow, is an individual swelling, or bouton, which constituted a complex branch point

FIGURE 4.29

Reconstruction of the HRP labelled plantaris Ia afferent collateral terminating in Clarke's column.

A single bouton is indicated by the arrow on this reconstruction. This bouton proved to exhibit a more complex configuration than expected, giving rise to three distinct branches of the collateral. This bouton and its collateral branches are shown in Fig. 4.30.

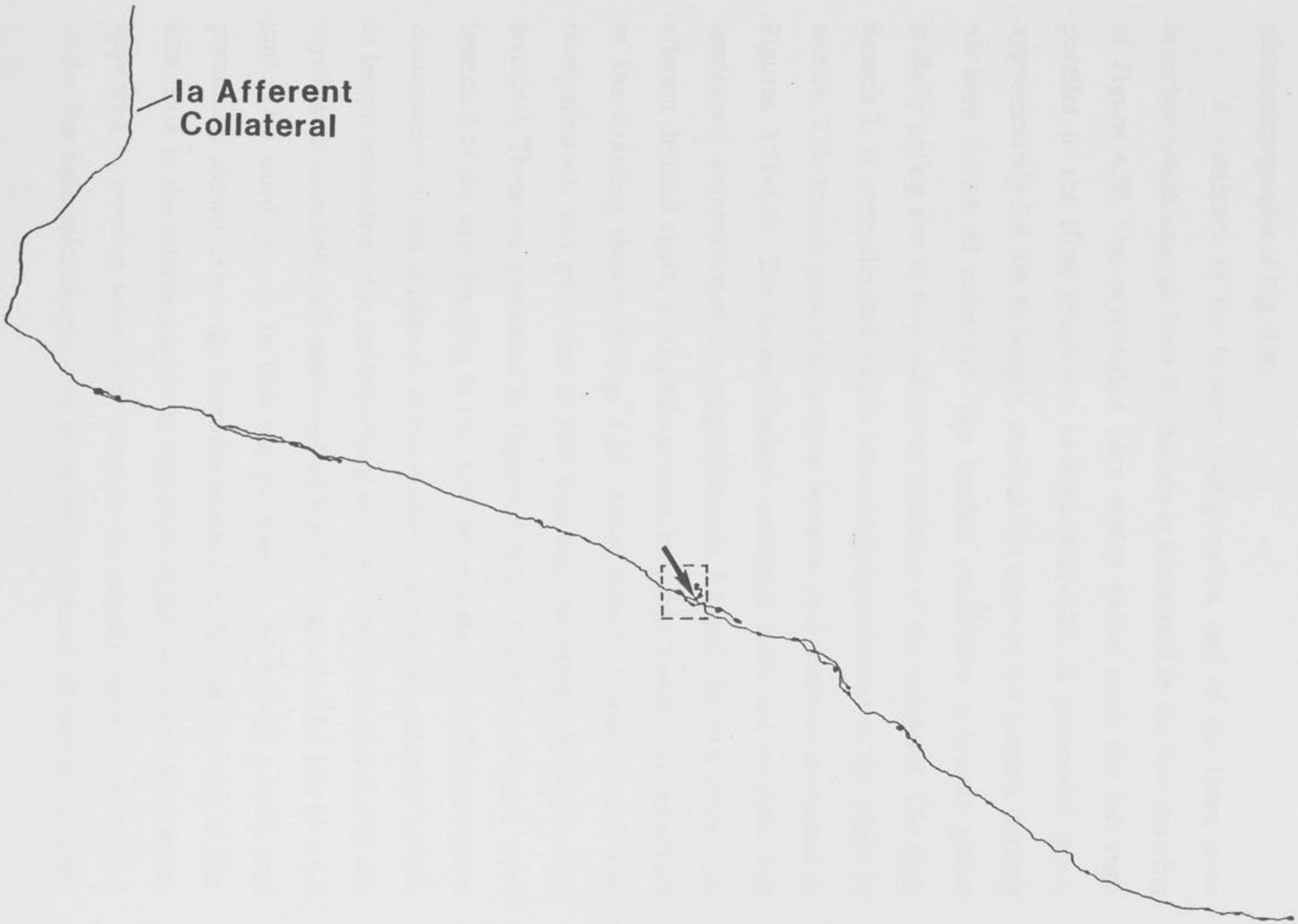
Ia Afferent
Collateral

(of greater complexity than indicated on the light reconstruction in Fig. 4.2). A sequence of the sections taken through this bouton and the collateral branches which arise from it is presented in the photomicrographs of Fig. 4.30.

A summary of the bouton configuration and of the three axon branches which emerge from the bouton is illustrated in the line drawing of Figure 4.30. The myelinated fibre which enters from the left runs parallel to the fibre presented in Figs. 4.25-4.28. A paranodal zone, approximately 2.8 μm in length, reaches the edge of the bouton, leaving no bare stretch of collateral. The bouton constitutes a branch point, initially giving rise to two individual branches of the collateral. The first, branch 1, is unmyelinated and is oriented perpendicular to the plane of section. This branch gave rise to three boutons, and these are presented in Figures 4.31-4.35. The second branch emerged from the bouton, and continued unmyelinated for approximately 1.2 μm. At this point, the afferent divided again, giving rise to axon branches 2 and 3, as presented in the drawing shown in Fig. 4.30. Axon branch 2 was narrow and unmyelinated, and gave rise to two boutons, the second of which was terminal. These are presented in Figures 4.36-39. The other branch, axon branch 3 of the line drawing in Fig. 4.30 became the remyelinated caudal continuation of the collateral. A paranodal region approximately 1.8 μm in length coincided with the branching of axon branches 2 and 3, and the myelinated axon branch 3 continued with a diameter D of 1.1 μm (d = 0.8 μm). This third branch in fact ran parallel to the branch which was previously shown to emerge from the boutons in the line drawing in Fig. 4.28. Due to the orientation of the branches, these two continuing axons appeared to overlap with each other in the sagittal sections examined under the light microscope, and the resolving power of that microscope

FIGURE 4.30

A selection of the serial sections taken through the bouton indicated in the reconstruction of Fig. 4.29 are presented in the upper photomicrographs.

This bouton gave rise to a complicated branching arrangement, which is indicated in the line drawing.

Branch 1, which emerged directly from the bouton, ran perpendicular to the remainder of the labelled collateral. This terminal branch is presented in Figs. 4.31-4.35.

A second branch which emerged from the collateral subsequently branched again, giving rise to branch 2 and branch 3.

Branch 2 was unmyelinated, and is presented in Figs. 4.36 - 4.39.

Branch 3 was the myelinated continuation of the labelled collateral. It ran in parallel with the branch of the collateral which emerged from the final bouton in Fig. 4.28.

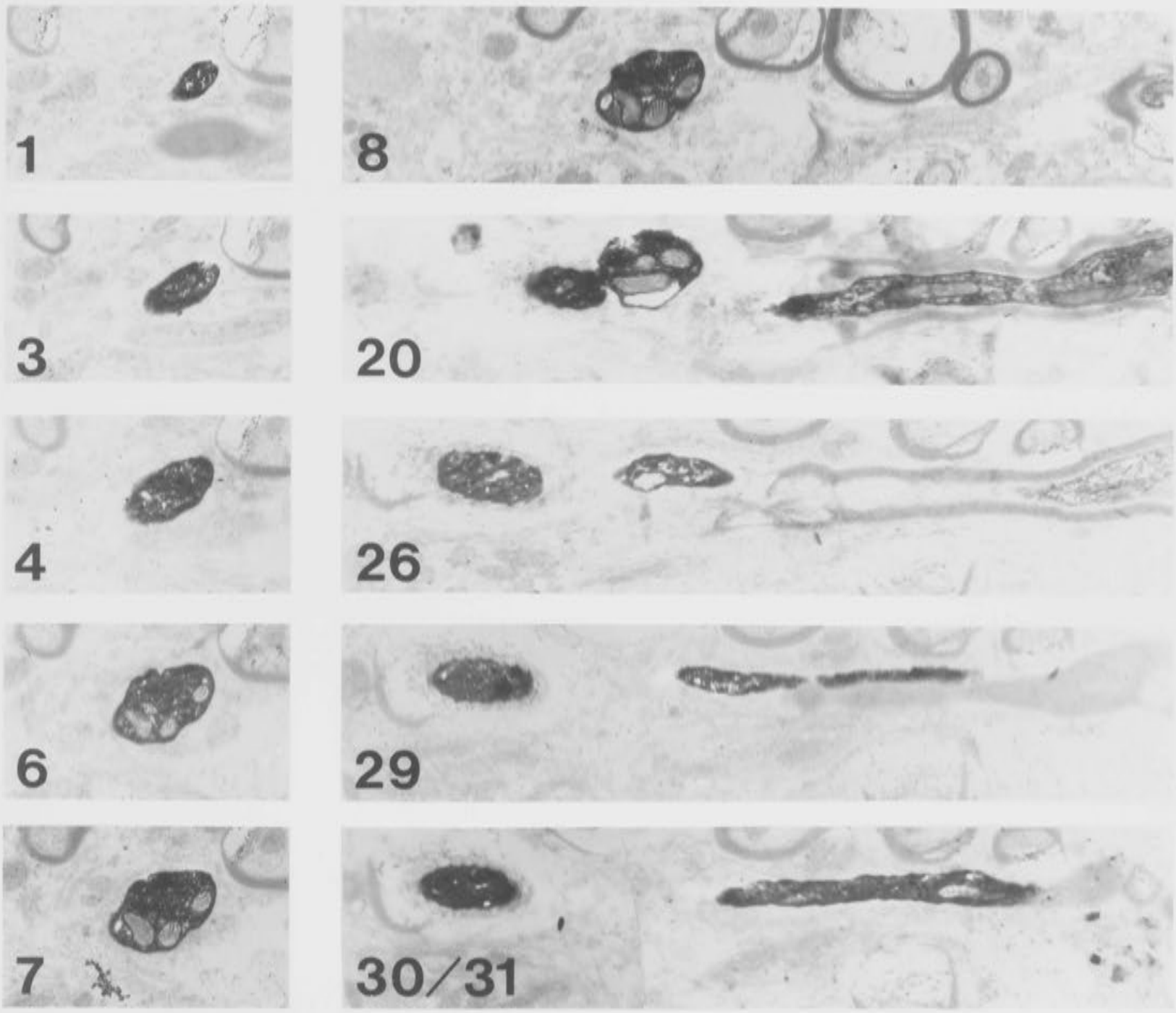
1
8
3
20
4
26
6
29
7
30/31

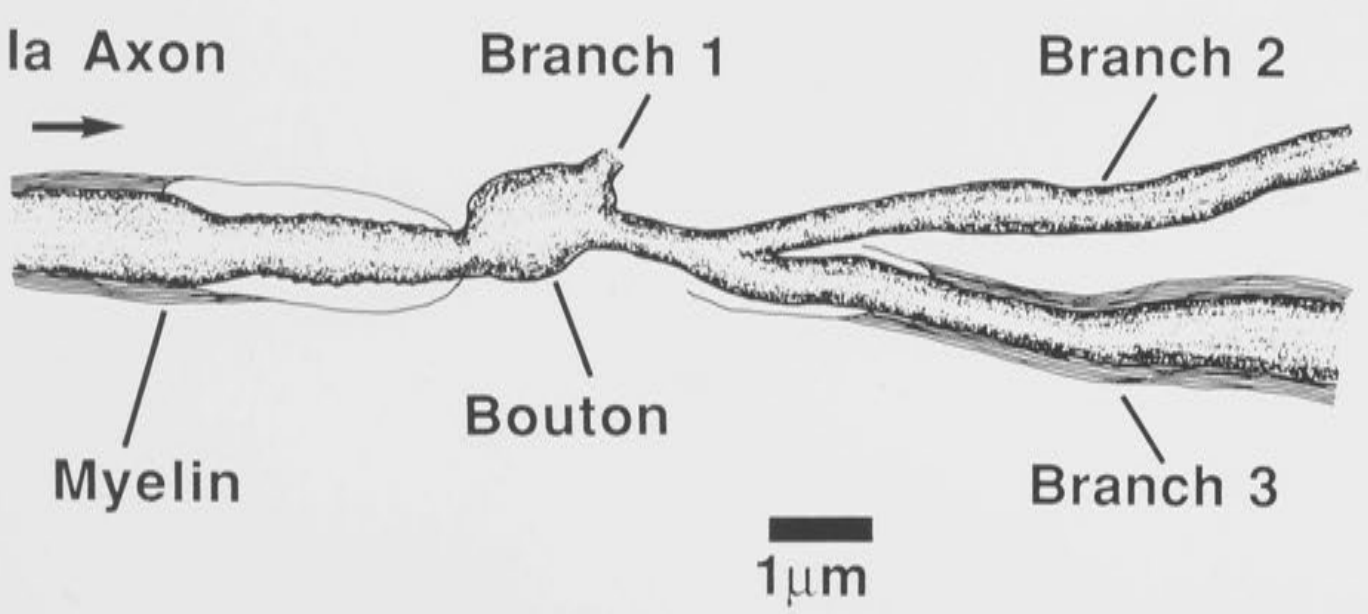
Ia Axon
Branch 1
Branch 2
Myelin
Bouton
Branch 3
1μm

FIGURE 4.31

Reconstruction of the HRP labelled plantaris Ia afferent collateral terminating in Clarke's column.

The boutons indicated in this reconstruction by the arrows as A, B and C, and enclosed in the dotted box, were situated on branch 1 of Fig. 4.30. This branch ran perpendicular to the remainder of the labelled collateral, towards the top of the section, and was terminal. The three boutons are presented in the sequence of photomicrographs in Figs. 4.32-4.35.

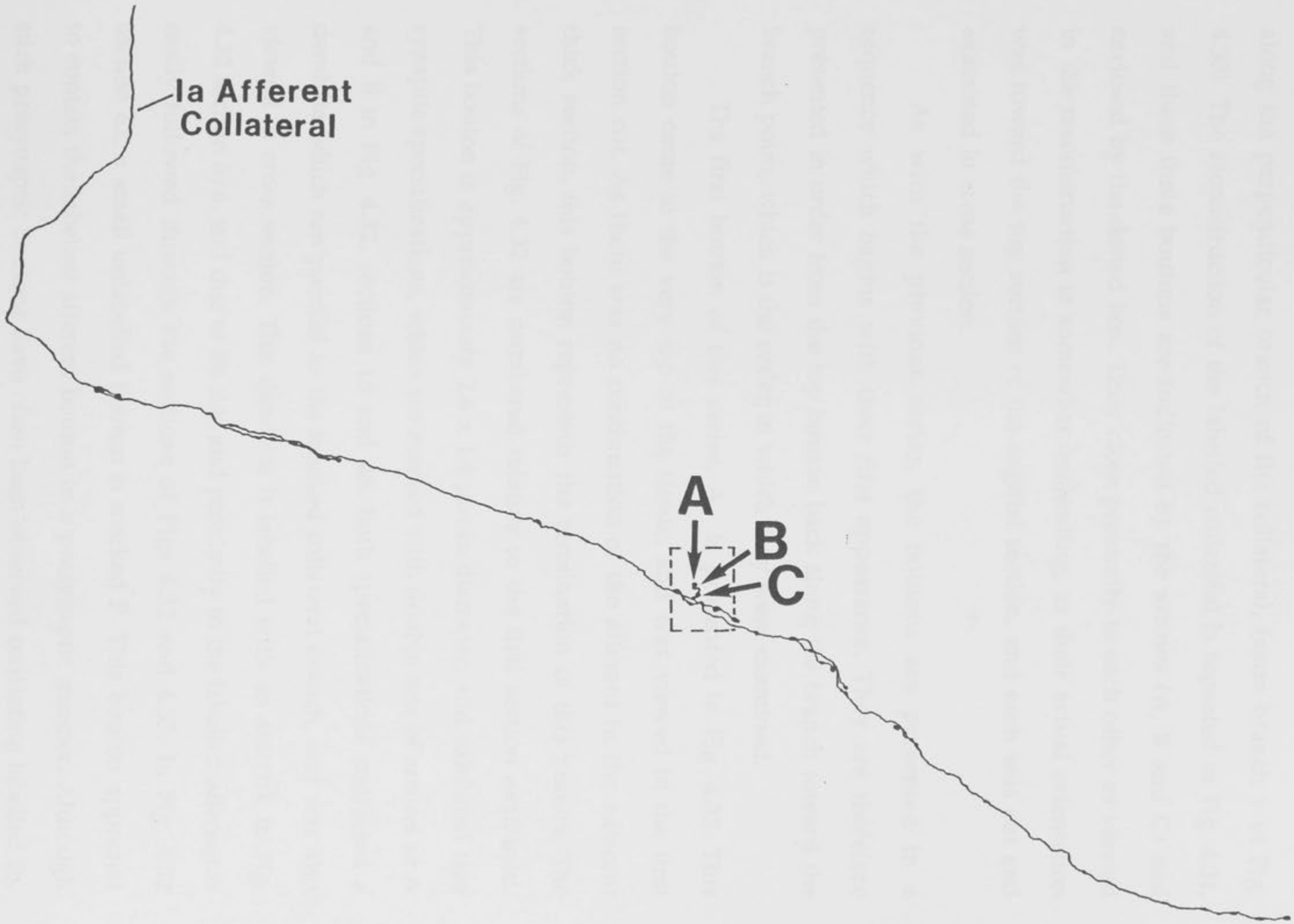
Ia Afferent
Collateral
A
B
C

was not sufficient to show the existence of two axon branches. Thus a single axon only was indicated on the tracing (see Figs. 4.2 and 4.29).

The following series of figures show the boutons that were situated along the perpendicular branch of the collateral, (axon branch 1 of Fig. 4.30). The reconstruction of the labelled collateral is repeated in Fig. 4.31, and these three boutons are indicated by the arrows (A, B and C) and enclosed by the dotted box. Their close proximity to each other as viewed in the reconstruction is somewhat misleading, as their actual orientation was toward the top surface of the sagittal section, and each was cut and examined in cross section.

As with the previous series, the boutons are presented in a sequence which begins with their first appearance. They are therefore presented in order from the top bouton back along the branch toward the branch point, which is the order in which they were examined.

The first bouton of this series, A, is presented in Fig. 4.32. This bouton came to the very top of the tissue, and was viewed in the first section cut. As there was no continuation of the afferent in the adjacent thick section, this bouton represents the termination of this branch. The sections of Fig. 4.32 are numbered relative to the first section examined. This bouton is approximately 2.6 x 1.6 μm in diameter, and exhibited two synaptic specializations, which are marked with double sets of arrows as A and B in Fig. 4.32, sections 18 and 48. Both specializations contacted a dendrite which ran parallel to the labelled collateral branch, and was also viewed in cross section. This dendrite is labelled with an asterisk in Fig. 4.32 section 5/6, and due to its size and proximity to the labelled afferent is easily followed through the sections of Figs 4.32 and 4.33. In Fig. 4.32 section 62, a small unlabelled bouton is marked P. This bouton appeared to contact the labelled afferent bouton in a presynaptic manner. Although such presynaptic boutons have often been observed contacting labelled Ib,

FIGURES 4.32 - 4.35

The following four figures show a sequence of photomicrographs taken through the sections along branch 1 of Fig. 4.30, and indicated in the reconstruction of Fig. 4.31.

The boutons were examined from the top section down, and are presented as they were observed, running from the top of the tissue back along the branch towards the branch point.

The first bouton, (A), illustrated in Fig. 4.32, exhibited two synaptic specializations, marked A and B, both with the dendrite marked with an asterisk in the first micrograph.

A small unlabelled bouton, P was found to make presynaptic contact with this bouton.

Fig. 4.33 shows a selected sequence of the sections through the second bouton, (B). This bouton also exhibited two synaptic specializations, marked with double sets of arrows as A and B. Each of these specializations was made with the same dendrite indicated by the asterisk in Fig. 4.32.

A sequence of the sections through the third bouton, (C) is presented in Figs. 4.34 and 4.35. The dendrite contacted by the previous two boutons is marked with an asterisk (for reference) in the first micrograph of Fig. 4.34. This bouton exhibited three synaptic specializations, marked with double sets of arrows as A and B in Fig. 4.34 and C in Fig. 4.35.

A small unlabelled bouton, P, is seen to make presynaptic contact with this bouton in Fig. 4.34.

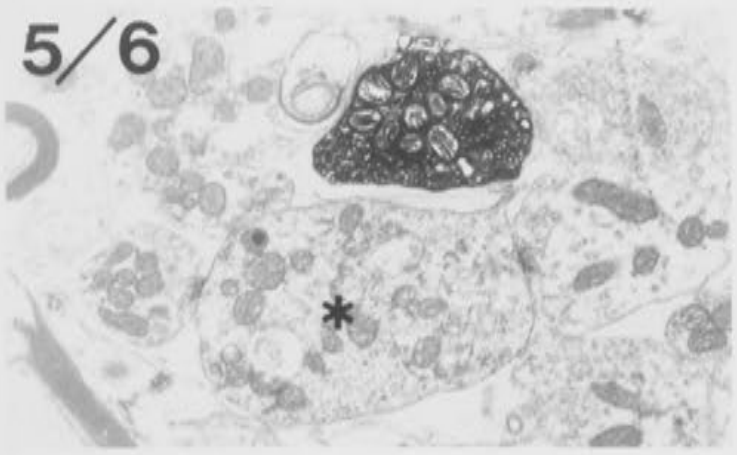
5/6
*

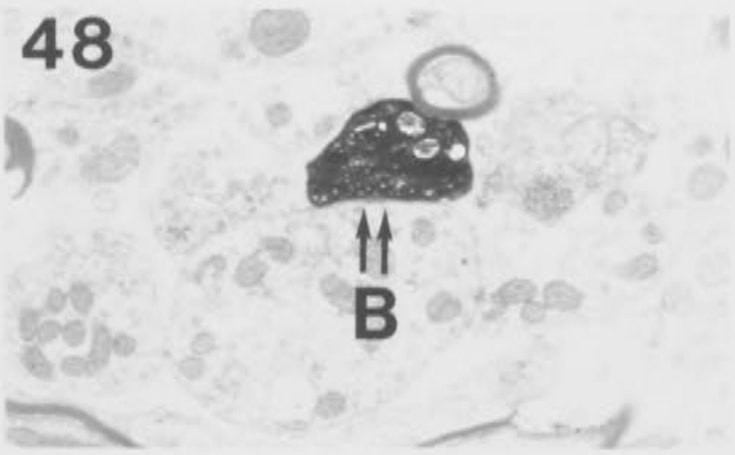
48
B

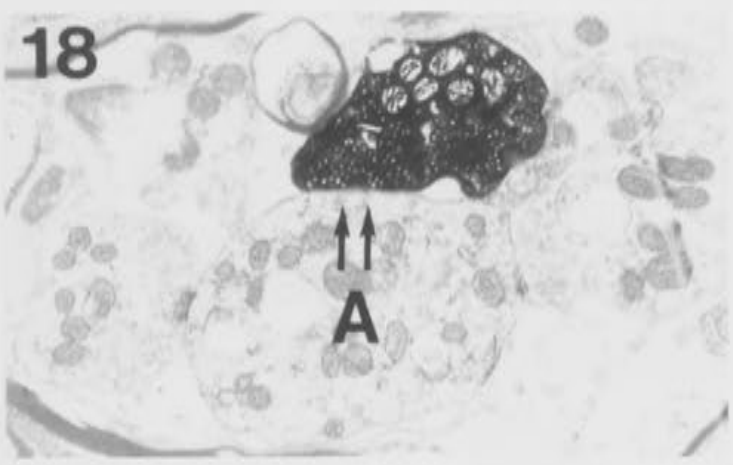
18
A

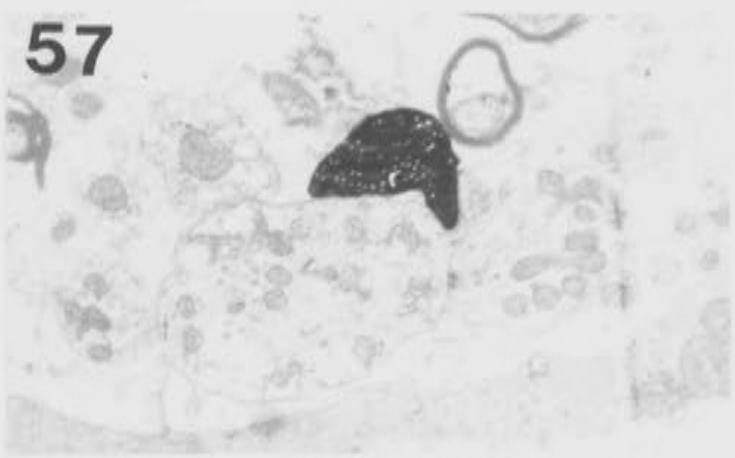
57

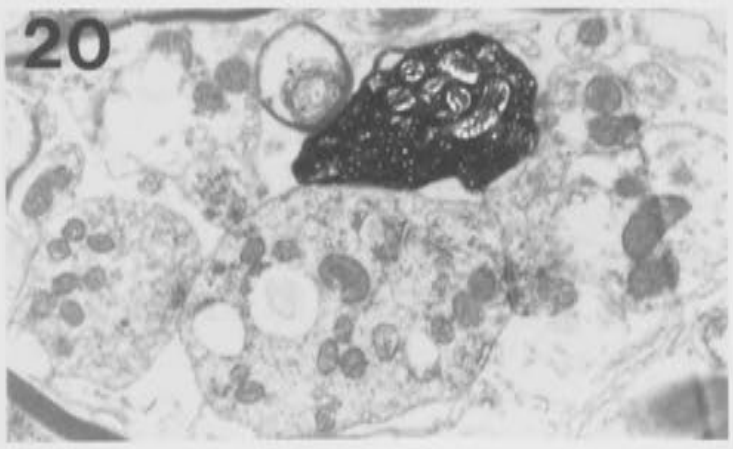
20

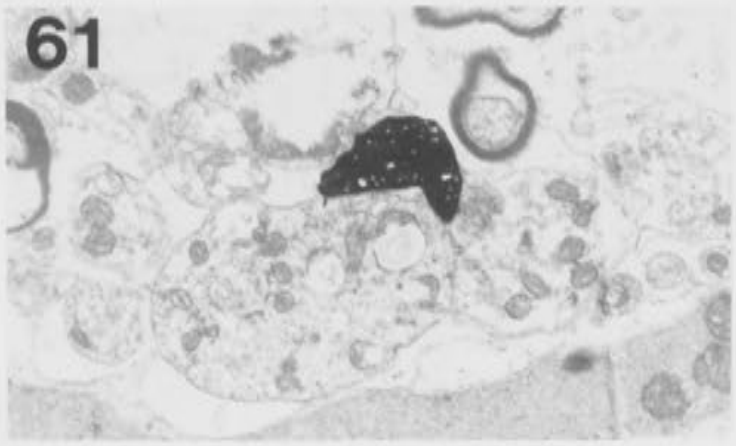
61

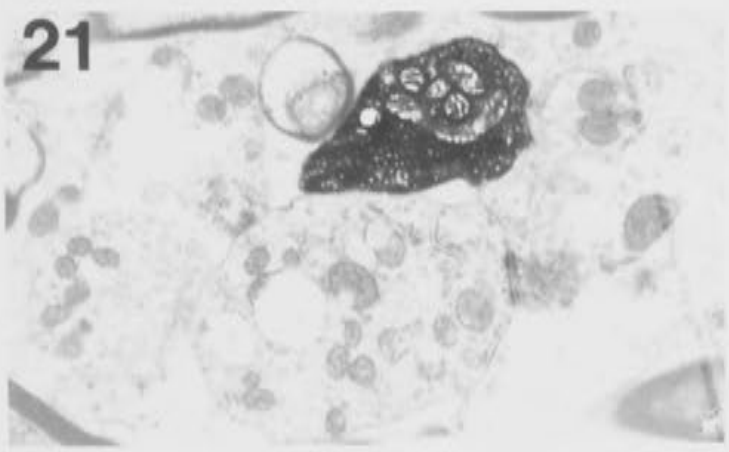
21


62
1 µm
P

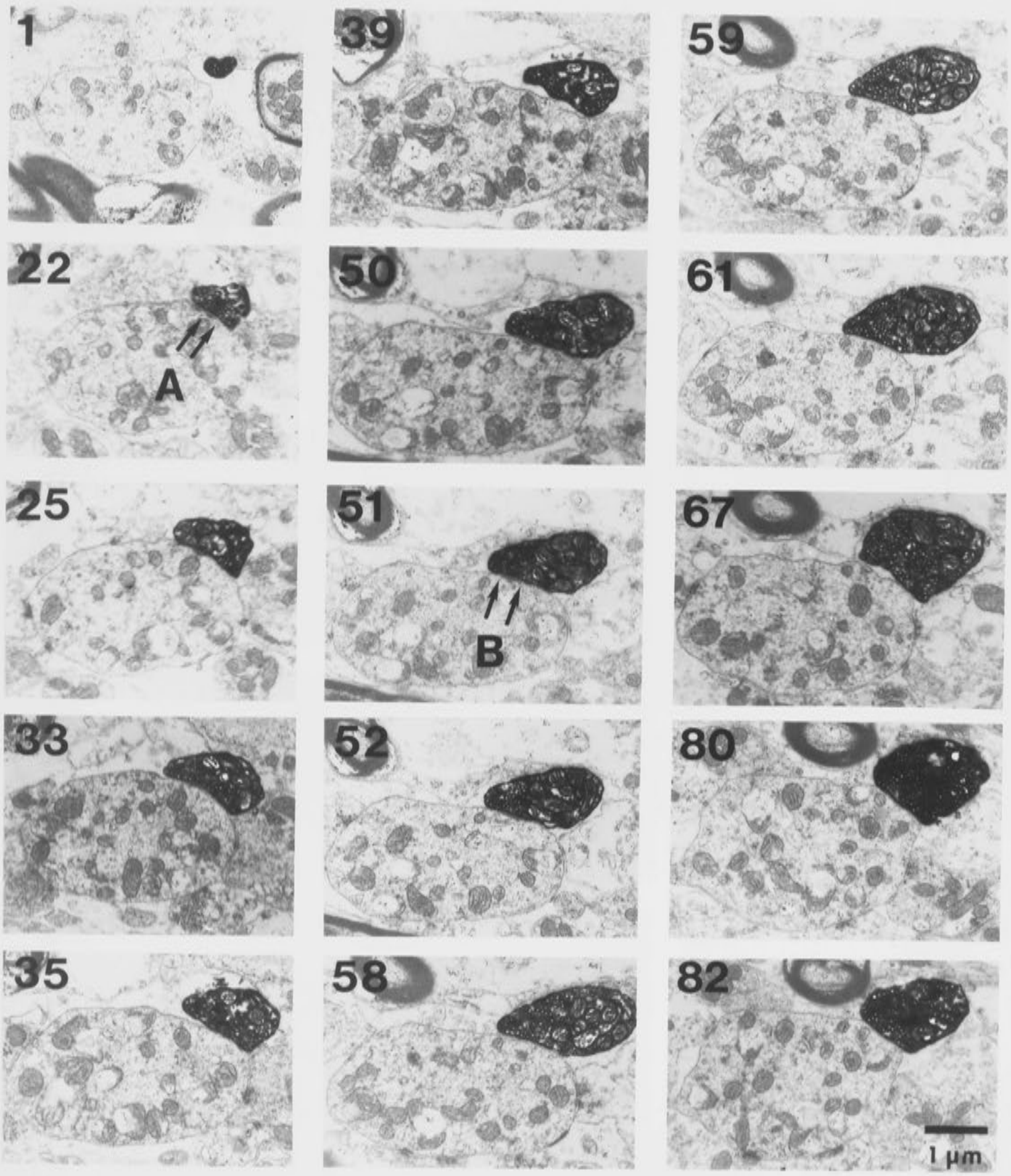
1
39
59
22
A
50
61
25
51
B
67
33
52
80
35
58
82
1 µm

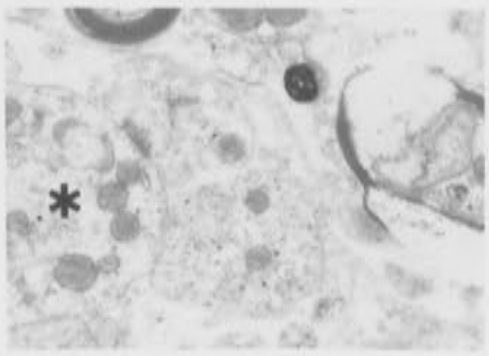
*

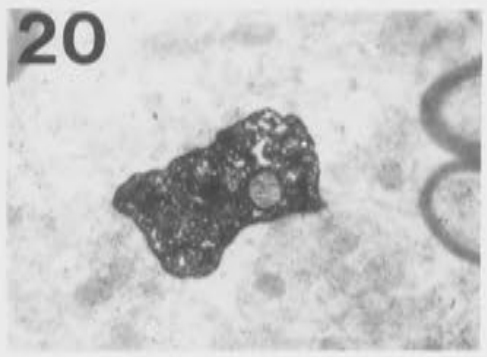
20

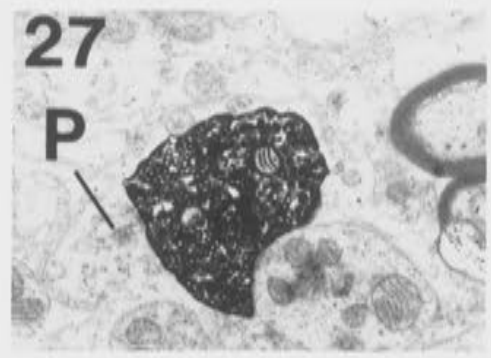
27
P


8

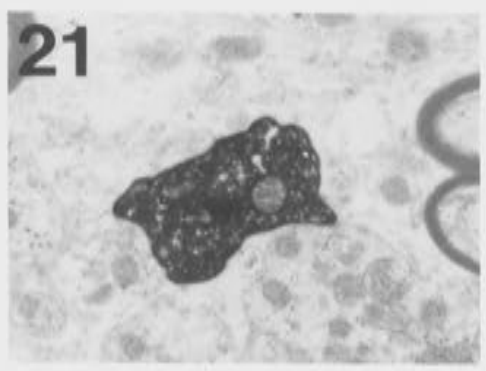
21


28


15
A


22

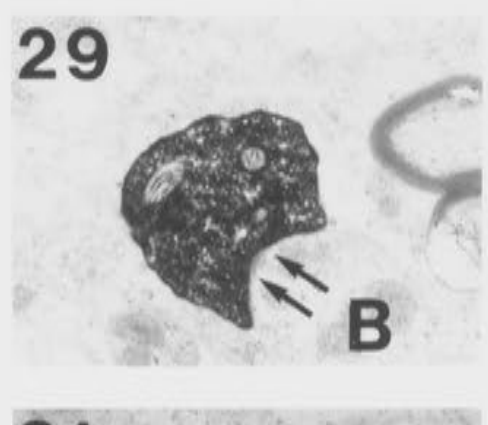
29
B

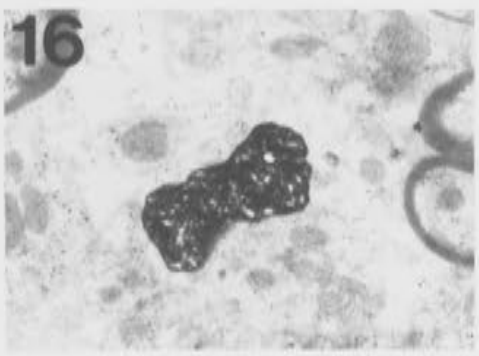
16

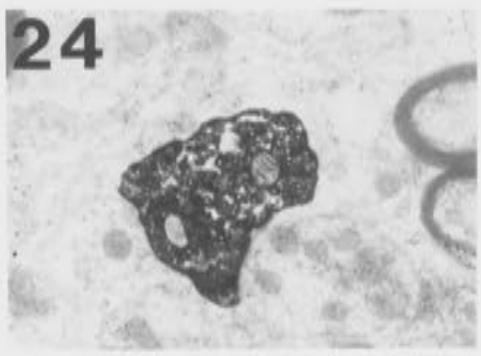
24

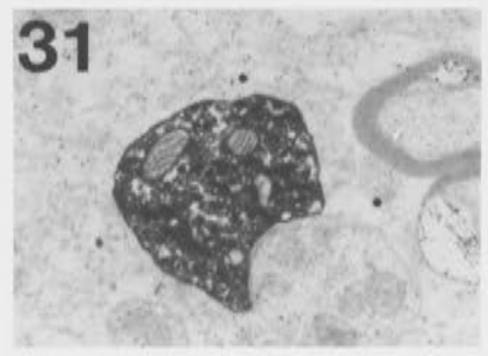
31


19

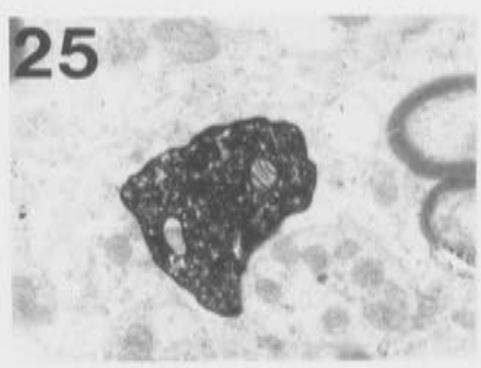
25

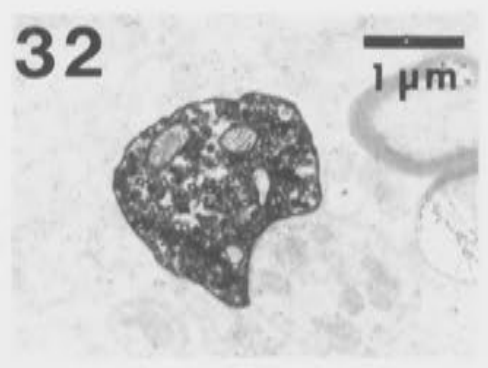
32
1 µm

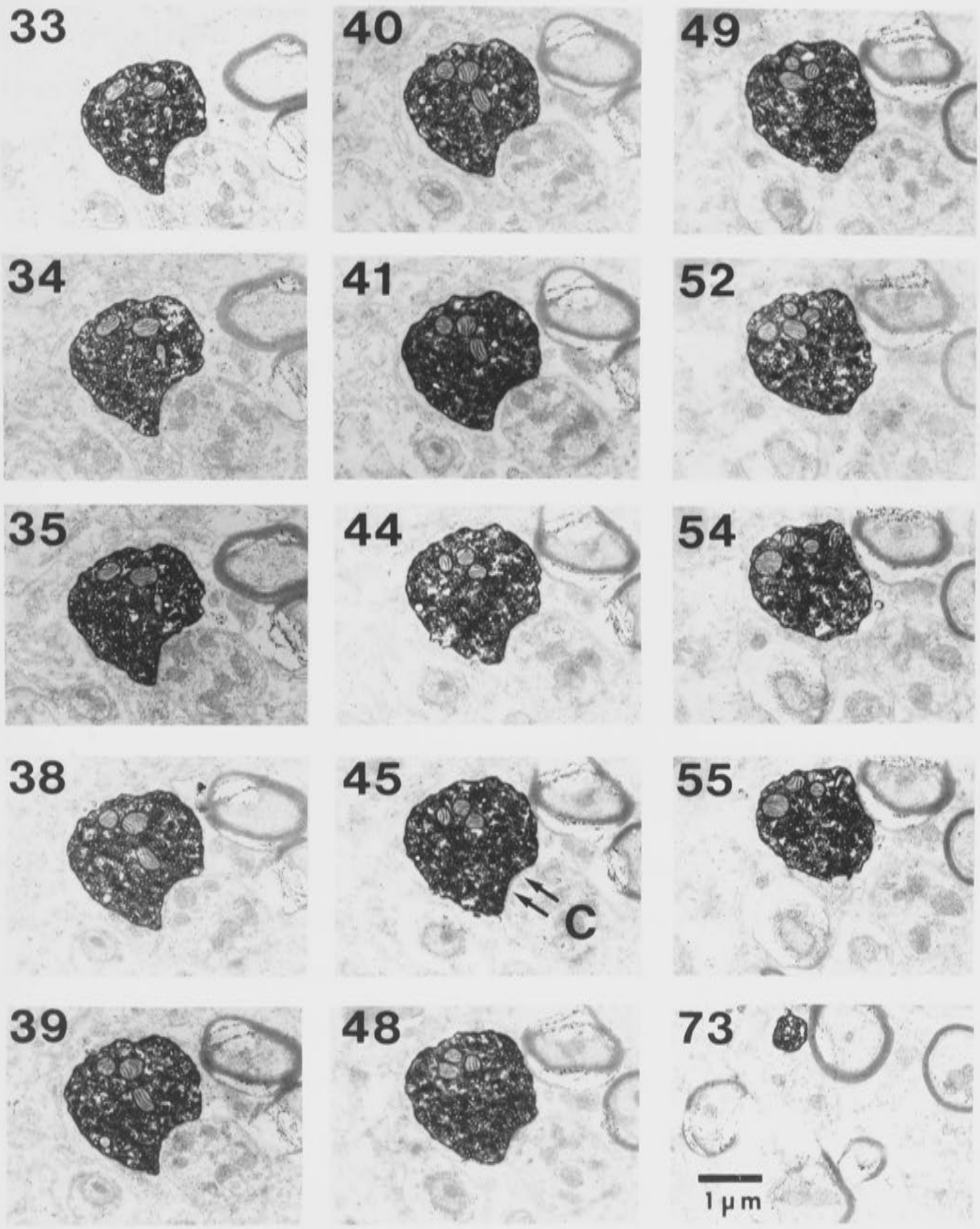
33
40
49
34
41
52
35
44
54
38
45
C
55
39
48
73
1 µm

and more rarely Ia boutons in Clarke's column (See Appendix II and Chapter 5), such an occurrence was extremely rare along the length of this labelled Ia afferent collateral. Following a reduction in size which correlated with a necking of the afferent, a second swelling or bouton, B, was exhibited. A series of photomicrographs through this boutons is presented in Fig. 4.33. This bouton reached approximately 2.3 x 1.6 μm in cross section, and was seen to exhibit two synaptic specializations which are labelled with double sets of arrows as A and B in Fig. 4.33 sections 22 and 51. Both contacts appeared to be with the same dendrite contacted by the previous bouton in Fig. 4.32. The dendrite is marked with an asterisk in Fig. 4.32 section 5/6, and continues to run parallel to the bouton, and very close to the labelled afferent, throughout the sections presented in Fig. 4.33.

The same dendrite is indicated by an asterisk in Fig. 4.34. At this stage, the dendrite and the labelled collateral have separated, and the bouton, C, presented in Figs 4.34 and 4.35, makes synaptic contact with another dendrite. The first section in Fig. 4.34 is not numbered. This section was chosen to show (in cross section) the narrow bridge which connected the previous bouton (Fig. 4.33) and this one. The bouton is first shown in the second photomicrograph of the series, Fig. 4.34 section 8. (The sections are again numbered from the first appearance of the bouton). The bouton reached a maximum diameter of 1.9 μm, and was followed through over 60 sections. Three synaptic specializations were exhibited by this bouton, and they are marked with double arrows as A and B in Fig. 4.34 sections 15 and 29, and C in Fig. 4.35 section 45. Each of these three specializations apparently contacted the same dendrite. This dendrite was also cut in cross section, and ran in parallel with the labelled collateral branch. In Fig. 4.34 section 27, a small unlabelled bouton marked P is shown to make a presumed contact with the labelled bouton. In Fig.

4.35 section 73, the bouton has narrowed to the small collateral branch which gave rise to these three boutons.

The line drawing of Fig. 4.30 showed the bouton giving rise to two branches of the collateral. The first branch was presented in Figs. 4.31-4.35. The other branch subsequently divided again, giving rise to axon branches 2 and 3. Branch 2, which is terminal, gave rise to synaptic boutons, and is presented in Figs. 4.36-4.39.

The reconstruction of the labelled collateral is repeated in Fig. 4.36. The arrows indicate two boutons, A and B, arising from axon branch 2 of Fig. 4.30 enclosed in the dotted box shown. From the light microscopic observations it appeared that the first of these boutons might be a branch point. However, serial section electron microscopy has shown that this was not the case.

The drawing in Fig. 4.37 shows that axon branch 2 is a terminal branch which does not remyelinate along its length. From the branch point, an unmyelinated fibre bridge 6.4 µm long and 0.45um in diameter extends to the first bouton. Bouton A is *en passant*. A second unmyelinated fibre bridge 5.5 µm long and 0.3 µm in diameter subsequently gives rise to bouton B, which is terminal.

Bouton A is 3.6 x 1.9 µm, and exhibits one synaptic specialization, marked with double arrows as A1 in Figure 4.37 section 34. Both boutons lay along the same dendrite, and this can clearly be seen in Fig 4.37 section 34 and Fig. 4.38 sections 35-39. No release sites were recognized for bouton B, which is 5.3 x 2.8 µm. This seems unusual for a bouton of this size and proximity to a dendrite, and suggests that potential release sites may have been masked by the angle of section relative to bouton and dendrite. Bouton B is packed full of vesicles, and presents a clear example of the packaging of the mitochondria. Throughout the sections in Fig. 4.39 a

FIGURE 4.36

Reconstruction of the HRP labelled plantaris Ia afferent collateral terminating in Clarke's column.

The two boutons indicated with arrows as A and B and enclosed by the dotted box in this reconstruction arise from branch 2 of the line drawing shown in Fig. 4.30. They are shown in the sequence of photomicrographs presented in Figs. 4.37-4.39.

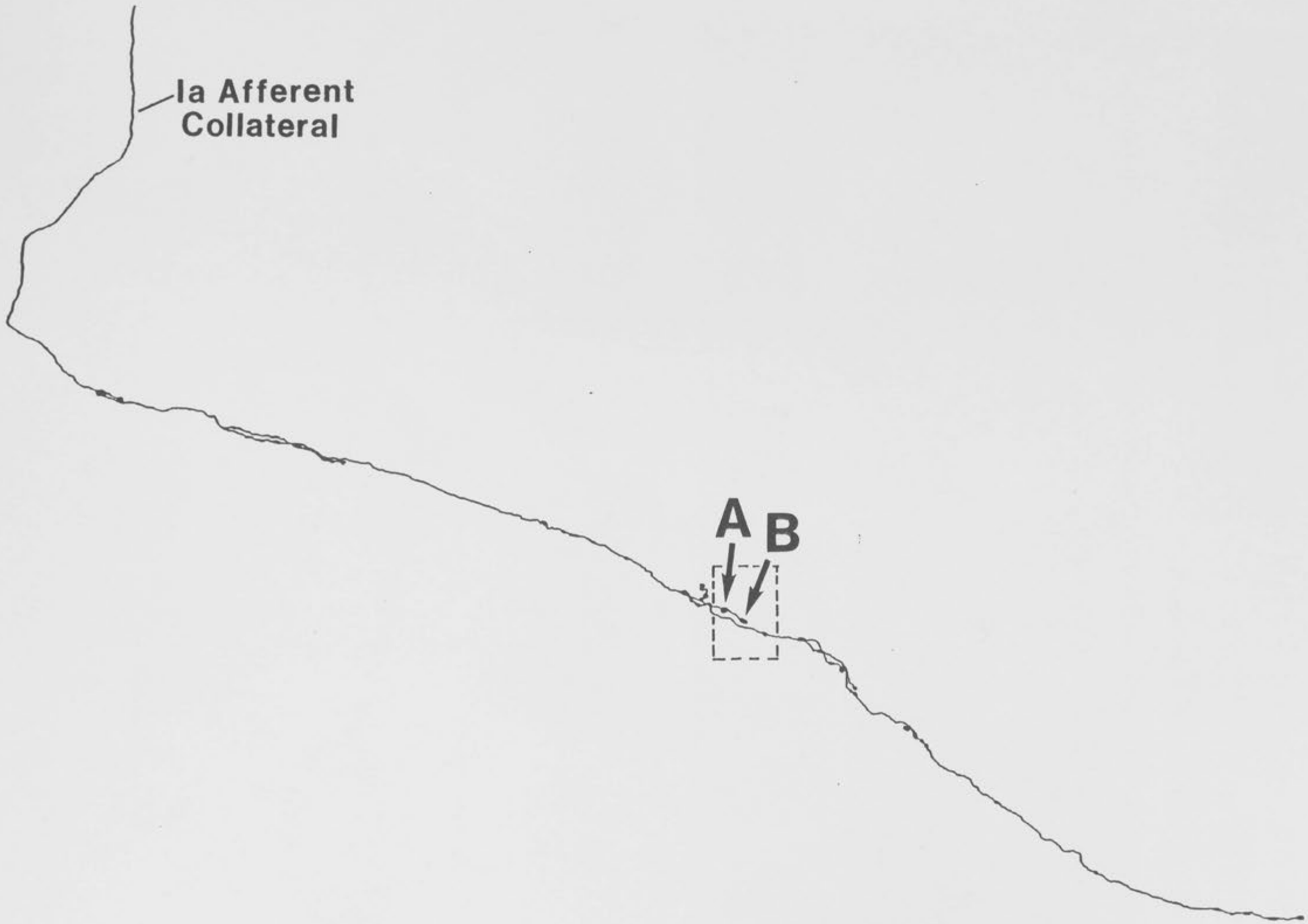
Ia Afferent
Collateral
A
B

FIGURES 4.37-4.39

The following three figures show a sequence of photomicrographs of the two boutons, A and B, which arose from branch two of Fig. 4.30. Their configuration and relation to the branch point is illustrated by the line drawing of Fig. 4.37.

Bouton A was seen to exhibit 1 synaptic specialization, indicated with double arrows as A1 in Fig. 4.37.


5

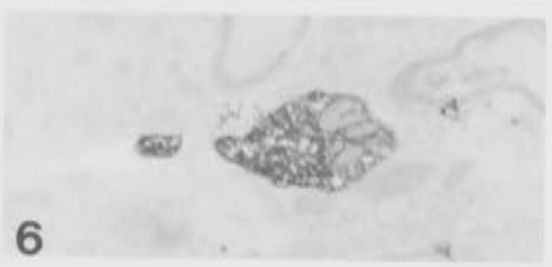
6

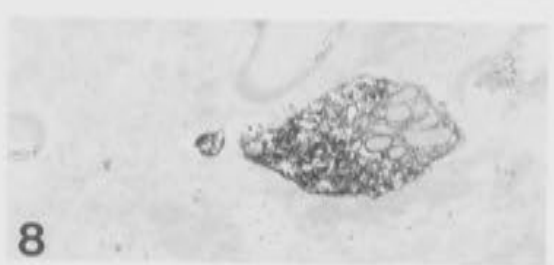
8

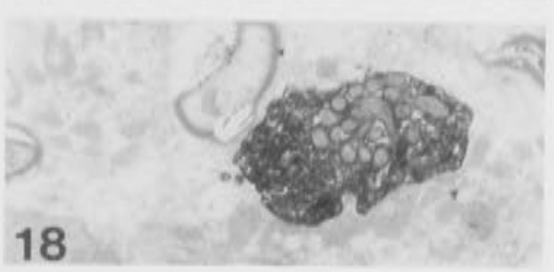
18

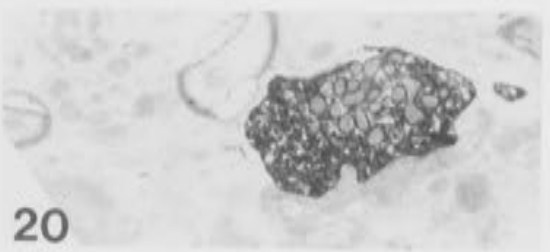
20


24

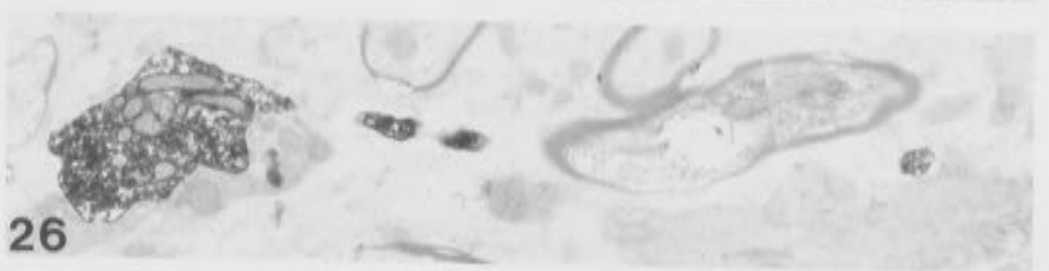
26

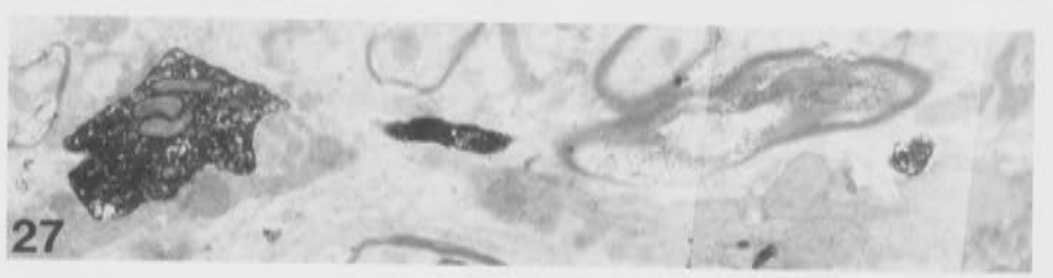
27


33


34
A1

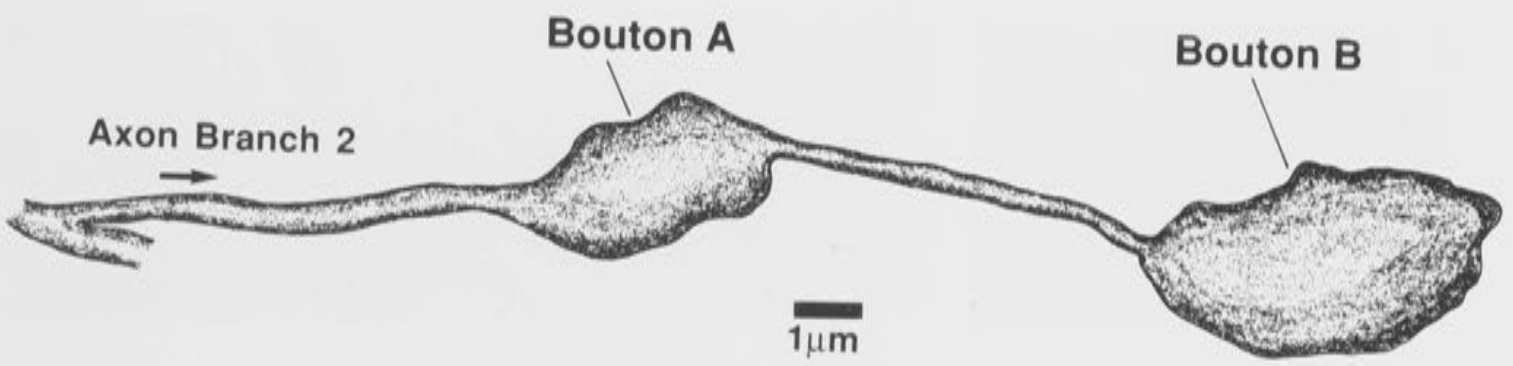
Bouton A
Bouton B
Axon Branch 2
1μm


35

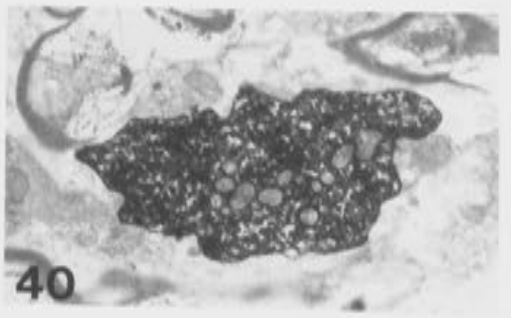
40

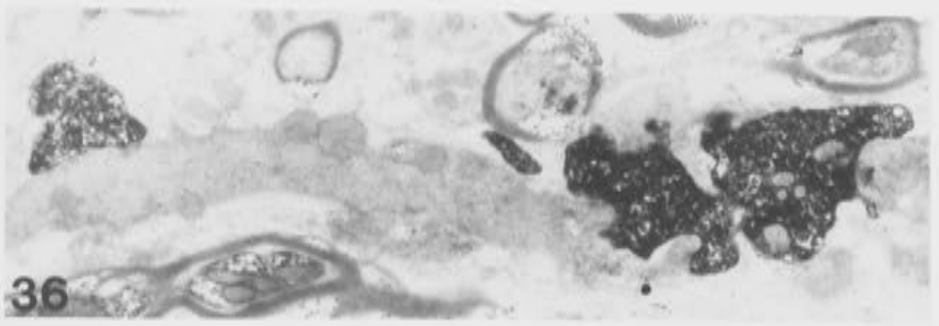
36


44


37

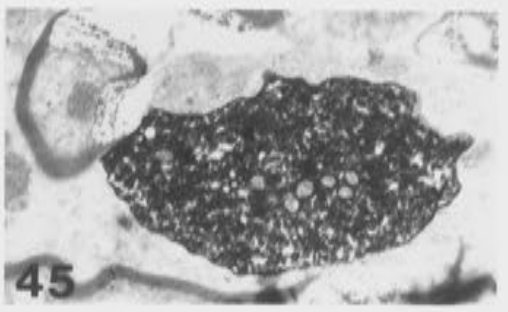
45

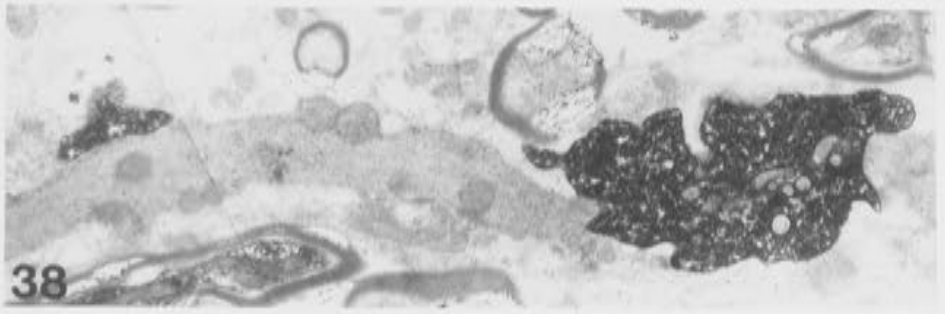
38


49

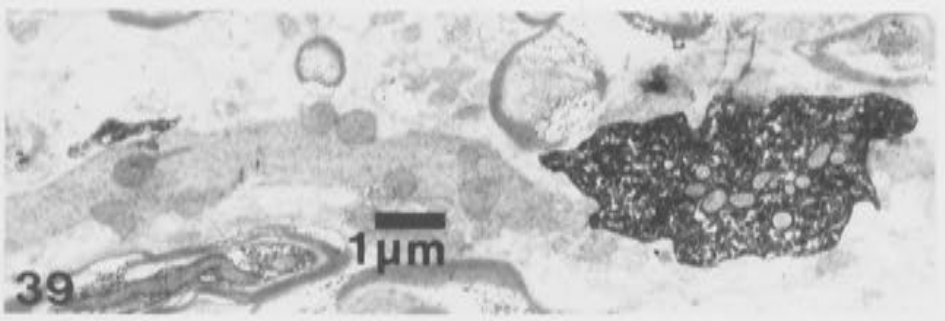
1µm
39


51

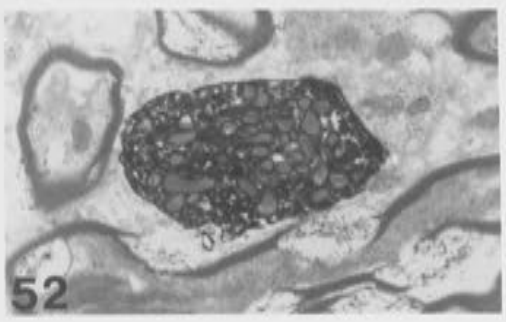
52

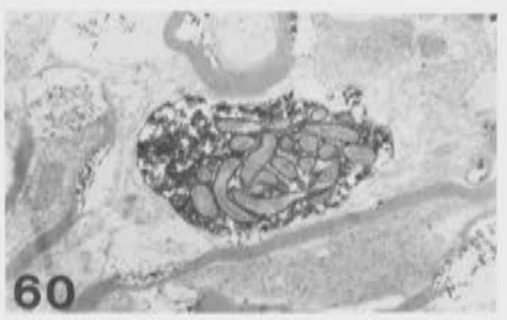
60


53


61


54


62


58


63

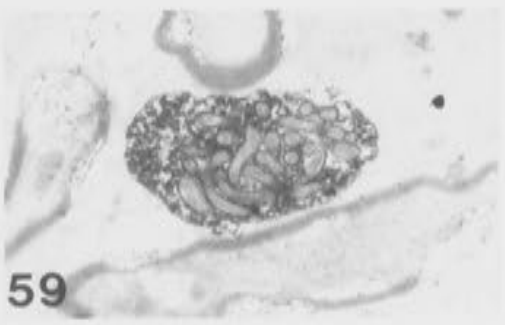
59


65
1µm

large number of mitochondria can be seen closely packed towards the middle and the right side of the bouton.

In Fig. 4.38 sections 35-39, an HRP labelled myelinated fibre can be seen in the lower left corner of the micrographs. This fibre is the third axon branch which emerged from the bouton illustrated in Fig. 4.30. Its proximity to the HRP labelled series presented in Fig. 4.36-4.39 explains why light microscope observations were unable to resolve all labelled structures.

The reconstruction of the labelled collateral is repeated in Fig. 4.40. The dotted box encloses a number of features marked with arrows (A-E), or with circles (open or closed). Despite the appearance of the two collateral branches in the tracing (Fig. 4.2, and 4.40) the boutons which follow are all situated on the same, terminal, unmyelinated collateral branch.

An important point to recognize is that two myelinated collateral branches, not one, were present from the beginning of this series. These were not resolved under the light microscope. Although the first arrowed feature on the reconstruction Fig. 4.40 is shown as a branch point, this was not the case. This was simply the point at which the two collateral branches separated sufficiently to be resolved individually under the light microscope. The first branch is dealt with in the following figures, 4.41-4.46.

This branch is shown fully reconstructed in the line drawing of figure 4.41. The break evidenced in the line drawing by slashed lines at the upper right and the lower left was necessary to include the entire branch on one figure. The pieces of afferent join directly at these slash marks, and no length has been ommitted from the drawing. The ultrastructure of the incoming myelinated afferent appears to be disrupted just prior to the point at which the myelin sheath began to unwind, possibly due to the

FIGURE 4.40

Reconstruction of the HRP labelled plantaris Ia afferent collateral terminating in Clarke's column.

Eight structural profiles are indicated with arrows and circles, and enclosed in the dotted box in this reconstruction.
The five arrows, A-E, indicate synaptic boutons, and these are presented in the series of Figures 4.41-4.46.
The open circle indicates a profile recognized as a bouton under the light miscroscope, which proved to be a region of the collateral itself which showed dark HRP labelling and ultrastructural disruption. This is shown in Fig. 4.41.
The two filled circles indicate specializations present in sections which were accidentally damaged during the staining process.

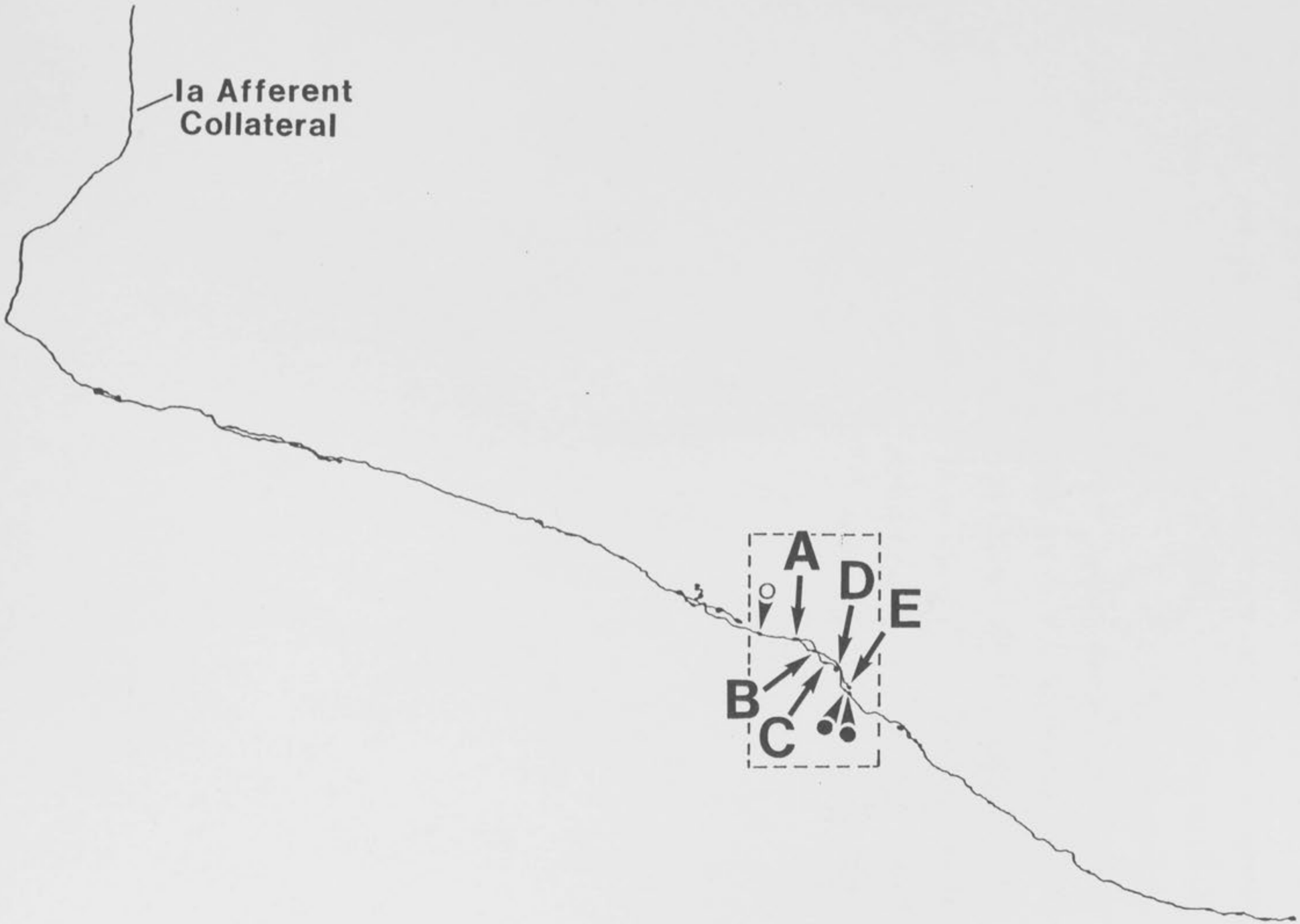
Ia Afferent
Collateral
A
D
E
B
C

FIGURE 4.41

The inset micrograph shows the collateral undergoing some form of disruption, after which the myelin sheath is lost. The disruption of the collateral ultrastructure coincides with the open circle indicated on the reconstruction in Fig. 4.40.

After losing its myelin sheath, the collateral gave rise to five discrete boutons labelled A to E on the drawing. Remyelination did not occur along the length of this branch, and bouton E was terminal. The five boutons correspond to the arrows in the reconstruction of Figure 4.40. These boutons are presented in the following sequence of photomicrographs, Figs. 4.42 - 4.46.

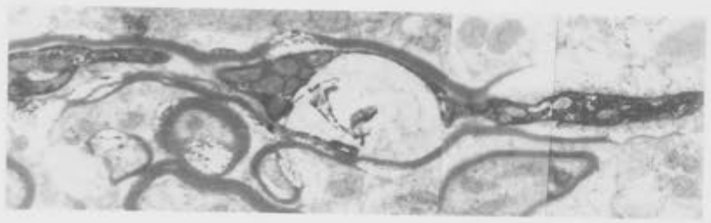

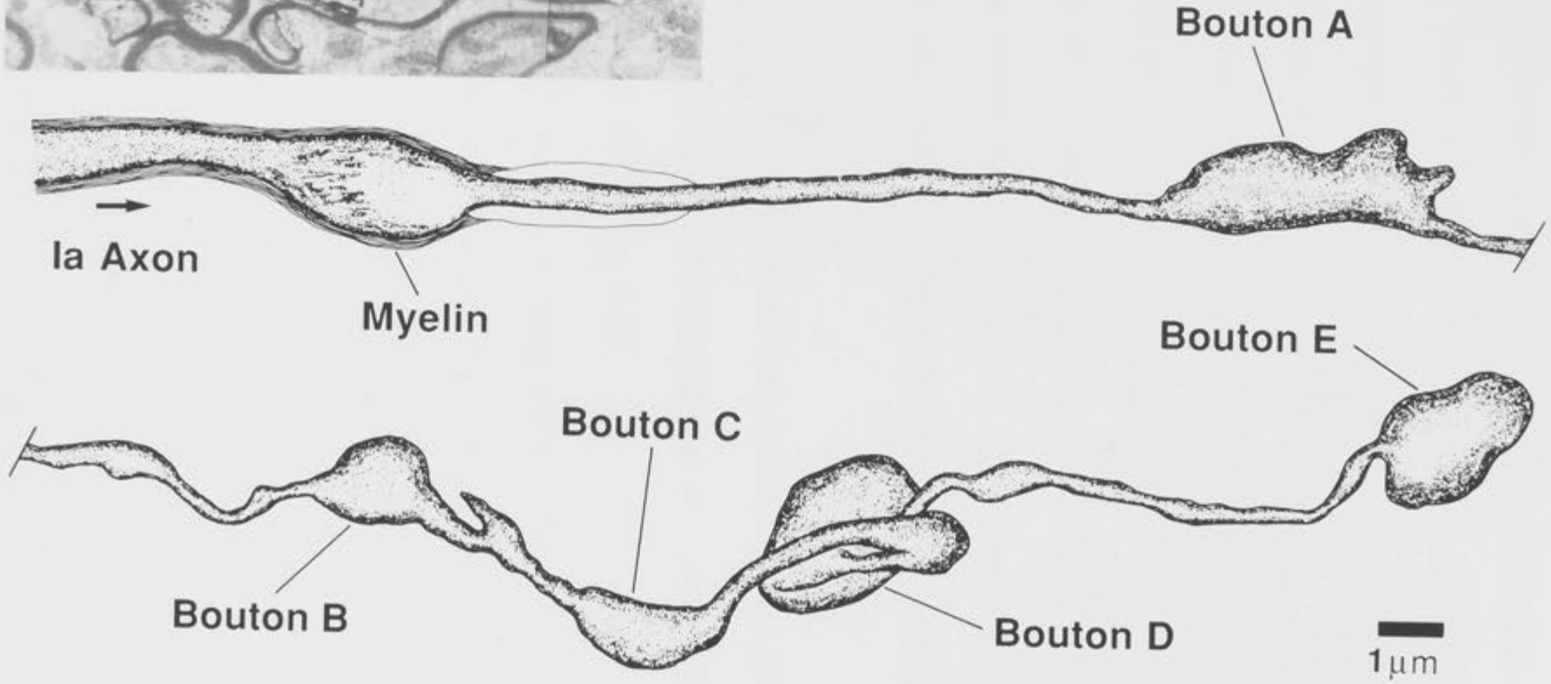
Bouton A
Ia Axon
Myelin
Bouton E
Bouton C
Bouton B
Bouton D
1μm

fixation of the collateral at this point. This enlargement of the afferent is illustrated in the inset photomicrograph, and reproduced in the line drawing of Fig. 4.41. Under the light microscope, this swelling of the collateral was recognised and recorded on the original tracing as a synaptic bouton (see Fig. 4.2). On the reconstruction in Fig. 4.40, the explosion of the collateral has been marked with an open circle. Its position, traced under the light microscope, correlatated exactly with its position as recorded from serial electron microscope sections. Following this disruption, the afferent shed its myelin sheathing over a distance of 3.5 μm, as seen in the inset photomicrograph of figure 4.41. The collateral branch then gave rise to five discrete boutons, A-E, the last of which was terminal. Remyelination never occurred along the length of this terminal branch, and no synaptic specializations could be recognized in any of the boutons.

Figures 4.42 - 4.46 show a selected sequence of the sections taken through the series of five boutons. This sequence is numbered relative to the first appearance of bouton A in Fig. 4.41.

After losing its myelin sheath, a long unmyelinated bridge of fibre 0.3 μm in diameter extended over 7.2 μm before giving rise to bouton A. Bouton A is irregular in shape, approxiamtely 4.4 μm long and 1.3 μm in diameter at its widest point. A sequence of the sections examined through bouton A is presented in Fig. 4.42. The long unmyelinated neck can be seen coming in from the left of the photomicrographs in Fig. 4.42 sections 6-10. Packaging of the mitochondria is very clear in Fig. 4.42 section 8-19. The bouton is seen to overlie a dendrite in Fig. 4.42 section 22-27, but no clear synaptic specializations were evident. This is probably due in part to the angle at which the bouton was sectioned, and also to the extremely dark HRP labelling of this bouton. In the upper right corner of Fig. 4.42 sections 5 and 6, a small part of the myelinated afferent which runs

FIGURES 4.42 - 4.46

The following figures show a sequence of selected photomicrographs taken through the five boutons, A-E, presented in the line drawing of Fig. 4.41. The sequence is numbered from the first appearance of bouton A in Fig. 4.42.

Bouton A is presented in Fig. 4.42, labelled darkly with HRP and packed with mitochondria and vesicles.

Bouton B is presented in Fig. 4.43.

Boutons C and D are seen in Fig. 4.44, and bouton D, which is of an extremely irregular shape, continues through the sections in Figs. 4.45 and 4.46. Bouton E is terminal, and seen in Figs. 4.45 and 4.46.

The bridge of the afferent fiber which connects boutons D and E crosses the path of the myelinated collateral branch, seen in Fig. 4.46.

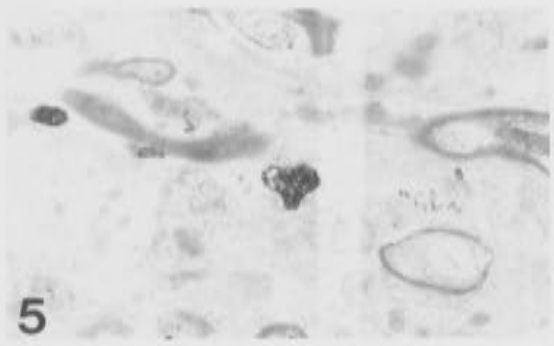
5


11


23

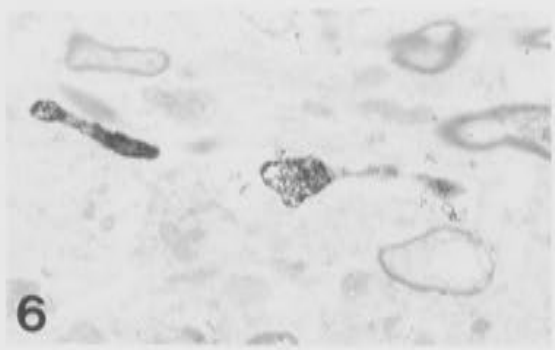
6

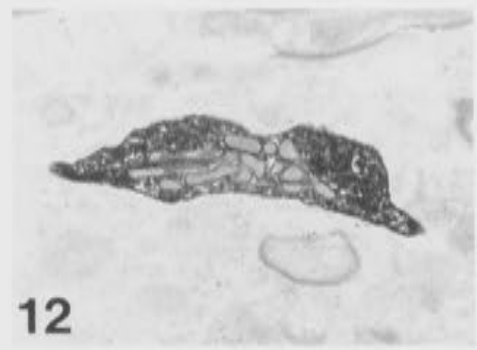
12

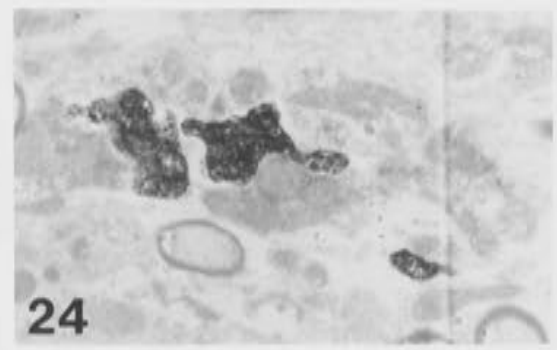
24

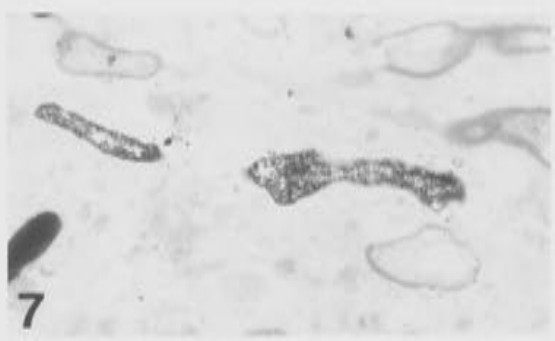
7


18

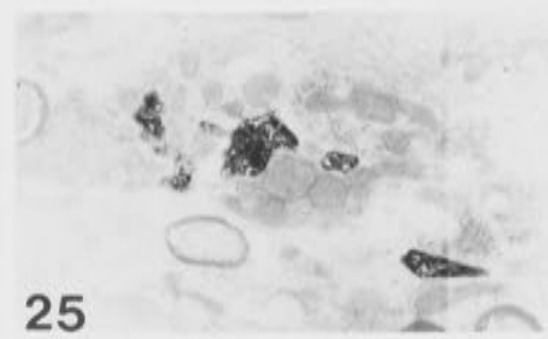
25


8

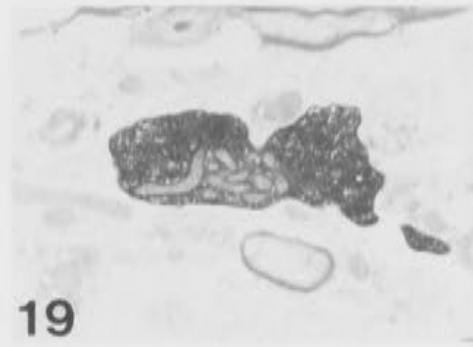
19

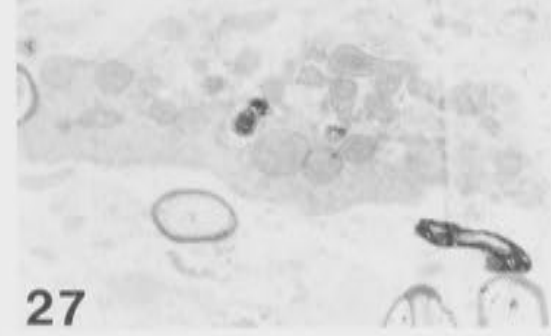
27


10

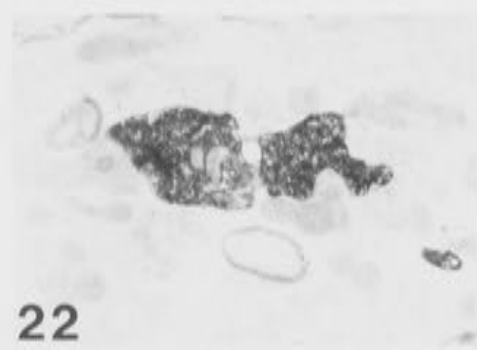
22

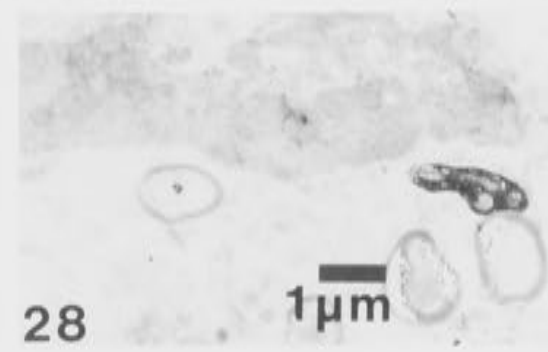
28
1µm

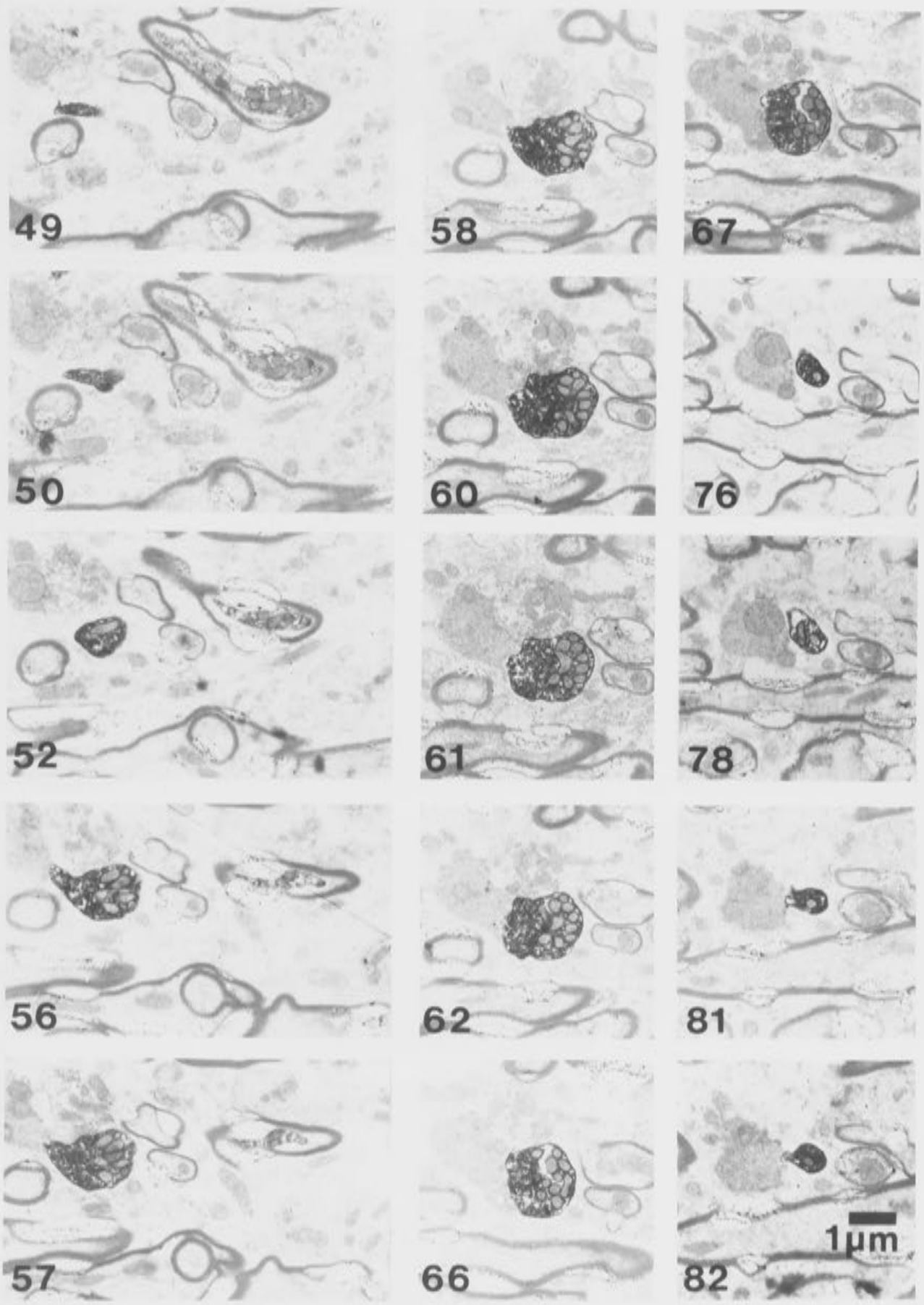
49
58
67
50
60
76
52
61
78
56
62
81
57
66
82
1µm

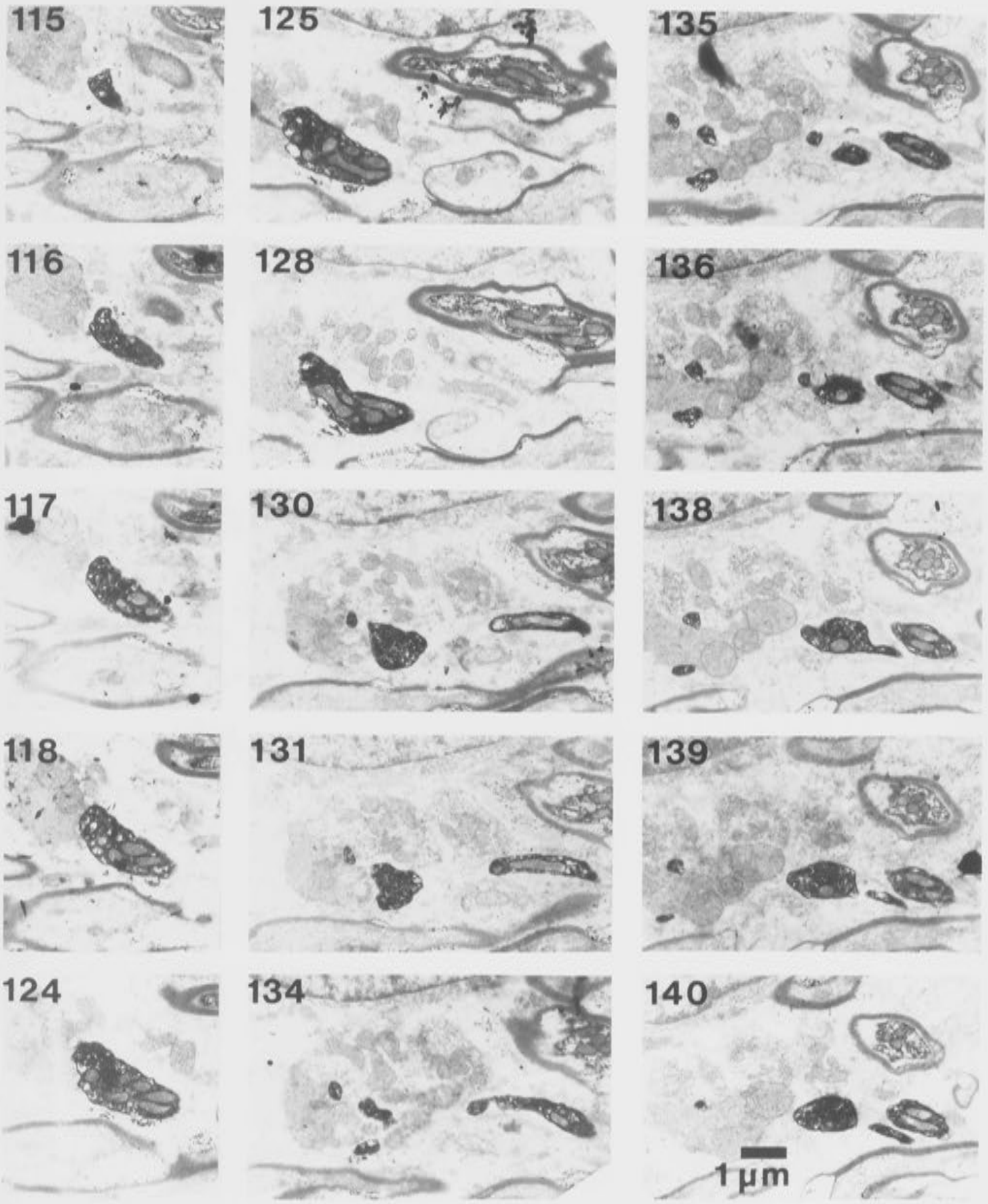
115
125
135
116
128
136
117
130
138
118
131
139
124
134
140
1 µm

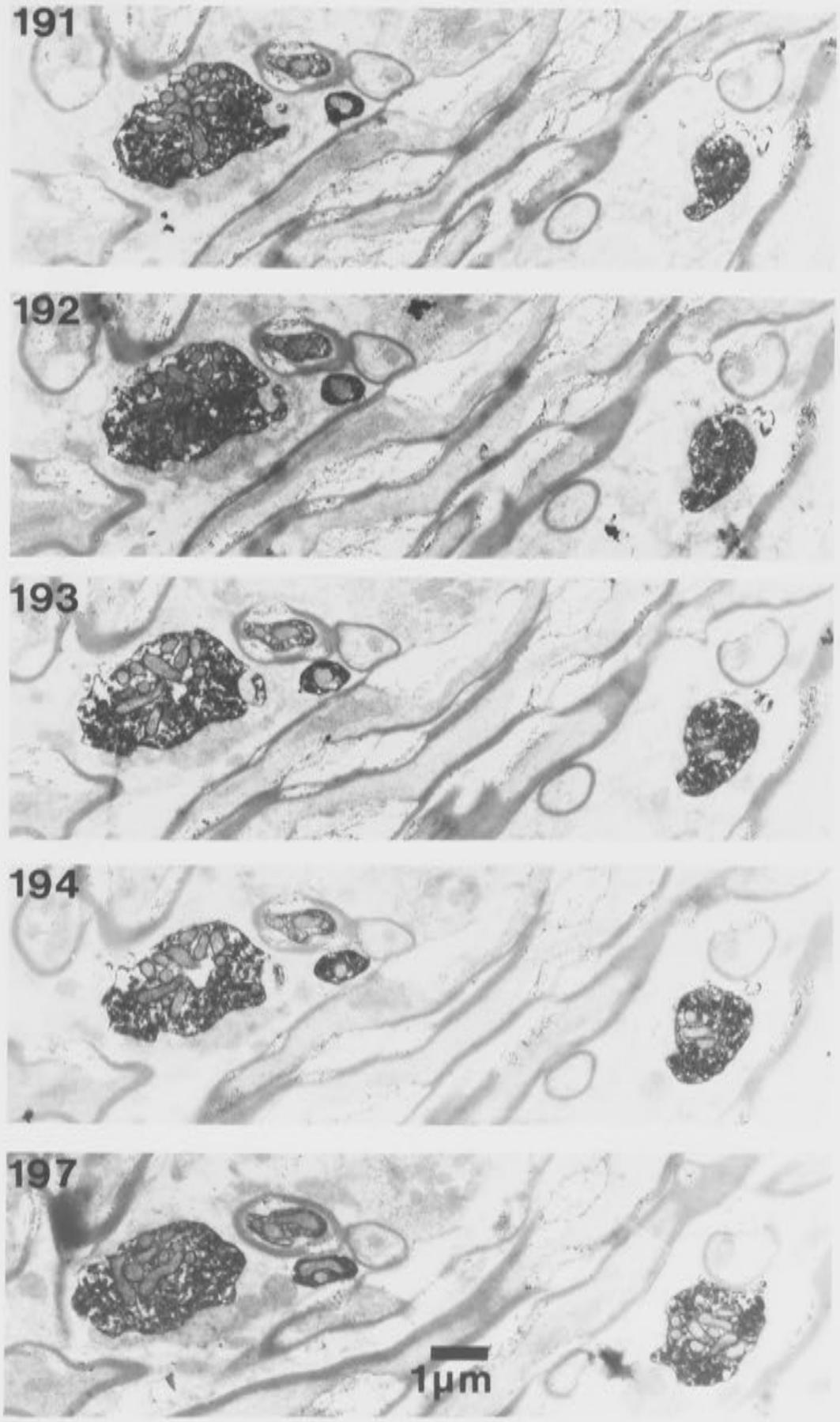
191
192
193
194
197
1μm

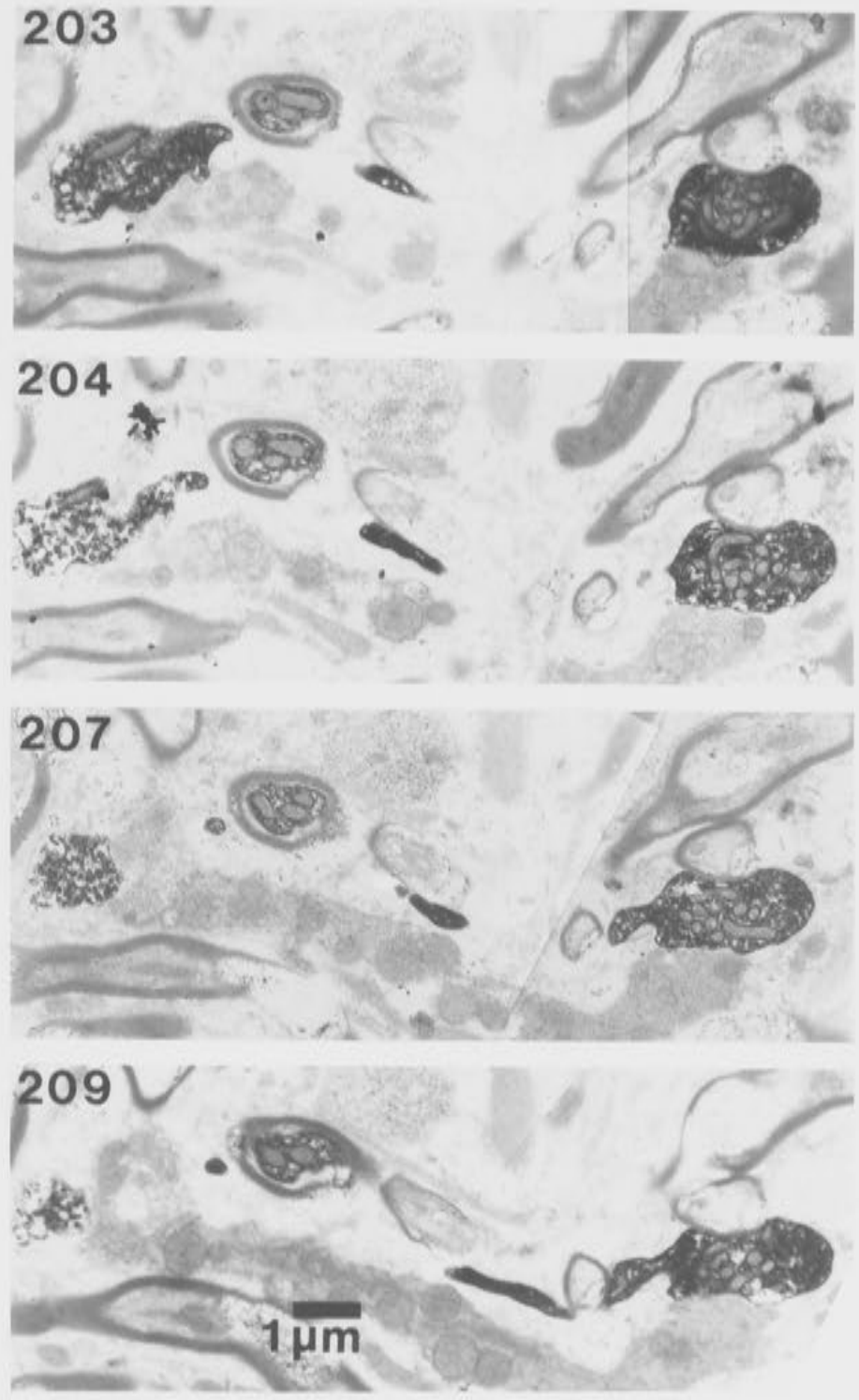
203
204
207
209
1 µm

parallel to this branch can be seen. Its proximity to bouton A probably explains why this bouton was proposed as a branch point in the light microscope reconstruction.

In Fig. 4.42 section 28, a small, unmyelinated length of the fibre is see leaving the bouton to the right of the section. This same section of fibre can be recognised from its shape and size on the left of the lower portion of the line drawing in Figure 4.41. This fibre travelled 6.4 μm, and subsequently gave rise to bouton B.

Bouton B is shown in the photomicrograph series of Fig. 4.43 sections 52-67. This bouton was 1.6 x 1.3 μm, and again, no synaptic specializations could be positively identified. The myelinated afferent which ran in parallel with this collateral branch is included in Fig. 4.43 sections 49-57.

As the fibre emerges from bouton B, an unusual configuration is evident. The fibre becomes very narrow, and then gives rise to a small, pointed extrusion, or extension, before another narrow neck extends to bouton C. It is not clear whether this extension is an inherent part of bouton B, or of bouton C, or whether it should in fact be labelled as a separate bouton. It can be seen in the micrographs of Fig. 4.43 sections 76 and 77.

After another short unmyelinated bridge, the afferent gave rise to bouton C. This bouton is 2.3 μm long, and 1.0 μm in diameter at its widest, and is shown in the photomicrographs of Fig. 4.44 sections 116-140. The dendrite to the left of bouton C, and in close proximity to it in Fig. 4.44 section 115-140, is the same dendrite seen physically contacting boutons A and B of this series. The myelinated afferent running in parallel to this branch of the collateral is seen in Fig. 4.44. A thin bridge of the afferent can be seen leaving bouton C in Fig. 4.44 sections 130-134. This bridge continued for approximately 5.0 μm before giving rise to bouton D.

Bouton D was most irregularly shaped. The extremely complex arrangement with which the afferent approached this bouton and emerged from it meant that it appeared as a series of small pieces of unattached, HRP labelled material in Fig. 4.44 sections 135-140. Reconstruction from the serial sections examined under the EM showed the configuration of the bouton to be that presented in Fig. 4.41. The bouton itself, shown on the left in Fig. 4.45 sections 191-197 and Fig. 4.46 sections 203-209 was 2.9 x 2.1 μm. This bouton was also closely associated with the same dendrite described previously in close proximity to boutons A, B and C. This dendrite is also closely associated with bouton E, as seen in Fig. 4.46 sections 207-209. The bridge between boutons D and E was extremely narrow, on average 0.3 μm in diameter, and extended over 7.9 μm in length.

Interestingly, this narrow bridge of fibre between boutons D and E actually crossed the path of the myelinated collateral branch which had been running in parallel. This is shown in Fig. 4.46 section 209. Close inspection of the reconstruction from LM observation (Fig. 4.2) indicates that the proposed configuration of these two afferent branches was close to that determined from EM observations, but that the resolution of the light microscope was not sufficient to determine that this was a cross over rather than a branch point. Bouton E, 2.7 x 1.8 μm, was terminal, and thus the last point on this unmyelinated branch of the labelled collateral.

The myelinated branch of the collateral, after crossing the path of the unmyelinated branch, continued caudally. The final two boutons indicated on the reconstruction in Fig. 4.40 indicated by the filled circles were in sections which were, unfortunately, damaged during the staining process, and therefore the ultrastructure of these two features could not be determined.

FIGURE 4.47

Reconstruction of the HRP labelled plantaris Ia afferent collateral terminating in Clarke's column.

The following series of figures, Figs. 4.48-4.52 show a selected series of the micrographs taken through the two boutons, indicated by the arrows as A and B, which are enclosed in the dotted box on this reconstruction.

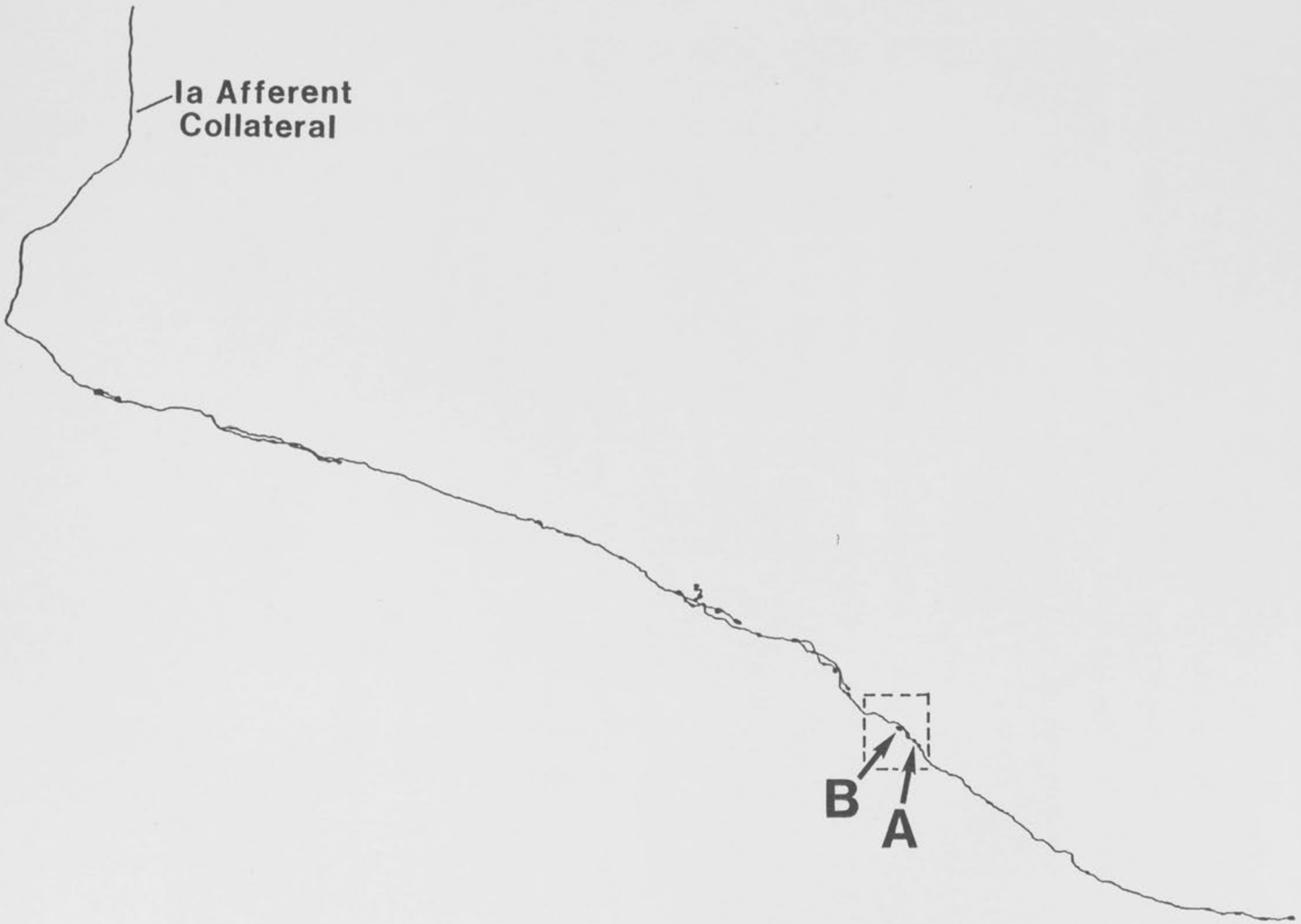
Ia Afferent
Collateral
B
A

FIGURES 4.48-4.52

The following series of figures shows a selected sequence of the photomicrographs taken through the two boutons indicated as A and B in the reconstruction of Fig. 4.47.

The line drawing of Fig. 4.50 shows the configuration of these two boutons, with the collateral branching back along its own length from bouton A to give rise to the terminal bouton B.

Figures 4.48-4.50 show a series of the micrographs through bouton B, and the backwards branching collateral. These sections are numbered from the first appearance of bouton B. A single synaptic specialization recognized in Bouton B is marked with a double set of arrows in Fig. 4.48. The major myelinated continuation of the collateral is seen in close proximity to this unmyelinated branch in all of the sections. The final micrographs of Fig. 4.50 show the myelinated and unmyelinated branches approaching the branch point at bouton A.

Bouton A is presented in the micrographs of Fig. 4.51 and 4.52. Sections are numbered relative to the first appearance of this bouton. Two synaptic specializations were recognized in this bouton, and they are marked with double sets of arrows as A and B in Fig. 4.51. A small unlabelled bouton, marked P in Fig. 4.52, appears to make synaptic contact with the labelled Ia bouton at the site marked with the open arrow.

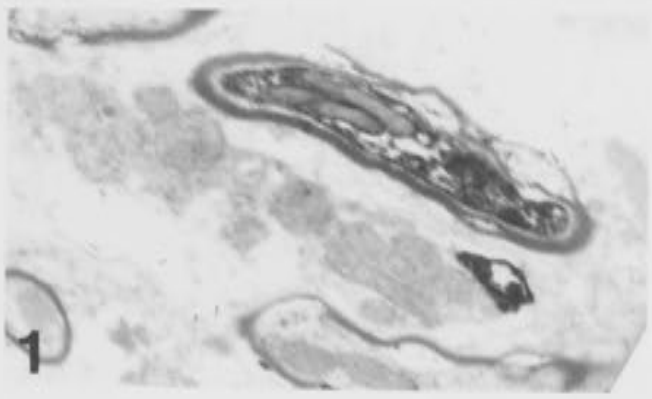
1

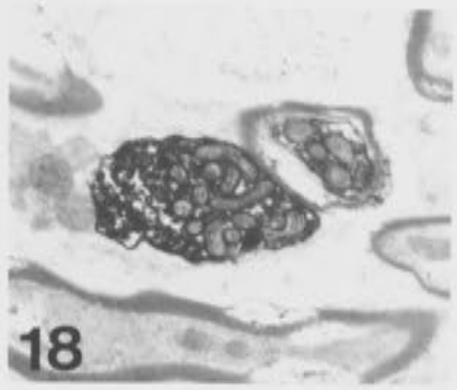
18


24


6

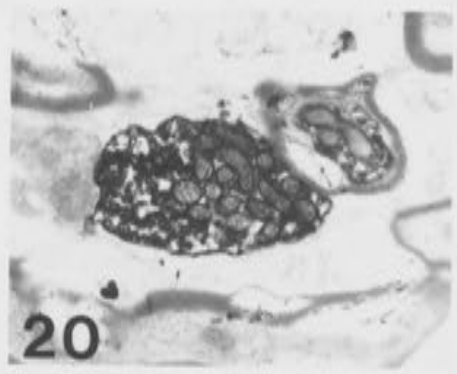
20


27


10


21


28

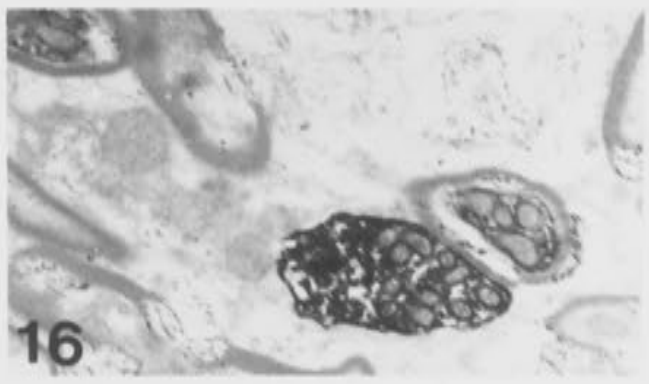
16


22

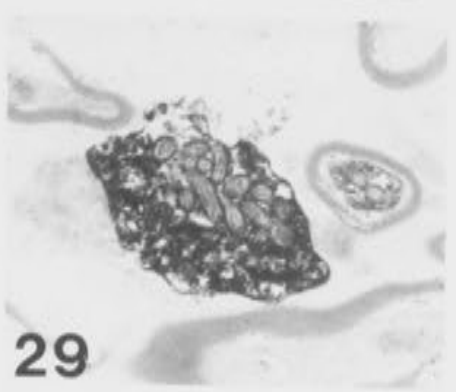
29

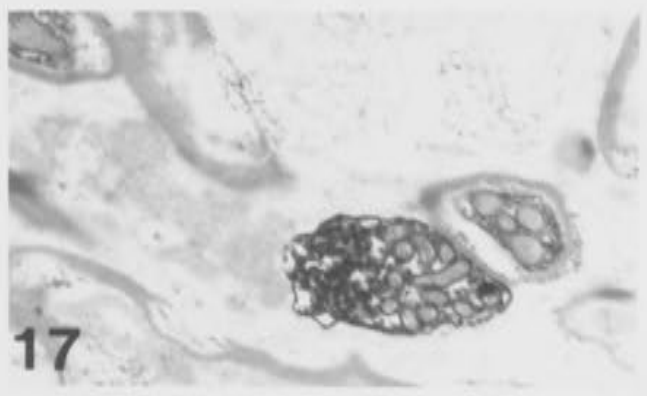
17


23

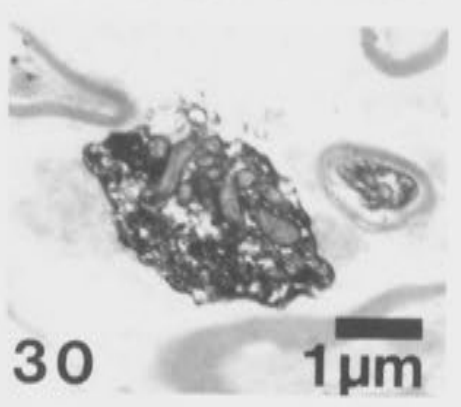
30
1µm


31


38

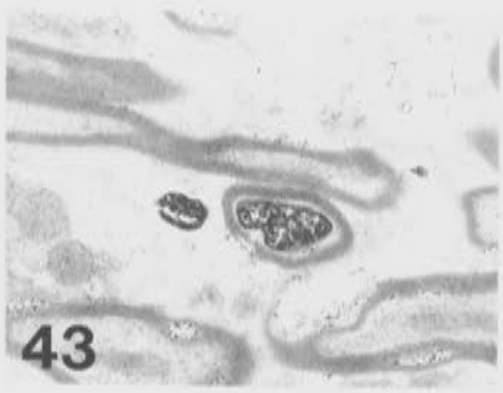
43

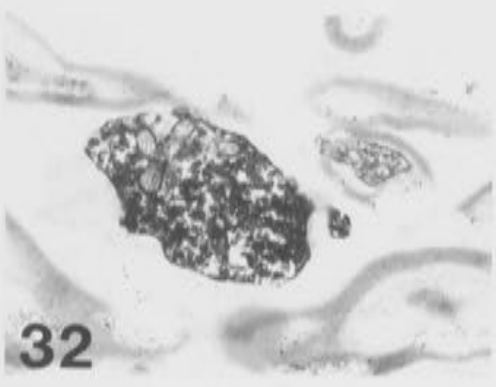
32


39


46


34

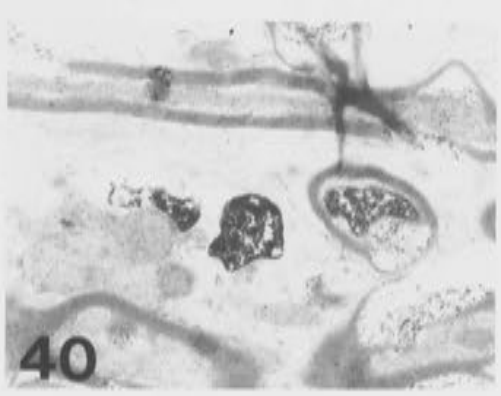
40


51


35

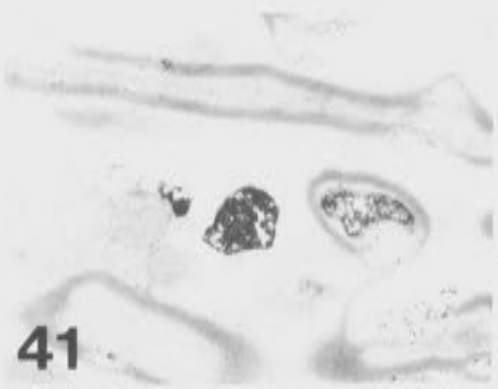
41


59

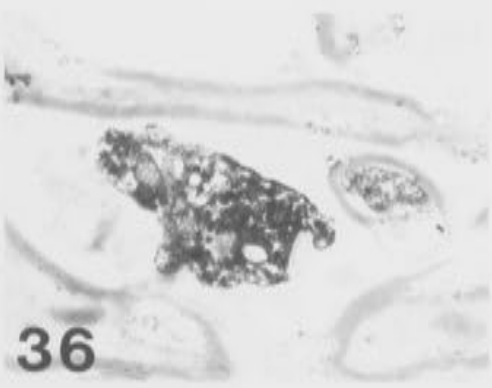
36


42


63
1um

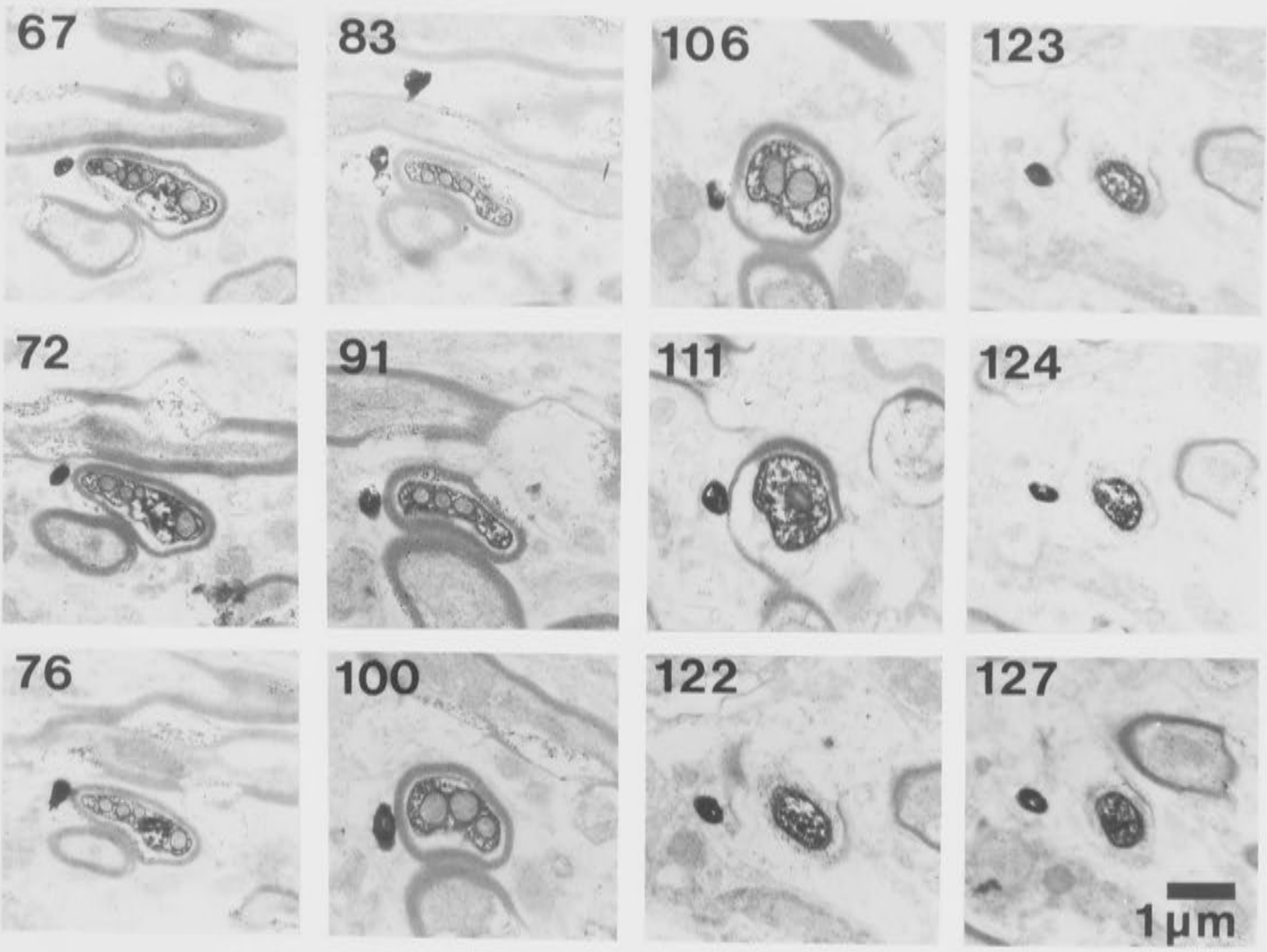
67
83
106
123
72
91
111
124
76
100
122
127
1 µm

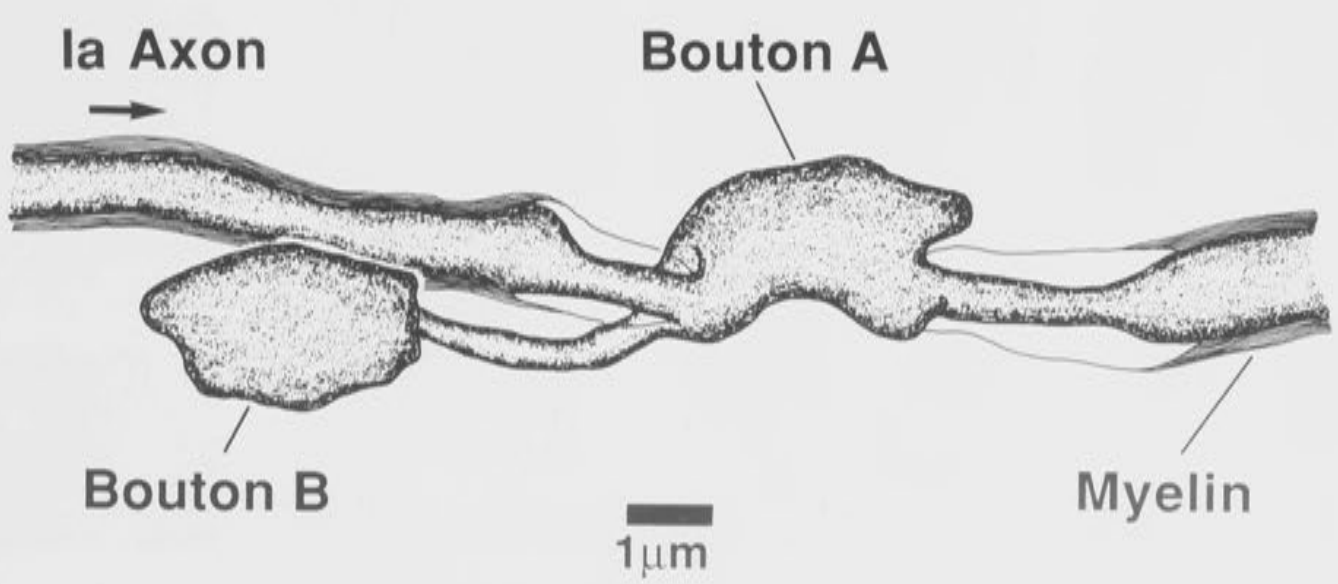
Ia Axon
Bouton A
Bouton B
Myelin
1µm

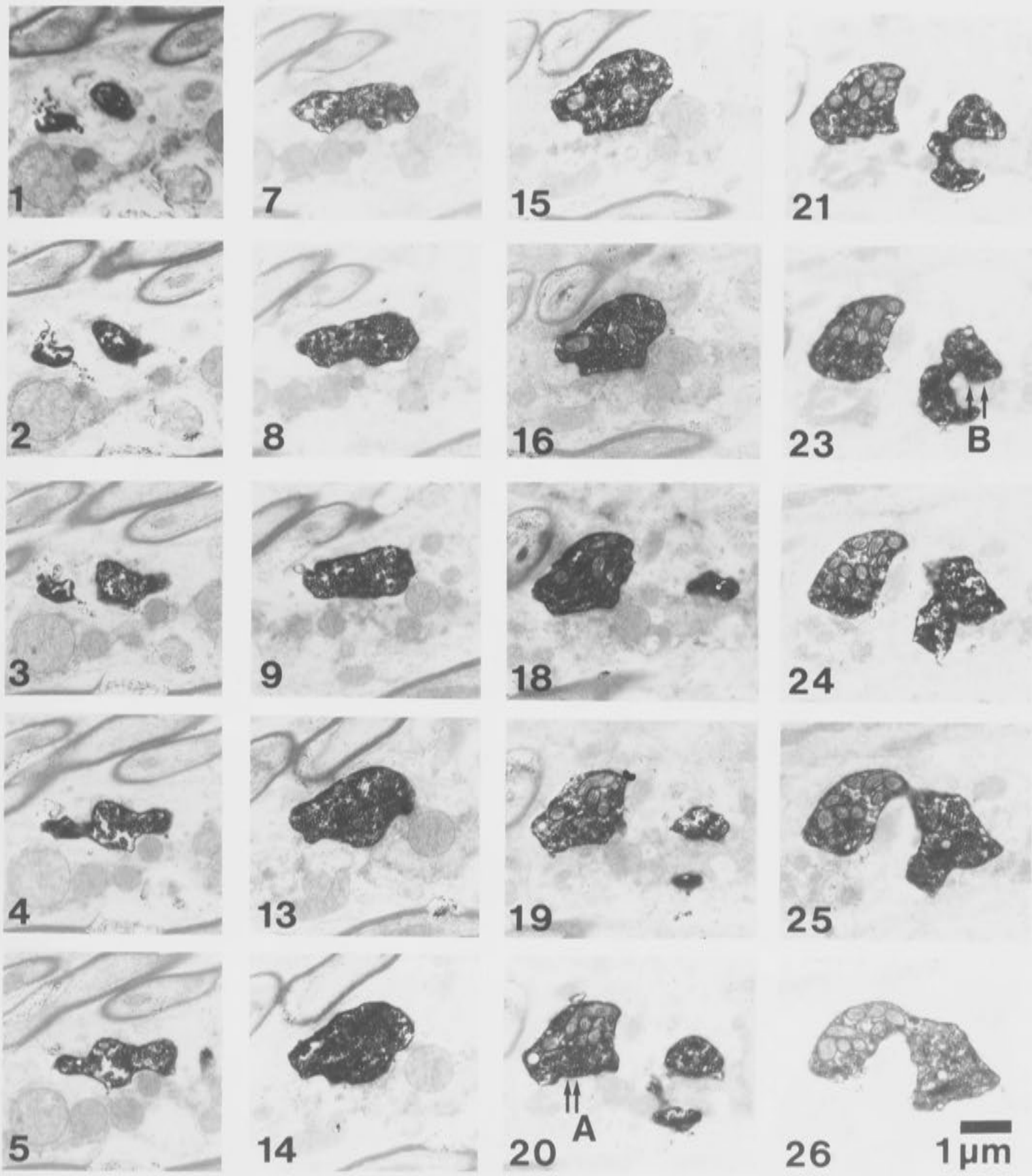
1
7
15
21
2
8
16
23
B
3
9
18
24
4
13
19
25
5
14
20
A
26
1 µm


27

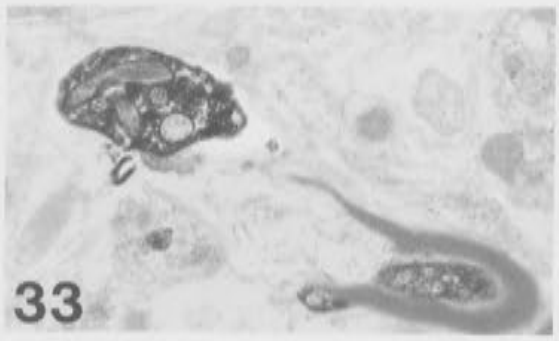
33


39


28


34


40


P
29

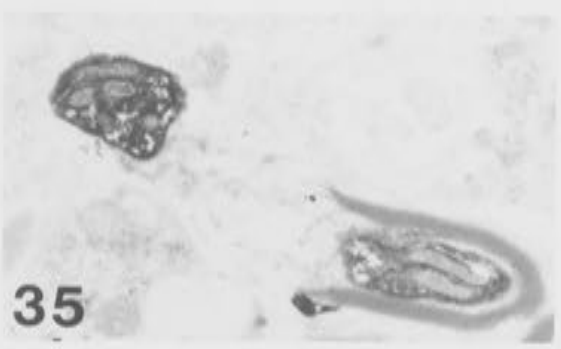
35

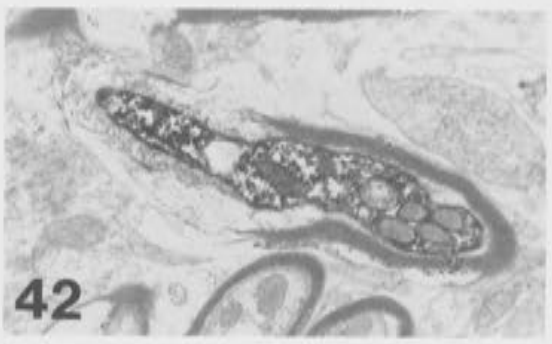
42

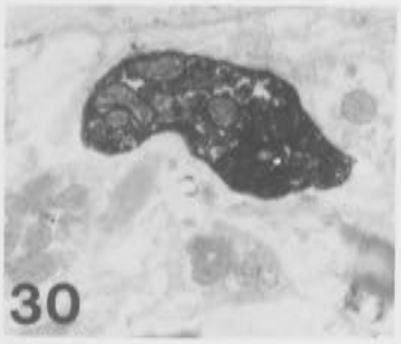
30

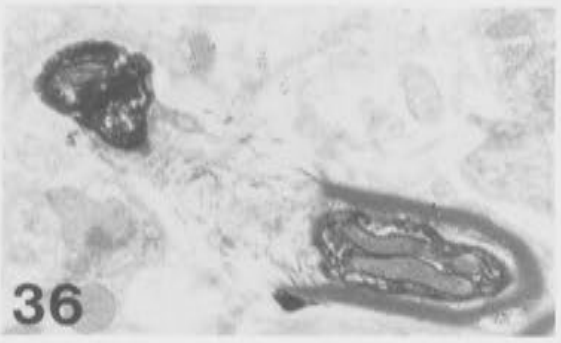
36

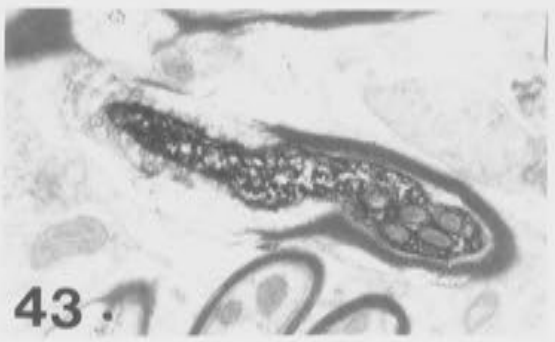
43


31


37


1µm
48

In Figure 4.47, the reconstruction of the afferent collateral is repeated, with the boutons to be presented in the following figures (Figure 4.48-4.52) shown enclosed in the dotted box, and marked with two arrows, A and B. On the original light microscopic reconstruction (Fig. 4.2) it was proposed that 3 boutons existed in this region. However, serial section electron microscopy has shown that only two boutons are apparent. As shown in Figure 4.2 and repeated in Fig. 4.47, the resolution of the light microscope was sufficient to suggest an unusual configuration of the collateral, which branched at the second bouton. The reconstruction suggested that from this branch point, a branch ran backwards along the collateral.

The true configuration of this backward branching collateral as revealed under the electron microscope is shown in the drawing in Fig. 4.50. The main collateral was seen to lose its myelin sheathing at the edge of bouton A. Bouton A was 4.0 x 1.8 μm, and constituted the branch point. A narrow unmyelinated branch of the collateral, 0.6 μm in diameter, emerges from the lower left corner of bouton A, and runs for 8.6 μm back along the main collateral, in very close proximity to it. This gives rise to the second and terminal bouton, bouton B, which is 3.4 x 2.0 μm. From the right side of bouton A, the major collateral branch emerges and remyelinates, continuing in a caudal direction, with a diameter D of 1.5 μm (d = 1.2 μm).

Figs. 4.48-4.52 show a sequence of the serial sections through these two boutons, A and B, and the afferent neck which connects them. Bouton A is shown in the series of photomicrogaphs in Figs 4.51 and 4.52. Fig. 4.48 section 1 shows the first small traces of the terminal bouton of the series, bouton B, lying below and very close to the major, myelinated collateral. For much of its length, the unmyelinated branch and the myelinated collateral physically contact each other. Also in direct contact

with bouton B is a large diameter dendrite, running in parallel with the myelinated afferent fibre in Fig. 4.48 sections 1-17. Bouton B appears to contact this dendrite, and a synaptic specialization is indicated by the double set of arrows in Fig. 4.48 section 22. This bouton was extremely densely labelled, which made recognition of presynaptic vesicles difficult. As with other boutons along this collateral, the mitochondria are packed closely together, and well away from the synaptic surface.

In Fig. 4.49 sections 43-64, an unmyelinated fibre neck can be observed. This neck connects bouton B to bouton A. This collateral branch was followed for over 80 sections through the tissue, as indicated by the section numbers in Fig. 4.50. The longitudinal lengths shown in the line drawing of Fig. 4.50 are somewhat foreshortened, due to the fact that much of the travel of these two profiles was perpendicular to the plane of section.

By Fig. 4.49 section 100, the myelinated afferent is seen to undergo a change. The myelin remains intact up to Fig. 4.50 section 111, but the diameter of the fibre itself (d) became smaller, widening the gap between the inner myelin layer and the axolemma. At Fig. 4.50 section 111 the unmyelinated collateral branch and the myelinated fibre remain in close proximity to one another, but the myelin sheathing begins to thin. This indicates that this cross section is directly through the paranodal region. Fig. 4.50 sections 122-127 show further advancement of the loss of myelin in the paranodal zone, which reaches right to the edge of bouton A. Bouton A constitutes the branch point, and is presented in the next two figures, Fig. 4.51 and 4.52.

A note regarding the line drawing of Fig. 4.50 is that the arrow to the left of the figure indicates the direction of an action potential travelling along the myelinated collateral, and that an action potential

invading bouton B would travel backwards from the branch point, in the opposite direction to the arrow shown.

Figs. 4.51 and 4.52 show a selected sequence of the serial sections examined through bouton A. The numbering of these sections starts again at a point where the myelin sheathing has almost disappeared, and the unmyelinated branch is in very close proximity. The actual branch point occurs in Fig. 4.51 between sections 3 and 4. Initial examination of bouton A, even under the electron microscope, appeared to show that, as suggested by the light microscope reconstruction, 2 separate boutons were situated close together. This is shown by Fig. 4.51 sections 18-25. However, further investigation showed that this was not the case, and Fig. 4.52 shows that only one bouton was present. Two possible synaptic specializations were recognised in this bouton, and though not as clearly defined as some previously presented, they are marked with double sets of arrows as A and B in Fig. 4.51 sections 20 and 23. In Fig. 4.52 section 29, a small unlabelled bouton (P) is marked, and an arrow in that section indicates a presumed contact with the HRP labelled bouton.

The rewinding of the myelin in the paranodal zone following bouton A is clearly illustrated in Fig. 4.52 sections 33-48. Fig. 4.52 sections 36 and 37 show the helical unwinding pattern of the myelin sheathing which forms a banding pattern across the paranodal zone. The final myelin layers are seen surrounding the neck of the bouton in Fig. 4.52 sections 39-43. Complete myelination of the afferent occurred approximately 2.9 μm distant from bouton A, and the caudal continuation of the collateral has a diameter D = 1.5 μm (d = 1.1 μm).

The boutons presented in Figs. 4.47-4.52 represent the final synaptic boutons on the piece of collateral contained in the first block of tissue. The remaining specializations were contained in the second block, and they are presented in the following figures.

The reconstruction of the plantaris Ia afferent collateral is repeated in Fig. 4.53. The bouton to be presented in the following figures, Figs. 4.54-4.60 is indicated by the arrow, and enclosed by the dotted box. The entire bouton, and the afferent either side of it were cut and examined in cross section. This is an example of an *en passant* bouton, and exhibits characteristic paranodal regions on both sides.

Figure 4.54 shows the afferent collateral branch as it appeared in cross section approaching this bouton. The diameter of the fibre, D, is maintained at approx D = 1.7 μm (d = 1.1 μm). In Fig. 4.54 section 1, the fibre and the inner layer of the myelin are quite close together, with only a small gap separating them. The fibre itself then reduces in diameter over the next 30 sections, while the diameter of the myelin sheathing remains approximately constant. Thus the gap between the innermost layer of the myelin sheathing and the axolemma of the fibre is quite marked by Fig. 4.54 sections 23-34. By Fig. 4.54 section 38, the myelin sheath can be seen to be thinning around the fibre, whose diameter is reduced to d = 0.5 μm. The first traces of the bouton are evident in Fig. 4.54 section 46.

Some remaining layers of myelin can be observed in Fig. 4.55 section 53, but these are lost by Fig. 4.55 section 54. These shreds of myelin contact the very edge of the bouton, such that none of the afferent approaching the bouton is left bare. An interesting configuration is seen in Fig. 4.55 sections 57-63. The labelled bouton apparently wraps, or surrounds, an unstained profile to its right. In Fig. 4.55 sections 61-63, the labelled bouton can be seen to completely surround this structure, suggesting that it may be a spine like dendritic protrusion viewed in cross section. It also appears that vesicles within the labelled bouton have lined up around the profile, suggesting that this portion of the membrane of the labelled bouton may be presynaptic. At its largest, this bouton measures 3.3 x 2.0 μm. However, by Fig. 4.56 section 86 the bouton

FIGURE 4.53

Reconstruction of the HRP labelled plantaris Ia afferent collateral terminating in Clarke's column.

The bouton indicated by the arrow and enclosed in the dotted box in this reconstruction was an example of a simple *en passant* bouton, with characteristic nodal and paranodal regions. The series of Figures 4.54-4.60 shows a selected sequence of the sections taken through the bouton, and through the collateral as it approached and emerged from that bouton.


Ia Afferent
Collateral

FIGURES 4.54-4.60

The following figures show an extensive series of the sections through the bouton indicated in Figure 4.53.

A possible synaptic specialization is indicated by a set of double arrows in Fig. 4.58.

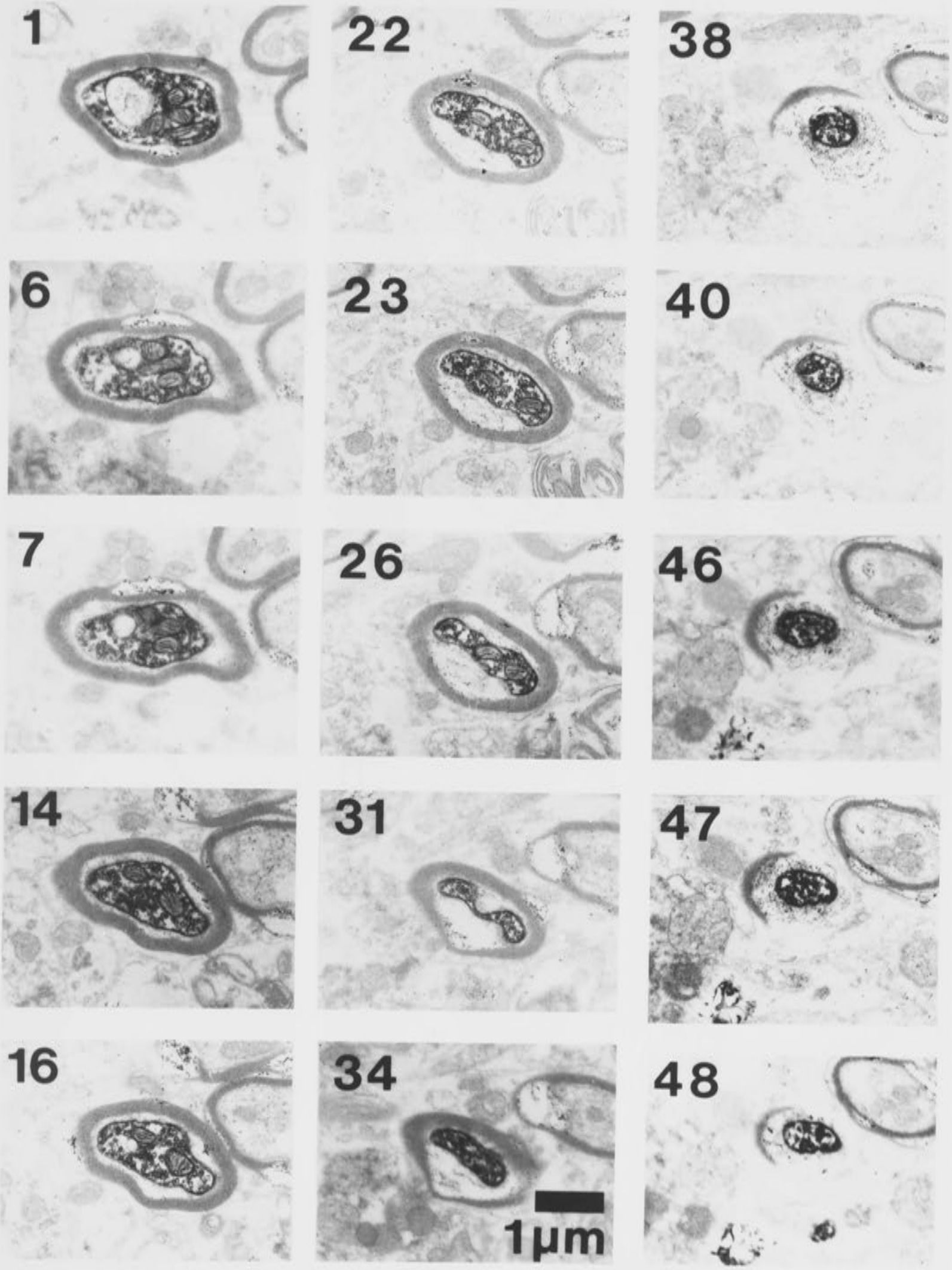
1
22
38
6
23
40
7
26
46
14
31
47
16
34
48
1µm


51


58


63


52


59


64


53


60


66


54

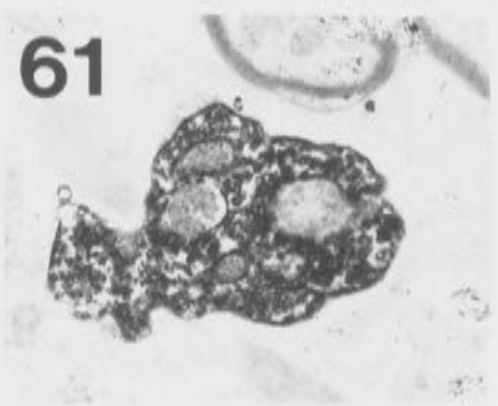
61


67

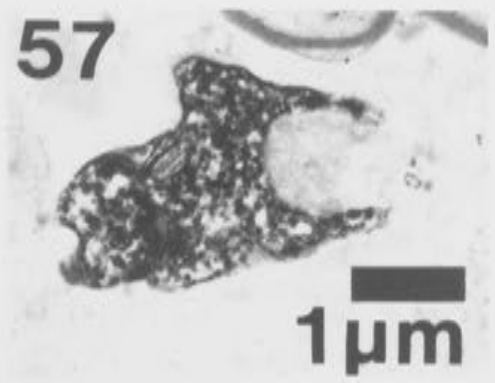
57
1µm


62


68


69


78


83


70


79


84


71


80


86


76


81


87


77


82


88
1µm

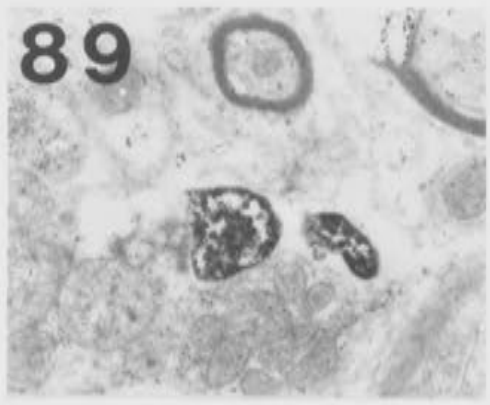
89

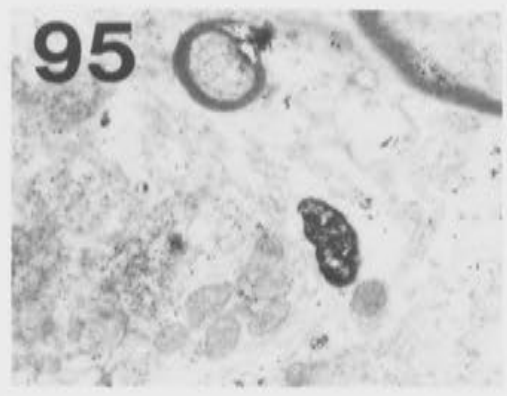
95


103


90

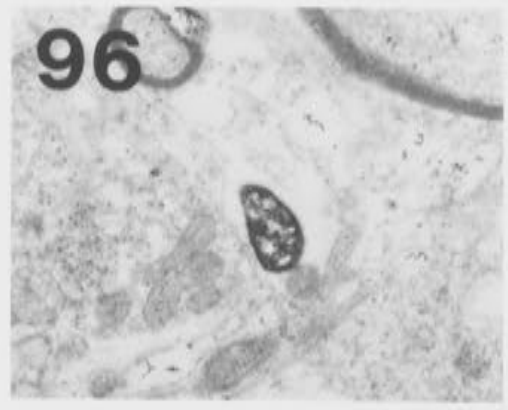
96

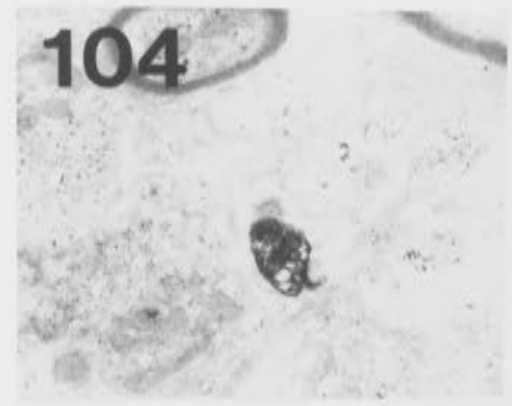
104

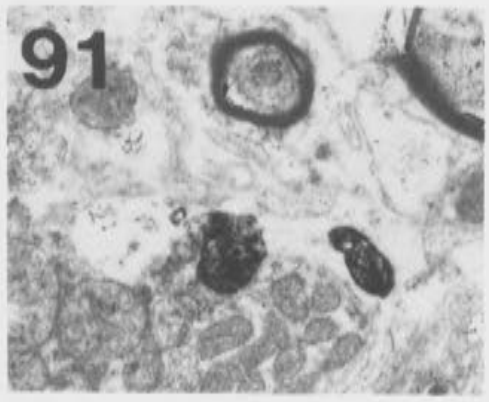
91


99

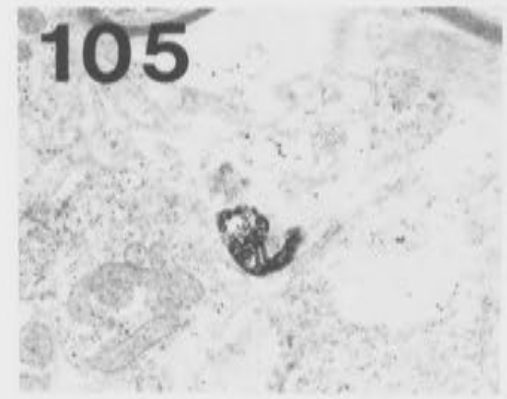
105


92


100


107


93

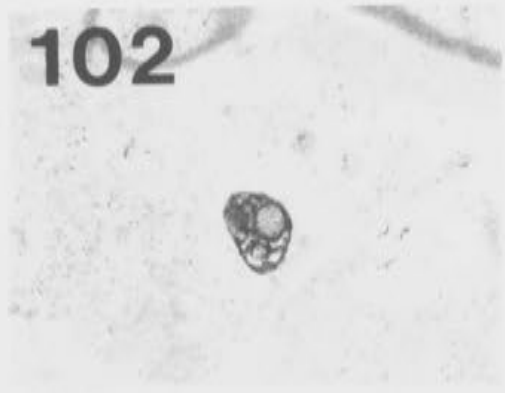
102

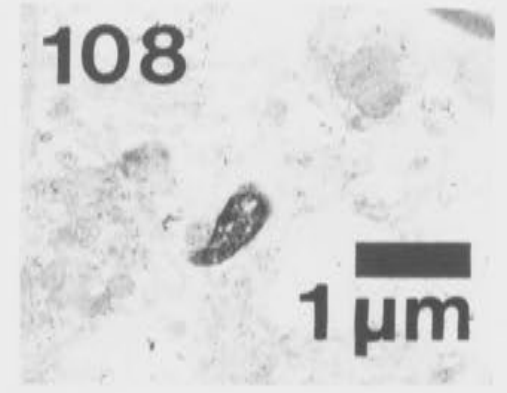
108
1 µm

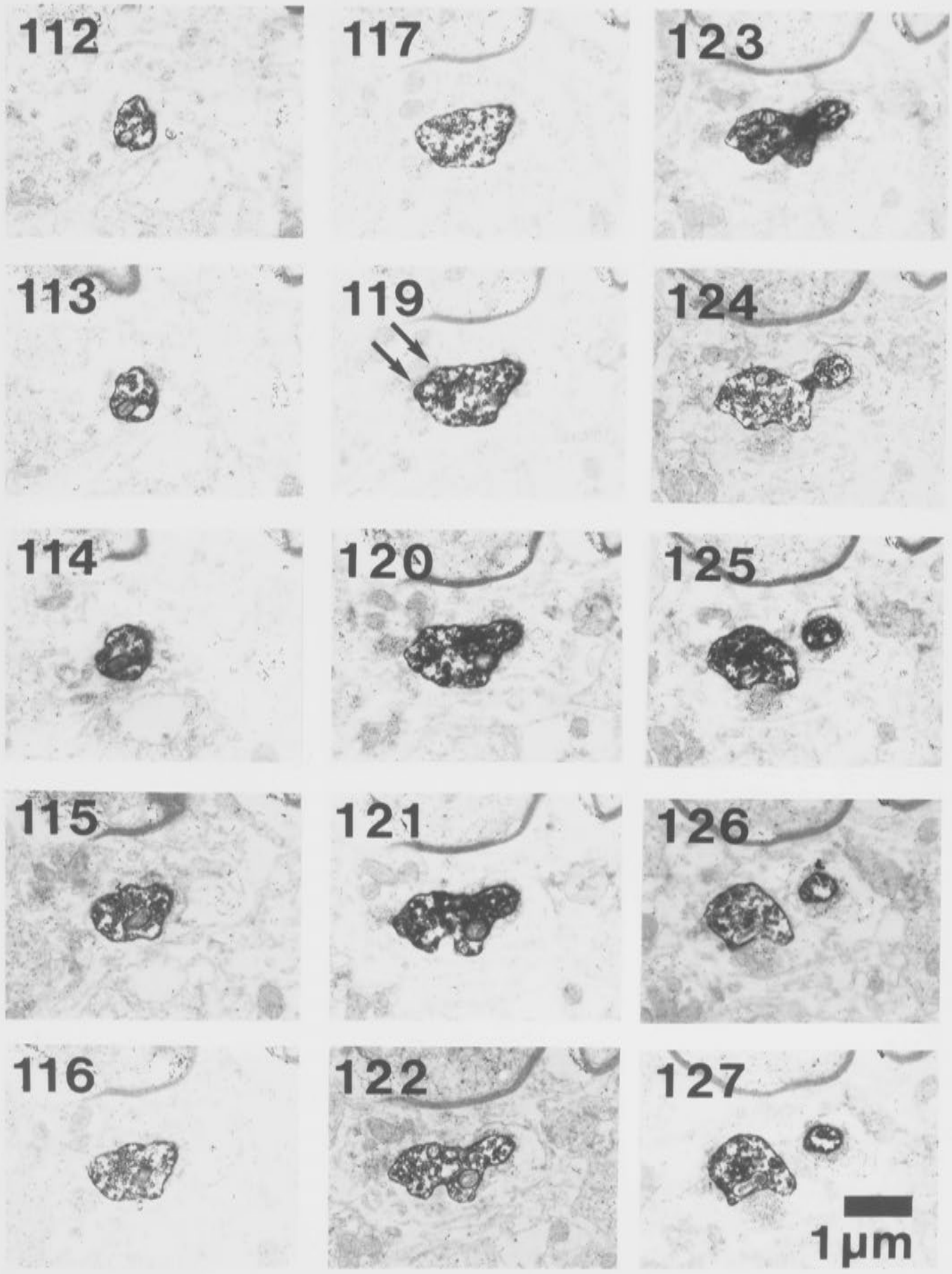
112
113
114
115
116
117
119
120
121
122
123
124
125
126
127
1 µm

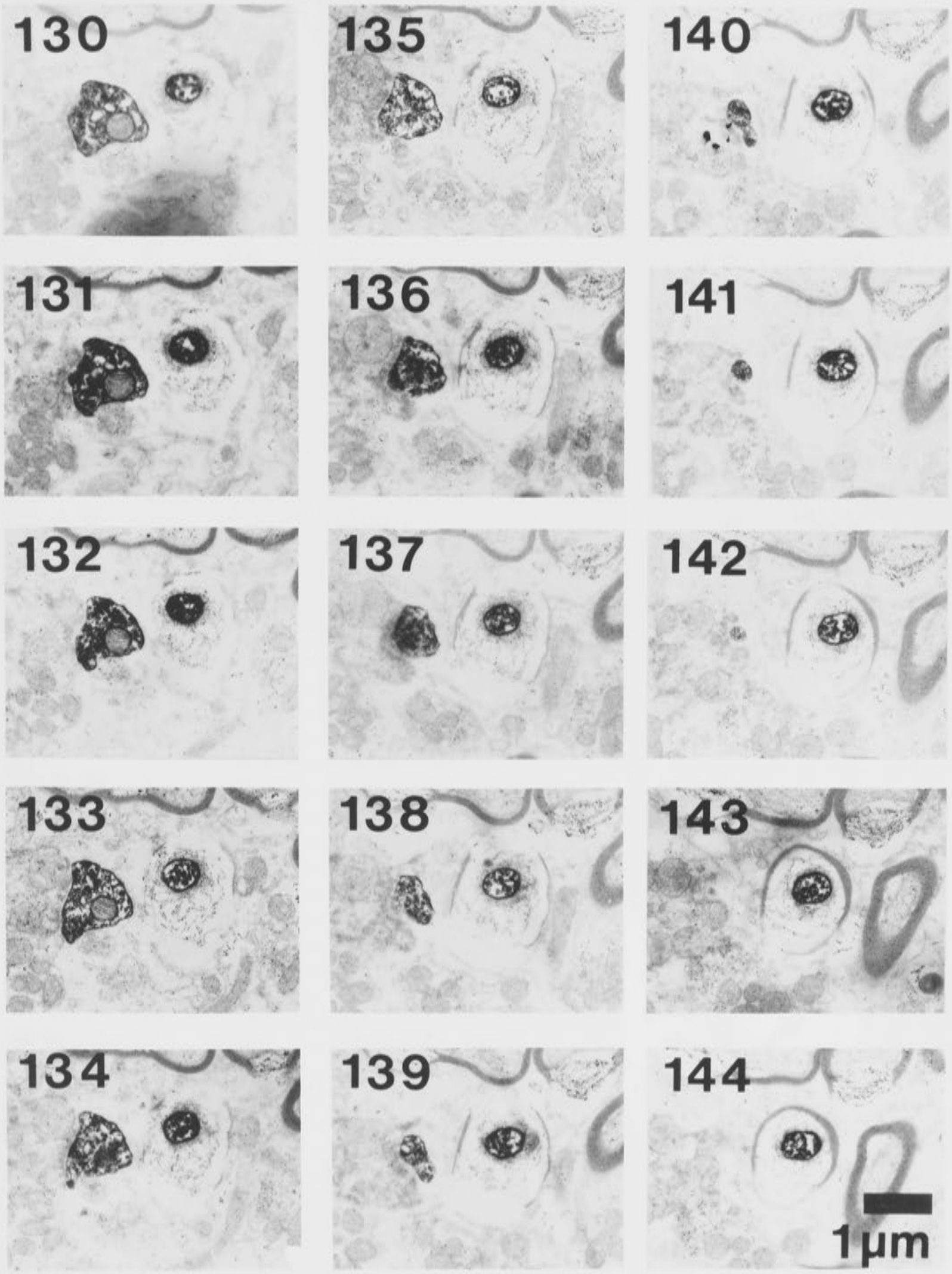
130
135
140
131
136
141
132
137
142
133
138
143
134
139
144
1µm


145


150


171


146


154


175


147


158


176


148

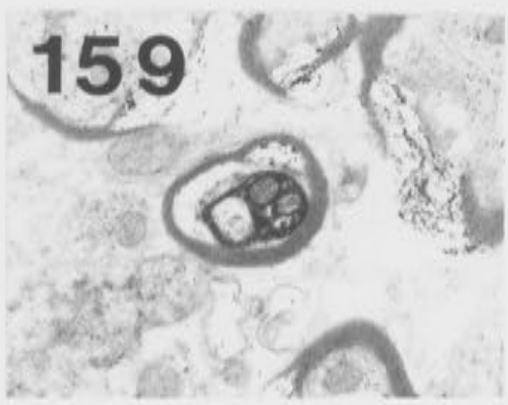
159


179

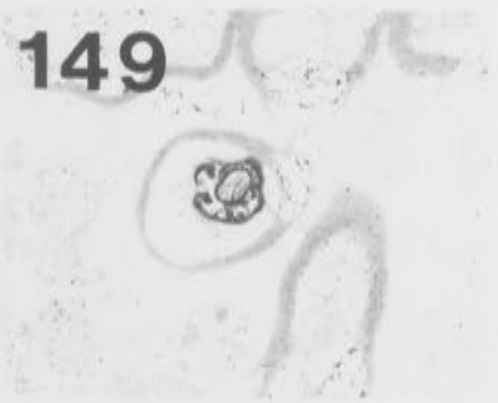
149


163


182
1 µm

becomes much smaller. This reduction in size continues through Fig. 4.57 sections 89-93, and here a small bridge begins to form. This bridge remains very small (0.3 μm in diameter) through to Fig. 4.57 section 108.

In Fig. 4.58, the bouton shows a size increase immediately prior to remyelination of the collateral. A single possible synaptic specialization was observed in this bouton, and is indicated by the double set of arrows in Fig. 4.58 section 119. A small protrusion from the bouton is seen to develop in Fig. 4.58 section 120, and by Fig. 4.58 sections 124-127 this piece has become entirely separate, and begun to show evidence of myelin sheathing. An extension of the bouton continues through the tissue in close proximity to this remyelinating branch of the collateral. The last traces of the bouton itself are seen in Fig. 4.59 sections 141 and 142, by which point the collateral approaches complete remyelination. The remyelinating zone has also been cut in cross section, and Fig. 4.60 shows a series of sections through the myelinating and myelinated fibre as it emerges from the bouton and continues caudally. By section 171 in Fig. 4.60, the myelin sheath is almost complete, and quite intact, yet the fibre diameter is not seen to fill that sheath until section 179. By Fig. 4.60 section 182, the fibre and its sheath are once again in close proximity, and the collateral has attained dimensions of D = 1.5 μm, and d = 1.0 μm.

After a further 55 μm, the collateral gave rise to another individual *en passant* bouton. This bouton is indicated by the arrow and enclosed in the dotted box in the reconstruction of 4.61, and shown in the series of photomicrographs through Figs. 4.62-4.64. The first trace of the bouton can be seen in Fig. 4.62 section 1, and the remainder of the sections are numbered relative to this section. This bouton reached a maximum of 2.0 μm in diameter, and exhibited no clear synaptic specializations. Fig. 4.62 sections 12-15 show the myelinated afferent approaching the bouton from the left. The sharp downward dip shown taken by the afferent in these

FIGURE 4.61

Reconstruction of the HRP labelled plantaris Ia afferent collateral terminating in Clarke's column.

The following three figures, Figs. 4.62-4.64 show a sequence of sections through the bouton indicated by the arrow and surrounded by the dotted box in this reconstruction. This bouton was a further example of an individual *en passant* bouton.


Ia Afferent
Collateral

FIGURES 4.62-4.64

The following series of photomicrographs were taken through the bouton indicated by the arrow in the reconstruction of Figure 4.61. The series is numbered from the first appearance of this bouton.

The myelinated afferent can be seen approaching the bouton in the large photomicrographs of Figs. 4.62 and 4.63, and the emerging branch is seen on Fig. 4.64. A small, extraneous whorl of myelin whose function is unknown is seen in Figs. 4.62 and 4.63, to the left of the bouton. No synaptic specializations were recognized in this bouton.


1

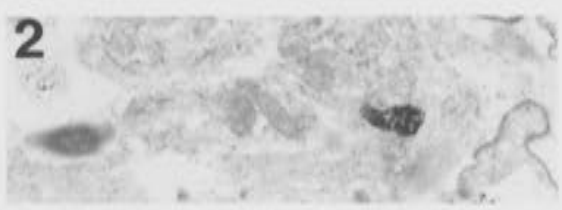
2


3


4

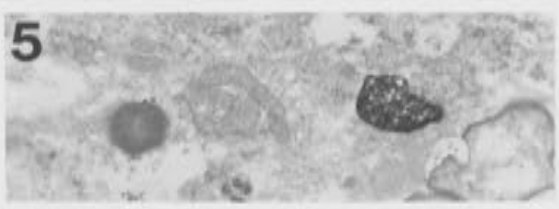
5


6


8


11


12


13


14


15
1µm

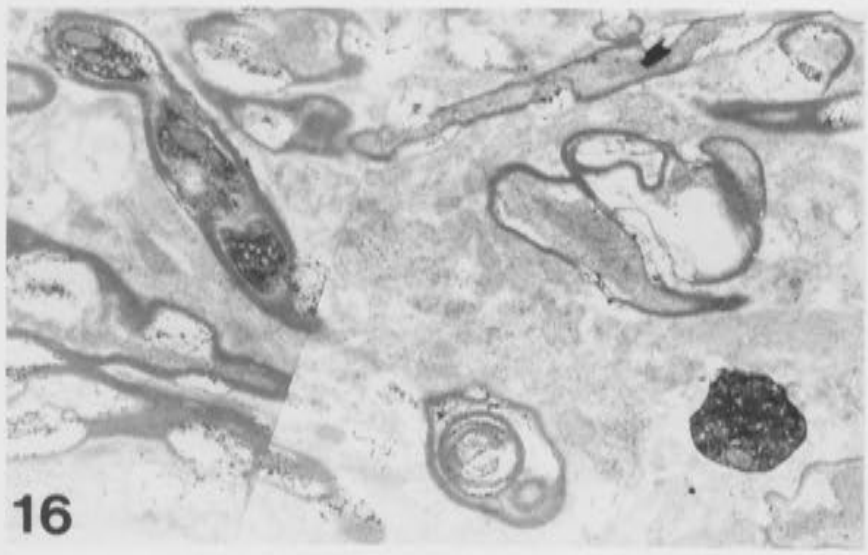
16


17


18


20


21


22


23


24


25

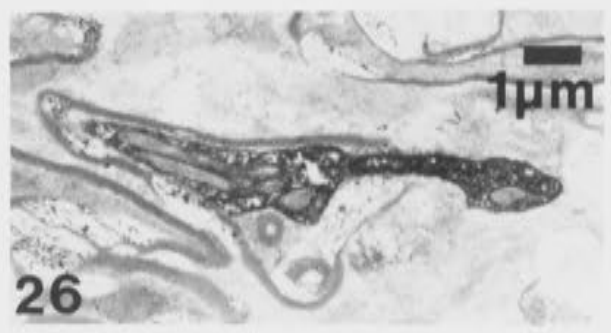
1µm
26


27

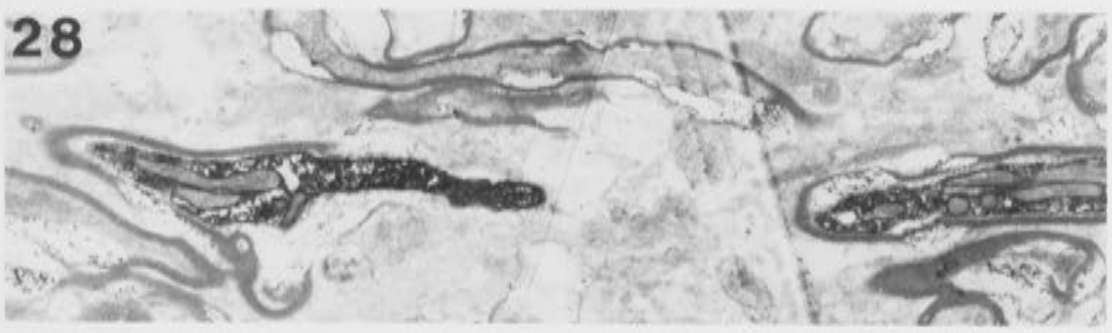
28

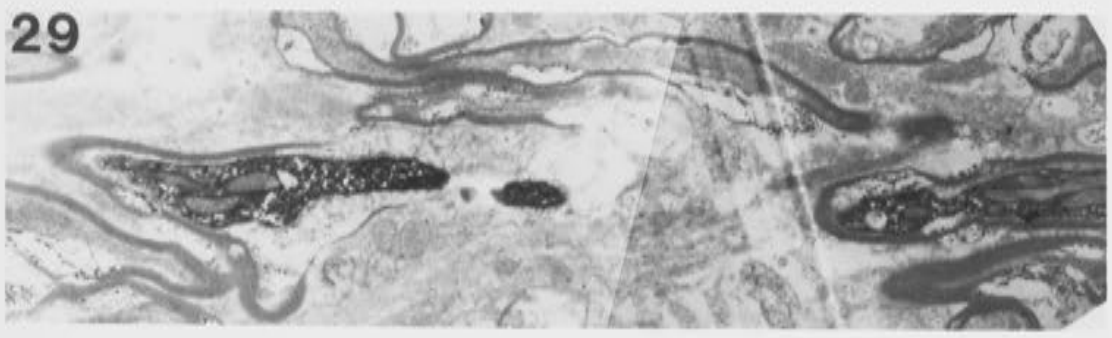
29

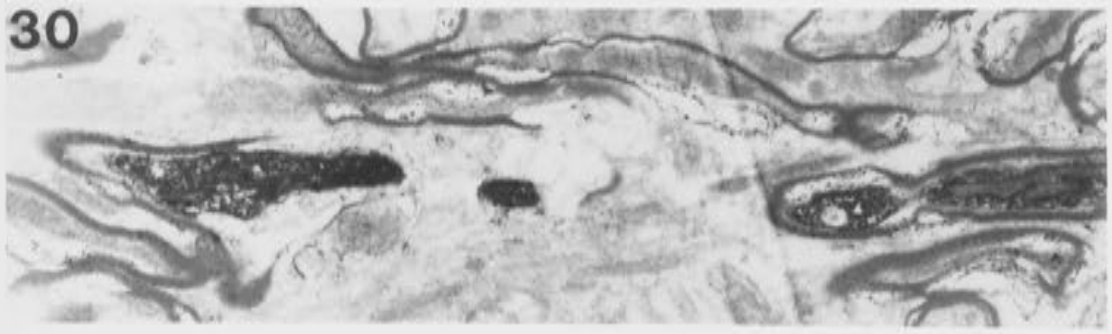
30

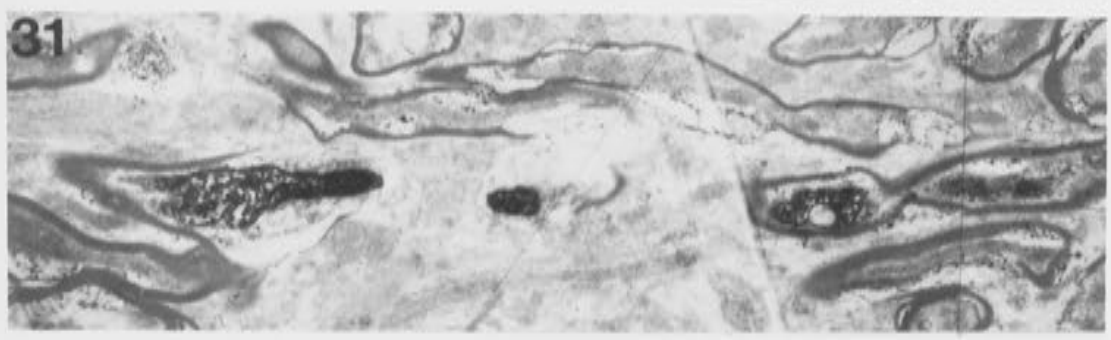
31


32

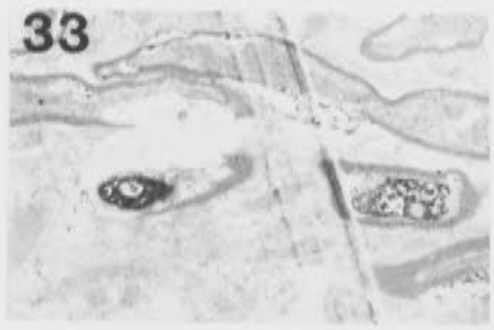
33


35


36


37

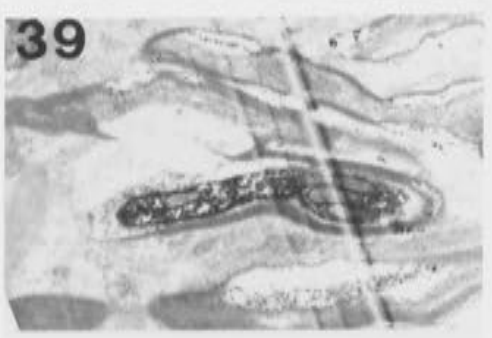
39


41
1µm

sections can be directly correlated with the original light microscopic reconstruction, (see Figs. 4.2 and 4.61). The collateral is seen approaching the bouton in Fig. 4.63 sections 16-20, with a diameter of D = 1.5 μm (d = 1.0 μm). Loss of myelination occurs over a paranodal zone 2.6 μm in length, illustrated in Fig. 4.63 sections 24-26, and in Fig. 4.64. An unusual feature of this series is the inclusion within the myelin sheathing just prior to the paranodal zone of a whorl of myelin, whose function is unclear. This extraneous myelin appeared to be continuous with the myelin sheathing of Fig. 4.64 sections 27-30, and could be traced back through the sections to termination in Fig. 4.53 section 4. It was therefore not a through travelling axon which had somehow been surrounded by the myelin sheath of this collateral, but apparently represented an integral part of the sheath itself. The paranodal zone in this region showed the characteristic banding described previously. This can be seen clearly in Fig. 4.63 sections 24-26. On either side of the bouton, the final layers of myelin are seen to directly contact the bouton itself, and therefore, no part of the actual collateral neck was left bare. The afferent emerges from the bouton in Fig. 4.64. Remyelination of the collateral is seen in Fig. 4.64 section 30. The caudal continuation of the afferent is shown on the right in Fig. 4.64 sections 27-29, with a diameter of D = 1.4 μm, and d = 0.9 μm.

From this point, the collateral continued caudally for a further 55 μm before approaching the final series of boutons. The original observations under the light microscope suggested that the final series consisted of five boutons. The reconstruction in Fig. 4.65 shows 5 boutons labelled with arrows (A-E) and enclosed in the dotted box. However, these arrows do not correspond with all of those on the original tracing in Fig. 4.2. The first of the proposed boutons in Fig. 4.2 proved to be the point at which the afferent lost its myelin sheathing for the last time, recognized under the electron microscope as very darkly HRP labelled, and exhibiting

FIGURE 4.65

Reconstruction of the HRP labelled plantaris Ia afferent collateral terminating in Clarke's column.

The final series of boutons on this HRP labelled Ia afferent collateral is indicated by five arrows, A-E, surrounded by the dotted box in this reconstruction. Five boutons were found to make up this series. However, their configuration was not as indicated on the original light microscopic reconstruction (see text). The following figures 4.66-4.72 show a sequence of the sections taken through these five boutons. The last bouont is the final termination of this labelled collateral.


Ia Afferent
Collateral
A
B
C
E
D

FIGURES 4.66-4.72

The series of photomicrographs shown in the following figures were taken of the five boutons situated in the area indicated by the arrows, A-E, on the reconstruction of Fig. 4.65. Their positions, however, differed from that proposed by the light reconstruction (Fig. 4.2).

The line drawing in Fig. 4.66 shows the configuration of the five boutons. Remyelination did not occur along the length of this branch, and the final bouton E was terminal, marking the end point of this labelled collateral.

The photomicrographs in Figs 4.66 - 4.72 are numbered relative to the first appearance of bouton A. Bouton B exhibits two synaptic specializations, indicated by the single arrow in Fig. 4.68, and the double arrows in Fig. 4.69. The specialization in Fig. 4.68 is made with a spine-like protrusion.

Final traces of the myelinated part of the collateral are present in Fig. 4.69. Bouton C also appears to surround a small unlabelled spine-like protrusion in Fig. 4.71.

Final traces of the terminal bouton E are shown in Fig. 4.72, proving that the collateral terminated at the point proposed by the reconstruction under the light microscope.

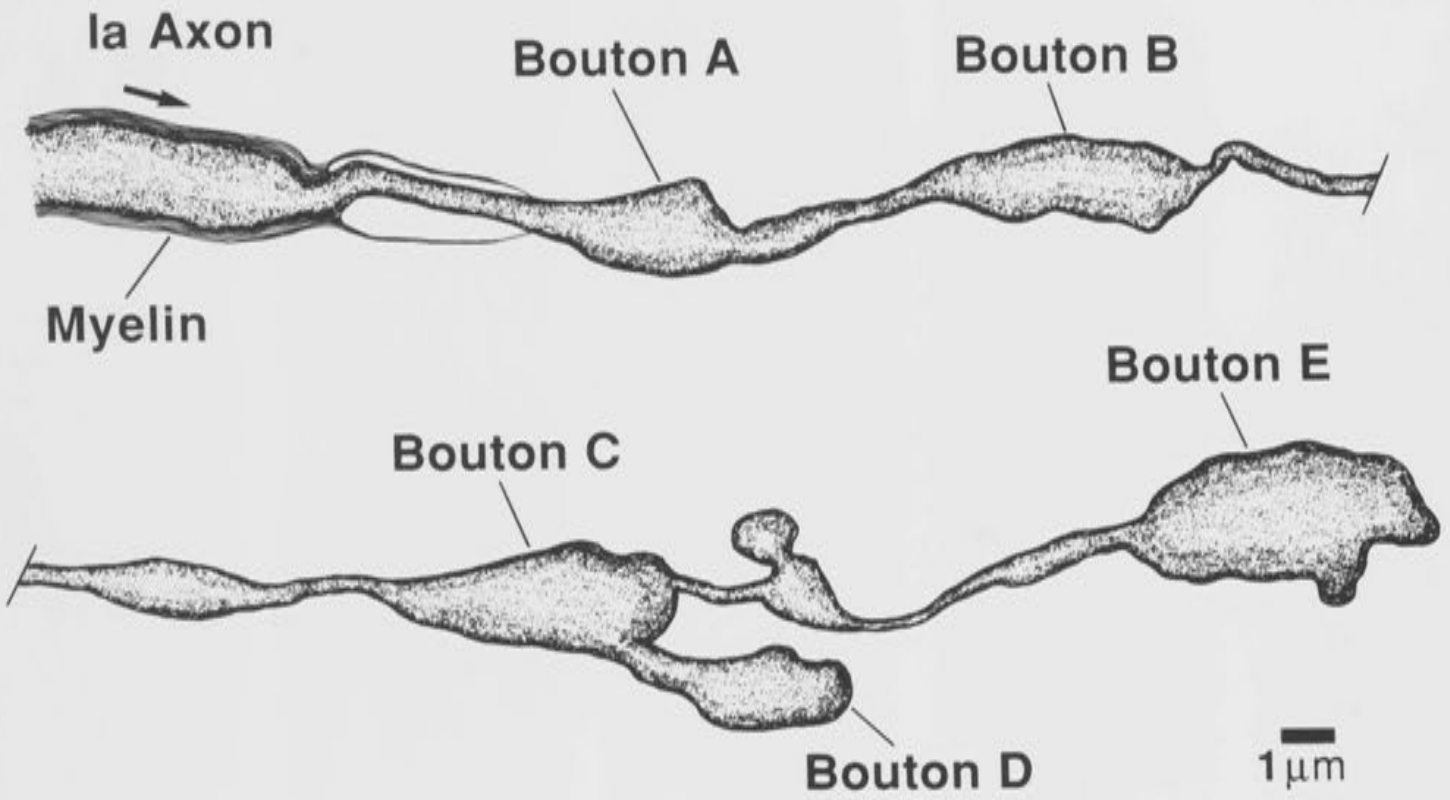
Ia Axon
Bouton A
Bouton B
Myelin
Bouton E
Bouton C
Bouton D
1 µm


2


8


3


9


4


10


5


13

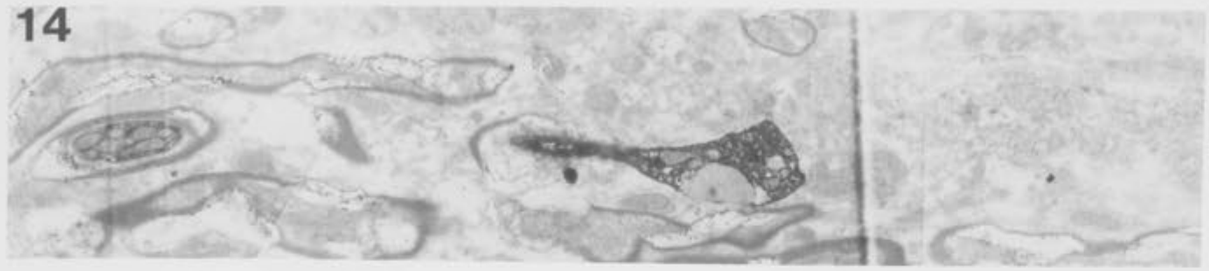
14

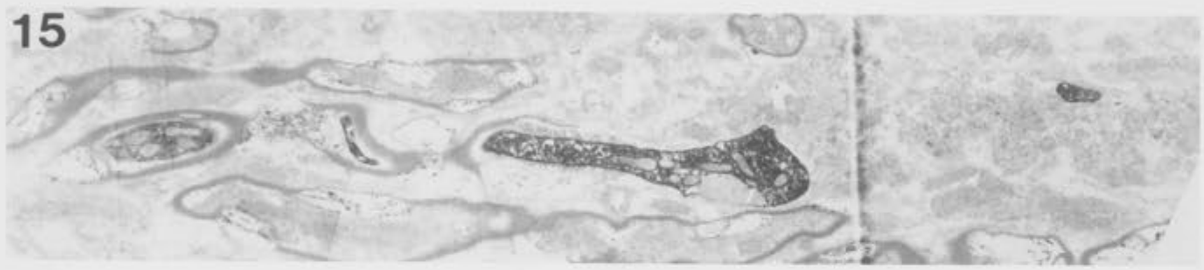
15


16


19

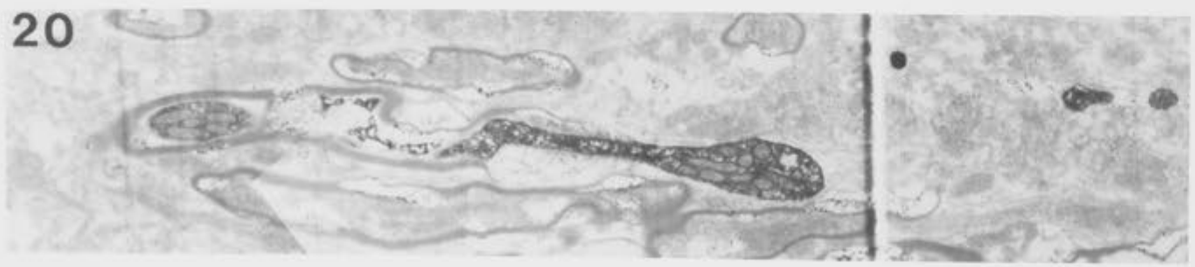
20


23

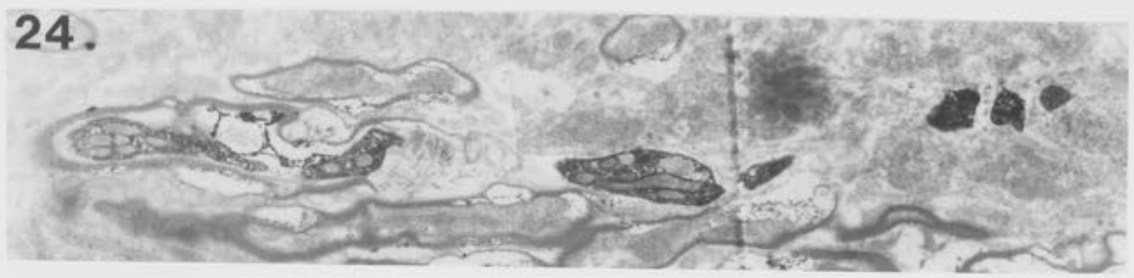
24.


25


26


27
1µm

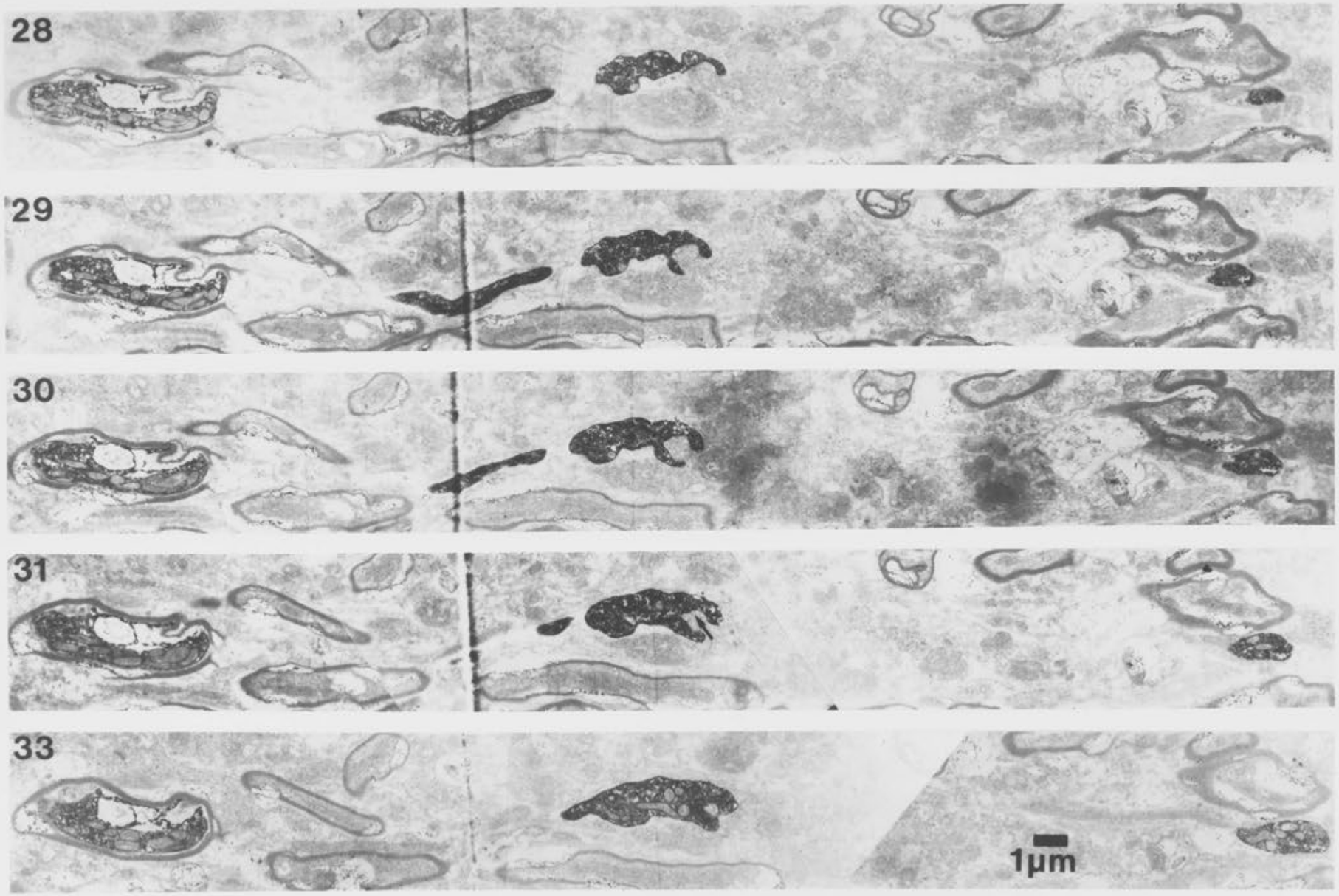
28
29
30
31
33
1µm


34

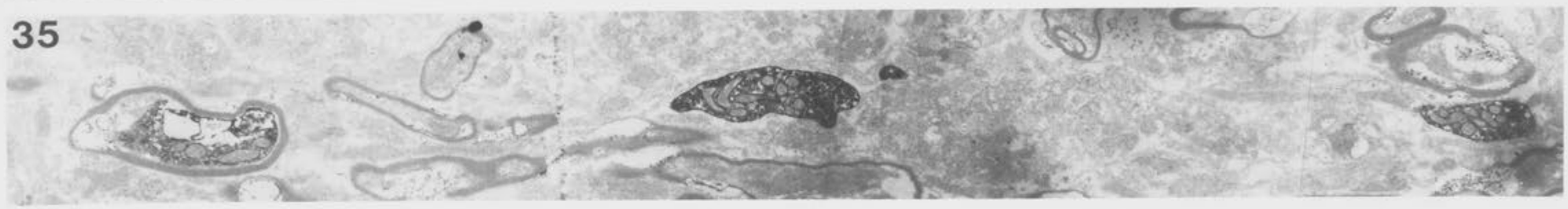
35


36


38

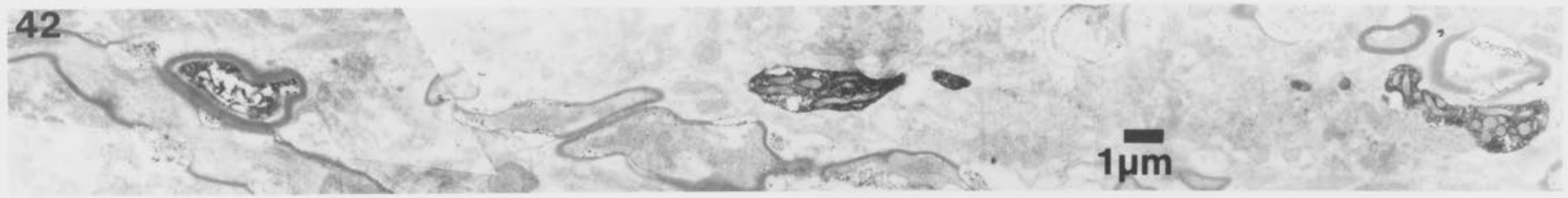
42
1µm

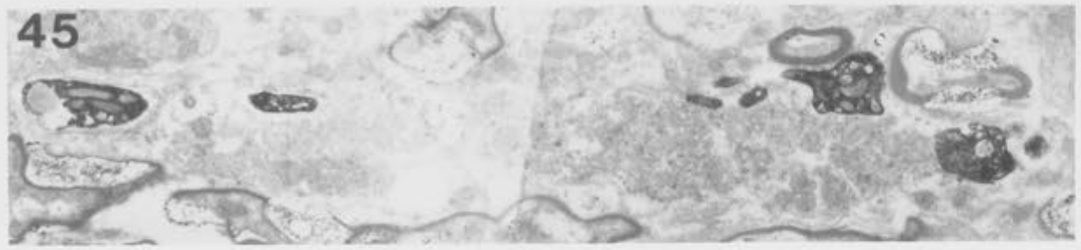
45

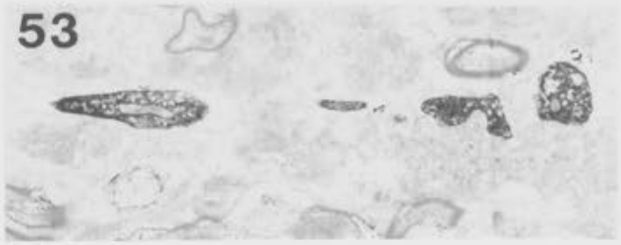
53

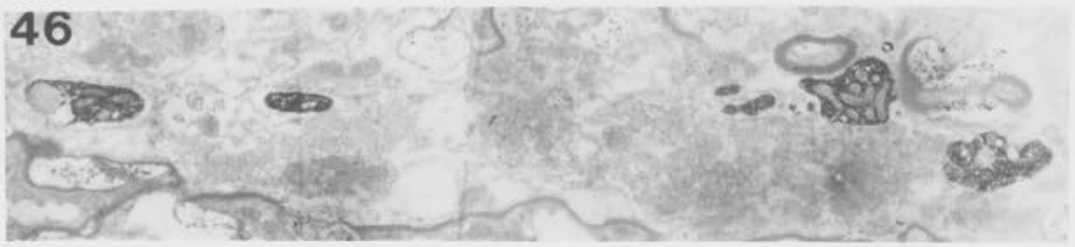
46


54


50

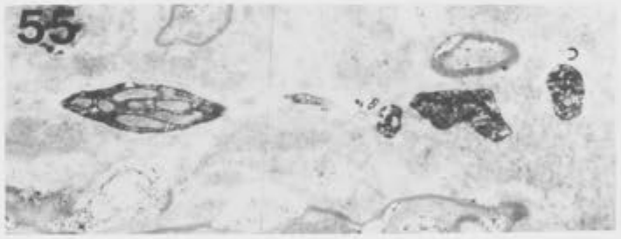
55

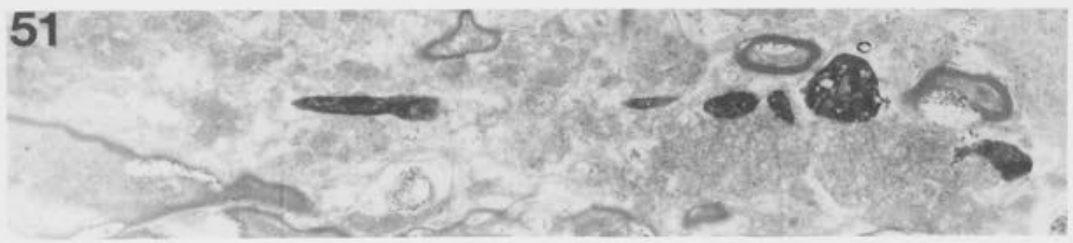
51

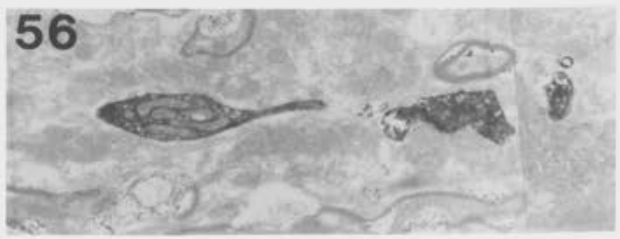
56

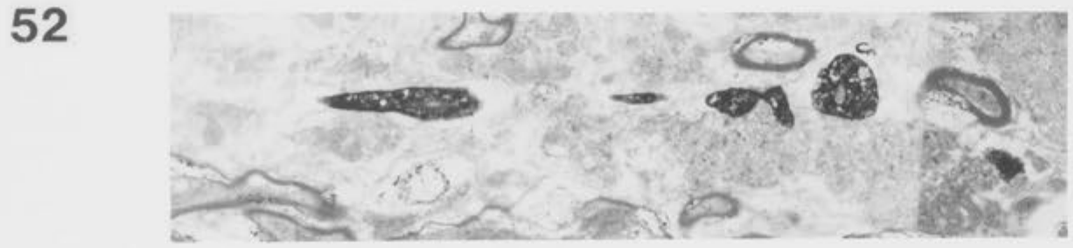
52

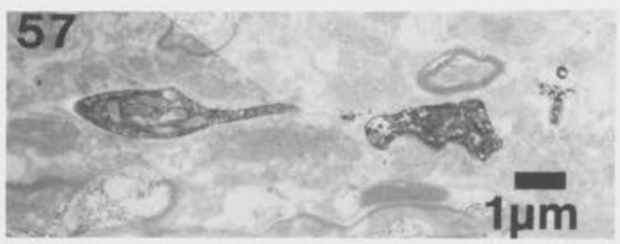
57
1µm


59

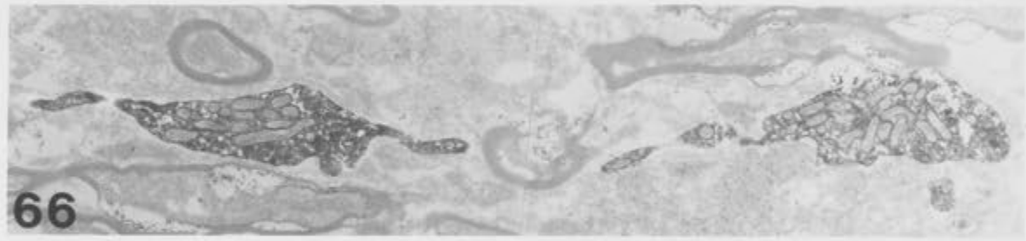
66


60

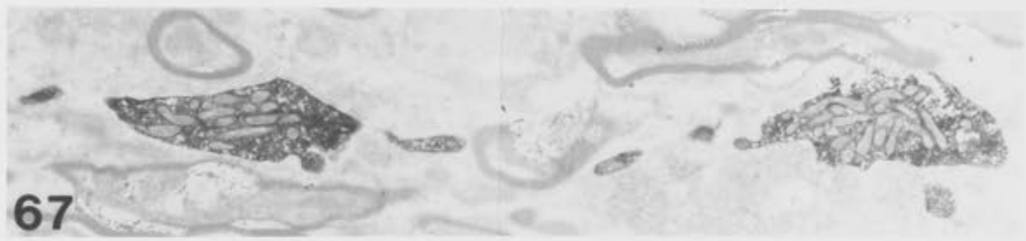
67

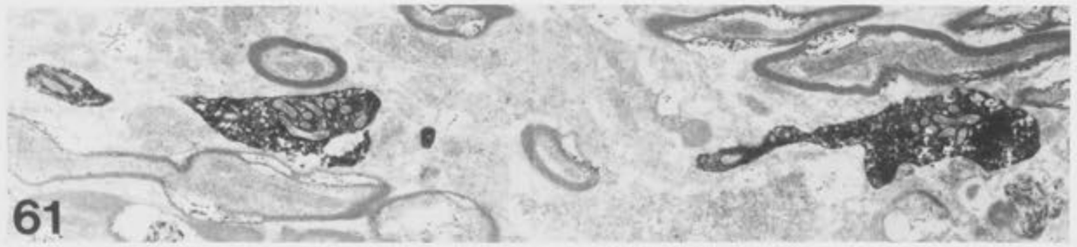
61

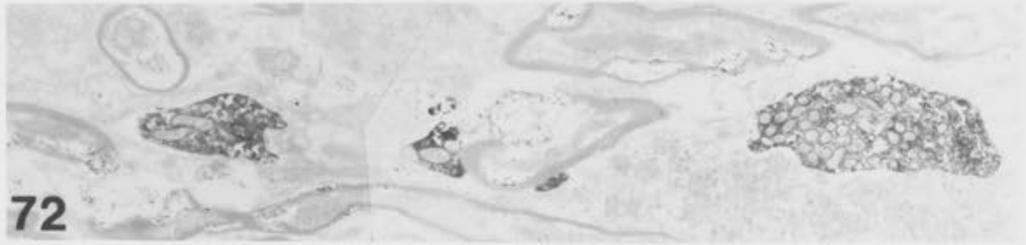
72


62

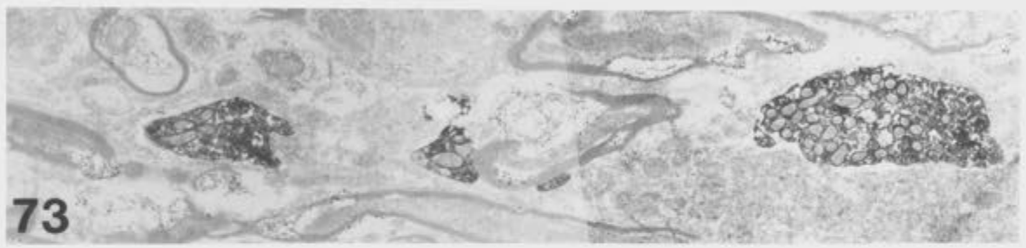
73


65

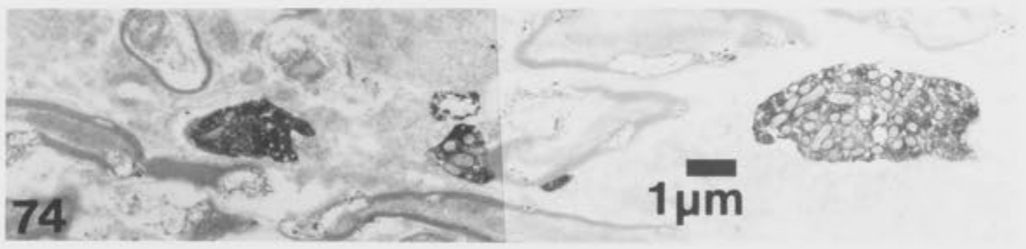
74
1µm

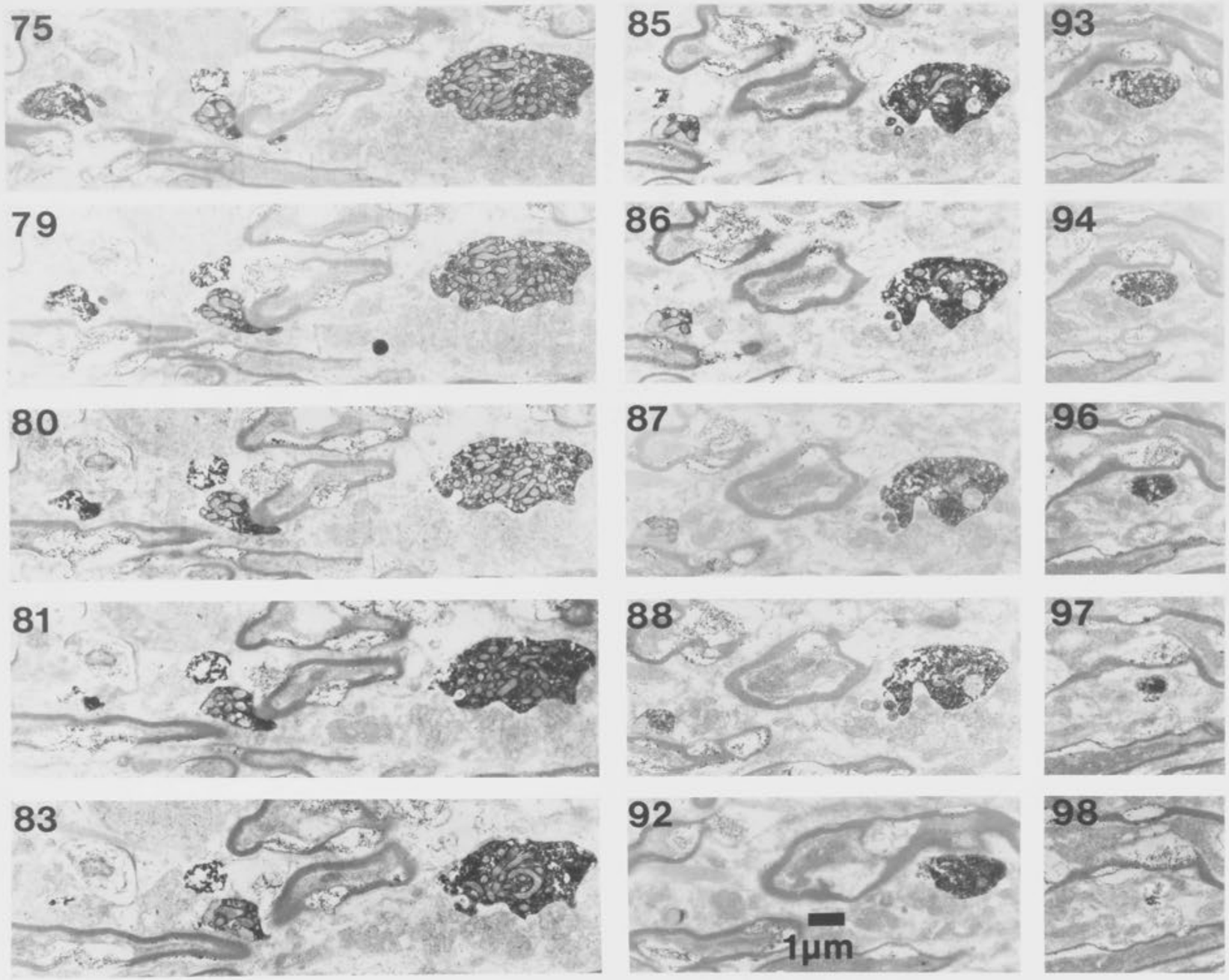
75
79
80
81
83
85
86
87
88
92
1µm
93
94
96
97
98

a slightly larger diameter than the remainder of that internode. The following two boutons proposed in Fig. 4.2 correspond to boutons A and B of Fig. 4.65. The region indicated by the 4th arrow in Fig. 4.2 was shown under the electron microscope to constitute 2 individual boutons, C and D of Fig. 4.65. Bouton E (Fig. 4.65), was terminal, as indicated on the original reconstruction (Fig. 4.2).

A summary line drawing in Fig. 4.66 shows the collateral at the top left corner losing its myelin sheathing for the last time. The unmyelinated fibre subsequently gave rise to five individual boutons, labelled A to E in the line drawing of Fig. 4.66. The final bouton, E, was terminal, marking the end point of this HRP labelled Ia collateral. The 5 boutons are presented in series through the sequence of photomicrographs in Figs. 4.66-4.72. The sequence is numbered relative to the first appearance of bouton A.

The diameter of the myelinated fibre in the last sections in which it appeared was approximately D = 1.7 μm (d = 1.4 μm). This indicated that over the 800 μm trajectory of this collateral, no tapering of the myelinated portions had occurred. The loss of the myelin sheathing around the neck of bouton A is shown in Figure 4.66 section 13, and Fig. 4.67 sections 14-23. Fig 4.66 section 13 shows an example of the familiar banding pattern across the paranodal zone proximal to bouton A. The final myelin layers come into direct contact with the edge of bouton A, which is approximately 3.4 x 1.8 μm. Bouton A is connected to bouton B via a narrow bridge of fibre, which can be seen emerging in Fig. 4.67 sections 24-27. The bridge of fibre, 3.9 μm in length and on average 0.5 μm in diameter, is seen giving rise to bouton B in Fig. 4.68. Bouton B is 4.9 x 1.6 μm, and shows a configuration similar to that described for the bouton in Fig. 4.56, in that it appears to surround a profile which is presumably post synaptic. This unlabelled profile, seen in Fig. 4.68 sections 28-33 appears to

be a spine like protrusion, possibly dendritic in origin. A potential site of synaptic connection betwen bouton B and this unlabelled profile is indicated by the arrow in Fig. 4.68 section 31. A second possible synaptic specialization recognized in bouton B is marked with double arrows in Fig. 4.69 section 36. A bridge of the unmyelinated fibre 9.9 μm in length, which subsequently gives rise to bouton C, can be seen emerging from bouton B in Fig. 4.69, especially in sections 38 and 42. The last traces of the myelinated collateral can also be seen in Fig. 4.69 section 42 on the far left. As noted, this region had been proposed as a bouton under the light microscope, and is therefore indicated with an arrow in the reconstruction of Fig. 4.2. The line drawing in Fig. 4.66 indicates a swelling of the unmyelinated bridge of fibre just prior to bouton C, and this is seen in Fig. 4.69 sections 52-57. This swelling appears to be filled predominantly with mitochondria. Bouton C was characterized by the presence of clear round vesicles which appeared to be much larger than those exhibited by every other bouton along this collateral, and were seen to line up in a most unusual configuration. However, the functional nature of these vesicles is not clear.

Bouton C (5.2 x 2.0 μm) constitutes a branch point, and gives rise to the smaller bouton, D (2.8 x 1.5 μm). This is shown in the line drawing of Fig. 4.66. A bridge of afferent fibre which emerges from bouton C subsequently gives rise to bouton E. Fig. 4.70 sections 45-57 show disjointed pieces of labelled tissue on the right. These are fragments of boutons C and D, and clearly indicate how essential serial section electron microscope techniques were for reconstruction of this series of boutons. In Fig. 4.71, bouton C is shown to envelope a small unlabelled profile in a manner similar to that described for bouton B. Although no synaptic specialization is evident, it is assumed that this inclusion is post synaptic, and most probably a spine-like dendritic protrusion.

The afferent fibre is shown emerging from bouton C in Fig. 4. 72 sections 62-67. The small irregularly shaped swelling of the fibre seen between boutons C and E in the line drawing of Fig. 4.66 is shown in the photomicrographs of Fig. 4.71 sections 72-74, and Fig. 4.72 sections 78-92. Following this swelling, an extremely narrow bridge of fibre 0.2 μm in diameter and 5.4 μm in length gave rise to the final bouton on this collateral, bouton E. This bouton was 5.6 x 2.7 μm, and irregularly shaped. Fig. 4.72 shows the last sequence of photomicrographs taken through boutons C and E. Fig. 4.72 section 98 shows the final traces of the labelled Ia collateral presented in this chapter. Subsequent sections were examined, but contained no HRP labelled structures. This bouton was therefore terminal as suggested by the initial light microscopic observations.

4.4 Discussion

This chapter has presented a detailed ultrastructural analysis of an HRP labelled plantaris Ia afferent collateral and its terminations within Clarke's column. This is the first comprehensive serial section electron microscope study of its kind, in which an entire collateral, including all of its branches and synaptic contacts, has been examined.

General LM and EM observations of the Plantaris collateral.

The plantaris Ia collateral entered the spinal grey matter and travelled 800 μm to terminate in Clarke's column. Initial observations under the light microscope suggested that 37 probable, and 4 further possible boutons were situated along this collateral and its branches. Serial section electron microscopy was performed on the entire collateral, and 35 boutons were recovered and examined. During the EM analysis, two

boutons were found whose presence had not been recognised under the light microscope, and 7 of those predicted were found not to be boutons. Of these, 2 cases existed where 2 proposed boutons were proven to be linked parts of a single bouton. Significantly, 4 cases existed where darker areas of the collateral itself had been incorrectly proposed as boutons. The very first small, *en passant* bouton, situated at the point where the collateral changed its trajectory, had been indicated as a possible, rather than a probable bouton. Not only did this bouton exist, but it exhibited two clear individual synaptic specializations.

These examples indicate that although light microscopic observations were useful in predicting the existence of boutons, they may not be entirely accurate. Light microscope observations were also not without error in resolving the branching pattern of the collateral. This failure was attributed to the close proximity of these branches.

On the other hand, the light microscopic reconstructions were extremely useful for orientation of the tissue under the electron microscope, and the combined use of the two techniques ensured that the entire labelled collateral was examined. Previous studies in which light and electron microscopic observations of the same tissue have been carried out have indicated that each bouton proposed under the light microscope has proven to be a synaptic bouton under subsequent electron microscopy, although discovery of further boutons under the electron microscope has also been reported (Conradi et al., 1983). In the present study, a number of boutons were recognized under the electron microscope which had not been identified under the light microscope, and not all proposed boutons proved to be synaptic boutons. These results suggest, therefore, that caution is required in the prediction of collateral trajectory, branch points, and presence of synaptic boutons following obvervations under the light microscope.

The true configuration of the collateral, as demonstrated by serial section electron microscopy is illustrated shematically in Fig. 4.73. This drawing also indicates the myelination pattern of the axon, shaded in red.

Morphology of the Boutons.

The results of this study provide a unique opportunity for comparison of 35 identified labelled Ia boutons, situated along the same collateral.

i) Size and Shape

The boutons ranged in length from small (< 1.5 μm in diameter) to large boutons, up to 9.2 μm in length. The average bouton size was 3.9 x 1.9 μm. Of these, the terminal boutons exhibited an average size of 3.7 x 2.1 μm, which did not differ greatly from the average size exhibited by the *en passant* boutons, of 3.9 x 1.8 μm.

The smaller boutons, up to 2 μm in diameter, were approximately spherical in shape. The larger boutons, 3-9 μm in length, rarely exceeded 3 μm at the widest point, and thus exhibited an elongated shape.

Since the discovery of the giant boutons in Clarke's column, many reports have suggested a minimum size for these boutons. Szentagothai and Albert (1955) originally described the giant boutons reaching 10-15 x 6-8 μm. Kuno et al (1973b) and Saito (1974) proposed that any bouton larger than 5 μm be regarded as a giant, although much larger boutons have been reported in Clarke's column (Rethelyi, 1970; Tracey and Walmsley, 1984). Hongo et al. (1987) have recently proposed that only boutons over 7 μm in length be regarded as giant, based on observations of primary afferent terminations in other parts of the lumbar spinal cord to 7 μm in

FIGURE 4.73

Schematic representation of the HRP labelled plantaris Ia collateral, as determined by serial section electron microscopy. This diagram, which is not to scale, emphasizes the configuration of the branch points, bouton locations and myelination pattern exhibited by the collateral. Myelin sheathing is indicated in red.

Discontinuities in the collateral indicate regions where there was an unfortunate loss of sections.

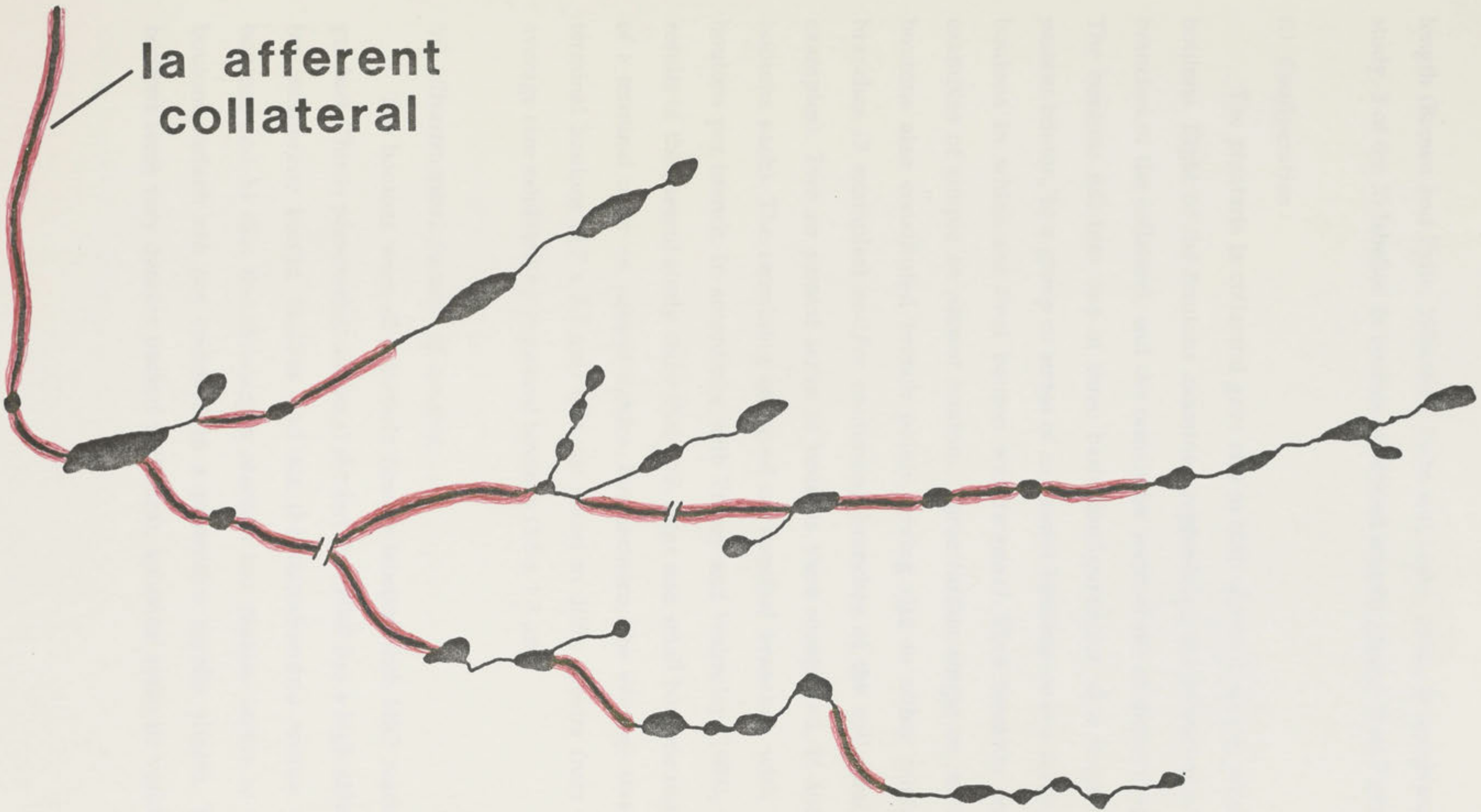
la afferent
collateral

length (Brown and Fyffe, 1978,1981; Fyffe and Light, 1984). In the present study, 3 of the 35 labelled Ia boutons exhibited lengths greater than 7 μm.

ii) Configuration

The plantaris Ia collateral gave rise to both terminal and *en passant* boutons. Eight of the boutons examined represented the termination of branches of the collateral, and the remainder were of the *en passant* type. The boutons fell into one of three basic configurations: a) a single *en passant* bouton, b) a group or series of *en passant* boutons, or c) a series of boutons in which the final bouton was *terminal*. Five boutons were examples of simple *en passant* boutons. Three further single *en passant* boutons also constituted branch points, giving rise to either teminal branches (3 examples) and/or continuing branches of the collateral (3 examples). Two *en passant* series of boutons were recognized, (2 and 4 boutons each). The remaining occurred on terminal branches, with 1-5 boutons per branch. In accordance with Tracey and Walmsley (1984), the results of the present study show that both large and small boutons can be of a terminal or an *en passant* nature. Furthermore, the average size of terminal boutons (3.7 x 2.1 μm) was not found to differ greatly from the average size exhibited by *en passant* boutons (3.9 x 1.8 μm).

iii) Ultrastructural features of boutons.

The boutons were all extremely heavily labelled with HRP reaction product. This is presumably due to a) the fact that HRP has a high affinity for membrane bound vesicles and for the mitochondria within the bouton, and b) that the chromogen reaction has readier access to the boutons, which are not enclosed in a protective myelin sheath. The boutons were very densely packed with clear, spherical synaptic vesicles,

and mitochondria. The mitochondria were characteristically seen to be tightly clustered, away from the synaptic surface of the bouton.

Morphology of the Synaptic Specializations.

Synaptic specializations were identified on the basis of three criteria: a) clusters of vesicles at the presynaptic site, b) presence of pre- and post-synaptic thickenings, and c) density of the synaptic cleft (Szentagothai, 1970). For most of the specializations exhibited by the boutons along this collateral, the presence of a post-synaptic thickening was the most obvious indication of a specialization. Clustering of vesicles was observed at the pre-synaptic membrane of these specializations. However, it was sometimes difficult to identify distinct clustering of vesicles, partly because of the intensity of the HRP reaction product, but especially because of the great density with which the vesicles were packed into the bouton. An interesting configuration was commonly observed, whereby the vesicles were lined up in neat rows at the presynaptic membrane. This was particularly observed at contacts on spines, or spine like protrusions.

i) Observation of Multiple synaptic specializations.

A notable observation in the present study was that not only large, or giant boutons, contained multiple synaptic specializations. The number of identified specializations in each bouton ranged from 1-7. Two of the smallest boutons along the collateral, 1.4 µm and 1.8 µm in length, exhibited two specializations each, and other small boutons (up to 3 or 4 µm in length) were shown to include 2 or 3 synaptic specializations. Two of the largest boutons, (9.2 and 9.0 µm in length) exhibited large numbers of release sites (6 and 7 respectively).

The anatomical demonstration of multiple synaptic specializations in the giant boutons (Rethelyi, 1970), has formed the basis for a hypothesis that quantal synaptic transmission is dependent on the independent operation of release sites, (Tracey and Walmsley, 1984), rather than the operation of the bouton as a whole (Redman and Walmsley, 1983a,b). The existence of multiple transmitter release sites is usually associated with the giant boutons in Clarke's column (Rethelyi, 1970). However, the present serial electron microscopic study has demonstrated that even the smallest boutons may exhibit multiple specializations. This finding suggests that light microscope observation and prediction may seriously underestimate the population of release sites at a connection, with obvious implications for studies modelling quantal transmitter release (see Discussion in Appendix I).

Some boutons exhibited no identifiable synaptic specializations. This was true of 2 of the largest boutons along the collateral. In some cases, boutons which exhibited no clear specializations were observed in close apposition to dendrites, and all of these boutons were packed with vesicles and mitochondria. In all such cases it seemed surprising that no specializations were recognized. The reasons for the apparent oversight of synaptic specializations in these boutons relate to the angle at which the synaptic surface was sectioned. If the plane of section was not perpendicular to the synaptic surface of the bouton, then the contact regions appeared smeared, and if the synaptic surface was parallel to the plane of section, specializations could not be positively identified. In a study such as this, in which a large number of boutons have been examined, it would be extremely fortuitous (and most unlikely) to achieve the exact sectioning plane required to identify specializations in all boutons. This indicates therefore that even serial section electron

microscopy may result in an underestimate of the total population of specializations at a connection.

ii) Configuration of the synaptic specializations.

The configuration of the individual synaptic specializations in a large bouton was reconstructed and illustrated in Fig. 4.20. This bouton was 9.2 μm in length, and exhibited 7 individual synaptic specializations. The synaptic surface in contact with the postsynaptic dendrite is shown in Fig. 4.20B. The specializations were shown to be of an extremely irregular shape, and varied sizes. Two examples of perforated synapses are shown. Perforated synapses, first described by Peters and Kaisermann-Abramof, (1969) and Cohen and Siekevitz (1978) in the cortex, are those in which the post synaptic density is discontinuous in any one of the sections through the specialization (Calverly and Jones, 1987). These perforated synapses can be of annular (doughnut), U (horseshoe) or W (irregular) configuration (Nieto-Sampedro et al., 1982; Dyson and Jones, 1984; Calverly and Jones, 1987). The bouton shown in Fig. 4.20 exhibits examples of both annular and irregular shaped perforated synapses (specializations 4 and 7 respectively).

Perforation, or extreme irregularity of shape, has been proposed as an indication that the specialization is undergoing development, or change (Carlin and Siekevitz, 1983; Dyson and Jones, 1984). As the synapse grows and develops, it appears to split into 2 or more specializations, and this splitting is indicated by the presence of perforations (Carlin and Siekevitz, 1983). In accordance with this hypothesis, perforated synapses are often seen to be much longer than non-perforated (e.g. Peters and Kaiserman-Abramof, 1969; Cohen and Siekevitz, 1978: Dyson and Jones, 1984; Calverley and Jones, 1987). The large size of the perforated synapses shown in Fig. 4.20 is also in accordance with this hypothesis. In one

example shown in Fig. 4.20, two of the release sites (2 and 3) were shown in very close proximity to each other. Serial section reconstruction of the bouton indicated that these specializations were in fact discontinuous. Although speculative, the possibility exists that this pair may originally have been one release site, which then perforated and divided, in the manner proposed by Carlin and Siekewitz (1983). Perforated or dividing synapses have often been shown to occur in association with dendritic spines, and spinule like protrusions (Carlin and Siekewitz, 1983, Spacek and Hartmann, 1983; Dyson and Jones 1984; Calverly and Jones, 1987). These spines may play some functional role in the recycling of synaptic membrane at the perforating synapse (Calverly and Jones, 1987) although that role is not yet clear. In this Chapter, examples were presented in which the bouton apparently engulfed or encompassed a small, spinelike postsynaptic protrusion (see 4.3 Results). Interestingly, on each occasion the vesicles in the bouton appeared to line up very closely at the presynaptic membrane around the spine.

These examples of spinelike projections into the boutons, and of perforated synapses, may indicate continued development and change of the synaptic surface of the boutons in Clarke's column. These observations suggest the interesting possibility of continuous modification of synaptic efficacy at the connections between primary afferent fibres and neurones in Clarke's column.

Myelination pattern of the collateral, and Nodal morphology.

Myelinated fibres in the central nervous system can be divided into 3 regions (for Reviews, see Waxman, 1972; Hirano and Dembitzer, 1978):
1) The *internodal region*, where the afferent is closely wrapped in spiral layers of myelin sheathing. Myelin sheathing in the CNS is provided by

oligodendrocytic cells, in the same manner as that provided by the Schwann cells of the peripheral nervous system (PNS). The internode is the non-excitable section of the afferent.

2). The *node*. Here the myelin sheathing is disrupted, leaving the axonal membrane bare, and exposed to the extracellular (perinodal) space. The node provides the basis for saltatory conduction in the central nervous system, and for synaptic specialization. Nodes were first described in the peripheral nervous system in 1874 by Ranvier, and later demonstrated in the central nervous system by Cajal (see Waxman, 1972 for review). The nodes of the CNS differ markedly from those of the PNS, and may exhibit varied geometry, even along the same collateral.

3) The *paranodal region* links the node and the internode. In the paranodal region, the myelin sheathing has been shown to undergo a helical process of unwinding, such that the outermost layers unwind last, and their termination at the axolemma is closer to the node than the termination of the innermost layers (Peters, 1966). Although the sheath unwinds in this region, the afferent is still completely enclosed by myelin, and isolated from the extracellular space.

Bodian and Taylor (1963) first indicated that the central nodes may be synaptically specialized. This has since been confirmed (e.g.Khattab, 1967; Sotelo and Palay, 1970; Waxman, 1970, Witkovsky, 1971), and is clearly illustrated by the examples presented in this chapter. Specialization of the node increases the surface area of the nodal membrane, and provides a site for synaptic transmission. All of the nodal regions examined in this chapter were synaptically specialized.

i). The Internode

Internode distances along the collateral presented in this chapter ranged from 40-80 μm in length. The diameter of the myelinated

collateral as it approached the first bouton was D = 1.5 μm, (d = 1.0 μm). At the point where the collateral lost its myelin sheath for the last time, the diameter D was 1.7 μm, d = 1.4 μm, which indicates that no overall tapering of the collateral occurred throughout its entire length.

ii). The Node.

Five examples of simple *en passant* boutons were presented in this chapter, either in longitudinal or cross section. The nodal gap incorporating these individual *en passant* boutons ranged from 2.3 - 2.7 μm. This gap was measured from the last terminating myelin layer on the proximal side of the node to the last terminating myelin layer on the distal side. In one case, the nodal gap was specialized to include 2 boutons, and in one case a string of 4 boutons were exhibited at a node as an *en passant* series. This nodal gap was 19.4 μm in length, and was the largest gap exhibited by this collateral. Waxman (1974) has noted that in the CNS, the nodal gap may range from < 1 μm, to > 8 μm. Apart from these examples of *en passant* boutons, every other case along this collateral can be described as a terminal heminode. This configuration occurs when the myelin unwinds and terminates, and the fibre then gives rise to an unmyelinated terminal branch. In each case examined, the terminal branch of the heminode gave rise to 1-5 boutons.

iii). The Paranode.

The internode and the node are linked by an intermediate region, the paranode, described by Ranvier as the site of attachment for the myelin sheath (in Wurtz and Ellisman, 1986). Here, the myelin, which forms a spiral sheath around the afferent unwinds in a helical, or corkscrew fashion, such that each successive turn overlaps and projects

past the lamellae inside it (Peters, 1966). Thus the innermost layers of the myelin sheath terminate furthest from the node.

In some of the examples presented in this chapter, the myelin layers can be seen terminating individually at the axolemma of the paranode, although this was not always clear. Studies have shown the presence of paranodal dense material around the afferent close to the node, and of banding across the paranodal zone, which runs perpendicular to the afferent. The perinodal material and banding are believed to result from the helical unwinding of the myelin in this region.

In this chapter, the dense strands of the perinodal matrix were often clearly visible. Examples of the paranodal banding were also observed. In longitudinal sections, the paranodal region was characterized by separation of the myelin sheathing from the afferent. The sheathing appeared to widen out and away from the afferent, as the fibre diameter narrowed down to a thin neck. This was particularly clear for those examples which were presented as a series in cross section through the node (*en passant* bouton). At the internode, the myelin sheathing was closely apposed to the axolemma. However, on approaching the paranode the afferent diameter (d) narrowed substantially. The myelin sheathing, which was quite intact at this point, maintained its diameter. This effectively created a gap between the axolemma and the inner layers of the myelin. In cross section, the paranodal region was again characterised by the presence of dense strands of perinodal material surrounding and contacting the fibre.

The reduction in size of the fibre diameter at the paranode was also noted by Moore et al. (1978). They termed it strangulation of the fibre, and sugested that the amount of strangulation was dependent on the fibre diameter. Reduction on the fibre diameter close to the node may be

related to ensuring propagation of the action potential into the nodal region, presumably due to a smaller amount of current required to depolarize the axon to firing threshhold. Moore et al. (1978) have shown that the reduction in diameter has no effect on the conduction velocity of the action potential, which is largely determined by internodal structure and length.

iv). Termination of the Myelin.

Examples have been shown in this chapter of the myelin sheathing and perinodal dense material terminating at, or on, the very edge of the bouton, both at the proximal and distal paranodal regions. In the case of the single *en passant* boutons, this leaves none of the afferent neck bare, and thus the bouton surface itself is the only true nodal membrane. In some cases, the collateral was seen to lose its myelin sheath, and then continue on for up to 7.2 μm before giving rise to a bouton. This was especially observed at the the six terminal heminodes examined, where the collateral lost its myelin sheath, and then continued, unmyelinated, before giving rise to a terminal series of 1-5 boutons. This termination of the sheath some distance from the bouton has the effect of presenting bare, axonal membrane to the extracellular space prior to the fibre diameter increase at the bouton.

v). The Nodal Membrane.

The node is specialized for ensuring the generation and conduction of the action potential, with conduction between nodes occurring in a saltatory manner. A number of studies suggest that generation of the action potential at the node is ensured by the local presence of voltage-activated sodium channels in the axonal membrane. Ritchie and Rogart (1977) used labelled saxitoxin and tetrodotoxin as markers for Na^+

channels, and concluded that in myelinated perpipheral fibres, the density of sodium channels was approximately 25/um^2 in internodal membrane, and 12,000/um^2 in nodal membrane. They also concluded that Na^+ channels were approximately 2 orders of magnitude more concentrated in nodal membrane of myelinated fibres than in the axolemma of unmyelinated fibres. Their findings therefore suggest that neither the internodal, nor the paranodal membrane exhibit a substantial degree of Na^+ channel concentration. Schrager (1987) has disputed this finding, suggesting that Na^+ channels are in fact present in internodal membrane, although he concurs that the concentration of Na^+ channels is higher in nodal membrane. The complimentary situation has been proposed for K^+ channels, which are apparently concentrated in internodal and paranodal regions, but not at the node (Chiu and Ritchie, 1981; see also review by Ritchie, 1986).

In an interesting study, Brigant and Mallart (1982) examined preterminal and terminal regions of the mouse motor end plate, using pharmacological techniques, and were able to show that the voltage-activated Na^+ channels were present in the preterminal, but not the terminal region. A complimentary situation existed for voltage-activated K^+ channels, which were present in the terminal, but not the preterminal region. Waxman and Wood (1984) have suggested that not only the number of Na^+ channels but also the distribution of these channels will influence conduction of an action potential, especially at a transition region (such as paranode/node, or preterminal/terminal).

In light of this evidence, an important question remains. Where, along the collateral, are the voltage activated Na^+ and K^+ channels, which are vital to the propagation of the action potential? It seems likely that for the single *en passant* boutons, the Na^+ channels may be concentrated solely on the surface of the bouton itself. In the situations where bridges of

nodal membrane extend from the bouton, particularly in the examples of the terminal heminodes, Na^+ channels could conceivably be located along this membrane. Brigant and Mallart (1982) proposed that relagation of the voltage-activated sodium channels to the preterminal region would leave more space in the terminal for cellular inclusions required for transmitter release. The existence of voltage-activated K^+ channels at the bouton membrane is also an important issue, since their presence will affect the amplitude and time course of the presynaptic action potential (Brigant and Mallart, 1982).

Modelling studies indicate that geometric variations of a fibre, particularly at a transition zone, are important in determining the amplitude and time course of an action potential (Revenko et al., 1973; Goldstein and Rall, 1974; Waxman and Wood, 1984)*. In turn, transmitter release from a synaptic bouton is influenced by the amplitude and duration of the presynaptic action potential (Katz and Miledi, 1968; see review by Martin, 1977). The study presented in this chapter has revealed considerable variation in the geometry and myelination pattern along the same identified, labelled Ia collateral. Of extreme importance now will be a determination of the location and density of the voltage-activated Na^+ and K^+ channels. Following the work of Ritchie and Rogart (1977) such a study is presumably feasible, for example, with the use of labelled toxin binding.

This knowledge, coupled with information on the ultrastructural morphology of the collateral, provided in the present study, will be extremely useful in describing the propagation of an action potential, its invasion of the synaptic boutons, and subsequently to our understanding of synaptic transmission between primary afferent fibres and neurones in Clarke's column of the spinal cord.

* see also: Stockbridge, N. and Stockbridge, L.L. (1988) J. Neurophysiology 59:1277-1285, and Stockbridge, N. (1988) J. Neurophysiology 59:1286-1295.

CHAPTER FIVE

GENERAL DISCUSSION

CHAPTER FIVE: GENERAL DISCUSSION

Morphology of DSCT Neurones in Clarke's column.

The results of two separate studies on the morphology of dorsal spinocerebellar tract neurones in Clarke's column have been presented and discussed in Chapter 3. Briefly, Golgi studies had originally suggested that the cells in Clarke's column giving rise to the dorsal spinocerebellar tract were large, with profuse dendritic trees oriented primarily in a rostrocaudal direction (Boehme, 1968; Loewy, 1970). Subsequent attempts to label DSCT neurones intracellularly with HRP had shown conflicting results (Randic et al., 1981; Houchin et al., 1983). In the present study, experiments were carried out in which cells receiving afferent input from the hindlimb were intracellularly identified, labelled with HRP, and reconstructed under the light microscope, both in sagittal and transverse sections of the spinal cord. A further example of a DSCT neurone receiving group I muscle afferent input from the hindlimb is illustrated in Figure 5.1 (reprinted from Appendix I). The general finding of this study was that, in accordance with Houchin et al. (1983), DSCT neurones which receive muscle afferent input have large cell bodies, and extremely complex dendritic trees which may extend approximately 3 mm in the rostrocaudal direction. In the transverse plane, the profusely tangled appearance of these dendritic trees was striking, as was their vast spread within Clarke's column. In addition, the dendrites of these cells were often found to extend well beyond Clarke's column in the lateral, ventral and dorsal directions.

A number of cells which received convergent (deep + cutaneous) input were also intracellularly labelled with HRP (Figs 3.15 and 3.16). These cells were shown to be of comparable size and complexity to the cells which received muscle afferent input. Throughout the course of

FIGURE 5.1

Reconstruction in the sagittal plane of a DSCT neurone in Clarke's column. This neurone received group I muscle afferent input from the hindlimb.

This figure is reprinted from Appendix I.


100 µm

these experiments, only 6 cells were encountered which received purely cutaneous input. One possible reason for this small sample size is that the majority of DSCT neurones which receive purely cutaneous input may, as suggested by Aoyama et al. (1973) and Tapper et al. (1975), be situated caudal or lateral to the Clarke's column boundary.

Randic et al. (1981) proposed that DSCT neurones which receive deep, cutaneous or convergent inpuy may exhibit differing morphologies. They showed DSCT neurones which receive convergent input to be smaller, and exhibit far less complex dendritic branches than DSCT neurones which receive muscle input. The present study has shown that DSCT neurones which receive convergent input may be as large as those which receive muscle input, with a similar complexity and rostrocaudal extent of the dendritic trees.

Due to considerable difficulties encountered in obtaining stable intracellular penetrations of DSCT neurones, the sample sizes of all labelling studies (including the present study) are quite small. However, the results of the present study do not support distinct morphological separation of the DSCT neurones in Clarke's column, based on afferent input.

Somatotopic arrangement of cell bodies in Clarke's column.

The question of somatotopic arrangement of DSCT neurones within Clarke's column was discussed in some detail in Chapters 1 and 3. Recent studies by Hongo and his colleagues (Hongo et al., 1982; Hongo, 1985) have suggested that DSCT neurones in Clarke's column are organized such that those receiving input from the toe muscles are located in the dorsomedial part of the column, those with input from the shank muscles in an intermediate region, and those cells receiving input

from the thigh muscles in the ventrolateral part of the column. Thus, a somatotopic organization appeared to be based on the proximity of the source of afferent input, which governed the region in which both the cell body, and the dendrites of DSCT neurones were situated.

In the present study, a number of DSCT cells which received group I muscle input from the ankle extensor muscles were labelled, and subsequently examined and reconstructed in transverse section. Six of these reconstructed DSCT neurones are repeated in Figure 5.2. These reconstructions indicate that DSCT neurones which receive group I input from ankle extensor muscles can be found throughout Clarke's column in transverse section. The dendrites of these neurones were found to spread throughout much of the column, often extending over 50% or more of the area of the column in transverse section. Not only did the dendrites spread to fill a large area within the column, they were often seen to spread well beyond it in dorsal, ventral and lateral directions. Interestingly, the terminations of ankle extensor muscle afferents have recently been found in comparable regions outside Clarke's column by Hongo et al. (1987). Thus, it seems likely that DSCT neurones may also receive synaptic input from primary afferents via those dendrites which extend beyond the boundary of Clarke's column.

Nevertheless, the results of the present study do not support a strict musculotopic localization of DSCT neurones (and their dendrites) within Clarke's column.

Topographic location of afferent terminations within Clarke's column.

Szentagothai (1961) suggested that the primary afferent terminations in Clarke's column might obey some form of topographic organization. He proposed that the afferent terminations of any one

FIGURE 5.2

Reconstructions in the transverse plane of 6 DSCT neurones in Clarke's column. Each of these cells received input from one or more of the ankle extensor muscles.

This figure is a composite, constructed from results presented in Chapter 3.

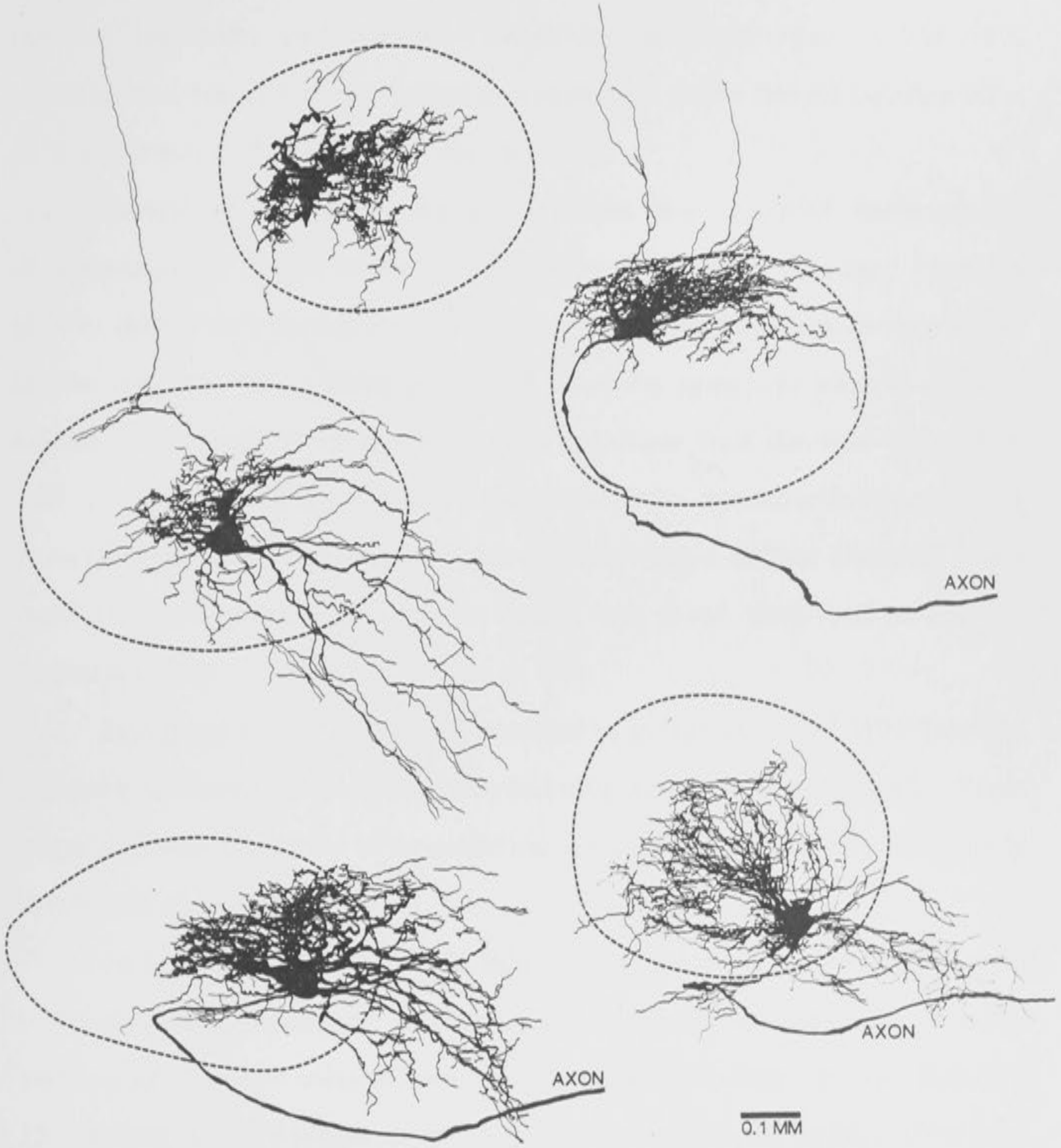
AXON
AXON
AXON
0.1 MM

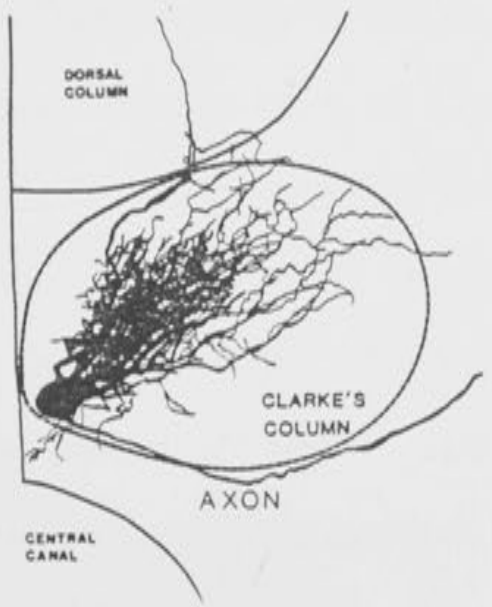
DORSAL COLUMN
CLARKE'S COLUMN
AXON
CENTRAL CANAL

collateral in the column were confined to a region which he described as a parallel oblique slice of the column, and that collaterals entered the column laterally, and travelled medially to termination. Collaterals entering the column more rostrally occupied a more lateral oblique slice of the column than those entering caudally.

Hongo et al. (1987) have proposed that a strict somatotopic organization of DSCT neurones in Clarke's column (Hongo, 1985) is closely linked to a topographic arrangement of the collateral terminations in the column. They have proposed that the group Ia and Ib muscle afferent collaterals from the hindlimb terminate in 4 discrete regions in and close to Clarke's column, and that the termination region is prescribed by the proximity of the muscle of origin of that afferent. The 4 termination regions appear to be similar to those described earlier by Rethelyi (1968).

Hongo et al. (1987) have illustrated reconstructions of HRP labelled primary afferent collaterals terminating in Clarke's column. These suggest discrete regions of termination for muscle afferents of toe, shank, thigh and hip origin.

In a recent transganglionic labelling study, Mense and Craig (1988) have shown terminals of gastrocnemius/soleus muscles in the medial portion of Clarke's column throughout its rostrocaudal length. Figs. 12, 13, 16 and 17 of Hongo et al. (1987) show collateral ramification and termination patterns for group Ia and Ib afferents of shank muscle origin spreading throughout most of the transverse area of Clarke's column. This does not seem to suggest such a strict topographic location of these afferents. Instead, this finding correlates well with the results presented in Chapter 3, which demonstrate that the cell bodies and dendritic trees of DSCT neurones receiving ankle extensor input can be situated throughout most of Clarke's column in transverse section. However, the

study of Hongo et al. (1987) suggests that the afferent terminations of toe and thigh muscles occupy a much more restricted area of Clarke's column than those of shank muscles.

The extensive spread of the dendrites of DSCT neurones illustrated in Chapter 3 (and see Fig. 5.1), suggests that an individual neurone may receive synaptic contacts throughout a large area of Clarke's column, and in many cases from beyond it. Terminations of hindlimb afferents have also been shown in regions lateral and ventrolateral to Clarke's column (Rethelyi, 1968; Hongo et al., 1987). The spread of DSCT neurone dendrites beyond Clarke's column, particularly in the lateral and ventrolateral directions, suggests that DSCT neurones with cell bodies inside Clarke's column may well receive synaptic contacts from afferents terminating outside Clarke's column. These contacts may even include the giant boutons (> 7 μm) described by Hongo et al. (1987) outside Clarke's column.

Future experiments, in which both an afferent fibre and its contacts with a DSCT neurone are visualised with HRP, will be very useful in clarifying this issue. Such results have been obtained previously in studies at the Ia fibre-motoneurone connection (Burke et al., 1979, 1981; Brown and Fyffe, 1981; Redman and Walmsley, 1983a,b). However, these experiments have proven to be extremely difficult in Clarke's column, although one successful result has been achieved during the present study. Results from this experiment are presented in the ultrastructural studies of Appendices I and II (see also Figs. 5.5 and 5.6).

Identified Afferent Boutons in Clarke's column.

i) Giant Boutons.

Giant boutons were first recognized in Clarke's column by Szentagothai and Albert (1955) during degeneration studies. Subsequent

ultrastructural observations found these boutons to be up to 10 μm in length, and to contain multiple sites for transmitter release (Rethelyi, 1970). Giant boutons, up to 25 μm in length have also been reported in Clarke's column (Saito, 1974).

Tracey and Walmsley (1984), first examined identified afferent terminations in Clarke's column under the light microscope, and demonstrated that giant boutons could arise from both Ia and Ib muscle afferents. They also showed that giant boutons could be of terminal or *en passant* types. Prior to the present studies, no examination of the ultrastucture of identified giant boutons in Clarke's column has been carried out.

Hongo et al. (1987) suggested that boutons over 7 μm in length be classified as giant boutons. On the basis of this classification, 3 of the 35 boutons recognized on the identified Ia afferent collateral presented in Chapter 4 were classified as giant boutons. These giant boutons measured 8.3 x 2.1 μm, 9.0 x 2.2 μm, and 9.2 x 3.1 μm in size.

During the course of the present experimental series, a number of much larger identified giant boutons have also been examined under the electron microscope. Figure 5.3 shows an HRP labelled giant bouton, over 20 μm long, which arose from an identified Ia afferent in Clarke's column. Fig. 5.3B shows the bouton as it appeared in a single sagittal section of the spinal cord, under the light microscope. This bouton was subsequently prepared for electron microscopy, and Fig. 5.3A shows a single electron micrograph of the bouton. Many of the characteristic features exhibited by other Ia boutons were also exhibited by this giant bouton, notably extremely close packaging of the synaptic vesicles and mitochondria.

A second serially sectioned giant bouton is presented in the sequence of three photomicrographs in Fig. 5.4. This bouton also arose

FIGURE 5.3

HRP labelled giant bouton. This bouton arose from an identified Ia afferent collateral in Clarke's column, and was over 20 μm in length.

A. Electron micrograph of the giant bouton showing dark HRP labelling, and closely packaged vesicles and mitochondria.

B. This photomicrograph shows the giant bouton as it appeared in a 100 μm thick sagittal section under the light microscope.

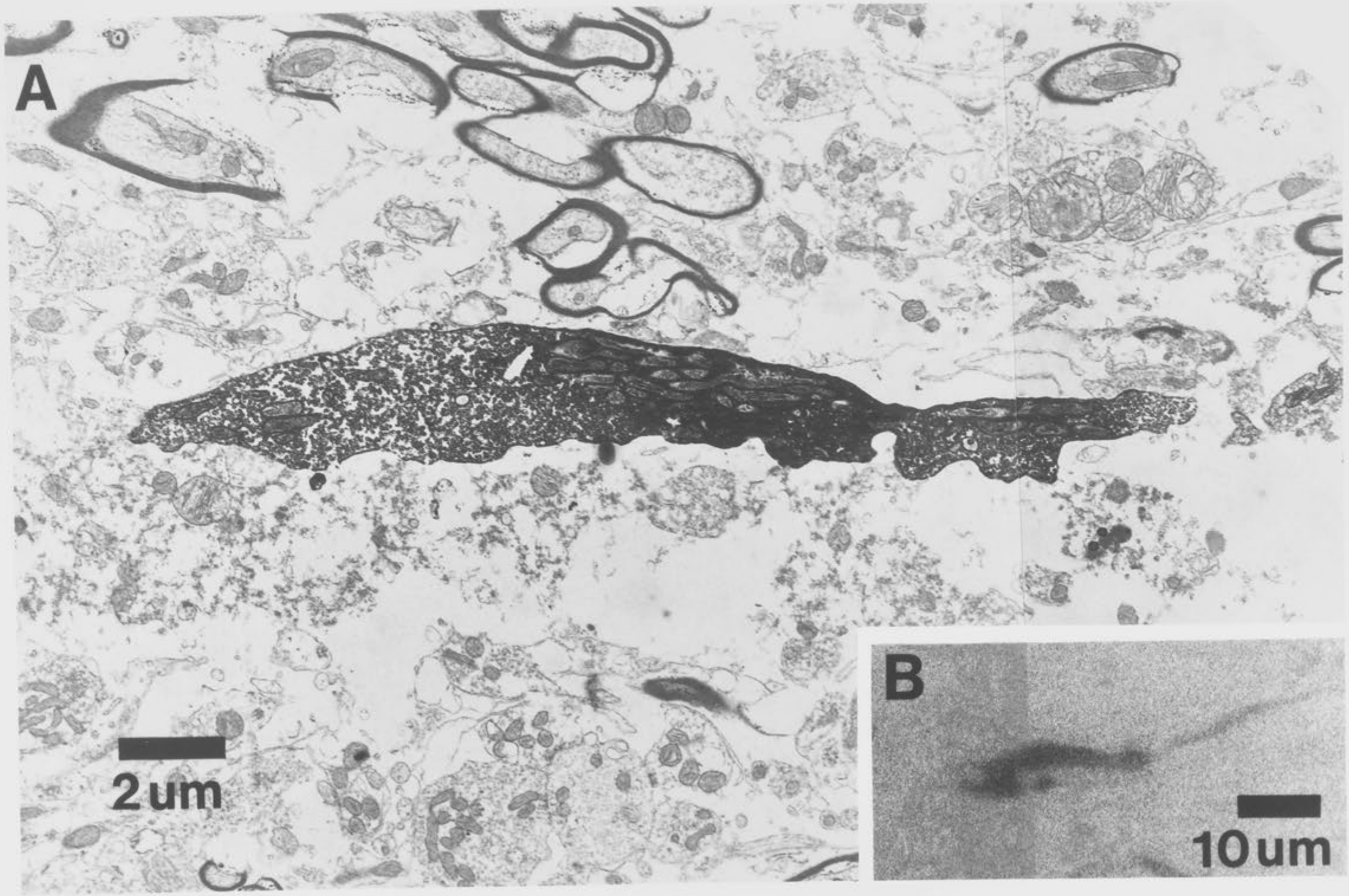
A
2um
B
10um

FIGURE 5.4

The giant bouton presented in this series of three photomicrographs arose from an identified Ia collateral fibre in Clarke's column. This is an example of a terminal bouton which reached 14 μm in length.

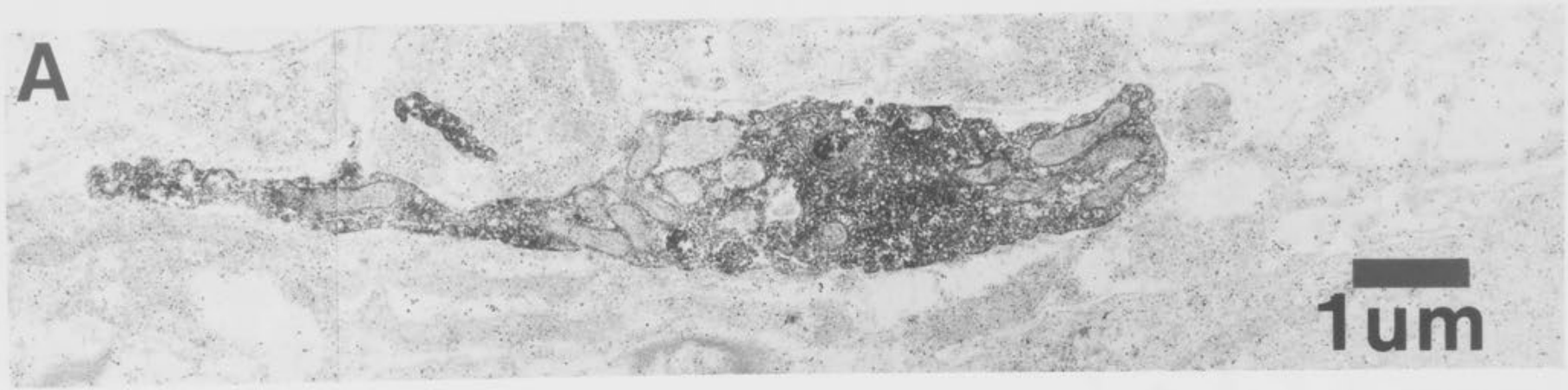
A
1um


B

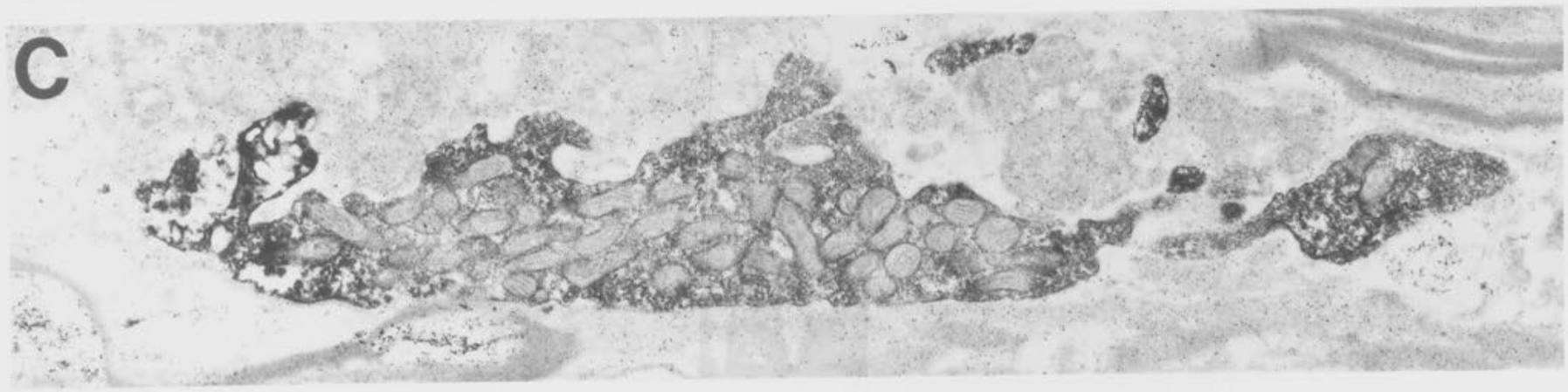
C

from a labelled Ia afferent collateral in Clarke's column, and was an example of a terminal giant bouton, 14 μm in length.

Saito (1974) described 3 different types of giant boutons making synaptic contact with Clarke's column cells. The first, elongated giant boutons with spherical (S) vesicles, appears to correspond to the two giant boutons presented in this chapter as Figs. 5.3 and 5.4. The second type of giant bouton described by Saito (1974) were elongated boutons with flattened (F) vesicles. The third type, the "club giant" boutons, described as having a contact length of 4-7.5 μm, appears to be similar to the large Ia boutons described in Chapter 4.

The existence of the giant boutons in Clarke's column has drawn attention to the fact that these boutons may contain multiple synaptic specializations (Rethelyi, 1970; Tracey and Walmsley, 1984). The present study has further demonstrated that even the smallest Ia boutons in Clarke's column may contain multiple synaptic specializations (see Chapter 4).

Such ultrastructural evidence on the existence of multiple sites for transmitter release within the same synaptic bouton provides further valuable evidence for studies on synaptic transmission at the connection between primary afferent fibres and DSCT neurones (Tracey and Walmsley, 1984; Walmsley et al., 1987,1988).

ii). Presynaptic boutons.

Subsequent to the discovery of giant boutons in Clarke's column, was the finding that they were often associated with small, presumably presynaptic boutons (Rethelyi, 1970; Saito, 1974, 1979; Houchin et al., 1983, and Appendix II). In accordance with previous suggestions (Gray, 1962), these boutons were proposed as the morphological correlate of presynaptic inhibition in Clarke's column. Presynaptic boutons in the

column are not, however, confined to contacts with giant boutons. They have been found to contact even small boutons presynaptically (see Chapter 4, and Appendix II). This is similar to the situation described at Ia muscle afferent contacts on motoneurones (Conradi et al., 1983; Fyffe and Light, 1984).

During the course of this study, a paper has been published in the Journal of Neuroscience detailing observations on presynaptic boutons in Clarke's column (see Appendix II), and a full discussion of the implications of this study is presented there.

The studies contained in Appendices I and II involved analysis of serial sections through 6 identified Ib, and 14 identified Ia afferent boutons in Clarke's column. Of the 6 Ib boutons, 5 were found to receive presynaptic connections from small, unlabelled boutons. In contrast, only one of the 14 Ia boutons was found to receive a presynaptic contact. Three of the serial sections through this bouton are shown in Fig. 5.5. In this experiment, both the presynaptic Ia bouton and the postsynaptic DSCT neurone were positively identified and labelled with HRP. This result is therefore unique in the study of afferent synaptic connections in Clarke's column. In Fig. 5.6 a single section through the labelled Ia bouton and labelled dendrite is shown at higher magnification. Below the micrograph is a schematic diagram and a serial reconstruction of the Ia bouton, the presynaptic bouton, and the dendrite as they appeared in serial sections.

In the study presented in Chapter 4, 3 of the 35 serially examined Ia boutons were shown to be contacted in a similar presynaptic manner. In total, this indicated that approximately 9% of the Ia boutons exhibited such a presynaptic contact, compared with approximately 80% of the Ib boutons. This is in accordance with other reports which have suggested that, in Clarke's column, Ib afferents are more likely to be subjected to

FIGURE 5.5

These photomicrographs show a sequence of sections through an identified HRP labelled plantaris Ia bouton which can be seen contacting a small, spine-like protrusion of an identified, HRP labelled DSCT neurone in Clarke's column. The labelled bouton is, in turn, contacted by a small, unlabelled presynaptic bouton, marked P in the second micrograph.

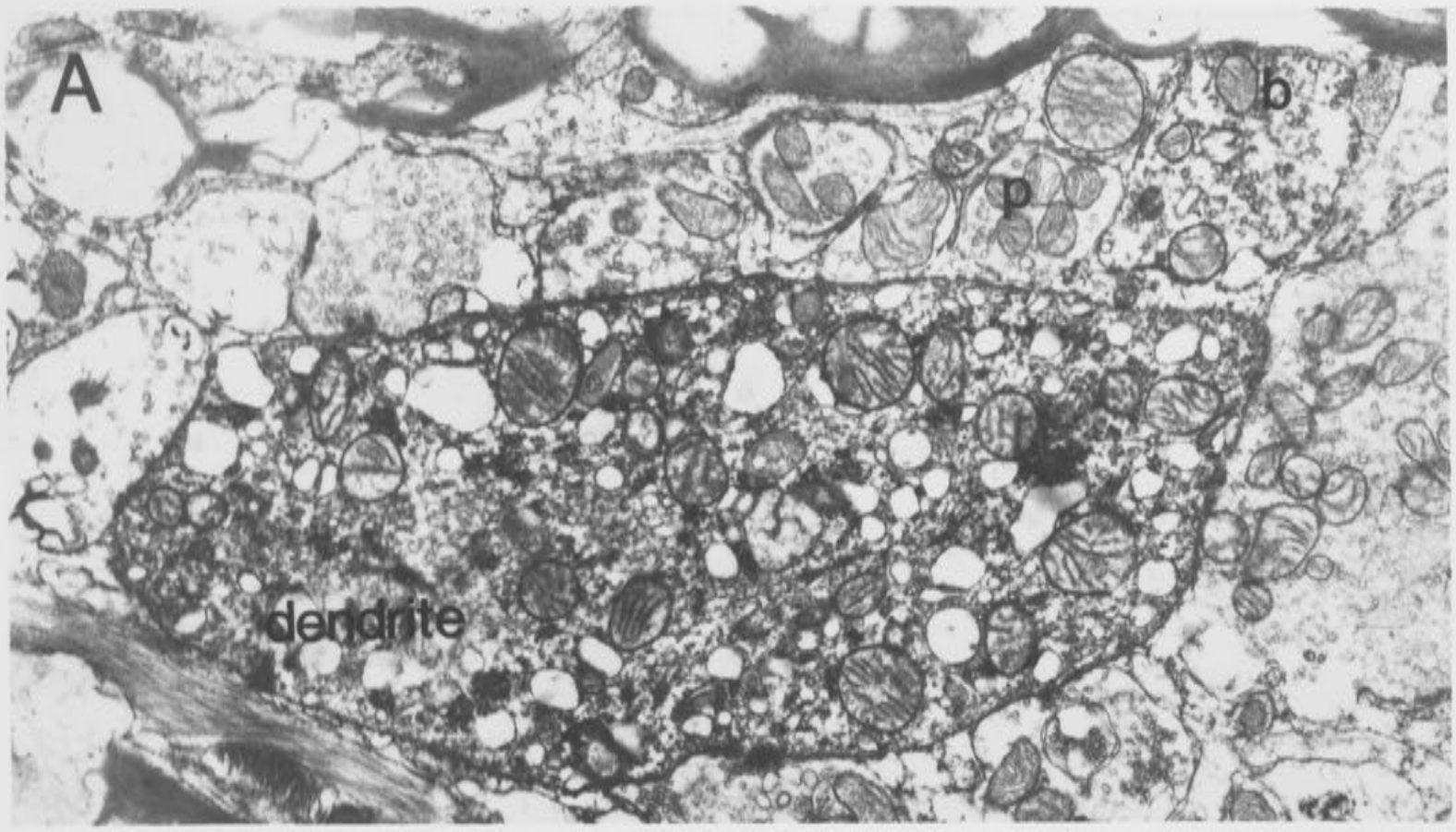
A
b
p
dendrite

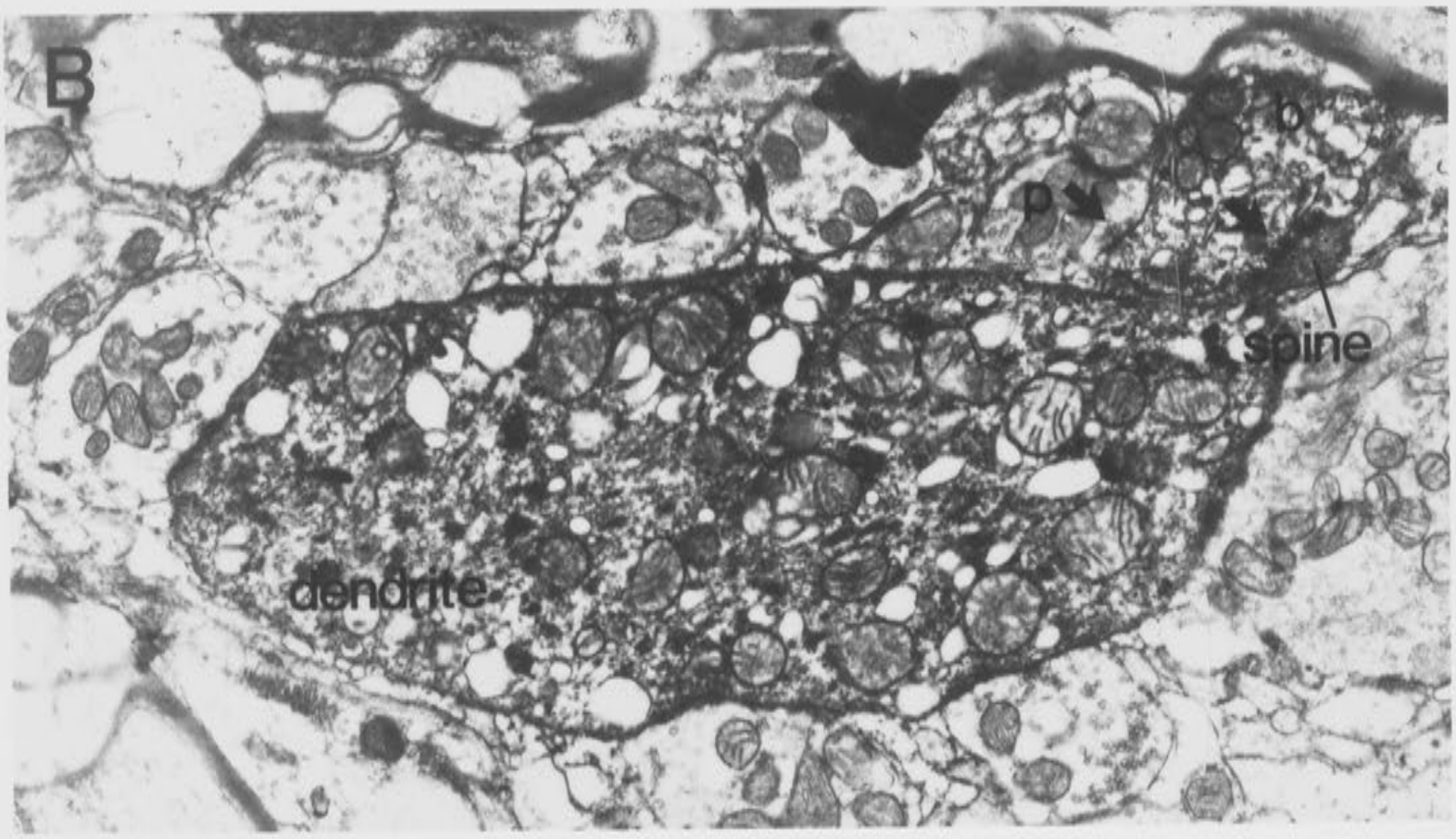
B
b
p
spine
dendrite

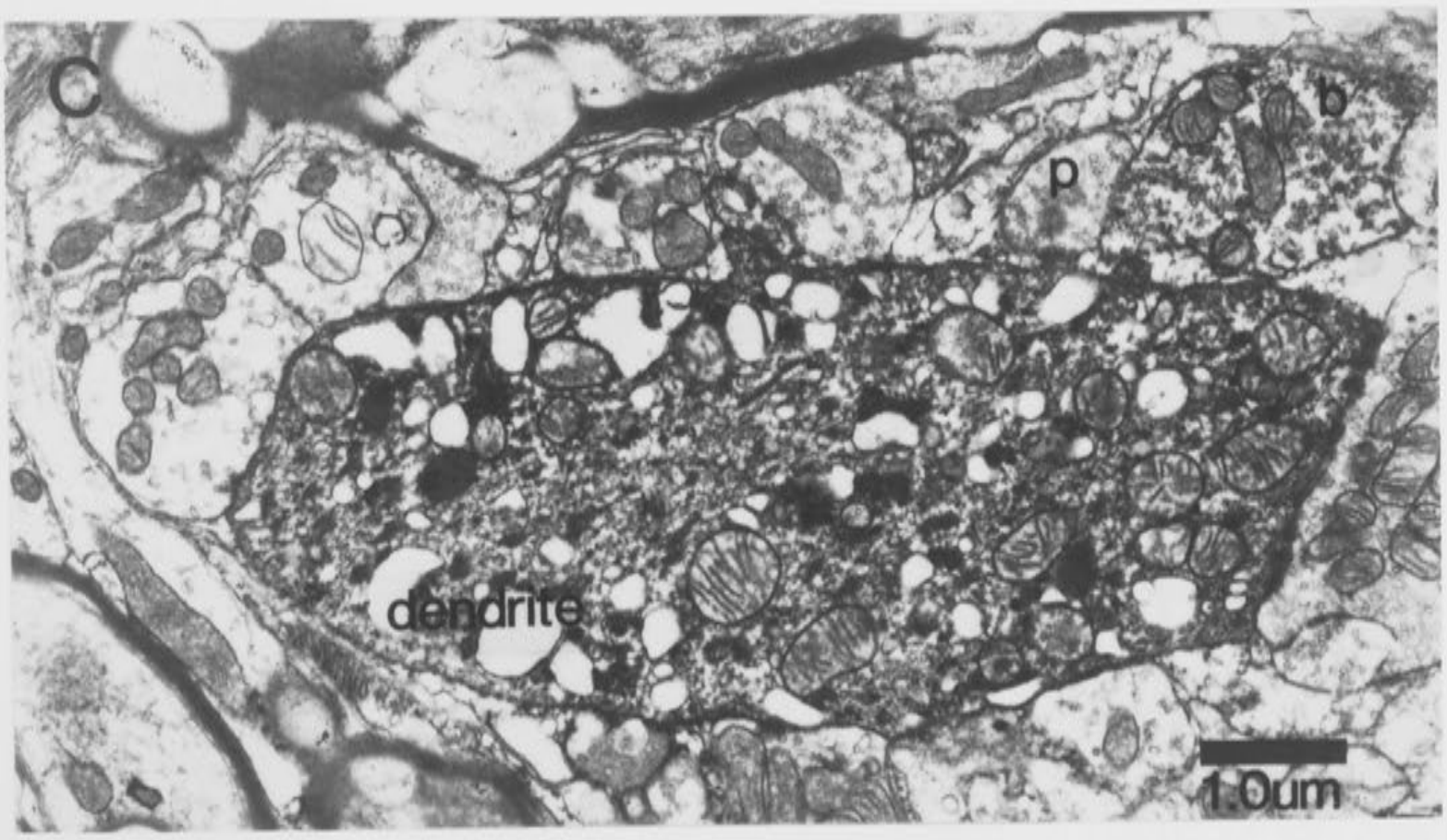
C
b
p
dendrite
1.0um

FIGURE 5.6

A. Higher magnification photomicrograph of one of the sections through the HRP labelled Ia bouton and the HRP labelled DSCT neurone dendrite presented in Figure 5.5.

B and C. Schematic reconstructions of the HRP labelled Ia afferent bouton contacting a spine-like protrusion of the DSCT neurone. The small, unlabelled presynaptic bouton is also indicated on these schematic drawings.

A

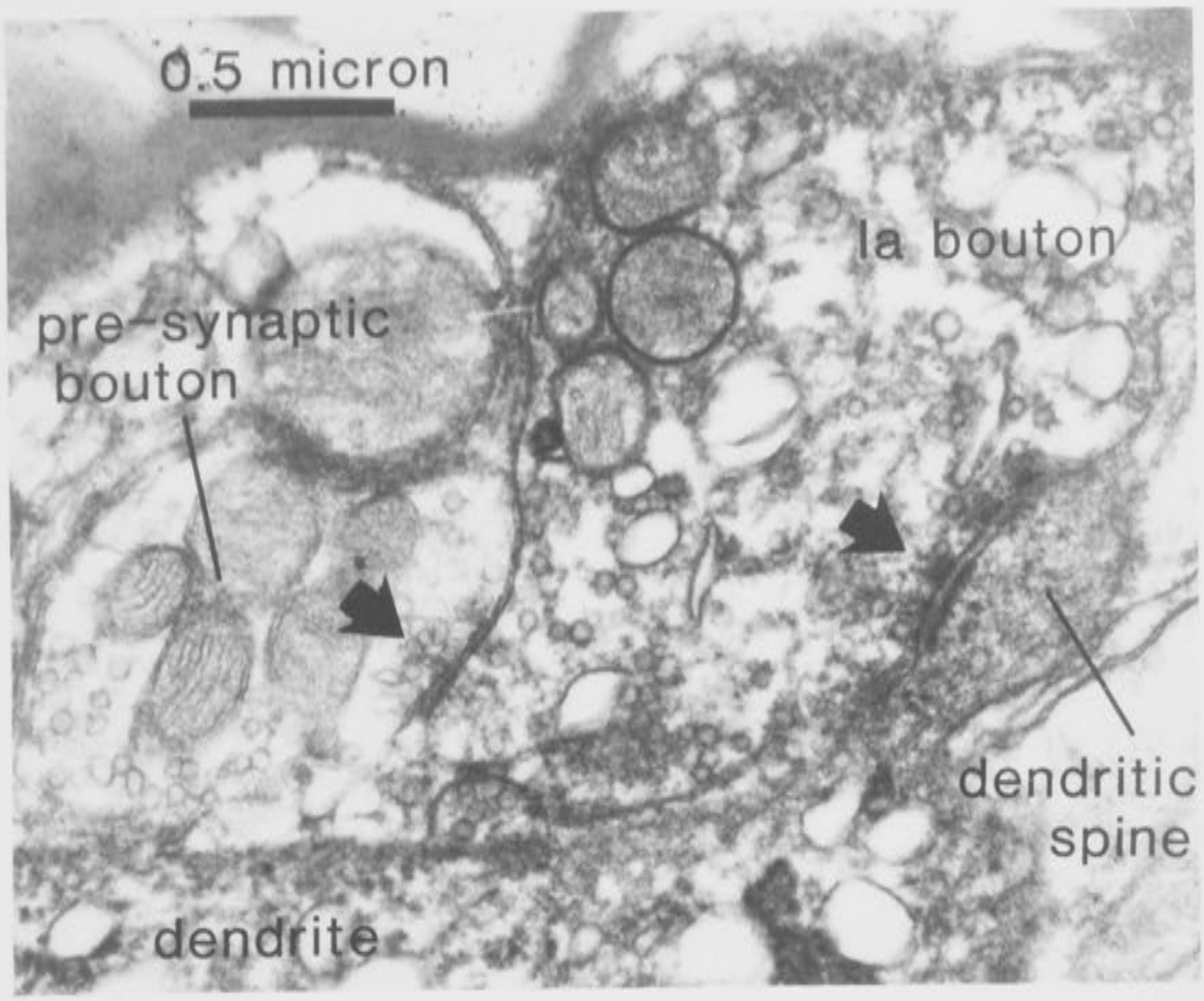

B

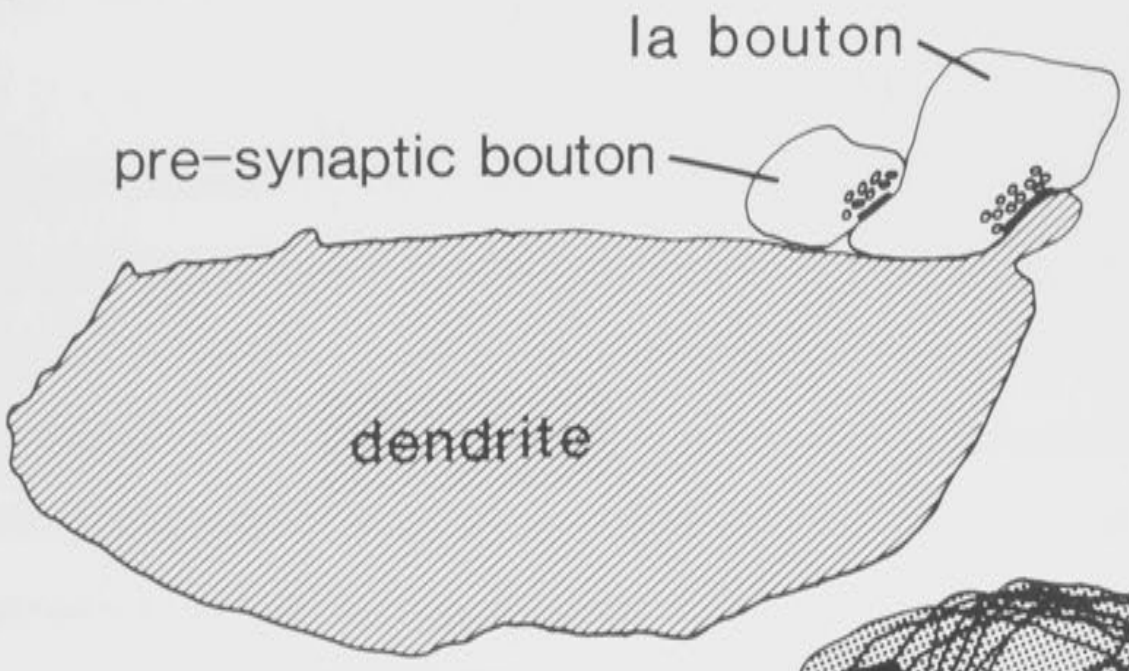

C

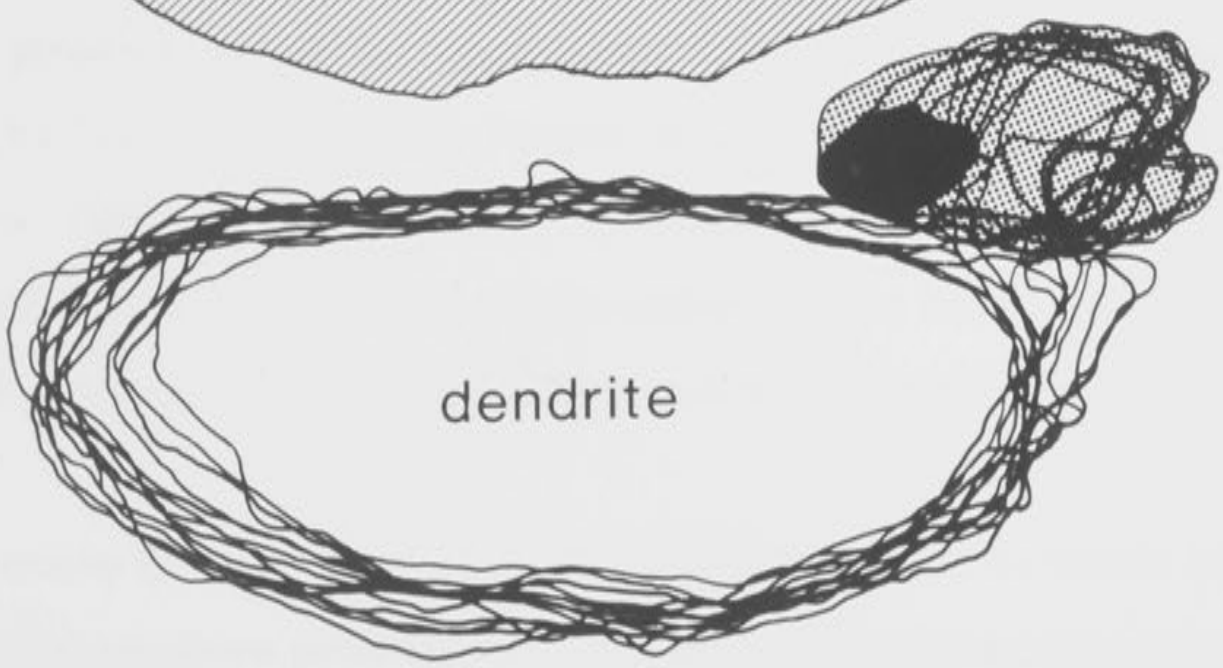

1.0 micron

presynaptic inhibition than Ia afferents (Jankowska et al., 1965, Hongo and Okada, 1967).

The results in Chapter 4 also concur with those presented in Appendix II, that boutons arising from the same Ia fibre do not necessarily all receive presynaptic contacts. In addition, the study presented in Appendix II demonstrates that not all boutons arising from the same Ia fibre and contacting the same postsynaptic DSCT neurone, receive presynaptic contacts. This implies that presynaptic inhibition may operate by selectively supressing synaptic transmission at only a proportion of the contacts arising from a single afferent fibre. (This hypothesis has also been suggested by the results of physiological experiments on the connection between single Ia fibres and motoneurones, Clements et al., 1987).

iii) Synaptic specializations.

Synaptic specializations, which are regarded as the active regions or transmitter release sites of boutons, are recognized ultrastructurally by the presence of vesicle accumulation at the presynaptic membrane, thickening of the postsynaptic membrane, dense material in the synaptic cleft and the presence of pre- and post-synaptic electron-dense material (see reviews by Szentagothai, 1970; Heuser and Reese, 1977; and Smith and Augustine, 1988). Determination of the morphological details of the synaptic specialization is important to our understanding of the synaptic events which accompany neurotransmitter release from a synaptic terminal.

Observations of synaptic specializations at identified Ia terminals in Clarke's column have been presented in Chapter 4. One of the interesting observations made in Chapter 4 was that, although the vesicles were often seen to cluster at the presynaptic site, a second configuration was also

observed, in which the vesicles appeared to line up in neat parallel rows against the presynaptic membrane. Strict organization of the synaptic surface has been associated with a regular array of dense projections from the presynaptic membrane, coupled with the presence of microtubules at the active zone, forming a presynaptic grid (Gray, 1963; Akert et al., 1972; Pfenniger et al., 1972; Gray, 1983; Westrum and Gray, 1986). The dense projections appear to organize the synaptic vesicles within the grid (Gray, 1983; Westrum and Gray, 1986). Triller and Korn (1982) have proposed that the size of the presynaptic grid may relate to efficiency of transmitter release. In fact, supporting evidence for a relationship between the morphology of the active zone and synaptic transmission has been described at a number of connections (see review by Akert, 1973). Furthermore, development and change in the morphology of the active synaptic zone have been implicated in modification of synaptic transmission (e.g. Herrera et al., 1985; Siekevitz, 1985; Chiang and Govind, 1986; see review by Atwood and Wojtowicz, 1986).

Perforated and irregular shaped synaptic specializations have been described as an indication that a synapse is undergoing change or development (Cohen and Siekevitz,1978; Carlin and Siekevitz, 1983; Nieto-Sampedri et al., 1983; Dyson and Jones, 1984; Calverley and Jones, 1987). The present studies have shown that perforated synapses may exist in the boutons arising from identified group Ia afferent fibres in Clarke's column (see Chapter 4 and Appendix I). This suggests possible plasticity of the bouton surface at Ia synapses, and associated modification of transmitter release.

Finally, it is interesting to speculate that the giant boutons of Clarke's column, characterized by the presence of multiple transmitter release sites, may be a manifestation of the exuberant growth, development and division of their synaptic specializations.

Axonal and Nodal Morphology

The importance of the structural features of axons and their relevance to the conduction of a presynaptic action potential has been emphasised in many previous studies (e.g. Revenko et al., 1973; Goldstein and Rall, 1974; Moore et al., 1978; Waxman and Wood, 1978; Parnas and Segev, 1979; Franciolini, 1987; see also review by Swadlow et al., 1980).

The results presented in this thesis have provided valuable information on the axonal morphology of an identified, labelled afferent in the spinal cord, and the implications of this have been discussed in Chapter 4.

In summary, a wide variety of axonal geometries was observed along an individual Ia collateral. The collateral exhibited nodes specialized with a single *en passant* bouton, nodes specialized to include a series of *en passant* boutons, and terminal heminodes, without myelination. In each case a paranodal region was observed over which the myelin sheathing was lost, giving rise to a node. Paranodal regions were examined in longitudinal and cross section, and were seen to exhibit the characteristic features associated with the unwinding of the myelin sheath.

In some examples, the myelin sheathing was seen to come right to the very edge of the bouton. In other cases, the myelin layers terminated some distance from the bouton, exposing a length of the axolemma as nodal membrane. These observations raise interesting questions concerning the location of the voltage-activated channels underlying the action potential. Previous studies have suggested that the voltage-activated Na^+ channels are situated almost exclusively in nodal membrane (Ritchie and Rogart, 1977, Ritchie 1986; see also Brigant and Mallart, 1982). If this were the case, then in the examples where the

myelin extends right to the edge of the bouton, the voltage-activated Na^+ channels must reside in the bouton membrane itself. In the alternative situation, where bridges of unmyelinated fibre join, or give rise to boutons, Na^+ channels may be restricted to the preterminal membrane, as described for the mouse motor end plate (Brigant and Mallart, 1982). Brigant and Mallart suggested that confining the voltage-activated Na^+ channels to the preterminal membrane would leave more room for synaptic specialization at the bouton. It will be of great interest to obtain information on the location of the channels underlying the action potential so that this can be related to these two alternative strategies for myelin disruption along an axon in the CNS.

All nodes arising from the labelled Ia afferent collateral in Clarke's column presented in Chapter 4 were specialized for synaptic transmission. A further example of a synaptically specialized node is presented in Fig. 5.7. The montage in Fig. 5.7A shows the paranodal region on the left giving rise to a bouton which contains many synaptic vesicles. The fibre then remyelinates on the right of the bouton. As decribed previously, the fibre diameter is markedly reduced in the paranodal regions, and in this example the individual layers of myelin can be seen terminating along the axolemma in the paranodal region, causing it to exhibit a scalloped appearance. This is shown more clearly at higher magnification in Fig. 5.7B.

During the course of these experiments, one example of a non-synaptically specialized node arising from an identified Ia afferent in Clarke's column was observed. A sequence of the serial sections examined through this node is presented in Fig. 5.8. Figure 5.8A shows the closely sheathed internodal region giving rise to the paranode, which is illustrated in Fig. 5.8B and C. The region of the node itself is shown in Fig.

FIGURE 5.7

A. Montage showing a synaptically specialized node in Clarke's column. This node arises from an identified Ia afferent collateral.

B. A single section through the nodal bouton presented in A, shown at higher magnification. The myelin layers can be seen terminating at the axolemma in the paranodal region, causing it to exhibit a scalloped appearance.


A
1um


B
1um

FIGURE 5.8

A selected sequence of serial sections examined through a non-synaptically specialized node in Clarke's column which arose from an identified, HRP labelled Ia afferent collateral.

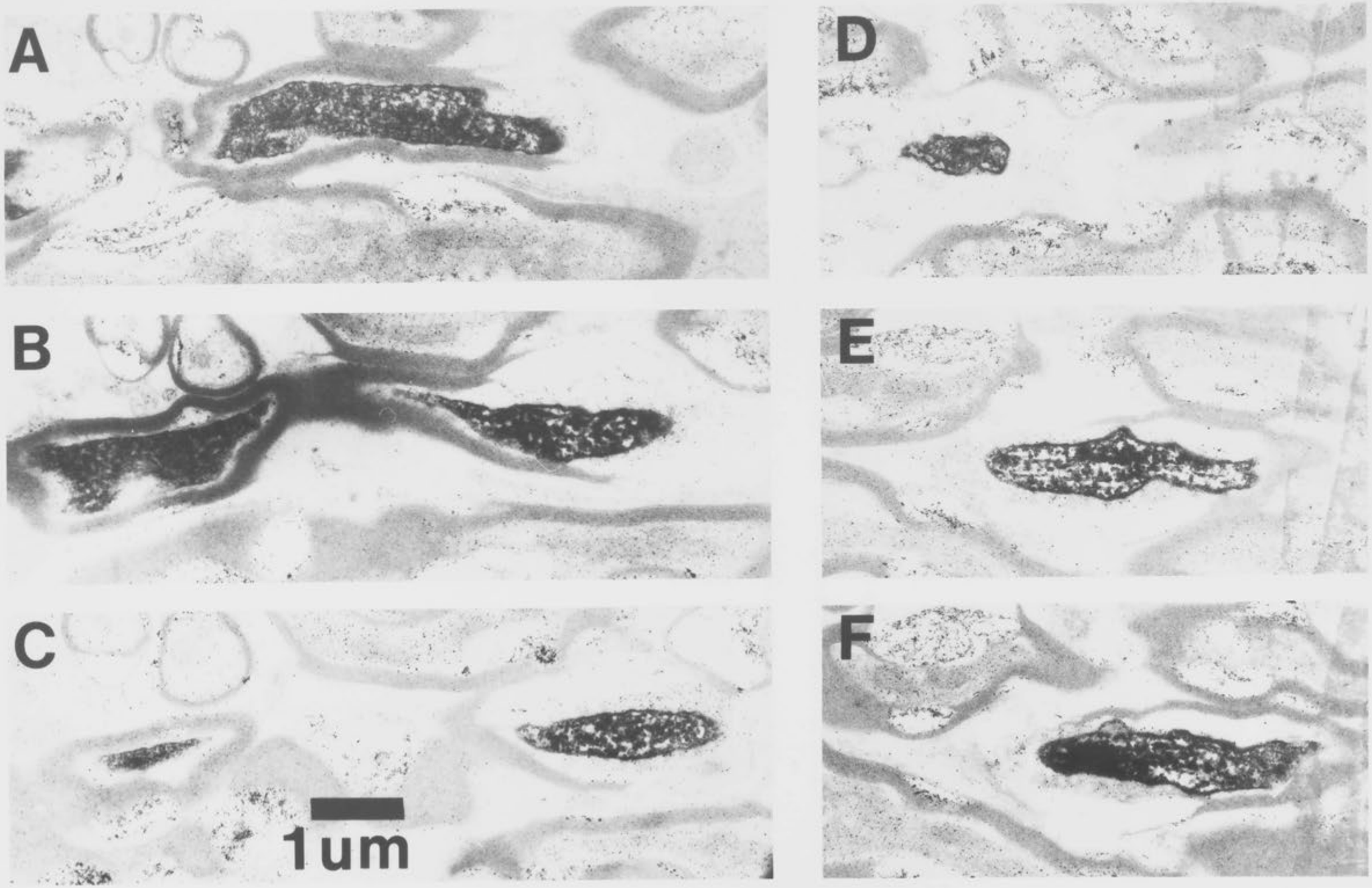
A
B
C
D
E
F
1 um

5.8D. No bouton-like swelling, vesicles or mitochondria are present. Remyelination of the fibre is seen in Fig. 5.8E and F.

Nodal geometry, as examined in the study presented in Chapter 4, was shown to differ from node to node, even along the same collateral. In summary, four nodal configurations have been determined for identified Ia afferent fibres in the present studies: 1) a single *en passant* bouton, 2) a series of boutons in the nodal gap, 3) a terminal heminode exhibiting single or multiple boutons, and 4) non-synaptically specialized node. Again the question is raised: with a number of alternative strategies available for loss of myelin, even along an individual collateral, how are the channels underlying the action potential distributed along the fibre?

A knowledge of the location of the voltage-activated channels, combined with the ultrastructural details of an afferent fibre, including its varying geometry, will greatly aid our understanding of the conduction of the presynaptic action potential, and subsequently of transmitter release.

In conclusion, the experimental studies presented in this thesis have emphasized the importance of structural, and particularly ultrastructural, observations to our understanding of synaptic connectivity in the nervous system.

REFERENCES

REFERENCES

Adams, J.C. (1977) Technical considerations on the use of horseradish peroxidase as a neuronal marker. Neuroscience 2:141-145

Adams, J.C. (1981) Heavy metal intensification of DAB based HRP reaction product. J. Histochem. Cytochem. 29:775

Akert, K. (1973) Dynamic aspects of synaptic ultrastructure. Brain Res. 49:511-518

Akert, K., Pfenniger, K., Sandri, C and Moor, H. (1972) Freeze etching and cytochemistry of vesicles and membrane complexes in synapses of the CNS. In Structure and Function of Synapses. Pappas, G.D. and Purpura, D.P. (eds.) Raven Press, N.Y. pp 67-86

Allbright, B.C. and Haines, D.E. (1973) The morphology of Clarke's column in the lesser bushbaby (*Galago senegalensis*). Brain, Behav. Evol. 8:165-190

Aoyama, M. Hongo, T. and Kudo, N. (1973) An uncrossed ascending tract originating from below Clarke's column and conveying group I impulses from the hindlimb muscles in the cat. Brain Res. 62:237-241

Atwood, H.L. and Wojtowicz, J.M. (1986) Short-term and long-term plasticity and physiological differentiation of crustacean motor synapses. Int. Rev. Neurobiol. 28:275-362

Berthold, C-H. (1978) Morphology of normal peripheral axons. In: Physiology and Pathobiology of Axons. Waxman, S.G. (ed.) Raven Press, N.Y.

Bodian, D. and Taylor, N. (1963) Synapse arising at a central node of Ranvier, and Note on fixation of the central nervous system. Science 139:330-332

Boehme, C.C. (1968) The neural structure of Clarke's nucleus of the spinal cord. J.Comp.Neurol. 132:445-462

Brodal, A. and Rexed, B. (1953) Spinal afferents to the lateral cervical nucleus in the cat. J. Comp. Neurol. 98:179-212

Brodal., A. and Grant, G. (1962) Morphology and temporal course of degeneration in cerebellar mossy fibers following transection of spinocerebellar tracts in the cat. Exp. Neurol. 5:67-87

Brigant, J.L. and Mallart A. (1982) Presynaptic currents in mouse motor endings. J. Physiol. 333:619-636

Brown, A.G. and Fyffe, R.E.W. (1978) The morphology of group Ia afferent fibre collaterals in the spinal cord of the cat. J. Physiol. 274:119-127

Brown, A.G. and Fyffe, R.E.W. (1981) Direct observations on the contacts made between Ia afferent fibres and alpha motoneurones in the cat's lumbosacral spinal cord.

Brown, A.G. and Iggo, A. (1967) A quantitative study of cutaneous receptors and afferent fibres in the cat and rabbit. J. Physiol. 193:707-733

Burke, R.E. and Rudomin, P. (1977) Spinal neurones and synapses. In: Handbook of Physiology, The Nervous System I. Kandel, E.R. (ed.) American Physiological Society, Washington D.C. pp 877-944

Burke, R.E., Walmsley, B. and Hodgson, J.A. (1979) HRP anatomy of group Ia afferent contacts on alpha motoneurones. Brain Res. 160:347-352

Burke, R.E., Walmsley, B. and Hodgson, J. A. (1981) Structural-functional relationships in monosynaptic action on spinal motoneurones. In: Integration in the Nervous System. Asanuma, H. and Wilson, V. (eds.), Igaku-Shoin, Tokyo-New York

Calverley, R.K.S. and Jones, D.G. (1987) A serial-section study of perforated synapses in rat neocortex. Cell Tissue Res. 247:565-572

Carlin, R.K. and Siekevitz (1983) Plasticity in the central nervous system: Do synapses divide? Proc. Natl. Acad. Sci. USA 80:3517-3521

Chang, H.T. (1951) Caudal extension of Clarke's column in the spider monkey. J.Comp.Neurol. 95:43-51

Chen, D.H., Chambers, W.W. and Liu, C.N. (1977) Synaptic displacement in intracentral neurons of Clarke's nucleus following axotomy in the cat. Exp. Neurol. 57:1026-1041

Chiang, R.G. and Govind, C.K. (1986) Reorganization of synaptic ultrastructure at facilitated lobster neuromuscular terminals. J. Neurocyt. 15:63-74

Chiu, S.Y. and Ritchie, J.M. (1981) Evidence for the presence of potassium channels in the paranodal region of acutely demyelinated mammalian single nerve fibres. J. Physiol. 313:415-437

Clarke, J. (1851) Researches into the structure of the spinal cord. Philos. Trans. Roy. Soc. 1:607-621

Clarke, J. (1859) Further researches on the gray substance of the spinal cord. Philos. Trans. Roy. Soc. 149:437-467

Clements, J.D., Forsythe, I.D. and Redman, S.J. (1987) Presynaptic inhibition of synaptic potentials evoked in cat spinal motoneurones by impulses in single group Ia axons. J. Physiol. 383:153-169

Cohen, R.S. and Siekevitz, P. (1978) Form of the post-synaptic density. A serial section study. J. Cell. Bio. 78:36-46

Conradi, S. (1969) Ultrastructure of dorsal root boutons on lumbosacral motoneurones of the adult cat, as revealed by dorsal root section. Acta physiol. scand. Suppl. 332:85-115

Conradi, S., Cullheim, S., Gollvik, L. and Kellerth, J-O. (1983) Electron microscopic observations on the synaptic contacts of group Ia muscle spindle afferents in the cat lumbosacral spinal cord. Brain Res. 265:31-39

Curtis, D.R., Eccles, J.C. and Lundberg, A. (1958) Intracellular recording from cells in Clarke's column. Acta physiol. scand. 43:303-314

Dyson, S.E. and Jones, D.G. (1984) Junction differentiation and splitting as a mechanism for modifying connectivity. Dev. Brain res. 13:125-137

Eccles, J.C., Schmidt, R.F. and Willis, W.D. (1963) Inhibition of discharges onto the dorsal and ventral spinocerebellar tracts. J. Neurophysiol. 26:635-645

Egger, M.D. and Egger, L.D. (1982) Quantitative morphological analysis of spinal motoneurones. Brain Res. 253:19-30

Franciolini, F. (1987) Spontaneous firing and myelination of very small axons. J. theor. Biol. 128:127-134

Fyffe, R.E.W. and Light, A.R. (1984) The ultrastructure of group Ia afferent fiber synapses in the lumbosacral spinal cord of the cat. Brain Res. 300:201-209

Goldstein, S.S. and Rall, W. (1974) Changes of action potential shape and velocity for changing core conductor geometry. Biophys. J. 14:731-757

Grant, G. (1962) Spinal course and somatotopically localized termination of the spinocerebellar tracts. Acta physiol. scand. 56(Suppl. 193):1-45

Grant, G. and Rexed, B. (1958) Dorsal spinal root afferents to Clarke's column. Brain 81:567-576

Grant, G., Wiksten, B., Berkley, K.J. and Aldskogius, H. (1982) The location of cerebellar-projecting neurones within the lumbosacral spinal cord in the cat. An anatomical study with HRP and retrograde chromatolysis. J.Comp.Neurol. 204:336-348

Gray, E.G. (1959) Axosomatic and axodendritic synapses of the cerebral cortex: an electron microscope study. J. Anat. 93:420-433

Gray, E.G. (1962) A morphological basis for pre-synaptic inhibition. Nature 193:82-83

Gray, E.G. (1963) Electron microscopy of presynaptic organelles of the spinal cord. J. Anat. 97:101-106

Gray, E.G. (1983) Neurotransmitter release mechanisms and microtubules. Proc. R. Soc. Lond. B 218:253-258

Grundfest, H. and Carter, W.B. (1954) Afferent relations of inferior olivary nucleus. I. Electrophysiological demonstration of dorsal spino-olivary tract in the cat. J. Neurophysiol. 17:72-91

Grundfest, H. and Campbell, B. (1942) Origin, conduction and termination of impulses in the dorsal spino-cerebellar tract in cats. J. Neurophysiol. 5:275-294

Hanker, J.S., Yates, P.E., Metz, C.B. and Rustioni, A. (1977) A new, specific, sensitive and non-carcinogenic reagent for the demonstration of horse radish peroxidase. Histochemical J. 9:789-792

Herrera, A.A., Grinnell, A.D. and Wolowske, B. (1985) Ultrastructural correlates of experimentally altered transmitter release efficacy in frog motor nerve terminals. Neuroscience 16(3):491-500

Heuser, J.E. and Reese, T.S. (1977) Structure of the Synapse. In: The Handbook of Physiology, Section I. The Nervous System Vol.1, part 1, Kandel, E.R. (ed.) pp 261-294 American Physiological Society, Bethesda, MD.

Hirano, A. and Dembitzer, H.M. (1978) Morphology of normal central myelinated axons. In: Physiology and Pathobiology of Axons. Waxman, S.G. (ed.) Raven Press, N.Y.

Hongo. T. (1985) Functional and morphological organizations of DSCT cells in Clarke's column. In Development, Organization and Processing in Sensory Pathways. Rowe, M. and Willis, W.D. (eds.) Alan R. Liss, Inc. N.Y. pp149-156

Hongo, T., Kudo, N., Sasaki, S., Yamashita, M., Yoshida, K., Ishizuka, N. and Mannen, H. (1982) Somatotopic organization of Clarke's column in the cat. Neurosci. Lett. 9(Suppl.):S107

Hongo, T., Kudo, N., Sasaki, S., Yamashita, M., Yoshida, K., Ishizuka, N. and Mannen, H. (1987) Trajectory of group Ia and Ib fibers from the hind-limb muscles at the L3 and L4 segments of the spinal cord of the cat. J. Comp. Neurol. 262:159-194

Hongo, T. and Okada, Y. (1967) Cortically evoked pre- and post synaptic inhibition of impulse transmission to the dorsal spinocerebellar tract. Exp. Brain Res. 3:163-177

Hongo, T., Okada, Y. and Sato, M. (1967) Corticofugal influences on transmission to the dorsal spinocerebellar tract from hindlimb primary afferents. Brain Res. 3:135-149

Houchin, J., Maxwell, D.J., Fyffe, R.E.W. and Brown, A.G. (1983) Light and electron microscopy of dorsal spinocerebellar tract neurones in the cat: An intracellular horseradish peroxidase study. Qu. J. Exp. Physiol. 68:719-732

Jankowska, E., Jukes, M.G.M. and Lund, S. (1964) On the presynaptic inhibition of transmission to the dorsal spinocerebellar tract. J. Physiol. 177:19-21P

Jankowska, E., Jukes, M.G.M. and Lund, S. (1965) The pattern of presynaptic inhibition of trnansmission to the dorsal spinocerebellar tract of the cat. J. Physiol. 178:17-18P

Jankowska, E., Rastad, J. and Westman, J. (1976) Intracellular application of horseradish peroxidase and its light and electron microscopical appearance in spinocervical tract cells. Brain Res. 105:557-562

Jansen, J.K.S. and Rudjord, T. (1965) Dorsal spinocerebellar tract. Response pattern of nerve fibers to muscle stretch. Science 149:1109-1111

Katz, B. and Miledi, R. (1968) The effect of local blockage of motor nerve terminals. J. Physiol. 199:729-741

Khattab, F. (1967) Synaptic structures at nodes of Ranvier in spinal cords of mice. Nature 216:496-497

Kitai, S.T. and Morin, F. (1962) Microelectrode study of dorsal spinocerebellar tract. Amer. J. Physiol. 203:799-802

Kuno, M., Munoz-Martinez, E.J. and Randic, M. (1973a) Sensory inputs to neurones of Clarke's column from muscle, cutaneous and joint receptors. J. Physiol.
228:327-342

Kuno, M., Munoz-Martinez, E.J. and Randic, M. (1973b) Synaptic action on Clarke's column neurones in relation to afferent terminal size. J. Physiol. 228:343-360

Laporte, Y. and Lundberg, A. (1956) Functional organization of the dorsal spino-cerebellar tract in the cat. III. Single fiber recording on Flechsig's fasciculus on adequate stimulation of primary afferent neurones. Acta physiol. scand. 36:204-218

Laporte, Y., Lundberg, A. and Oscarsson, O. (1956a) Functional organization of the dorsal spino-cerebellar tract in the cat. I. Recording of mass discharge in dissected Flechsig's fasciculus. Acta physiol. scand. 36:175-187

Laporte, Y., Lundberg, A. and Oscarsson, O. (1956b) Functional organization of the dorsal spino-cerebellar tract in the cat. II. Single fiber recording in Flechsig's fasciculus on electrical stimulation of various peripheral nerves. Acta physiol. scand. 36:188-203

Larsell, O. (1953) The cerebellum of the cat and the monkey. J.Comp.Neurol. 99:135-199

Liu, C-N. (1956) Afferent nerves to Clarke's and the lateral cuneate nuclei in the cat. Arch. Neurol. Psychiat. 75:67-77

Lloyd, D.P.C. and McIntyre, A.K. (1950) Dorsal column conduction of group I afferent impulses and their relay through Clarke's column. J. Neurophysiol. 13:39-54

Loewy, A.D. (1970) A study of neuronal types in Clarke's column of the adult cat. J.Comp.Neurol. 139:53-80

Low, J.S.T., Mantle St-John, L.A. and Tracey, D.J. (1986) Nucleus Z in the rat: Spinal afferents from collaterals of the dorsal spinocerebellar tract neurons. J. Comp. Neurol. 243:510-526

Lundberg, A. and Oscarsson, O. (1956) Functional organization of the dorsal spino-cerebellar tract in the cat. IV. Synaptic connections of afferents from Golgi tendon organs and muscle spindles. Acta physiol. scand. 38:53-75

Lundberg, A. and Oscarsson, O. (1959) Identification of a third subdivision of the dorsal spino-cerebellar tract. Experientia 15:195

Lundberg, A. and Oscarsson, O. (1961) Three ascending pathways in the dorsal part of the lateral funiculus. Acta physiol. scand. 51:1-16

Mann, M.D. (1971) Axons of the dorsal spinocerebellar tract which respond to activity in cutaneous receptors. J. Neurophysiology 34:1035-1050

Mann, M.D. (1973) Clarke's column and the dorsal spinocerebellar tract: A review. Brain, Behav. Evol. 7:34-83

Mann, M.D., and Tapper, D.N. (1970) Cutaneous subdivision of the dorsal spinocerebellar tract. The Physiologist. 13:255

Martin, A.R. (1977) Junctional Transmission. II. Presynaptic mechanisms. In: The Handbook of Physiology, Section I. The Nervous System Vol.1, part 1, Kandel, E.R. (ed.) pp 329-355 American Physiological Society, Bethesda, MD.

Matsushita, M. and Hosoya, Y. (1979) Cells of origin of the spinocerebellar tract in the rat, studied with the method of retrograde transport of horseradish peroxidase. Brain Res. 173:185-200

Matsushita, M., Hosoya, Y. and Ikeda, M. (1979) Anatomical organization of the spinocerebellar system in the cat, a study by retrograde transport of horseradish peroxidase. J. Comp. Neurol. 184:81-106

Matsushita, M. and Ikeda, M. (1970) Spinal projections to the cerebellar nuclei in the cat. Exp. Brain Res. 10:501-511

Mense, S. and Craig, A.D. (1988) Spinal and supraspinal terminations of primary afferent fibers from the gastrocnemius-soleus muscle in the cat. Neuroscience 26(3):1023-1035

Moore, J.W., Joyner, R.W., Brill, M.H., Waxman, S.D. and Najar-Joa, M. (1978) Simulations of conduction in uniform myelinated fibers. Relative sensitivity to changes in nodal and internodal parameters. Biophys. J. 21:147-160

Morin, F. (1955) A new spinal pathway for cutaneous impulses. Am. J. Physiol. 183:245-252

Morin, F., Lindner, D. and Catalano, J. (1957) Afferent projections to posterior lobe of the cerebellum and their spinal pathways in the cat and in the monkey. Am. J. Physiol. 188:257-262

Nieto-Sampedro, M., Hoff, S.F. and Cotman, C. W. (1982) Perforated postsynaptic densities: probable intermediates in synapse turnover. Proc. Natl. Acad. Sci. USA 79:5718-5722

Oscarsson, O. (1957) Primary afferent collaterals and spinal relays of the dorsal and ventral spinocerebellar tracts. Acta. physiol. scand. 40:222-231

Oscarsson, O. (1965) Functional organization of the spino-and cuneocerebellar tracts. Physiol. Rev. 45:495-522

Oscarsson, O. (1973) Functional organization of spinocerebellar paths. In: Somatosensory System, Handbook of Sensory Physiology. Iggo, A. (ed.) Vol. 2, Springer, Heidelberg, pp 339-380

Parnas, I. and Segev, I. (1979) A mathematical model for conduction of action potentials along bifurcating axons. J. Physiol. 295:323-343

Pass, I.J. (1933) Anatomical and functional relationships of the nucleus dorsalis (Clarke's column) and the dorsal spino-cerebellar tract. Arch. Neurol. Psychiat., Chicago 30:1025-1045

Peters, A. (1966) The node of Ranvier in the central nervous system. Quart. J. exp. Physiol. 51:229-236

Peters, A. and Kaisermann-Abramof, I.R. (1969) The small pyramidal neuron of the rat cerebral cortex. The synapses upon dendritic spines. Z. Zellforsch. Nilenos Aust. 100:487-506

Petras, J. M. (1977) Spinocerebellar neurons in the rhesus monkey. Brain Res.130:146-151

Petras, J.M. and Cummings, J.F. (1977) The origin of spinocerebellar pathways. II. The nucleus centrobasalis of the cervical enlargement and the nucleus dorsalis of the thoracolumbar spinal cord. J.Comp.Neurol. 173:693-716

Pfenniger, K., Akert, K., Moor, H. and Sandri, C. (1972) The fine structure of presynaptic membranes. J. Neurocytol. 1:129-149

Ramon y Cajal, S. (1909) Histologie du Systeme Nerveux de L'Homme et des Vertebres. Consejo Superior de Investigaciones Scientificas, Madrid

Randic, M., Miletic. V. and Loewy, A.D. (1981) A morphological study of cat dorsal spinocerebellar tract neurones after intracellular injection of horseradish peroxidase. J.Comp.Neurol. 198:453-466

Randic, M., Myslinski, N.R. and Gordon, J.H. (1976) Spinal localization of neurones receiving inputs from cutaneous afferents in the cat hindlimb. Brain Res. 105:573-577

Redman, S.J. and Walmsley, B. (1983a) The time course of synaptic potentials evoked in cat spinal motoneurones at identified group Ia synapses. J. Physiol. 343:117-133

Redman, S.J. and Walmsley, B. (1983b) Amplitude fluctuations in synaptic potentials evoked in cat spinal motoneurones at identified group Ia synapses. J. Physiol. 343:135-145

Rethelyi, M. (1968) The Golgi architecture of Clarke's column. Acta morph. hung. 16:311-330

Rethelyi, M (1970) Ultrastructural synaptology of Clarke's column. Exp. Brain Res. 11:159-174

Revenko, S.V., Timin, YE. N. and Khodorov, B.I. (1973) Special features of the conduction of nerve impulses from the myelinized part of the axon into the non-myelinated terminal. Biofizika 18(6):1074-1078

Rexed, B. (1954) A cytoarchitectonic atlas of the spinal cord in the cat. J. Comp. Neurol. 100:297-379

Reynolds, E.S. (1963) The use of lead citrate at high pH as an electron opaque stain in electron microscopy. J. Cell Biol. 17:208

Ritchie, J.M. (1986) Distribution of Saxitoxin-binding sites in mammalian neural tissue. Annals NY Acad. Sci. 479:385-401

Ritchie, J.M. and Rogart, R.B. (1977) Density of sodium channels in mammalian myelinated nerve fibers and nature of the axonal membrane under the myelin sheath. Proc. Natl. Acad. Sci. USA 74(1):211-215

Rose, P.K. and Richmond, F.J. (1981) White matter dendrites in the upper cervical spinal cord of the adult cat: a light and electron microscopic study. J. Comp. Neurol. 199(2):191-203

Saito, K. (1972) The initial segment of DSCT (dorsal spinocerebellar tract) neurones in the cat. J. Electron microscopy. 21(4):325-326

Saito, K. (1974) The synaptology and cytology of the Clarke cell in nucleus dorsalis of the cat: an electron microscopic study. J. Neurocytol. 3:179-197

Saito, K. (1979) Morphometrical synaptology of Clarke cells and of distal dendrites in the nucleus dorsalis: an electron microscope study in the cat. Brain Res. 178:233-249

Sedar, A.W. and Moskowitz, N. (1967) Differentiation of synaptic bulbs in Clarke's column. Nature 214:391-392

Sherrington, C.S. and Laslett, E.E. (1903) Remarks on the dorsal spinocerebellar tract. J. Physiol. 29:188-194

Shrager, P. (1987) The distribution of sodium and potassium channels in single demyelinated axons of the frog. J. Physiol. 392:587-602

Siekevitz, P. (1985) The postsynaptic density: A possible role in long-lasting effects in the central nervous system. Proc. Natl. Acad. Sci. 82:3494-3498

Smith, S.J. and Augustine, G.J. (1988) Calcium ions, active zones and synaptic transmitter release. TINS 11(10):458-464

Snow, P.J., Rose, P.K. and Brown, A.G. (1976) Tracing axons and axon collaterals of spinal neurons using intracellular injection of horseradish peroxidase. Science 191:312-313

Snyder, R.L., Faull, R.L.M. and Mehler, W.R. (1978) A comparitive study of the neurones of origin of the spinocerebellar afferents in the rat, cat and squirrel monkey based on the retrograde transport of horseradish peroxidase. J.Comp.Neurol. 181:833-852

Sotelo, C. and Palay, S.L. (1970) The fine structure of the lateral vestibular nucleus in the rat. II. Synaptic organization. Brain Res. 18:93-115

Spacek, J. and Hartamnn, M. (1983) 3-dimensional analysis of dendritic spines. I. Quantitative observations related to dendritic spine and synaptic morphology in cerebral and cerebellar cortices. Anat. Embryol. 167:289-310

Spurr, A.R. (1969) A low-viscosity resin embedding medium for electron microscopy. J. Ultrastruct. Res. 26:31-43

Swadlow, H.A., Kocsis, J.D. and Waxman, S.G. (1980) Modulation of impulse conduction along the axonal tree. Ann Rev. Biophys. Bioeng. 9:143-179

Szentagothai, J. (1961) Somatotopic arrangement of synapses of primary sensory neurones in Clarke's column. Acta morph. hung. 10:307-310

Szentagothai, J. (1970) The morphological identification of the active synaptic region: Aspects of general arrandement of geometry and topology. Excitatory Synaptic Mechanisms. Andersen, P. and Jansen, J. (eds.) Universtetforlaget, Oslo

Szentagothai, J. and Albert, A. (1955) The synaptology of Clarke's column. Acta morph. hung. 5:43-51

Tapper, D.N., Mann, M.D., Brown, P.B. and Cogdell, B. (1975) Cells of origin of the cutaneous subdivision of the dorsal spinocerebellar tract. Brain Res. 85:59-63

Tracey D.J. and Walmsley, B. (1984) Synaptic input from identified muscle afferents to neurones of the dorsal spinocerebellar tract in the cat. J. Physiol. 350:599-614

Triller, A. and Korn, H. (1982) Structural evidence for sungle synaptic grids in individual terminal boutons. Neurosci. Lett. 10(Suppl.):S488-S489

Uchizono, K. (1965) Characteristics of excitatory and inhibitory synapses in the central nervous system of the cat. 207:642-643

Ulfhake, B. and Kellerth, J-O. (1981) A quantitative light microscopic study of the dendrites of cat spinal a-motoneurones after intracellular staining with horseradish peroxidase. J.Comp.Neurol. 202:571-583

van Beusekom, G.T. (1955) Fibre analysis of the anterior and lateral funiculi of the cord in the cat. Eduardo Ijdo, N.V. Leiden.

Walmsley, B., Edwards, F.R. and Tracey, D.J. (1987) The probabilistic nature of synaptic transmission at a mammalian excitatory central synapse. J. Neurosci. 7(4):1037-1046

Walmsley, B., Edwards, F.R. and Tracey, D.J. (1988) Nonuniform release probabilities underlie quantal synaptic transmission at a mammalian excitatory central synapse. J. Neurophysiol. 60(3):889-908

Waxman, S.G. (1970) Closely spaced nodes of Ranvier in the teleost brain. Nature 227:283-284

Waxman, S.G. (1972) Regional differentiation of the axon: A review with special reference to the concept of the multiplex neuron. Brain Res. 47:269-288

Waxman, S.G. (1974) Ultrastructural differentiation of the axon membrane at synaptic and non-synaptic central nodes of Ranvier. Brain Res. 65:338-342

Waxman, S.G. and Wood, S.L. (1984) Impulse conduction in inhomogeneous axons: Effects of variation in voltage-sensitive ionic conductances on invasion of demyelinated axon segments and preterminal fibres. Brain Res. 294:111-122

Westrum, L.E. and Gray, E.G. (1986) New observations on the substructure of the active zone of brain synapses and motor endplates. Proc. R. Soc. Lond. B. 229:29-38

Witkovsky, P. (1971) Synases made by myelinated fibres running to teleost and elasmobranch retinas. J. Comp. Neurol. 142:205-222

Wurtz, C.C. and Ellisman, M.H. (1986) Alterations in the ultrastructure of peripheral nodes of Ranvier associated with repetitive action potential propagation. J. Neurosci. 6(11):3133-3143

Yamomoto, S. and Miyajima, M. (1959) Activation of spinocerebellar neurones by adequate exteroceptive and proprioceptive stimulation. Exp. Neurol. 1:427-440

Yoss, R.E. (1952) Studies of the spinal cord. I Topographical localization within the dorsal spinocerebellar tract in *Macaca mulatta*. J.Comp.Neurol. 97:5-20

APPENDIX I

THE ULTRASTRUCTURAL BASIS FOR SYNAPTIC TRANSMISSION BETWEEN PRIMARY MUSCLE AFFERENTS AND NEURONS IN CLARKE'S COLUMN OF THE CAT.

by

B. Walmsley, E. Wieniawa-Narkiewicz,
and M.J.Nicol

The Journal of Neuroscience, (1985), 5(8):2095-2106

0270-6474/85/0508-2095$02.00/0

The Journal of Neuroscience
Vol. 5, No. 8, pp. 2095-2106
August 1985

The Ultrastructural Basis for Synaptic Transmission between Primary Muscle Afferents and Neurons in Clarke's Column of the Cat[1]

B. WALMSLEY,[2] E. WIENIAWA-NARKIEWICZ,[3] AND M. J. NICOL

Experimental Neurology Unit, John Curtin School of Medical Research, Australian National University, Canberra, Australian Capital Territory, Australia.

Abstract

The synaptic connection between primary muscle afferents and dorsal spinocerebellar tract (DSCT) neurons has been studied in an attempt to reveal some of the mechanisms underlying excitatory transmission in the mammalian central nervous system. Previous electrophysiological experiments have shown that the excitatory postsynaptic potentials (EPSPs) evoked DSCT neurons by impulses in a single muscle afferent fluctuate in amplitude. These fluctuations occur between discrete amplitudes which are separated by quantal increments. Two alternative hypotheses relate such a quantal increment to all-or-nothing transmitter release from either (1) an entire synaptic bouton or (2) an individual transmitter release site, given that a bouton may contain multiple release sites. The present study was undertaken primarily to gain ultrastructural evidence on these proposals. Electrodes filled with horseradish peroxidase (HRP) were used to label single identified group Ia afferent fibers and DSCT neurons in the lumbar spinal cord of anesthetized cats. HRP-labeled Ia synaptic boutons, and the contacts formed between HRP-labeled Ia boutons and the dendrites of a DSCT neuron labeled intracellularly with HRP, were examined in serial sections under the electron microscope. Group Ia boutons were found to contain multiple synaptic specializations, as evidenced by pre- and postsynaptic thickenings and presynaptic clusters of vesicles. Careful examination of a bouton in serial sections revealed each specialization as a separate structure. These observations support the proposal that synaptic transmission between group I muscle afferents and DSCT neurons occurs with discrete all-or-nothing EPSPs associated with transmitter release sites, rather than boutons per se.

Primary afferents from hindlimb muscle spindles and tendon organs make monosynaptic connections with dorsal spinocerebellar tract (DSCT) neurons, situated in Clarke's column (Mann, 1973). In a previous study (Tracey and Walmsley, 1982, 1984), the excitatory postsynaptic potentials (EPSPs) evoked in DSCT neurons by impulses in a single primary muscle afferent were found to fluctuate in amplitude from trial to trial. These fluctuations occur between discrete amplitudes separated by a quantal increment. In an earlier electrophysiological/anatomical study on single group Ia fiber EPSPs evoked in cat spinal motoneurons (Redman and Walmsley, 1981, 1983a, b), it was proposed that such a quantal increment is due to all-or-nothing transmitter release from a synaptic bouton. Light microscopic observations on the synaptic connections between horseradish peroxidase (HRP)-identified primary muscle afferents and DSCT neurons have revealed that these afferent boutons vary greatly in size, from 1 × 1 μm up to "giant" boutons of 20 × 3 μm (Tracey and Walmsley, 1984). Electron microscopic studies in Clarke's column have revealed the presence of several types of synaptic contacts, including giant boutons (Szentagothai and Albert, 1955; Rethelyi, 1970; Saito, 1974, 1979; Houchin et al., 1983). It was suggested that the giant boutons contain multiple transmitter release sites and that synaptic transmission between group I muscle afferents and DSCT neurons occurs with the quantal increments underlying EPSP amplitude fluctuations associated with these transmitter release sites (Tracey and Walmsley, 1984).

However, until the present study, no information has been available on the ultrastructure of identified terminals contacting DSCT neurons. We have employed electron microscopy to examine in detail the ultrastructure of group Ia synapses in Clarke's column and the synaptic contacts between Ia muscle afferents and DSCT neurons, both identified by intracellular labeling with HRP. A complete picture of the synaptic specializations contained within each bouton was constructed, using serial sections. The results indicate that some of the Ia synaptic terminals on DSCT neurons contain multiple transmitter release sites. These observations are taken as support for the proposed relationship between quantal EPSPs and individual transmitter release sites rather than synaptic boutons.

Materials and Methods

Experiments were performed on cats weighing 1.5 to 2.5 kg. The cats were anesthetized with sodium pentobarbitone (35 mg/kg, i.p.) and maintained with supplementary doses (5 mg, i.v.). Mean arterial pressure and end-tidal CO_2 were monitored.

HRP labeling of axons and neurons. The following muscles were exposed in the left hindlimb: medial gastrocnemius, lateral gastrocnemius, soleus, and plantaris. The tendons of these muscles were separated and cut at their insertion to allow each muscle to be individually stretched. The cat was fixed in a rigid animal frame, and a laminectomy was performed from L7 to L3. The exposed hindlimb muscles and spinal cord were covered with pools of mineral oil, maintained at 35 to 37°C by infrared heating. Bipolar stimulating electrodes were placed on the sciatic nerve and its branches to the exposed muscles.

Glass microelectrodes containing 10% HRP in 1 M KCl were inserted into the dorsal columns near the junction of L3 and L4 segments of the spinal cord, about 200 μm lateral to the midline. On intracellular penetration of a primary muscle afferent, its conduction time was recorded, allowing a preliminary classification into group I or group II. Fibers were classified as group Ia if they had high dynamic sensitivity to passive stretch and a silent period during active muscle contraction. Once the afferent was identified, HRP was iontophoresed into the axon for up to an hour. Iontophoresis of HRP was continued only while the intracellular action potential was greater

Received August 20, 1984; Revised February 19, 1985;
Accepted February 28, 1985

[1] We are grateful to Dr. R. E. W. Fyffe and Dr. E. G. Jones for comments and suggestions on this paper, and to Mrs. M. Wiechert for typing the manuscript.

[2] To whom correspondence should be addressed.

[3] Present address: Department of Anatomy, Faculty of Medicine, The University of Calgary, 3300 Hospital Dr., N.W., Calgary, Alberta, Canada T2N 4N1.

than 10 mV. Good results were obtained when the charge transfer was in the range 100 to 400 nA/min.

In the same experiments, intracellular recordings were made from DSCT neurons in Clarke's column at the level of L3 and L4 segments of the cord. Antidromic identification of DSCT neurons was performed by stimulation of the dissected dorsolateral fasciculus of the spinal cord at the C2 level (Houchin et al., 1983; Tracey and Walmsley, 1984). The dorsal columns were removed for approximately 2 cm to avoid stimulation spreading to them. Electrodes, filled with 10% HRP in 1 M KCl, were driven into Clarke's column in the spinal cord approximately 200 to 300 μm from the midline. Only DSCT neurons receiving monosynaptic excitation from group I muscle afferents were injected with HRP (10 to 30 nA for 10 to 40 min).

Following a 2- to 5-hr post-injection survival time, the animal was perfused with 3% glutaraldehyde in phosphate buffer (pH 7.2). The spinal cord segments L3 and L4 were removed and post-fixed for about 10 hr. Parasagittal sections (100 μm) of these segments were cut using a Vibratome and reacted for HRP using diaminobenzidene (DAB).

Light microscopy. Sections were serially mounted on gelatin-coated slides and cleared in alcohols and xylene to enable complete reconstruction of DSCT neurons (See Fig. 1) by light microscopy.

Electron microscopy. Sections immersed in glycerol were carefully examined under the light microscope. Structures filled with HRP reaction product were readily observed, even in the nondehydrated tissue. Small areas (2 × 1 mm) containing stained fibers or neurons were cut from the sections and transferred to 0.1 M phosphate buffer (pH 7.4), washed, and left for 2 to 3 hr at 4°C. Subsequently, the tissue was post-fixed in 2% O_sO_4, stained *en bloc* with 2% uranyl acetate, dehydrated in alcohol, and embedded in Spurr resin. Thin sections (~100 nm) were cut with a diamond knife (Diatome) on a Reichert microtome, collected on parlodion-coated slot grids, and examined in a Phillips 301 electron microscope.

HRP-labeled structures were easily observed, and in the majority of cases staining was light enough not to obscure intracellular components. Criteria for identification of synapses were as follows: (*1*) thickening of the apposed cellular membranes; (*2*) accumulation of synaptic vesicles close to the presynaptic membrane; and (*3*) synaptic cleft. Sequential sections of each labeled structure were examined and relevant sections were photographed.

The possibility that observed contacts were actually autapses rather than afferent contacts could be ruled out because the axons of DSCT neurons do not give rise to recurrent collaterals (Randic et al., 1981; Houchin et al., 1983; personal observation of HRP-labeled DSCT neurons). Such a possibility does exist, for example, with spinal motoneurons.

Results

Results were obtained from experiments on 22 cats weighing 1.5 to 2.5 kg.

Light microscopy of DSCT neurons. In confirmation of earlier HRP studies (Houchin et al., 1983; Tracey and Walmsley, 1984), the dendritic trees of DSCT neurons were very profuse and extended over 3 mm in the rostrocaudal direction. Figure 1 shows a camera lucida reconstruction of a typical DSCT neuron receiving group I muscle afferent input. Many fine branchlets can be seen arising from both proximal and distal dendrites, in contrast to the DSCT neurons illustrated in the HRP study by Randic et al. (1981).

Electron microscopy of contacts between Ia fibers and DSCT neurons. A previous light microscopic study (Tracey and Walmsley, 1984) failed to observe contacts between a single HRP-labeled afferent fiber and intracellularly labeled DSCT neurons. We were, however, successful in obtaining some results in the present study.

Staining of both DSCT neurons and Ia fibers was sufficient to allow easy recognition without obscuring ultrastructural details. (In a number of experiments, a cobalt enhancement of the DAB-HRP reaction was used (Adams, 1977, 1981), but the resulting strong label usually obscured the fine details of terminals in the electron microscope.)

Since one of our primary interests was to investigate whether a single primary afferent bouton contained multiple synaptic specializations, it was essential to examine serial sections of each contact. (Otherwise, an irregularly shaped specialization would appear as multiple contacts if examined only in a single section.) Eight HRP-labeled Ia boutons were examined fully in serial sections under the electron microscope. Figures 2 to 6 illustrate connections between

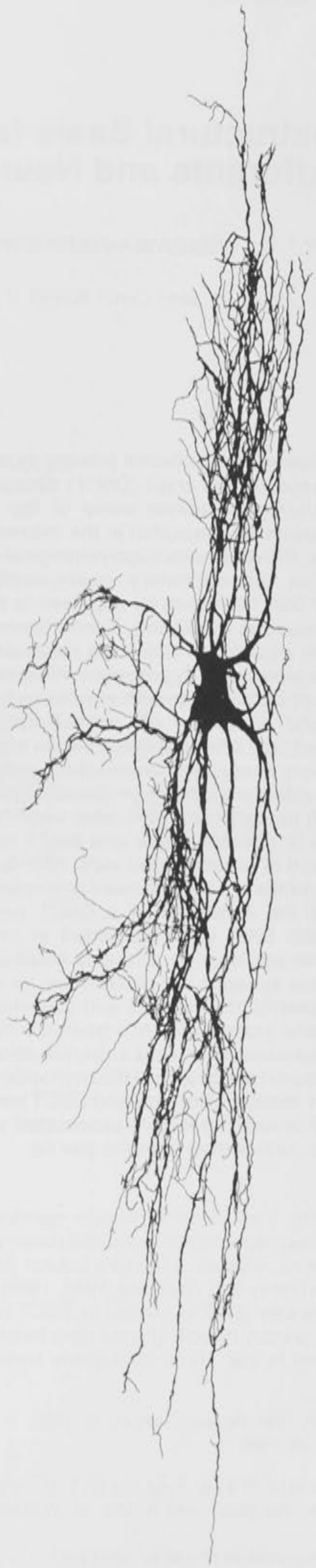

Figure 1. Reconstruction of a DSCT neuron receiving group I muscle afferent input. The HRP-injected neuron was reconstructed from 100-µm-thick sagittal sections in the L3 spinal cord segment.

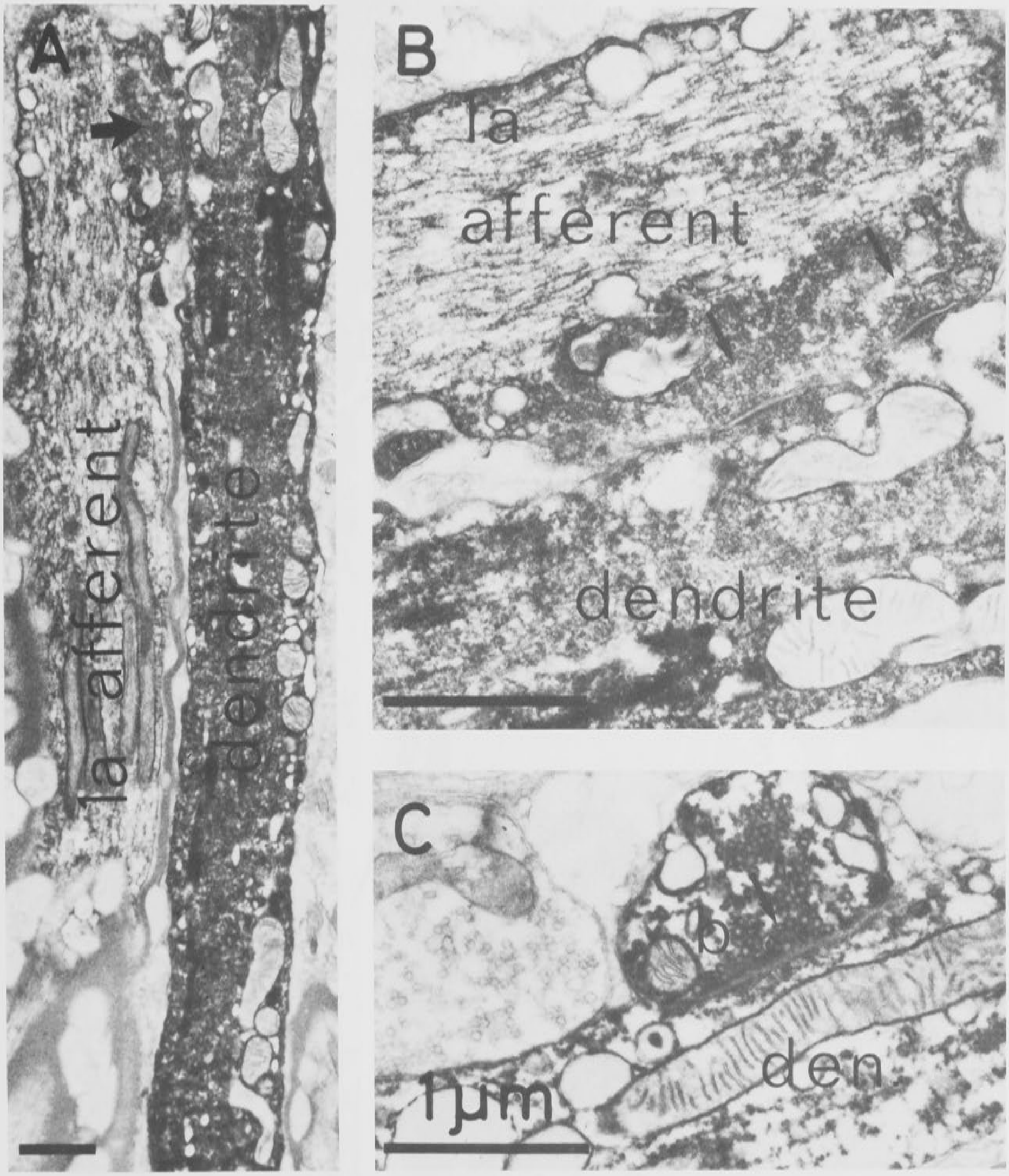

Figure 2. Electron micrographs of the connection between an HRP-stained Ia afferent and an HRP-stained DSCT neuron. An en passant connection between the Ia afferent and a dendrite of the DSCT neuron (*arrow* in *A*) is shown in more detail in *B*. The *two arrows* in *B* indicate two synaptic specializations found at this connection. *C* illustrates a contact (*arrow*) between a terminal Ia bouton and a dendrite (*den.*) of the DSCT neuron.

Figure 3. Serial sections through an HRP-labeled Ia bouton shown in sequential order, *A* to *J*. The Ia bouton made contact with two small branchlets (*single* and *double arrows*) which arise from a larger diameter dendrite of the HRP-labeled DSCT neuron. Details of the synaptic specializations in the Ia bouton are shown in Figure 4.

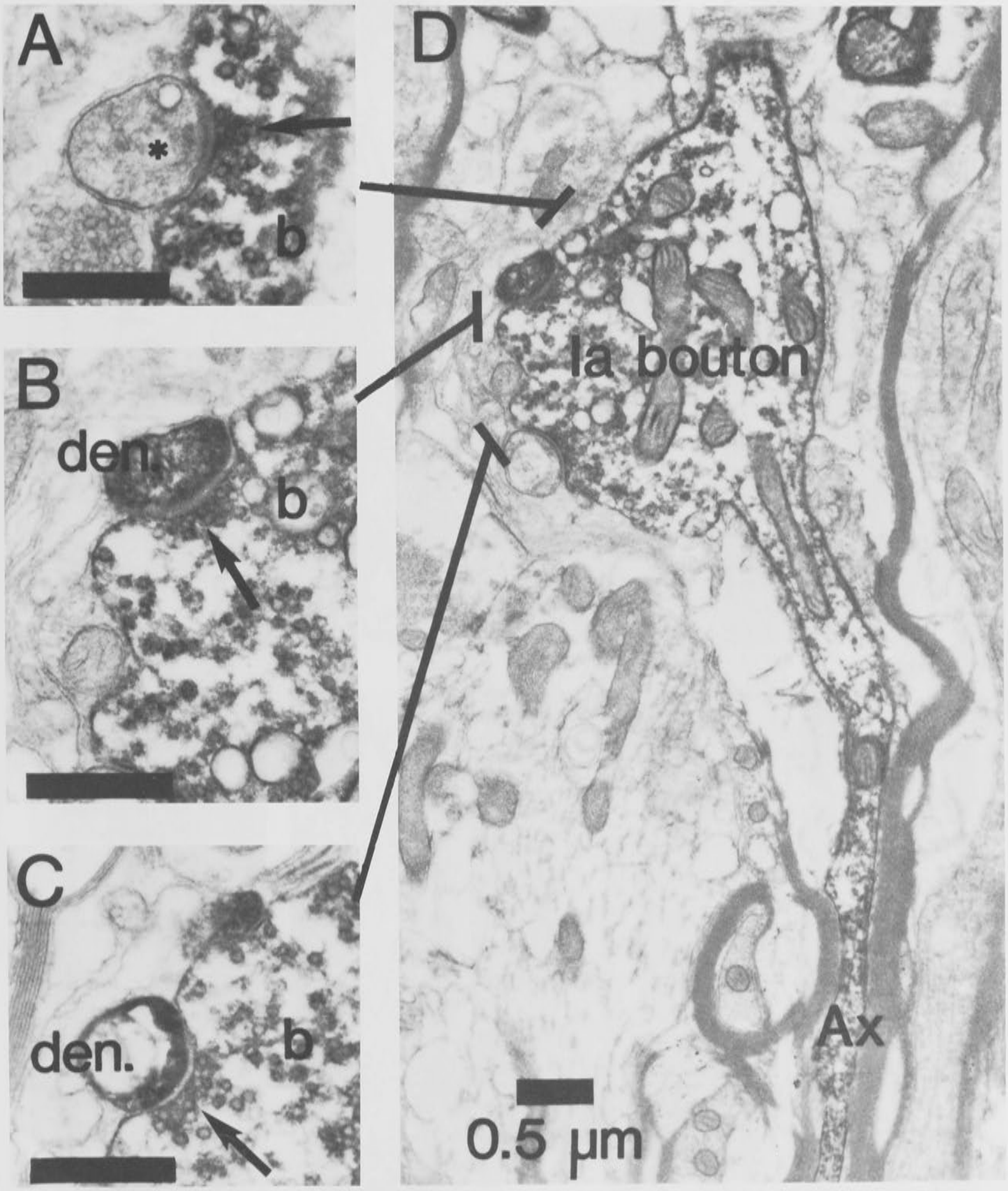

Figure 4. Contacts (*arrows*) formed by a Ia bouton (*D*), labeled with HRP (same bouton as shown in Fig. 3). Two contacts were formed with different HRP-labeled dendrites (*den.* in *B* and *C*), and a third contact was formed with an unlabeled structure (*asterisk*, in *A*). The approximate region in which these contacts were found is indicated by the *lines* joining the detailed photomicrographs (*A*, *B*, and *C*) and the photomicrograph in *D*. Only the postsynaptic dendrite of *A* can be seen in the single section in *D*. All *calibration bars* are 0.5 μm.

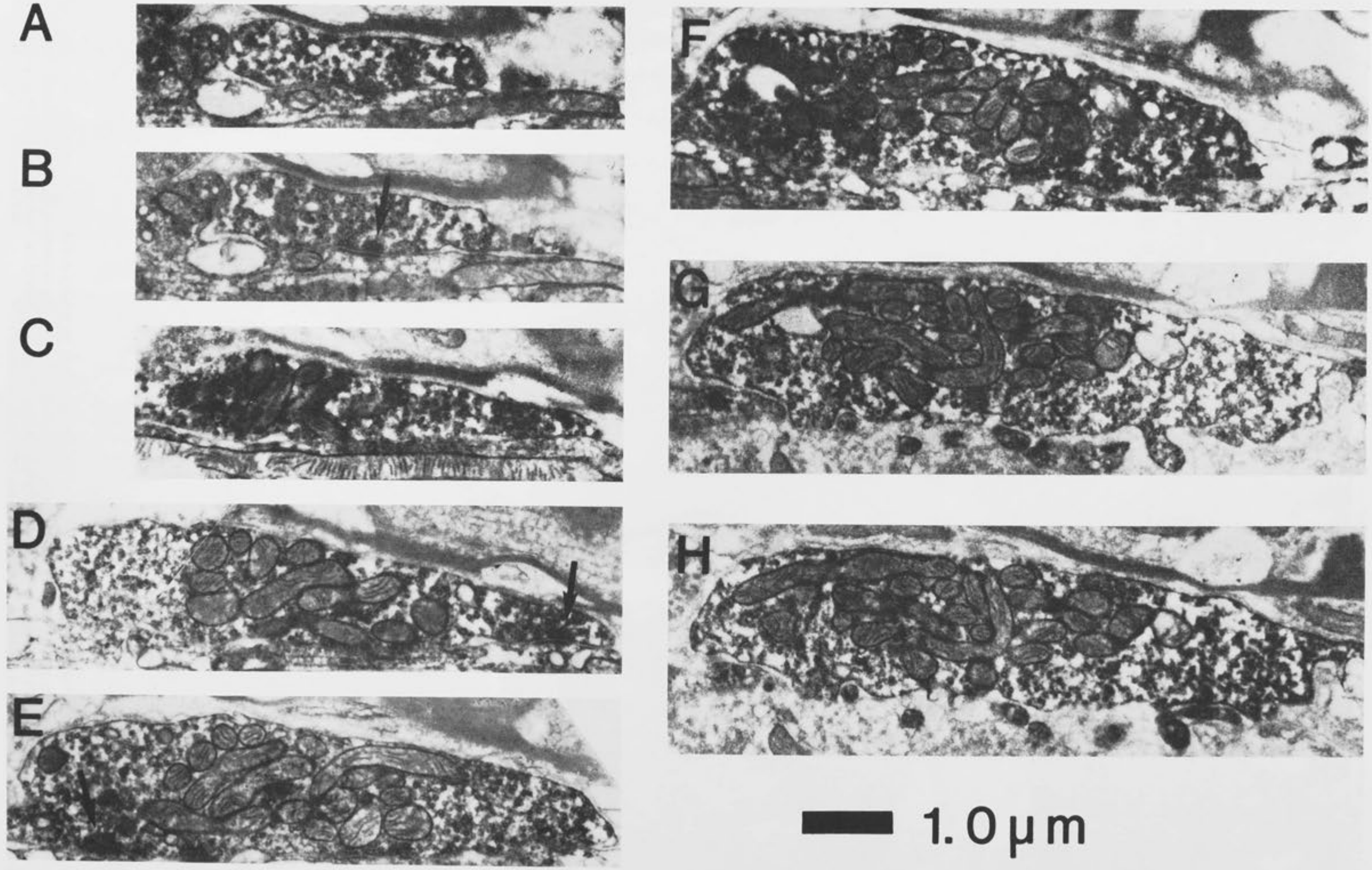

Figure 5. Serial sections through an HRP-labeled Ia bouton, shown in sequential order, *A* to *H*. The Ia bouton contacted an HRP-labeled dendrite of a DSCT neuron, which is shown in detail in Figure 6. Synaptic specializations are indicated by *arrows* in *B*, *D*, and *E*.

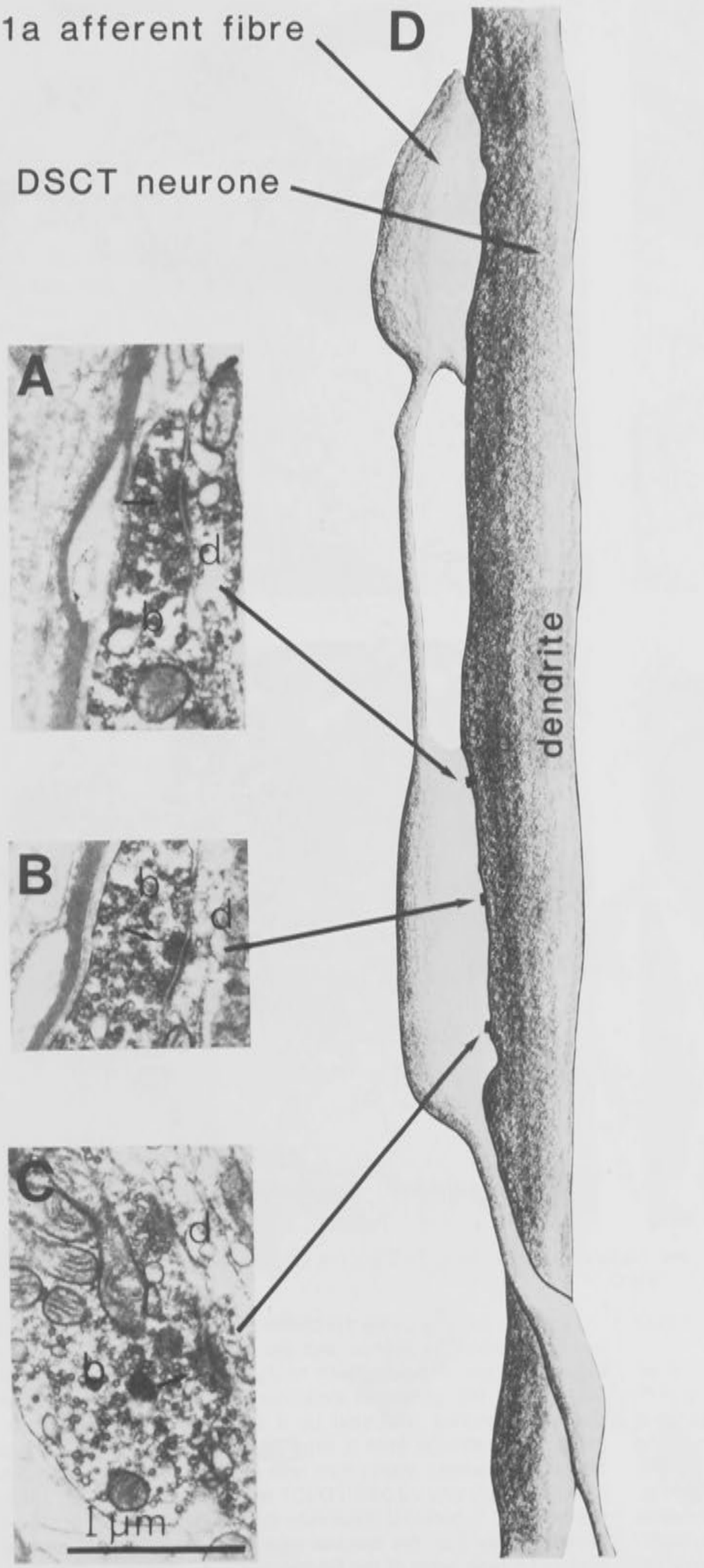

Figure 6. Details of the contacts between an HRP-labeled Ia bouton (same bouton as shown in Fig. 5) and the HRP-labeled dendrite of a DSCT neuron. Synaptic specializations (*arrows* in *A*, *B*, and *C*; *d*, dendrite; *b*, bouton) were found in the regions indicated by the *lines* joining *A*, *B*, and *C* to the drawing shown in *D*. This drawing was constructed from serial sections and is drawn to the same scale as the photomontage shown in *E*. *Calibration bar* in *E* is 1.0 μm.

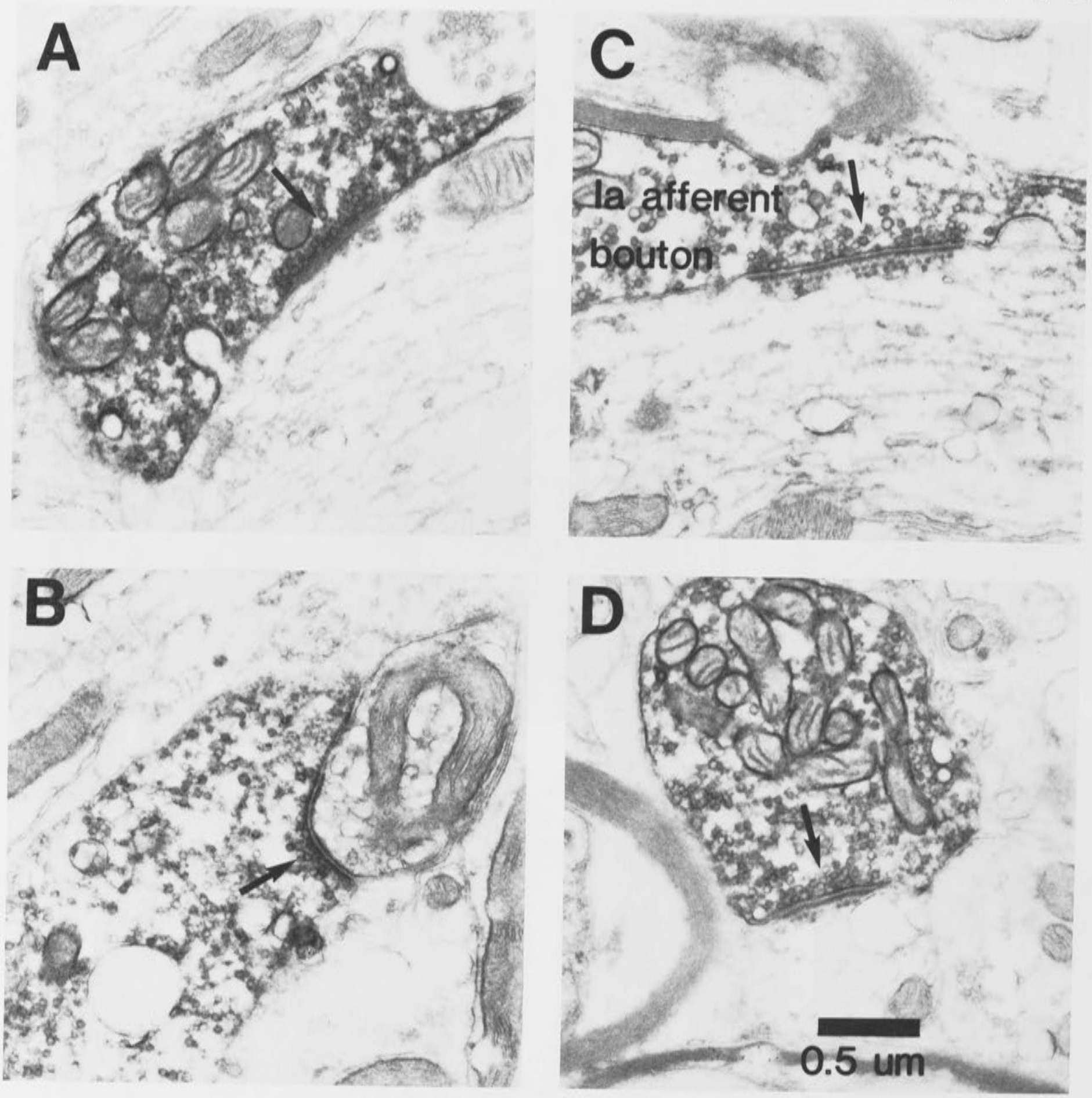

Figure 7. Contacts formed by HRP-labeled Ia boutons (*A* to *D*) within Clarke's column. Synaptic specializations are indicated by *arrows*. Note the array of postsynaptic dense bodies opposite the presynaptic thickenings in *C* and *D*.

an HRP-labeled Ia afferent fiber and dendrites of the same labeled DSCT neuron.

The synaptic boutons were of both terminal (Fig. 2C) and en passant (Fig. 2, *A* and *B*) types. The bouton in Figure 2, *A* and *B*, is of the en passant type and can be seen arising from a node of Ranvier and making connection with an HRP-labeled dendrite of the DSCT neuron. The appearance of this synapse is similar to the "outpocketing" synapses observed by Uchizono (1975, e.g., Fig. 128) in the cat spinal cord. In Figure 2*B*, two regions of synaptic specialization can be seen, as evidenced by pre- and postsynaptic thickenings and presynaptic clusters of vesicles. Serial examination revealed that these were separate specializations rather than sections of the same specialization.

Figures 3 and 4 illustrate the connections made between another serially sectioned Ia bouton and the HRP labeled DSCT neuron. Figure 3 shows a sequence (*A* to *J*) of photomicrographs of the bouton and the contacted dendrites. It appears that two small diameter branches (indicated by a *single* and a *double arrow*, respectively) emerge from a larger dendrite. Such branchlets are frequently observed arising from both proximal and distal dendrites of intracellularly labeled (HRP) DSCT neurons (Houchin et al., 1983; see also Fig. 1; personal observation). The bouton itself is of the en passant rather than the terminal type as the (myelinated) axon is evident on both sides of the bouton, labeled in Figure 3, *C* and *H*. The Ia bouton formed single synaptic specializations with both of the HRP-labeled branchlets as shown in detail in Figure 4, *B* and *C*.

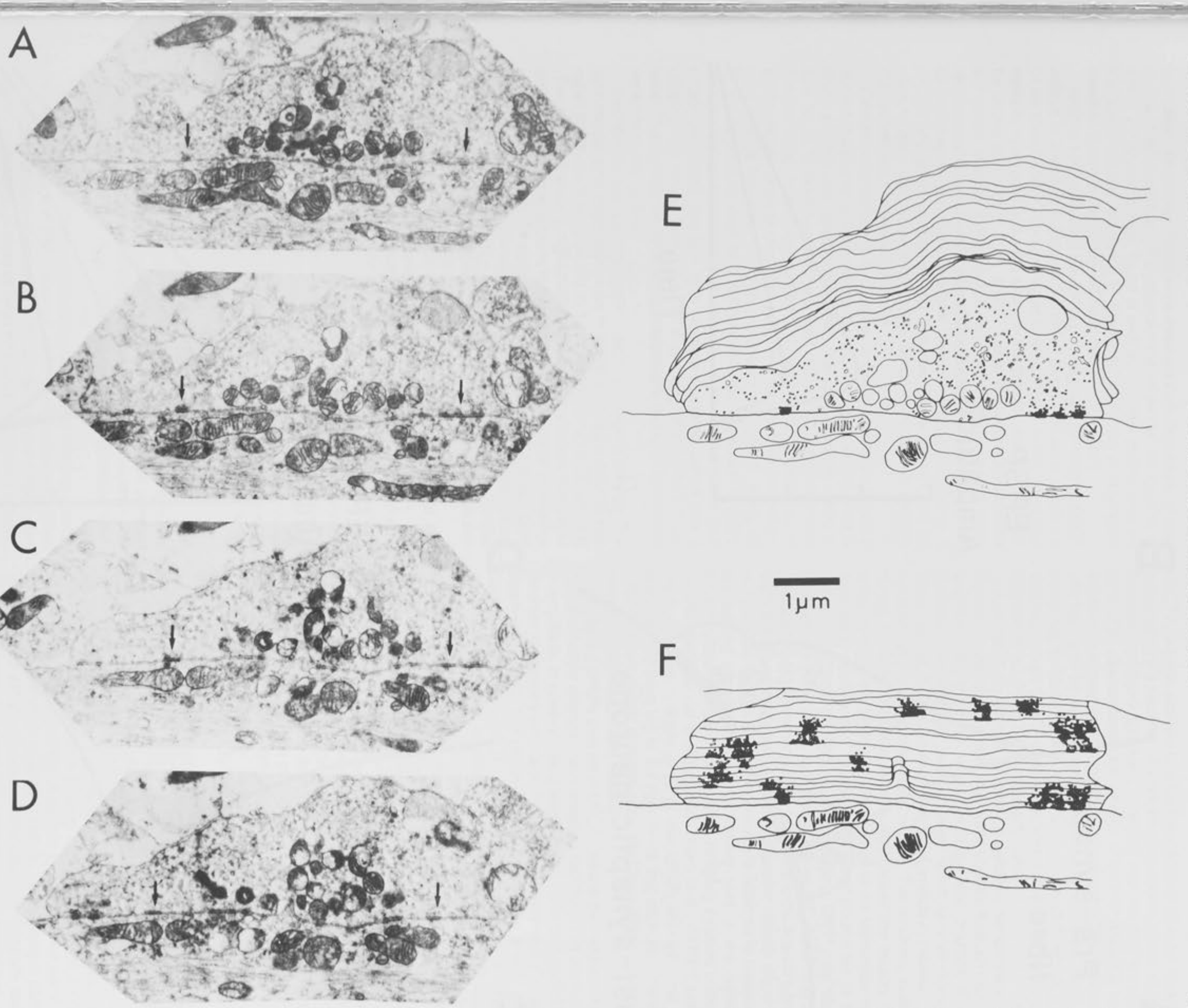

Figure 8. Reconstruction from serial sections of a "giant" bouton in Clarke's column. Photomicrographs of four serial sections are shown in *A* to *D* (*arrows* indicate regions of synaptic specialization). Reconstruction of the external profile of the bouton is shown in *E*, with the first section drawn in detail (same section as *A*). Synaptic specializations contained in this bouton (presynaptic densities and clusters of vesicles) have been reconstructed in *F*, which also shows the region of apposition between each section and the postsynaptic dendrite.

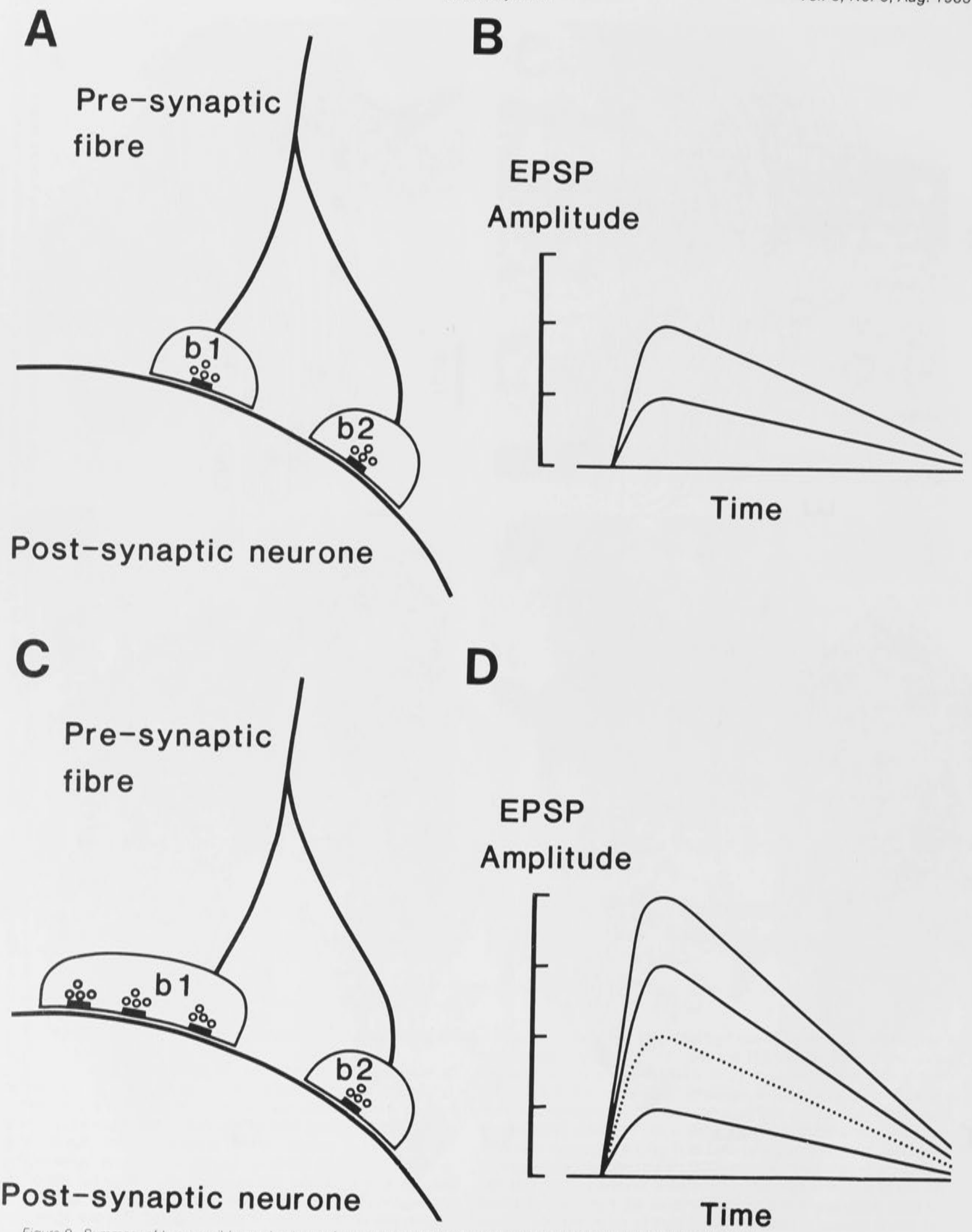

Figure 9. Summary of two possible mechanisms of synaptic transmission in the spinal cord. See the text for explanation.

In addition, the bouton contacted a small unlabeled structure, shown in Figure 4*A* (*asterisk*). The approximate region of the bouton in which the contacts were found is indicated by the joining lines on the single section illustrated in Figure 4*D* (only the postsynaptic dendrite shown in Fig. 4*B* is visible in this single section).

Another HRP-labeled Ia bouton contacting the HRP-labeled DSCT neuron is illustrated in Figures 5 and 6. Figure 5 shows a sequence of sections (*A* to *H*) through the Ia bouton. Three widely separated synaptic specializations were found in this bouton, and are indicated by *arrows* in Figure 5, *B*, *D*, and *E*. These synaptic specializations are shown in detail in Figure 6, *A* to *C*, which also shows a three-dimensional drawing which was reconstructed from serial sections of the bouton and the contacted dendrite. Figure 5*E* shows a photomontage of the bouton and dendrite. The Ia afferent can be seen to enter and leave the bouton, which forms an en passant connection with the labeled dendrite.

Electron microscopy of Ia boutons in Clarke's column. Figure 7 illustrates synaptic specializations found in boutons arising from Ia fibers intracellularly labeled with HRP. The specializations varied in size for all Ia boutons examined from 0.3 to 1.0 μm in diameter (longest axis). In two cases (Fig. 7, *C* and *D*) a regular array of postsynaptic dense bodies was observed, similar to those associated with the M-bouton found on motoneurons (Conradi, 1969). All of the Ia boutons examined contained round, agranular vesicles, and the synaptic contacts formed were of the asymmetrical type (Colonnier, 1968). The size of Ia boutons examined varied over a considerable range, from 1.6 to 11.5 μm long and 0.6 to 2.1 μm wide. The number of synaptic specializations found in Ia boutons varied from one to four.

Electron microscopy of a "giant" bouton in Clarke's column. The light microscopic observations on Ia fibers in Clarke's column indicated that these fibers give rise to "giant" terminals up to 20 μm long (Tracey and Walmsley, 1982, 1984). However, our limited sample of serially sectioned Ia boutons in this study did not allow us to examine such large boutons. To gain further information about these giant boutons, we have reconstructed an unlabeled giant bouton found within Clarke's column (Fig. 8), with the additional advantage that presynaptic elements were not obscured by the HRP-DAB reaction product found in the labeled boutons.

Reconstruction from 100-nm serial sections revealed that this bouton formed nine synaptic contacts with a large dendrite. The long axis of this dendrite was parallel to the long axis of the bouton. The size of the postsynaptic densities varied from 0.2 to 0.7 μm in diameter.

The three largest postsynaptic densities appeared as very irregular shapes similar to structures observed in rat cortex (Peters and Kaisermann-Abramof, 1969) and dog cortex (Cohen and Siekiewitz, 1978). A single section through such an irregularly shaped specialization (e.g., Fig. 8*A*) could be misinterpreted as multiple synaptic specializations. Serial reconstruction is obviously necessary to resolve such a problem (Fig. 8, *E* and *F*).

Discussion

The results from this study confirm and extend previous light and electron microscopic studies on the synaptic connections between primary afferent fibers and DSCT neurons in Clarke's column (Rethelyi, 1970; Houchin et al., 1983; Tracey and Walmsley, 1982, 1984).

We have studied these connections using serial electron microscopy of afferents and DSCT neurons which were positively identified by direct intracellular injection of HRP. Single Ia afferent fibers give rise to a wide range of sizes of synaptic boutons in Clarke's column. Results from the present study show that an individual Ia bouton may contain multiple synaptic specializations, which was verified by detailed examination of serial sections. A single bouton could make contact with one or several postsynaptic profiles. An example was illustrated in which an HRP-labeled Ia bouton formed synaptic contacts with two separate dendritic branches of the same HRP-labeled DSCT neuron, in addition to a third contact with an unlabeled profile, presumably the dendrite of a neighboring neuron. In our study all Ia boutons contained agranular, spherical vesicles and formed contacts of an asymmetrical type. Several of the HRP-labeled Ia boutons exhibited a regular array of postsynaptic dense bodies, a characteristic feature of the M-boutons on motoneurons (Conradi, 1969). Such postsynaptic dense bodies have not been found, however, in electron microscopy of HRP-identified Ia fiber contacts with motoneurons (Conradi et al., 1983; Fyffe and Light, 1984).

A number of previous studies on synaptic transmission in the central nervous system have attempted to relate fluctuations in EPSP amplitude to transmitter release from synaptic boutons. Figure 9 illustrates schematically two proposals which have emerged from these studies. Figure 9*A* illustrates the connection between a presynaptic fiber and a postsynaptic neuron. Two boutons, each containing a single transmitter release site, contact the neuron. Stimulation of the presynaptic fiber may result in no transmitter release from either release site, release from either bouton b1 or b2, or release from both b1 and b2. The resulting EPSP may fluctuate between the three levels indicated in Figure 9*B*, depending on the probabilities of transmitter release from b1 and b2. In such a scheme each bouton contains only a single transmitter release site and it is not possible to decide whether there is a relationship between the fluctuations and the number of release sites or the number of boutons. Such a situation exists at an inhibitory synaptic connection on the Mauthner cell in the goldfish (Korn et al., 1981). Studies on the fluctuations in single group Ia fiber EPSPs evoked in cat spinal motoneurons have led to the hypothesis that each increment in an EPSP is the synaptic potential generated by a single bouton (Redman and Walmsley, 1981, 1983b).

Studies of EPSPs evoked in DSCT neurons by impulses in single primary muscle afferents have revealed that these EPSPs fluctuated in amplitude. In general, these single fiber EPSPs fluctuate between discrete amplitudes separated by a quantal increment (Tracey and Walmsley, 1984). The present study has shown that a single Ia bouton contacting a DSCT neuron may contain multiple transmitter release sites. Such a situation is represented in Figure 9, *C* and *D*. Two boutons contact the postsynaptic neuron with one bouton containing three transmitter release sites and the other bouton contains only a single release site. The EPSP resulting from transmission at a bouton containing multiple release sites would be larger than that from a bouton containing only a single release site. If the boutons b1 and b2 in Figure 9*C* acted as all-or-nothing release elements, then the fluctuations would be nonquantal, as illustrated in Figure 9*D*, excluding the dotted EPSP. However, no large increments in EPSP amplitude fluctuations have been found (Tracey and Walmsley, 1984), and this possibility is considered unlikely. A more probable mechanism is that transmitter release sites within a single bouton act independently. In the illustration shown in Figure 9, *C* and *D*, the EPSP would fluctuate between five possible amplitude levels (including zero).

There are a number of factors which complicate the scheme presented in Figure 9, *C* and *D*. The probability that transmitter will be released following arrival of an action potential in a synaptic bouton may be different from bouton to bouton. For example, some boutons may be subjected to presynaptic inhibition whereas others are not, and the amount of calcium entering one bouton may be different from another. In a bouton containing multiple transmitter release sites, the probability of release may not be the same for all release sites. Although quantal in nature, the fluctuation pattern of single Ia fiber EPSPs in motoneurons does not obey any standard statistical distribution, such as Poisson or binomial (Jack et al., 1981). Such distributions (Poisson or binomial) would be expected if the probability of transmitter release were identical for all release sites. It seems likely, therefore, that the EPSP fluctuation pattern observed for single Ia fiber EPSPs in DSCT neurons (and probably motoneurons) is due to a combination of all-or-nothing transmitter

release from individual release sites, and that the probability of release may vary from release site to release site.

References

Adams, J. C. (1977) Technical considerations on the use of horseradish peroxidase as a neuronal marker. Neuroscience *2:* 141–145.

Adams, J. C. (1981) Heavy metal intensification of DAB based HRP reaction product. J. Histochem. Cytochem. *29:* 775.

Cohen, R. S., and P. Siekiewitz (1978) Form of the postsynaptic density. A serial section study. J. Cell. Biol. *78:* 36–46.

Colonnier, M. (1968) Synaptic patterns on different cell types in the different laminae of the cat visual cortex. An electron microscope study. Brain Res. *9:* 268–287.

Conradi, S. (1969) Ultrastructure of dorsal root boutons on lumbosacral motoneurons of the adult cat, as revealed by dorsal root section. Acta Physiol. Scand. Suppl. *332:* 85–115.

Conradi, S., S. Cullheim, L.Gollvik, and J. -O. Kellerth (1983) Electron microscopic observations on the synaptic contacts of group Ia muscle spindle afferents in the cat lumbosacral cord. Brain Res. *265:* 31–39.

Fyffe, R. E. W., and A. R. Light (1984) The ultrastructure of group Ia afferent fiber synapses in the lumbosacral spinal cord of the cat. Brain Res. *300:* 201–209.

Houchin, J., D. J. Maxwell, R. E. W. Fyffe, and A. G. Brown (1983) Light and electron microscopy of dorsal spinocerebellar tract neurones in the cat: An intracellular horseradish peroxidase study. Q. J. Exp. Physiol. *68:* 719–732.

Jack, J. J. B., S. J. Redman, and K. Wong (1981) The components of synaptic potentials evoked in cat spinal motoneurones by impulses in single group Ia fibres. J. Physiol. (Lond.) *321:* 65–96.

Korn, H., A. Triller, A. Mallart, and D. S. Faber (1981) Fluctuating responses at a central synapse: *n* of binomial fit predicts number of stained presynaptic boutons. Science (N.Y.) *213:* 898–901.

Mann, M. D. (1973) Clarke's column and the dorsal spinocerebellar tract. Brain Behav. Evol. *7:* 34–83.

Peters, A., and I. R. Kaisermann-Abramof (1969) The small pyramidal neuron of the rat cerebral cortex. The synapses upon dendritic spines. Z. Zellforsch. Nilenos Aust. *100:* 487–506.

Randic, M. M., V. Miletic, and A. D. Loewy (1981) A morphological study of cat dorsal spinocerebellar tract neurones after intracellular injection of horseradish peroxidase. J. Comp. Neurol. *198:* 453–466.

Redman, S. J., and B. Walmsley (1981) The synaptic basis of the monosynaptic stretch reflex. Trends Neurosci. *4:* 248–250.

Redman, S. J., and B. Walmsley (1983a) The time course of synaptic potentials evoked in cat spinal motoneurones at identified group Ia synapses. J. Physiol. (Lond.) *343:* 117–133.

Redman, S. J., and B. Walmsley (1983b) Amplitude fluctuations in synaptic potentials evoked in cat spinal motoneurones at identified group Ia synapses. J. Physiol. (Lond.) *343:* 135–145.

Rethelyi, M. (1970) Ultrastructural synaptology of Clarke's column. Exp. Brain Res. *11:* 159–174.

Saito, K. (1974) The synaptology and cytology of the Clarke cell in nucleus dorsalis of the cat: An electron microscopic study. J. Neurocytol. *3:* 179–197.

Saito, K. (1979) Morphometrical synaptology of Clarke cells and of distal dendrites in the nucleus dorsalis: Electron microscopic study in the cat. Brain Res. *178:* 233–249.

Szentagothai, J., and A. Albert (1955) The synaptology of Clarke's column. Acta Morphol. Hung. *5:* 43–51.

Tracey, D. J., and B. Walmsley (1982) Anatomy of the connection between identified primary afferents and neurones of the dorsal spinocerebellar tract. Proc. Aust. Physiol. Pharmacol. Soc. *13:* (2) 134P.

Tracey, D. J., and B. Walmsley (1984) Synaptic input from identified muscle afferents to neurones of the dorsal spinocerebellar tract in the cat. J. Physiol. (Lond.) *350:* 599–614.

Uchizono, K. (1975) *Excitation and Inhibition: Synaptic Morphology*, Elsevier Scientific Publishing Co., Amsterdam.

Wienawa-Narkiewicz, E., B. Walmsley, and M. J. Nicol (1984) Electron microscopy of the synaptic connection between primary afferents and DSCT neurones. Neurosci. Lett. Suppl. *15:* S63.

APPENDIX II

ULTRASTRUCTURAL EVIDENCE RELATED TO PRESYNAPTIC INHIBITION OF PRIMARY MUSCLE AFFERENTS IN CLARKE'S COLUMN OF THE CAT.

by

B. Walmsley, E. Wieniawa-Narkiewicz,
and M.J.Nicol

The Journal of Neuroscience, (1987), 7(1):235-243

The Journal of Neuroscience, January 1987, 7(1): 236–243

Ultrastructural Evidence Related to Presynaptic Inhibition of Primary Muscle Afferents in Clarke's Column of the Cat

B. Walmsley, E. Wieniawa-Narkiewicz,[a] and M. J. Nicol[1]

Neural Research Laboratory, School of Anatomy, University of New South Wales, Kensington, N.S.W., Australia, and [1]Experimental Neurology Unit, John Curtin School of Medical Research, Australian National University, Canberra, A.C.T., Australia

As part of an investigation on excitatory synaptic transmission in the mammalian CNS, we have examined ultrastructural details of the synaptic connection between primary afferent fibers and dorsal spinocerebellar tract (DSCT) neurons in Clarke's column of the cat spinal cord. Single primary muscle afferents (group Ia and Ib) and DSCT neurons were identified and stained intracellularly with HRP. The terminations of these afferent fibers were examined in serial sections under the EM. Five of 6 Ib boutons and 1 of 14 Ia boutons were contacted by small presynaptic boutons. An example was illustrated in which only 1 out of 7 boutons arising from the same Ia fiber and contacting the same postsynaptic DSCT neuron was contacted by a presynaptic bouton. It is likely that the presynaptic contacts are responsible for presynaptic inhibition of synaptic transmission between primary afferents and DSCT neurons. We have proposed that the observed differences in presynaptic contacts from bouton to bouton may be one of the causes of a nonuniformity in the probability of transmitter release between release sites at this connection.

In a previous light-microscopic study (Tracey and Walmsley, 1984), the anatomical details of the monosynaptic connection between primary muscle afferents and dorsal spinocerebellar tract (DSCT) neurons in Clarke's column were examined. It was found that the synaptic terminals from both group Ia and group Ib fibers varied greatly in size, from 1 × 1 μm up to "giant" boutons, 20 × 3 μm. Previous electron-microscopic studies in Clarke's column indicated that these giant boutons may contain multiple transmitter release sites, although the precise origin of the boutons was unknown (Szentagothai and Albert, 1955; Rethelyi, 1970; Saito, 1974, 1979; Houchin et al., 1983). In a recent study (Walmsley et al., 1985), the ultrastructure of identified Ia afferent terminations was examined, including the connection between Ia boutons and dendrites of a DSCT neuron, both labeled intracellularly with HRP. The results of this study confirmed earlier suggestions that Ia synaptic terminals in Clarke's column contain multiple transmitter release sites.

Received Apr. 7, 1986; revised June 30, 1986; accepted July 1, 1986.

We are grateful to Dr. E. G. Jones, Dr. D. R. Curtis, Dr. R. E. W. Fyffe, and Dr. D. J. Tracey for their comments on and suggestions concerning the manuscript.

Correspondence should be addressed to Dr. B. Walmsley, Neural Research Laboratory, School of Anatomy, University of N.S.W., P.O. Box 1, Kensington, N.S.W., Australia.

[a] Present address: Department of Anatomy, Faculty of Medicine, The University of Calgary, 3300 Hospital Drive, N.W., Calgary, Alberta T2N 4N1, Canada.

Electrophysiological experiments have shown that excitatory postsynaptic potentials (EPSPs) evoked in DSCT neurons by impulses in a single afferent fiber fluctuate in amplitude (Tracey and Walmsley, 1984). These fluctuations occur between discrete amplitudes that are separated by quantal increments. The electron-microscopic observations on Ia terminations (Walmsley et al., 1985) are consistent with the proposal that synaptic transmission between group I muscle afferents and DSCT neurons occurs with discrete all-or-nothing EPSPs correlated with the number of release sites (rather than the number of boutons). Although quantal in nature, the fluctuation pattern of single-fiber EPSPs evoked in DSCT neurons (Walmsley et al., in press), and motoneurons (Jack et al., 1981) does not obey any standard statistical distribution, such as Poisson or binomial. Such distributions would be expected only if the probability of transmitter release were identical at all release sites. Recent evidence has been obtained (Walmsley et al., in press) that the probability of transmitter release may vary considerably from release site to release site. This observation has led us in the present electron-microscopic study to examine ultrastructural differences in the terminals of both group Ia and group Ib afferent fibers in Clarke's column. The results demonstrate the existence of presynaptic contacts on some, but not all, Ia and Ib boutons. Furthermore, boutons arising from the same Ia afferent fiber and contacting the same DSCT neuron also show differences in the occurrence of presynaptic contacts. These presynaptic contacts are most likely responsible for presynaptic inhibition in the spinal cord, and they may be one of the causes of nonuniform release probability in synaptic transmission between single muscle afferents and DSCT neurons.

Materials and Methods

Experiments were performed on cats weighing 1.5–2.5 kg. The cats were anesthetized with sodium pentobarbital (35 mg/kg, i.p.) and maintained with supplementary doses (5 mg, i.v.). Mean arterial pressure and end-tidal CO_2 were monitored.

Identification and HRP-labeling of muscle afferents and neurons. The following muscles were exposed in the left hindlimb: medial gastrocnemius, lateral gastrocnemius, soleus, and plantaris. The tendons of these muscles were separated and cut at their insertion to allow each muscle to be stretched individually. The cat was fixed in a rigid animal frame and a laminectomy performed from L7 to L3. The exposed hindlimb muscles and spinal cord were covered with pools of mineral oil, maintained at 37°C by infrared heating. Bipolar stimulating electrodes were placed on the sciatic nerve and its branches to the exposed muscles.

Glass microelectrodes containing 10% HRP (Sigma type VI) in 1 M KCl were inserted into the dorsal columns near the junction of L3 and L4 segments of the spinal cord, about 200 μm lateral to the midline. On intracellular penetration of a primary muscle afferent, its conduction time in response to electrical stimulation of the appropriate nerve was

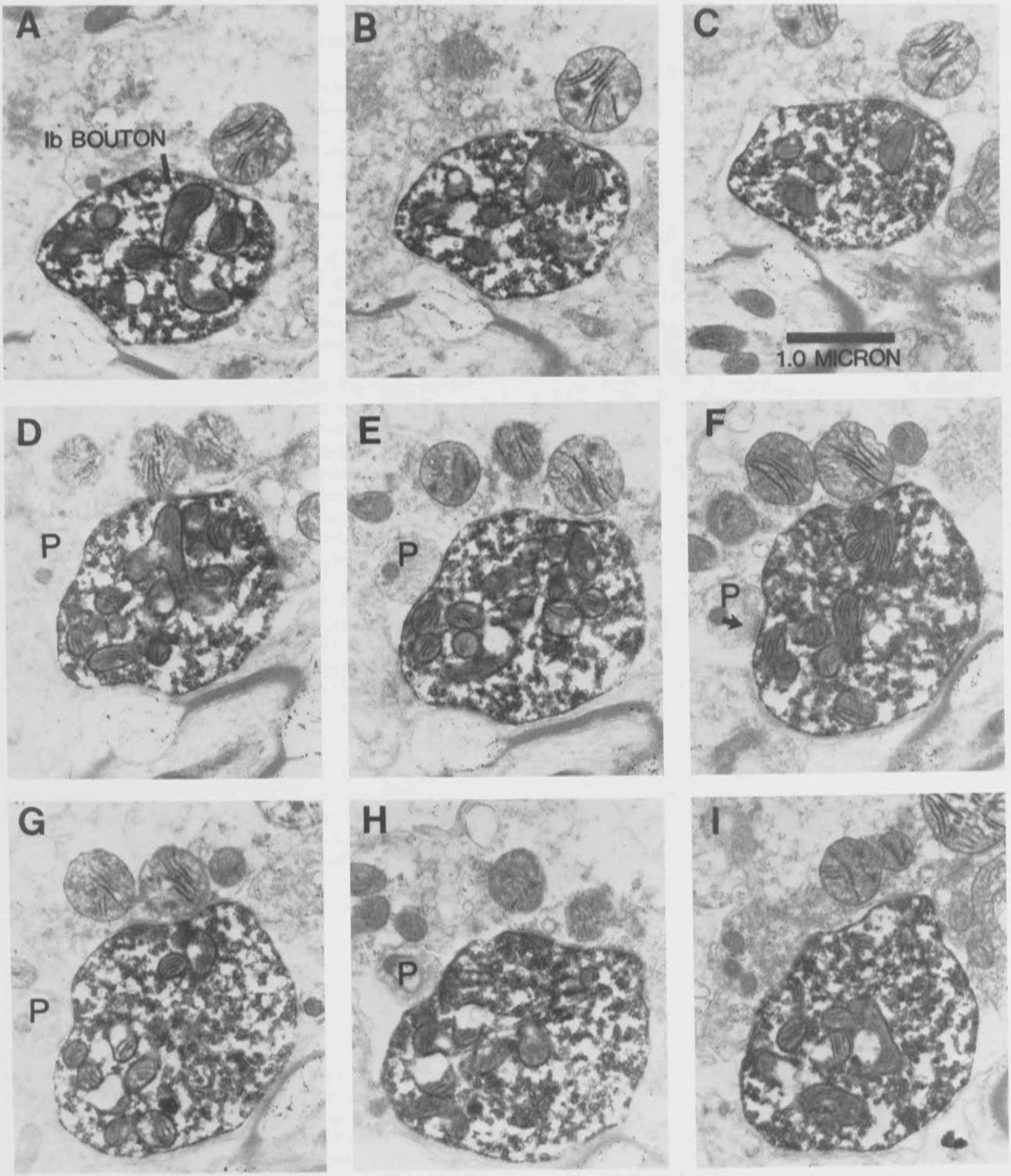

Figure 1. Serial sections through an HRP-labeled Ib bouton shown in sequential order (*A–I*). A small unlabeled bouton (*P*) contacted the Ib bouton (*arrow* in *F*).

recorded, allowing preliminary classification into group I or II. Fibers were classified as group Ia if they had high dynamic sensitivity to passive stretch and a silent period during active muscle contraction. Group Ib fibers had high thresholds and low dynamic sensitivity to passive stretch, and were activated during the period of a muscle twitch (Tracey and Walmsley, 1984). Once the afferent was identified, HRP was iontophoresed into the axon for up to an hour. Iontophoresis of HRP was continued only while the intracellular action potential was greater than 10 mV.

Good results were obtained when the charge transfer was in the range 100–400 nA min. (In any given experiment only Ia *or* Ib fibers, but not both, were injected with HRP.)

In the same experiments, intracellular recordings were made from DSCT neurons in Clarke's column at the level of the L3 and L4 segments of the spinal cord. Antidromic identification of the DSCT neurons was performed by stimulation of the dissected dorsolateral fasciculus of the spinal cord at the C2 level (Houchin et al., 1983; Tracey and Walmsley, 1984). The dorsal columns were removed for approximately 2 cm to avoid stimulation spreading to them. Electrodes filled with 10% HRP in 1 M KCl were driven into Clarke's column in the spinal cord approximately 200–300 μm from the midline. Only DSCT neurons receiving monosynaptic excitation from group I muscle afferents were injected with HRP (10–30 nA for 10–40 min). The staining of both neurons and afferent fibers in the same experiment allowed subsequent identification of both pre- and postsynaptic structures under the EM.

Following a 2–5 hr postinjection survival time, the anesthetized animal was perfused with 3% glutaraldehyde in 0.1 M phosphate buffer (pH 7.2). The spinal cord segments L3 and L4 were removed and postfixed for about 10 hr. Parasagittal sections (100 μm) of these segments were cut using a Vibratome and reacted for HRP using diaminobenzidine (DAB).

Electron microscopy. Sections immersed in glycerol were carefully examined under the light microscope. Structures filled with HRP reaction product were readily observed, even in the nondehydrated tissue. Small areas (2 × 1 mm) containing stained fibers were cut from the sections and transferred to 0.1 M phosphate buffer (pH 7.4), washed, and left for 2–3 hr at 4°C. Subsequently, the tissue was postfixed in 2% OsO_4, stained en bloc with 2% uranyl acetate, dehydrated in alcohols, and embedded in Spurr resin. Thin sections (ca. 1000 Å) were cut with a diamond knife (Diatome) on a Reichert microtome, collected on parlodion-coated slot grids, and examined in a Philips 301 EM. HRP-labeled structures were easily observed, and in the majority of cases staining was light enough not to obscure intracellular components. Sequential sections of each labeled structure were examined and relevant sections photographed. HRP-labeled boutons were examined completely in sequential sections so that the presence or absence of presynaptic structures could be confidently determined for each bouton.

Results

Electron microscopy of HRP-identified Ib boutons in Clarke's column

Six HRP-labeled Ib boutons from 2 afferent fibers were completely examined in serial sections under the EM. Figure 1 shows a sequence of sections through a Ib bouton. The HRP-DAB reaction product stained this terminal darkly enough for positive identification without obscuring the major ultrastructural details. Figure 2 shows different sections through the same bouton and illustrates the main features of most Ib boutons examined. Synaptic contacts of Ib fibers showed a pronounced postsynaptic density (Fig. 2*B*), indicating that these synapses were of the asymmetrical type. Figure 2*C* illustrates that this same Ib bouton received a contact from a small unlabeled bouton (see also Fig. 1). This was a common feature, as 5 out of 6 Ib boutons examined were contacted by presynaptic boutons, ranging in size from 0.5 to 1.5 μm in diameter. The bouton *not* receiving a presynaptic contact arose from the same Ib fiber that possessed terminals receiving presynaptic contacts.

Figure 3 illustrates the contacts formed between presynaptic boutons and 4 different HRP-labeled Ib boutons. One of these boutons (Fig. 3*B*) appeared to be contacted by 2 separate presynaptic terminals. The presynaptic terminals contained elliptical to round vesicles that accumulated close to the presynaptic membrane. Although the postsynaptic thickening was partly obscured by the HRP reaction product, these synapses appeared to be of the symmetrical type.

Electron microscopy of HRP-identified Ia boutons in Clarke's column

Fourteen boutons arising from 3 HRP-identified Ia fibers have been completely examined in serial sections under the EM. The main features of Ia boutons in Clarke's column have been described in a previous study (Walmsley et al., 1985). However, none of the boutons presented in that study was contacted by presynaptic boutons. We have now found an example of a presynaptic contact formed with a Ia bouton in Clarke's column, and this example is illustrated in Figures 4 and 5. In this experiment, both the Ia afferent and the DSCT neuron contacted by this afferent were labeled with HRP, allowing positive identification of both pre- and postsynaptic structures. (DSCT neurons do not possess recurrent axon collaterals and therefore the possibility of confusing Ia terminals and "autapses" can be dismissed.)

Figure 4 shows 3 sequential sections through the Ia bouton (and DSCT neuron dendrite). In Figure 4*B* the Ia bouton can be seen to make contact with a small spine arising from the DSCT neuron dendrite. In the same section, another bouton (p) appears to contact the labeled Ia bouton. This is shown in more detail in Figure 5. Figure 5*B* shows a schematic reconstruction of the dendrite, the Ia bouton, and the presynaptic bouton from 14 sequential sections. Figure 5*A* is a higher-magnification electron micrograph and clearly shows the arrangement between the Ia bouton, the presynaptic bouton, and the dendritic spine arising from the DSCT neuron dendrite. In total, 7 HRP-labeled boutons arising from the same Ia fiber and contacting the dendrites of this same HRP-labeled DSCT neuron have been completely examined in serial sections under the EM. The Ia bouton illustrated in Figures 4 and 5 is the only 1 of the 7 to receive a presynaptic contact.

Discussion

The major findings of the present study are as follows:

1. Identified boutons of both Ia and Ib primary muscle afferents in Clarke's column are contacted by presynaptic boutons.
2. Not all boutons arising from a single Ia or Ib fiber are contacted by presynaptic boutons.
3. Not all boutons from a single Ia fiber that contact the *same* postsynaptic DSCT neuron are contacted by presynaptic boutons.

It is probable that the presynaptic contacts observed are related to presynaptic inhibition of synaptic transmission between Ia and Ib afferents and neurons in Clarke's column. Jankowska et al. (1965, 1984) and Curtis et al. (in press) have reported excitability changes of group I muscle afferent fibers and their terminations in Clarke's column in response to stimulation of other primary afferents. Curtis et al. (in press) proposed that primary afferent depolarization of group I muscle afferents in Clarke's column is generated at bicuculline-sensitive receptors by GABA released at axoaxonic synapses on the terminations of these afferents (see also Eccles et al., 1963; Jankowska et al., 1981; Rudomin et al., 1981; Curtis and Lodge, 1982). The present electron-microscopic study has now demonstrated the existence of such axoaxonic contacts on positively identified group Ia and Ib afferent boutons in Clarke's column. Such contacts have also been observed on group Ia boutons in the motor nuclei

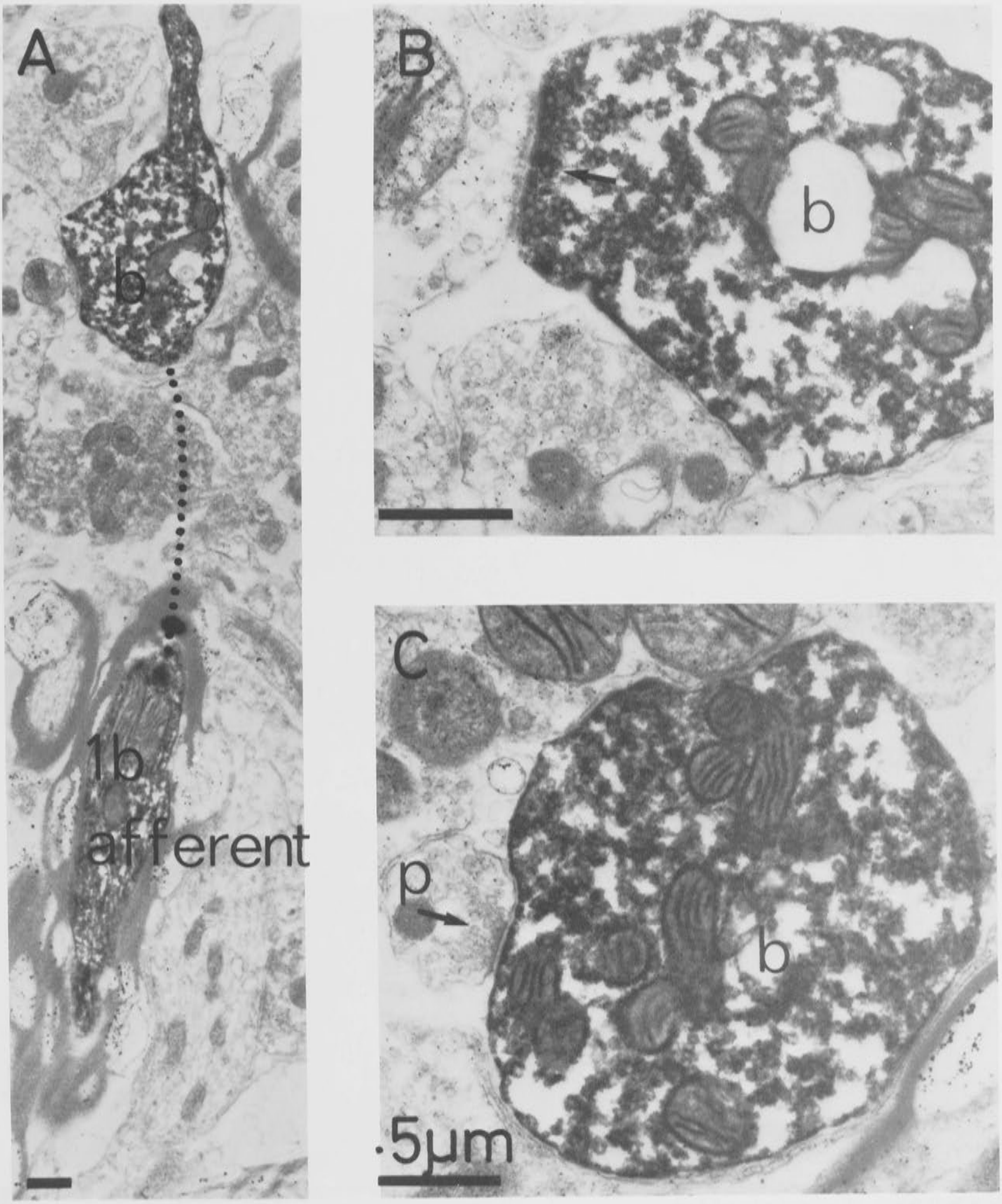

Figure 2. Photomicrographs of the same HRP-labeled bouton (*b*) shown in Figure 1. In *A* the afferent fiber can also be seen. The *dotted line* indicates the continuation of the Ib fiber that was followed in adjacent sections. *B*, Probable contact between the Ib bouton and an unlabeled postsynaptic profile. *C*, Small unlabeled bouton (*p*) makes contact with the Ib bouton. All calibration bars, 0.5 μm.

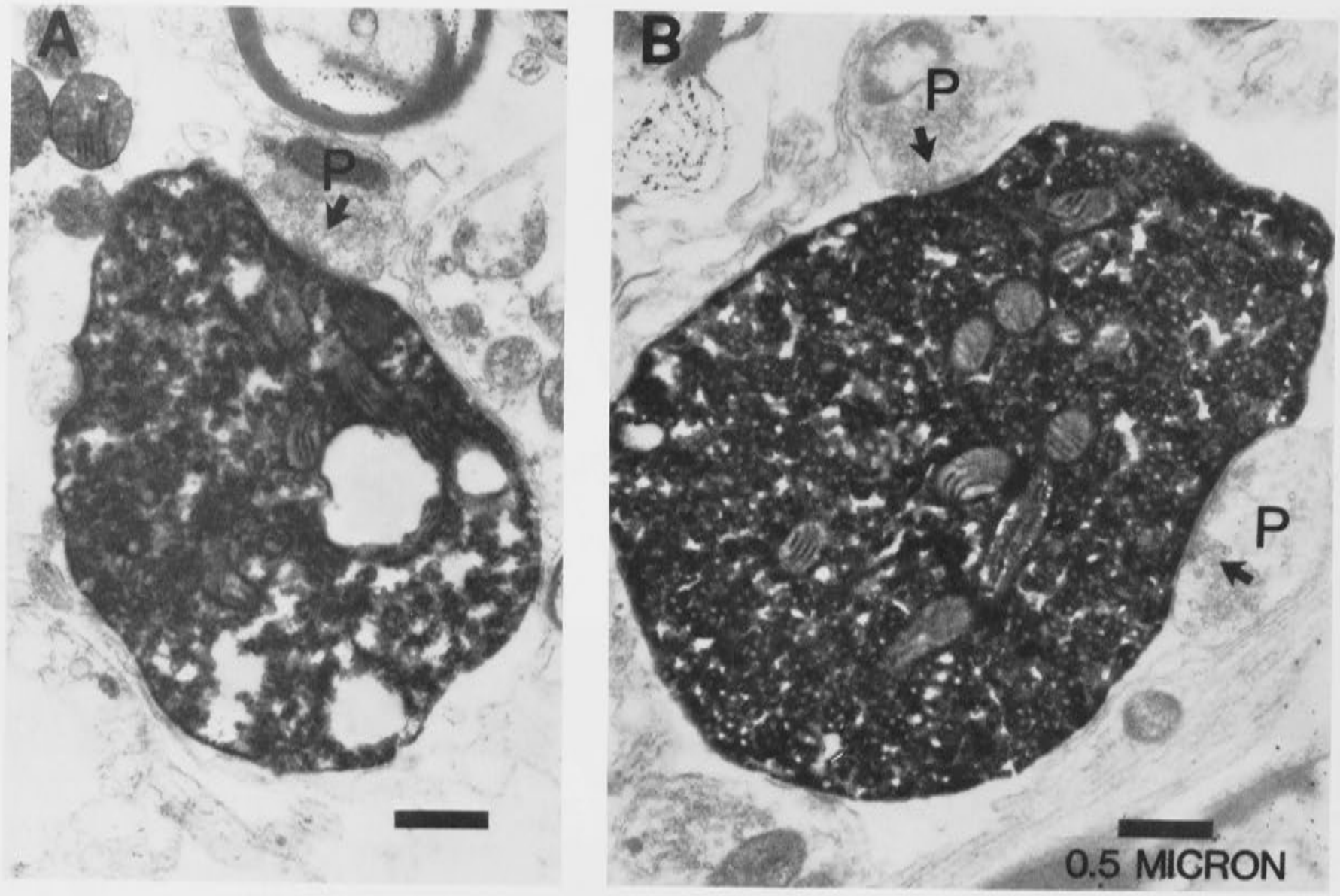

Figure 3. Presynaptic contacts between unlabeled boutons (*P*) and 4 different HRP-labeled Ib boutons. In *B*, 2 small boutons appear to contact the same Ib bouton. All calibration bars, 0.5 μm.

of the cat spinal cord (Fyffe and Light, 1984), where the action of GABA has also been demonstrated (Curtis and Lodge, 1982).

Clements et al. (in press) have recently examined presynaptic inhibition of single group Ia fiber EPSPs recorded in motoneurons. By analyzing the fluctuations in single-fiber EPSPs, they have demonstrated that the probability of transmitter release decreases during presynaptic inhibition (see also Dudel and Kuffler, 1961). Tracey and Walmsley (1984) examined synaptic

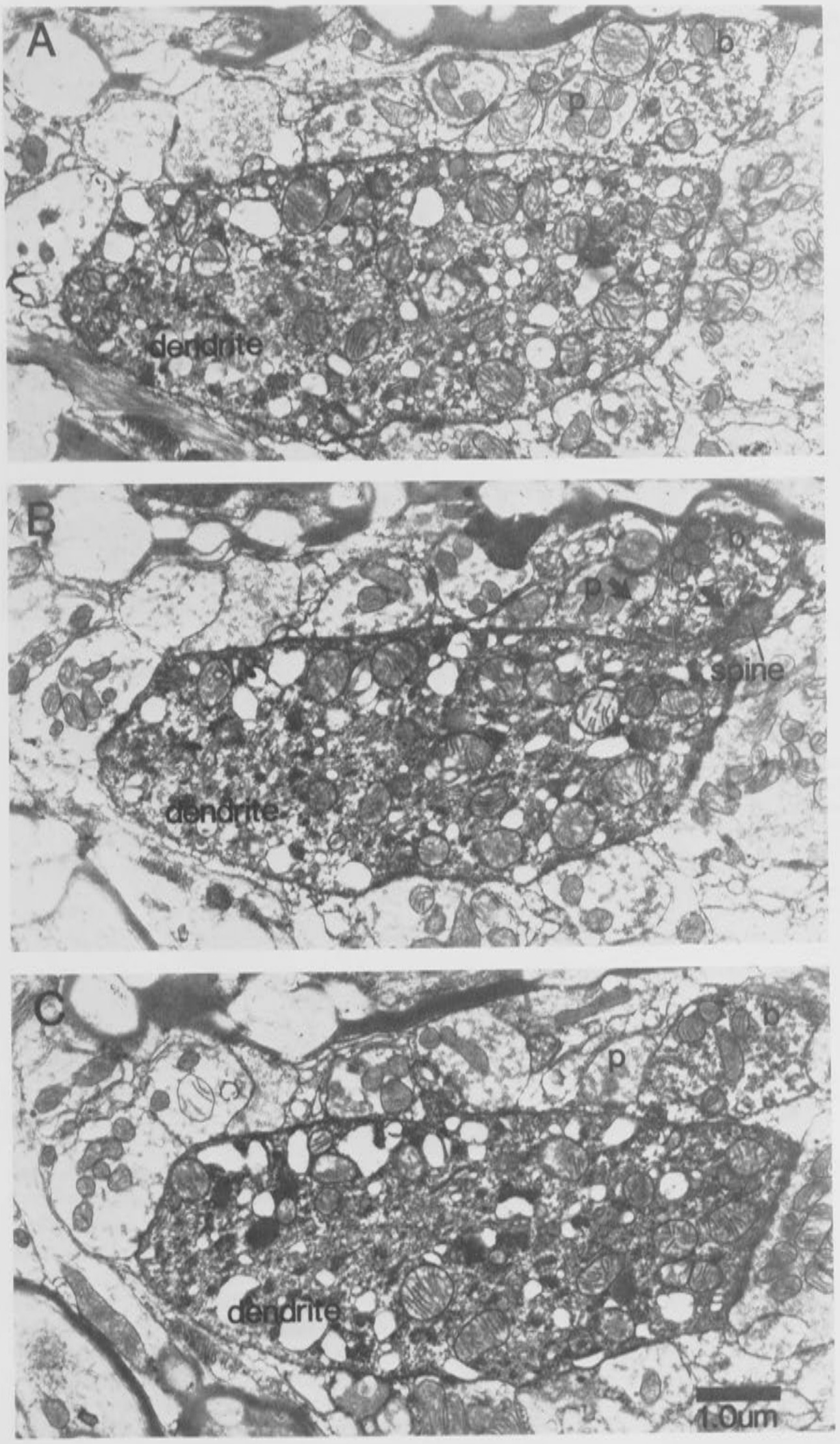

Figure 4. *A–C*, Three sequential sections through an HRP-labeled Ia bouton (*b*) and the dendrite of an HRP-labeled DSCT neuron. The Ia bouton contacts a spine of the DSCT neuron in *B* and, in the same section, receives a contact from an unlabeled bouton (*p*).

transmission between single primary muscle afferents and DSCT neurons in Clarke's column. They found that single-fiber EPSPs evoked in DSCT neurons fluctuate between discrete amplitudes that are separated by quantal increments. Previous studies on synaptic transmission in the mammalian CNS have attempted to relate fluctuations in EPSP amplitude with the *number* of synaptic boutons (Redman and Walmsley, 1981). In contrast, Tracey and Walmsley (1984) proposed that transmission be-

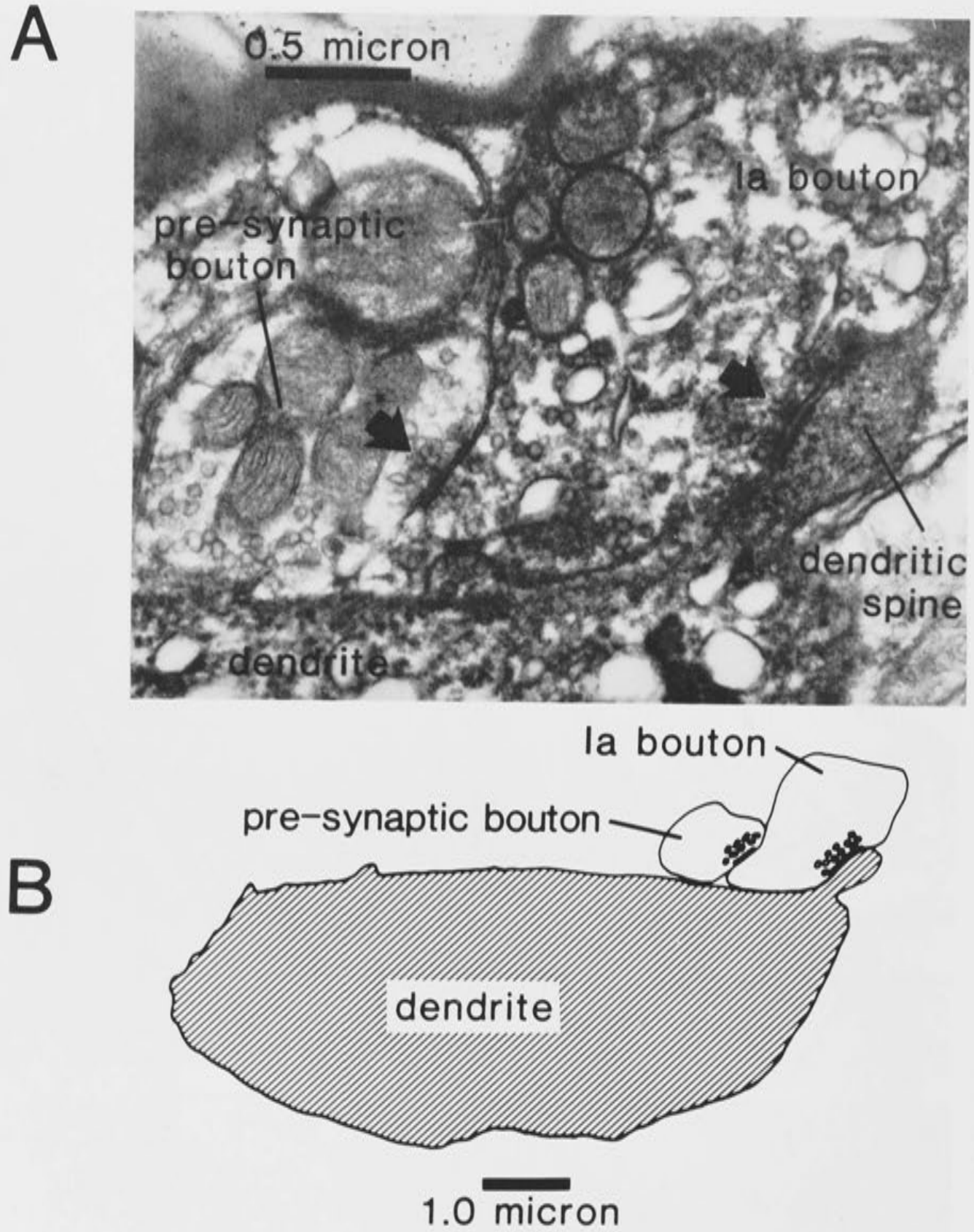

Figure 5. Details of the contact (also shown in Fig. 4) between an HRP-labeled Ia bouton and an HRP-labeled DSCT neuron dendrite. Fourteen serial sections were used in a reconstruction to obtain the schematic shown in *B*. An unlabeled bouton was found to be presynaptic to the Ia bouton (labeled in *A* and *B*). The contact is indicated by the *arrow* in *A*.

tween group I muscle afferents and DSCT neurons occurs with EPSP fluctuations related to transmitter release sites rather than boutons *per se*, since many boutons probably contain multiple transmitter release sites. In an EM study, Walmsley et al. (1985) demonstrated that group Ia boutons contacting DSCT neurons in Clarke's column contain multiple synaptic specializations, which probably correspond to transmitter release sites. Tracey and Walmsley (1984) concluded that the single-fiber EPSP amplitude fluctuation pattern is due to a summation of EPSPs arising from all-or-nothing transmission at individual release sites and that the probability of release may vary from release site to release site. The present electron-microscopic study has demonstrated that some boutons arising from the same single fiber may be subjected to presynaptic inhibition, and others may not. A difference in the presynaptic contacts would provide one explanation for nonuniform release probabilities. Such a scheme is illustrated in Figure 6. A presynaptic fiber is shown making contact at 2 boutons with a postsynaptic neuron. Each bouton contains 2 transmitter release sites. [The number of boutons arising from a group I muscle afferent and contacting a DSCT neuron may vary from 1 to greater than 18 (Tracey and Walmsley, 1984). In addition, the number of release sites within a single bouton may vary from 1 to greater than 9 (Walmsley et al., 1985).] Figure 6*A* illustrates a hypothetical EPSP amplitude fluctuation pattern, assuming uniform release probabilities for all release sites. (For simplicity, the contacts and recording site in this example are considered to be somatic.) In this example, the probability has been chosen to be 0.9 (i.e., $P1 = P2 = P3 = P4 = 0.9$), and simple binomial statistics have been assumed. The EPSP amplitude may fluctuate between the 4 levels shown (plus zero), and the probabilities for each amplitude level are illustrated. Figure 6*B* illustrates the situation in which only one of these boutons (b2) is subjected to presynaptic inhibition. The probability of transmitter release from b2 would be de-

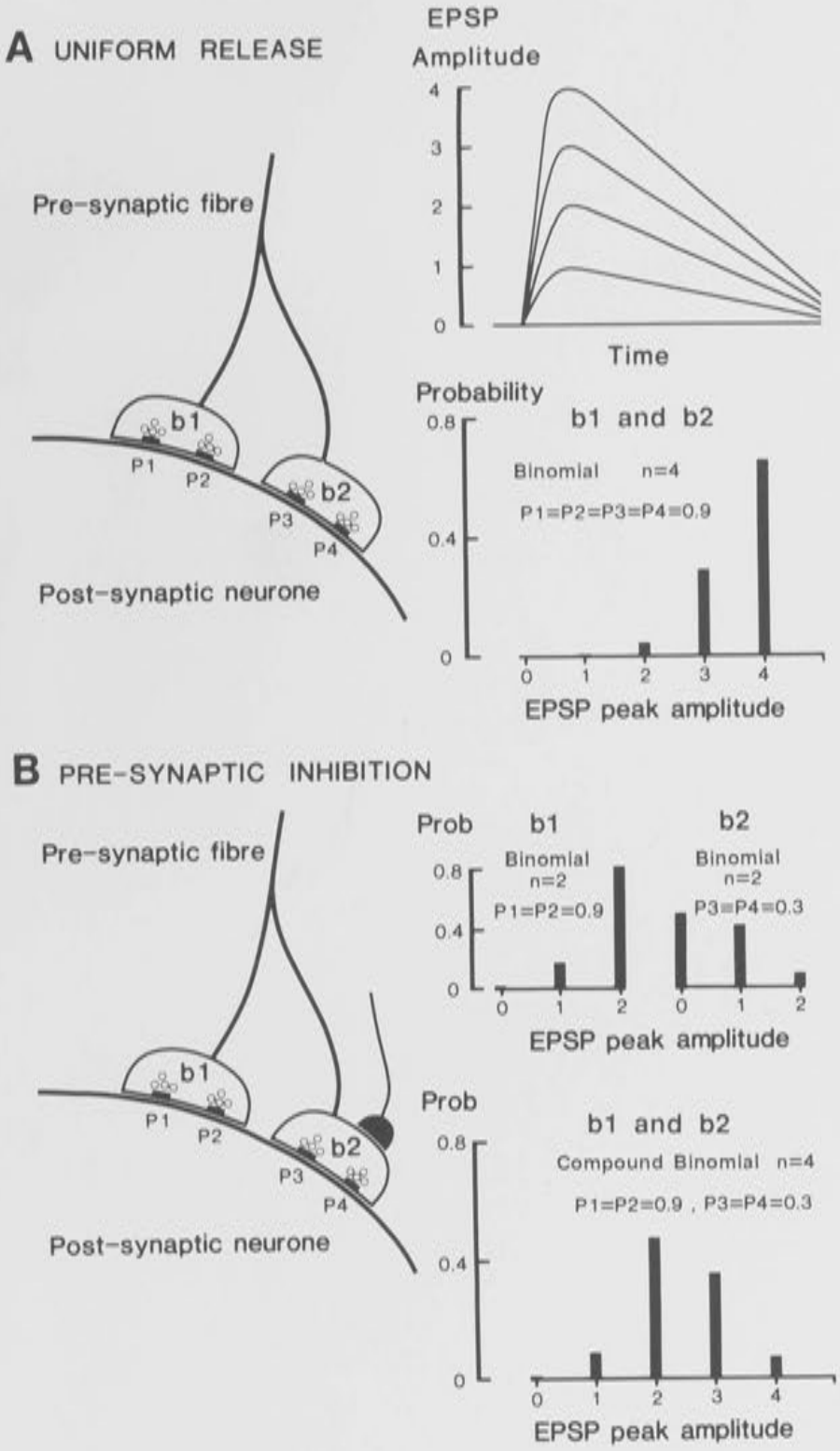

Figure 6. Summary of the possible effect of presynaptic contacts on synaptic transmission in the spinal cord. See text for explanation.

creased and, in this example, it has been arbitrarily reduced from 0.9 to 0.3. The release probabilities from release sites in b1 have been assumed to remain at 0.9. (The possibility exists for a polarization at b2 to spread to b1 and so influence the release probability at this bouton also, although to a lesser degree.) If it is now assumed that each bouton acts independently with simple binomial release probabilities (i.e., for b1, $n = 2$ and $P1 = P2 = 0.9$, and for b2, $n = 2$ and $P3 = P4 = 0.3$), then the overall fluctuation pattern could be described by a compound binomial model in which $n = 4$, $P1 = P2 = 0.9$ and $P3 = P4 = 0.3$, as shown in the lower right of Figure 6*B*.

Walmsley et al. (in press) have demonstrated that uniform binomial release statistics do not apply to the amplitude fluctuation pattern of single group I muscle afferent EPSPs recorded in DSCT neurons. Instead, the fluctuation pattern can be described if different release probabilities are assumed. The simple scheme presented in Figure 6*B* represents only one explanation for such nonuniform release probabilities, based on the electron-microscopic evidence presented in this study.

Continued investigation of the synaptic connection between primary afferent fibers and DSCT neurons will, we hope, allow us to formulate a general model of excitatory synaptic transmission in the mammalian CNS. The ultrastructural features of this connection provide a basis for our present investigations on the mechanisms underlying the probabilistic nature of synaptic transmission at this synapse.

References

Clements, J. D., I. D. Forsythe, and S. J. Redman (in press) Presynaptic inhibition of synaptic potentials evoked in cat spinal motoneurones by impulses in single group Ia axons. J. Physiol.

Curtis, D. R., and D. R. Lodge (1982) The depolarization of feline ventral horn group Ia spinal afferent terminations by GABA. Brain Res. *46:* 215–233.

Curtis, D. R., B. D. Gynther, and R. Malik (in press) A pharmacological study of group Ia muscle afferent terminals and synaptic excitation in the intermediate nucleus and Clarke's column of the cat spinal cord. Exp. Brain Res.

Dudel, J., and S. W. Kuffler (1961) Pre-synaptic inhibition at the crayfish neuromuscular junction. J. Physiol. (Lond.) *155:* 543–562.

Eccles, J. C., R. F. Schmidt, and W. D. Willis (1963) Pharmacological studies on presynaptic inhibition. J. Physiol. (Lond.) *168:* 500–530.

Fyffe, R. E. W., and A. R. Light (1984) The ultrastructure of group Ia afferent fiber synapses in the lumbosacral spinal cord of the cat. Brain Res. *300:* 201–209.

Houchin, J., D. J. Maxwell, R. E. W. Fyffe, and A. G. Brown (1983) Light and electron microscopy of dorsal spinocerebellar tract neurons in the cat: An intracellular horseradish peroxidase study. Q. J. Exp. Physiol. *68:* 719–732.

Jack, J. J. B., S. J. Redman, and K. Wong (1981) The components of synaptic potentials evoked in cat spinal motoneurones by impulses in group Ia fibres. J. Physiol. (Lond.) *321:* 65–96.

Jankowska, E., and Y. Padel (1984) On the origin of presynaptic depolarization of Group I muscle afferents in Clarke's column in the cat. Brain Res. *295:* 195–201.

Jankowska, E., M. G. M. Jukes, and S. Lund (1965) On the presynaptic inhibition of transmission to the dorsal spinocerebellar tract. J. Physiol. (Lond.) *177:* 19–20P.

Jankowska, E., D. McCrea, P. Rudomin, and E. Sykova (1981) Observations on neuronal pathways subserving primary afferent depolarization. J. Neurophysiol. *46:* 506–516.

Redman, S. J., and B. Walmsley (1981) The synaptic basis of the monosynaptic stretch reflex. Trends Neurosci. *4:* 248–250.

Rethelyi, M. (1970) Ultrastructural synaptology of Clarke's column. Exp. Brain Res. *11:* 159–174.

Rudomin, P., I. Engberg, and I. Jimenez (1981) Mechanisms involved in the generation of presynaptic depolarization of group I afferent and rubro-spinal fibers in the cat spinal cord. J. Neurophysiol. *46:* 532–547.

Saito, K. (1974) The synaptology and cytology of the Clarke cell in the nucleus dorsalis of the cat: An electron microscopic study. J. Neurocytol. *3:* 179–197.

Saito, K. (1979) Morphometrical synaptology of Clarke cells and of distal dendrites of the nucleus dorsalis: Electron microscopic study in the cat. Brain Res. *178:* 233–249.

Szentagothai, J., and A. Albert (1955) The synaptology of Clarke's column. Acta. Morphol. Hung. *5:* 43–51.

Tracey, D. J., and B. Walmsley (1984) Synaptic input from identified muscle afferents to neurones of the dorsal spinocerebellar tract in the cat. J. Physiol. (Lond.) *350:* 599–614.

Walmsley, B., F. R. Edwards, and D. J. Tracey (in press) The probabilistic nature of synaptic transmission at a mammalian excitatory central synapse. J. Neurosci.

Walmsley, B., E. Wieniawa-Narkiewicz, and M. J. Nicol (1985) The ultrastructural basis for synaptic transmission between primary muscle afferents and neurones in Clarke's column of the cat. J. Neurosci. *5:* 2095–2106.